

Université de Montréal

**Petit poisson deviendra grand?:
Évaluation du rôle de la contamination chimique dans le déclin des
populations de perchaudes (*Perca flavescens*) du lac Saint-Pierre**

par Mélissa Khadra

Département de sciences biologiques
Faculté des arts et des sciences

Thèse présentée
en vue de l'obtention du grade de Philosophiae Doctor (Ph. D.)
en Sciences Biologiques

Mai, 2019

© Mélissa Khadra, 2019

Université de Montréal
Département de sciences biologiques, Faculté des arts et des sciences

Petit poisson deviendra grand?: Évaluation du rôle de la contamination chimique dans le déclin des populations de perchaudes (*Perca flavescens*) du lac Saint-Pierre

Présentée par
Mélissa Khadra

A été évaluée par un jury composé des personnes suivantes

Bernadette Pinel-Alloul
Présidente-rapporteuse

Marc Amyot
Directeur de recherche

Dolors Planas
Codirectrice

Andrea Bertolo
Membre du jury

Nelson Belzile
Examinateur externe

Résumé

La qualité de l'eau du lac Saint-Pierre (LSP), le plus grand lac fluvial du fleuve Saint-Laurent, est notamment compromise par le déversement d'une mixture composée de métaux et de pesticides provenant des rejets des industries, des effluents municipaux et de l'exploitation des terres agricoles dans son bassin versant. Cette contamination est d'autant plus importante dans les zones du lac caractérisées par une végétation dense favorisant la rétention et la sédimentation de la matière en suspension. Or, ces herbiers aquatiques, qui occupent de vastes étendues du LSP, servent de frayère pour plusieurs poissons, dont la perchaude (*Perca flavescens*). Cette espèce est donc particulièrement affectée par la dégradation des habitats aquatiques du LSP. À la suite d'un déclin important de ses populations depuis la fin des années 1990 en raison de son important intérêt commercial et sportif, un moratoire de cinq ans sur la pêche de la perchaude a été imposé en 2012 et reconduit jusqu'en 2022, puisque l'incapacité de rétablissement des populations de perchaudes semble persister. La présente étude vise à évaluer l'hypothèse que cette incapacité de rétablissement, qui se reflète par un recrutement déficient, soit en partie attribuable à l'impact de la contamination chimique sur la reproduction, soit par des effets toxiques potentiels sur les femelles ovigères, sur les œufs ou sur les jeunes larves pendant les premiers mois.

Dans un premier temps, nous avons évalué l'hypothèse que le glyphosate, herbicide à large spectre et ingrédient actif de la formulation Roundup®, ait un impact indirect sur les jeunes perchaudes en décimant les communautés de biofilms périphytiques, source d'alimentation des invertébrés dont se nourrissent les jeunes larves. Cette suite d'effets contribuerait à l'accroissement de la mortalité hivernale des jeunes de l'année, due à une insuffisance de ressources énergétiques. Or, nos résultats démontrent que peu importe l'âge, et par le fait même l'épaisseur des biofilms, le glyphosate, en concentrations environnementales现实的, ne semble pas impacter négativement la composition des communautés ou le métabolisme de la chlorophylle des biofilms. Seul l'âge (2 mois, 1 an, 20 ans) de ces derniers semblait en effet influencer la composition taxonomique des communautés. Nous avons cependant observé une augmentation de l'abondance relative d'*Anabaena*, un taxon de cyanobactéries toxiques qui possède une forme résistante rare de l'enzyme EPSPS, cible principale du mode d'action du glyphosate. Cette étude contribue à l'avancement des connaissances sur les effets de l'herbicide le plus utilisé à l'échelle mondiale, actuellement au cœur de préoccupations d'intérêt international.

Nous avons également évalué le potentiel de toxicité associé au transfert maternel du mercure et du sélénium chez la perchaude à l'aide de techniques de fractionnement subcellulaire.

Le mercure est un contaminant d'intérêt en raison de son omniprésence dans l'environnement ainsi que de ses effets néfastes sur la reproduction des poissons à de très faibles concentrations. Il a également été démontré que des ratios molaires Se:Hg supérieurs à 1 atténuait les effet néfastes du mercure. Nos résultats démontrent une évidence de transfert maternel de la femelle à ses œufs, mais également aux mitochondries gonadiques, principales composantes sensibles de la cellule. Le transfert maternel représentant la source d'exposition aux contaminants la plus importante pour les embryons, nos observations pourraient contribuer à expliquer le recrutement déficient des jeunes perchaudes au LSP. Nous avons également mesuré des ratios molaires Se:Hg systématiquement supérieurs à 1 dans les différentes fractions subcellulaires hépatiques et gonadiques, résultats novateurs qui laissent sous-entendre un effet protecteur du Se.

Puisque nous avons confirmé l'occurrence d'un transfert maternel du mercure, l'étape logique subséquente était d'évaluer la bioaccumulation de ce contaminant au sein des différents stades ontogéniques du cycle de vie de la perchaude. Les stades embryo-larvaires et juvéniles précoces sont en effet des phases particulièrement sensibles aux contaminants organiques et inorganiques. Nos résultats démontrent que les concentrations de MeHg décroissent suivant un patron ontogénique, avec les plus hautes concentrations mesurées chez les juvéniles et les plus basses dans les masses d'œufs. Nous avons également démontré que presque 100% du mercure était présent sous forme de MeHg, forme toxique et bioamplifiable, chez les larves et les juvéniles. Les ratios molaires Se:Hg étaient quant à eux systématiquement supérieurs à 1, résultats comblant d'importantes lacunes au niveau des effets antagonistes entre le mercure et le sélénium chez les poissons.

Les résultats découlant des présents travaux de recherche ont un impact important sur la science de l'écotoxicologie en raison de leur caractère novateur. Tout d'abord, nous avons contribué à l'avancement des connaissances sur l'impact de concentrations environnementales de glyphosate sur des biofilms d'âge très contrasté. Ensuite, nous avons, pour la première fois, utilisé des outils de fractionnement subcellulaire afin d'évaluer le potentiel de toxicité lié au transfert maternel du mercure. Enfin, nous rapportons les premières données liées à la bioaccumulation simultanée du mercure et du sélénium aux stades de vie clés du développement de la perchaude. La présente thèse s'avère ainsi nécessaire afin de contribuer au progrès du savoir sur le devenir de certains contaminants d'intérêt au sein des écosystèmes aquatiques.

Mots-clés : mercure, méthylmercure, sélénium, glyphosate, perchaude, biofilms périphytiques, lac Saint-Pierre, fractionnement subcellulaire, transfert maternel

Abstract

Lake Saint Pierre (LSP) is the largest fluvial lake in the Saint Lawrence River. Water quality in LSP is heavily affected by inputs of nutrients and chemical pollution from tributaries which drain agricultural watersheds, from municipal effluents and from industrial discharges. This contamination is amplified in areas of LSP with dense vegetation because aquatic plants promote the retention and sedimentation of dissolved and particulate matter. Several fish species, including Yellow Perch (*Perca flavescens*), use these aquatic vegetation beds as their spawning grounds and are therefore particularly affected by the contamination of aquatic habitats in LSP. This study therefore tests the hypothesis that chemical contamination in Yellow Perch (YP) during their early life stages can help explain this species' lack of resilience despite the implementation of a fishing moratorium in 2012. This moratorium was extended until 2022 since populations are still undergoing a recruitment failure and a decline in juvenile abundance populations.

The phosphonate herbicide glyphosate, which is the active ingredient in Roundup®, is currently the most widely used herbicide in the world. Glyphosate-based herbicides are sprayed on food and feed crops during cultivation and are thus subject to leaching to streams and rivers. In aquatic ecosystems, periphytic biofilms, or periphyton, are important primary producers and are often the first trophic level to be in contact with runoff waters. Thus, a trophic cascade could occur if these biofilms are negatively impacted by glyphosate, potentially leading to larval fish mortality due to resource limitation. Results showed that submersion period (2 months, 1 year, 20 years) was the only significant contributor to community structure. However, the glyphosate-resistant Cyanobacteria *Anabaena* was found to be favoured by the use of glyphosate. This freshwater Cyanobacteria commonly forms toxic blooms, raising concern regarding the use of glyphosate. For all colonization stages, and therefore different thicknesses, chlorophyll *a* did not show an unequivocal decline over time. This study therefore provides an interesting snapshot of the biological processes related to periphytic biofilms' exposure to environmental concentrations of glyphosate. As this herbicide is currently of international concern, it is imperative to contribute to the advancement of knowledge about its effects.

Mercury (Hg) is a trace element of particular concern since it is ubiquitous in the environment and because its methylated form (MeHg) readily bioaccumulates and biomagnifies

in food webs. This latter process leads to elevated Hg concentrations in fish and thus induces toxicity. Maternal transfer of bioaccumulated contaminants to offspring is a suggested mechanism of impaired reproductive success in fish. We therefore assessed the toxicity potential of Hg during maternal transfer in YP from LSP using a sub-cellular partitioning approach. Results showed a strong relationship between Hg bioaccumulation in the liver and Hg concentrations in gonadal mitochondria, which corroborates the potential toxicity of maternal transfer. As selenium is a well-studied Hg antagonist, we also measured the Se:Hg molar ratios in all subcellular fractions. We found that these ratios were systematically above 1, which is the suggested threshold for Hg toxicity alleviation through sequestration by Se.

Since early developmental stages in aquatic biota are particularly sensitive to Hg, and after confirming the evidence of maternal transfer, we subsequently addressed Hg bioaccumulation in all parts of YP life cycle. This study is the first of its kind to follow Hg and Se during YP ontogenetic development, from the gravid female to the juvenile. Results show that MeHg follow an ontogenetic pattern, with concentrations decreasing from the juveniles to egg masses. We also found that nearly 100% of THg was measured as the toxic form MeHg in larvae and juveniles. Lastly, Se:Hg molar ratios were systematically above 1, suggesting a potentially protective effect of Se on Hg bioaccumulation. This study will thus provide much needed information on the changes in bioaccumulation patterns during the most sensitive life cycle stages of this declining fish population.

Results issued from the present research have significant impact when it comes to the advancement of knowledge in Ecotoxicology due to their novel characteristics. First, we have contributed to the advancement of knowledge on the effects of environmental concentrations of glyphosate on highly age-contrasted biofilms. Also, it is the first time that subcellular partitioning techniques are used in order to assess the toxicity potential of mercury during maternal transfer. Finally, we provide the very first results on the simultaneous bioaccumulation of mercury and selenium in key life stages of YP development. Therefore, this thesis is of particular interest when aiming to assess the fate of certain contaminants of interest within aquatic ecosystems.

Keywords: mercury, methylmercury, selenium, glyphosate, Yellow Perch, periphytic biofilms, Lake Saint Pierre, subcellular partitioning, maternal transfer

Table des matières

Introduction.....	1
Le lac Saint-Pierre, Réserve mondiale de la Biosphère	2
La perchaude au LSP: valeur écologique et socio-économique	4
Pérophyton et glyphosate, une relation toxique?	9
Le mercure, un contaminant historique qui demeure préoccupant	12
Le fractionnement subcellulaire, un outil qui permet de lier la bioaccumulation et la toxicité	16
Le sélénium: osciller entre carence et toxicité.....	19
Cadre conceptuel et objectifs généraux de la thèse	26
 CHAPITRE 1: Dis-moi ton âge et je te dirai qui tu es : Le temps de colonisation du pérophyton façonne la structure des communautés soumises à une exposition au glyphosate	31
Abstract.....	33
1. Introduction.....	34
2. Materials and methods	37
2.1 Study area and sampling	37
2.2 Experimental design.....	37
2.3 Periphyton analysis	40
2.3.1 Chlorophyll <i>a</i> (Chla).....	40
2.3.2 DNA extraction and sequence analyses.....	40
2.3.3 Essential aromatic amino acids.....	41
2.4 Water analysis.....	41
2.4.1 Glyphosate	42
2.4.2 Phosphorus.....	42
2.5 Statistical analyses	43
3. Results.....	44
3.1 Glyphosate concentrations.....	44
3.2 Dissolved and reactive phosphorus.....	45
3.3 Chlorophyll <i>a</i>	46

3.4 Community composition.....	47
4. Discussion	50
4.1 Environmentally relevant glyphosate concentrations are lost from water within 7 days under our experimental conditions.....	50
4.2 Glyphosate is a source of phosphorus but not in a bioavailable form	51
4.3 Chlorophyll <i>a</i> and essential aromatic amino acid contents are not adversely impacted by glyphosate in biofilms.....	53
4.4 Microbial communities are more influenced by biofilm age than glyphosate exposure	54
5. Conclusion	56
Acknowledgements.....	57
Supplementary information	58
Supplementary methods.....	58
Supplementary tables	61
Supplementary figures	62

CHAPITRE 2: Évaluation du potentiel de toxicité associé au transfert maternel du mercure et du sélénium chez la perchaude (<i>Perca flavescens</i>) à l'aide d'une approche de fractionnement subcellulaire	70
Abstract.....	72
1. Introduction.....	73
2. Methods.....	76
2.1. Study site.....	76
2.2. Fish sampling	76
2.3. Subcellular partitioning procedure.....	78
2.4. MeHg and THg Analyses.....	82
2.5. Se Analyses.....	82
2.6. Data Analyses	83
3. Results.....	84
3.1. Subcellular partitioning of MeHg in liver and gonads.....	84
3.2. MeHg concentrations in subcellular fractions	86

3.3. Maternal transfer of MeHg	88
3.4. Maternal transfer of Se.....	90
3.5. Se:Hg molar ratios in subcellular fractions.....	92
4. Discussion	94
4.1. Hg accumulates in sensitive fractions.....	94
4.2. MeHg is maternally transferred to gonadal mitochondria	97
4.3. Selenium is maternally transferred to eggs and might confer protection from Hg toxicity at a subcellular level	98
Acknowledgements.....	102
Supplementary Material.....	103
Supplementary table.....	103
Supplementary figures	105
Supplementary methods.....	112

CHAPITRE 3: Distribution du mercure et du sélénium dans différents tissus et stades de vie de la perchaude (<i>Perca flavescens</i>) au lac Saint-Pierre	115
Abstract.....	117
1. Introduction.....	118
2. Material and methods.....	121
2.1 Study site.....	121
2.2 Fish sampling	121
2.3 MeHg, THg and Se analyses.....	122
2.4 Statistical analyses	123
3. Results and discussion	125
3.1 Biodistribution of THg and MeHg in tissues of gravid YP	125
3.2 Bioaccumulation of THg and MeHg at different YP life stages.....	128
3.3 Differences in %MeHg among key tissues and early life stages	131
3.4 Biodistribution of Se in key tissues and early life stages.....	133
3.5 Se:Hg molar ratios in tissues and early life stages.....	136
3.6 Correlation between biometric data and metal concentrations	138
4. Conclusions.....	142

Acknowledgements.....	143
Supplementary Material.....	144
Supplementary tables.....	144
Supplementary figures	147
 Conclusion	152
Biofilms périphytiques et pesticides	152
Fractionnement subcellulaire et transfert maternel.....	155
Bioaccumulation des contaminants organiques et inorganiques	159
Perspectives.....	162
 Bibliographie.....	166
 ANNEXE I. Bande dessinée « La forteresse gluante »	i
ANNEXE II. Analyses préliminaires liées à l'aperçu de la contamination en retardateurs de flamme dans les tissus de perchaude au LSP.....	iv
ANNEXE III. Fractionnement subcellulaire du cuivre, du cadmium, du manganèse et du fer dans les foies de perchaudes au LSP.....	vii
ANNEXE IV. Bioaccumulation du manganèse, du fer, du cuivre, de l'arsenic et du cadmium dans les tissus et les stades de vie précoces de la perchaude au LSP	x

Liste des tableaux

Chapitre 1

Table 1. Name, nominal concentration and description of each treatment. Nominal initial concentrations of glyphosate were accurately measured in a preliminary study conducted in 2015 under the exact same experimental conditions. 39

Table S1. Adjusted p-values associated to Tukey's multiple comparison post hoc test following a two-way ANOVA on $\log+1$ transformed chlorophyll *a* concentrations for the 20-year-old biofilms. Alpha = 0.05. Significant results are indicated in grey cells. 61

Chapitre 2

Table S1. Length and weight of each gravid female that was sampled on the North shore (Maski) and on the south shore (BDF) of Lake Saint-Pierre..... 103

Chapitre 3

Table S1. MeHg (n=3) and Se (n=1) concentrations in water samples from all sampling stations (mapped in Fig. S1)..... 144

Table S2. Adjusted p-values associated to Tukey's multiple comparison post hoc test following a two-way ANOVA on *log* transformed THg and MeHg dry weight tissue concentrations. Alpha = 0.05. Significant results are indicated in grey cells. 145

Table S3. Comparison table for descriptive statistics related to MeHg, THg and Se concentrations in gonads, brain, gut, liver and muscle of gravid Yellow Perch (n=44)..... 146

Liste des figures

Introduction

Figure 1. Le lac Saint-Pierre et son archipel en amont. Adaptée de La Violette (2004).	3
Figure 2. Débarquement commercial de perchaudes entre 1986 et 2011. Un premier moratoire de 5 ans sur toute forme de pêche a été instauré en 2012. Adaptée de Magnan et al. (2017). ...	6
Figure 3. Courbe représentant la réponse des organismes en fonction de la concentration d'un élément trace qui est nécessaire à la survie, mais devient toxique lorsque présent en trop grande concentration. Adaptée de Mason (2013).	22
Figure 4. Ratios molaires Se:Hg mesurés dans le muscle de plusieurs espèces de poissons d'eau douce en Caroline du Sud et au Tennessee. Adaptée de Burger et Gochfeld (2013).	25
Figure 5. Cadre conceptuel de la thèse, illustrant les thèmes associés à chacun des chapitres.	26

Chapitre 1

Figure 1. Proportion of remaining glyphosate in the water for each treatment over time. (a) 2-month-old periphyton, (b) 1-year-old periphyton, and (c) 20-year-old periphyton.....	44
Figure 2. Reactive and total dissolved phosphorus (P) concentrations in the water throughout the experimental period for the glyphosate (G3) and P3 treatments in microcosms containing 20-year-old periphyton. Error bars represent the standard error of the mean (SEM) ($n = 3$). Data are log+1 transformed. T value is the sampling time in number of days.	46
Figure 3. Impact of glyphosate (G1, G2, and G3) and phosphorus (P1, P2, and P3) on chlorophyll <i>a</i> . (a) 2-month-old periphyton, (b) 1-year-old periphyton, and (c) 20-year-old periphyton. Data are log+1 transformed. Error bars represent the standard error of the mean (SEM) ($n = 3$). T value is the sampling time in number of days.....	47
Figure 4. Principal coordinates analysis of unweighted UniFrac distances. Community composition clusters by periphyton age for (a) cyanobacteria (permanova $R^2 = 0.366, p = 0.001$) and (b) eukaryotes (permanova $R^2 = 0.248, p = 0.001$). T0, beginning of the experiment; G, glyphosate treatment; P, phosphorus treatment.	48

Figure 5. Relative abundance of genera (a) *Anabaena* and (b) *Microcystis* for 1-year-old periphyton in control, glyphosate (G3), and phosphorus (P3) treatments throughout the experiment ($n = 1$). T value is the sampling time in number of days..... 49

Figure S1. Picture of 20-year-old periphyton on an artificial substrate. Substrate setups are anchored with a clay brick at 1 m depth. Biofilms grow on Teflon mesh disks. Disks are installed on Plexiglas plates at a 45-degree angle. Arrow is pointing from an empty to a colonized disk. A floating rope is attached at the top to facilitate location and sampling..... 62

Figure S2. Experimental design. Treatments were performed in triplicate, for a total of 21 microcosms per experiment. Three experiments were conducted independently for each colonization rate. At the beginning of each experiment, 4 colonized mesh disks were placed in each Pyrex® round dish filled with filtered lake water. Microcosms were randomly distributed in a growth chamber..... 63

Figure S3. 48-hour monitoring of glyphosate concentrations in a preliminary test during which 2.5 mg/L of glyphosate was added under the same experimental conditions ($n=1$)..... 64

Figure S4. Glyphosate concentrations in the water of microcosms with 20-year-old biofilms exposed for 7 days in a preliminary experiment that took place in 2015 under the same experimental conditions ($n=2$)..... 65

Figure S5. Principal coordinates analysis (PCoA) of weighted UniFrac distances. a. Community composition cluster by periphyton age for Cyanobacteria (Weighted UniFrac, permanova $R^2 = 0.582$, $p = 0.001$). Multivariate dispersion is significant ($p < 0.0001$). b. Community composition cluster by periphyton age for eukaryotes (Weighted UniFrac, permanova $R^2 = 0.255$, $p = 0.001$). Multivariate dispersion is not significant (betadisper, $p > 0.05$). 66

Figure S6. Aminomethylphosphonic acid (AMPA) concentrations in the water of microcosms with 20 years-old biofilms exposed to glyphosate (600 $\mu\text{g}/\text{L}$) for 7 days in a preliminary experiment that took place in 2015 under the same experimental conditions. Error bars represent standard error of the mean (SEM) ($n=3$). There is a significant increase between T0 and T3 (t-test, $p_{adj} < 0.05$)..... 67

Figure S7. Total phosphorus concentrations in glyphosate (G1, G2, G3) and phosphorus (P1, P2, P3) enriched treatments throughout the experimental period. a. 2-month-old periphyton. b. 1-year-old periphyton. c. 20-year-old periphyton. Error bars show standard error of the mean

(SEM) (n=3). While glyphosate concentrations decreased during incubations, we also noted a significant decrease in TP concentrations between T0 and T3 for the P2 treatment (t-test, adjusted $p < 0.005$), which included initial additions of phosphorus in equal amounts to the concentrations found in G2 (Fig. 2a&b). Time ($p < 0.0001$), treatment ($p < 0.0001$) and the interaction of these two factors ($p < 0.0001$) significantly explained differences in the early stages of the incubations, between T0 and T3 (multifactorial 2-way ANOVA) (Fig. 2a&b), with treatment alone explaining 68.54% of total variation. After 3 days (T3), there was a significant difference between control and all three glyphosate treatments (adjusted $p < 0.01$ for G1, $p < 0.05$ for G2 and $p = 0.0001$ for G3) (Dunnett's multiple comparisons post-hoc test). In Fig. 2c, the decrease in total phosphorus between T0 and T3 was significant for the P2 and P3 treatments (t-test $p < 0.05$). This might infer an incorporation of added phosphorus by periphyton. Time ($p < 0.0001$), treatment ($p < 0.0005$) and the interaction of the two factors ($p < 0.0001$) significantly explained differences in TP when comparing T0 to T3 (multifactorial 2-way ANOVA). Treatment explained 46.37% of total variation in TP concentrations. After 3 days (T3), we confirmed that there was a significant (adjusted $p < 0.005$) difference in TP concentrations between control and G3 treatment (Dunnett's multiple comparisons post-hoc test)..... 68

Figure S8. Aromatic amino acids concentrations in 20 years-old biofilms exposed to glyphosate for 7 days in a preliminary experiment that took place in 2015. Error bars represent standard error of the mean (SEM) (n=3). Neither time nor treatment had a significant effect on amino acid concentrations (2-way ANOVA, $p>0.05$). 69

Chapitre 2

Figure 1. Map of Lake Saint-Pierre (Quebec, Canada) showing sampling sites. Gravid females were sampled from Maskinongé (Maski) on the north shore and from Baie-du-Febvre (BDF) on the south shore. 77

Figure 2. Schematic illustration of the subcellular partitioning procedure used to separate Yellow Perch (a) gonads and (b) liver into operationally defined fractions. Small tubes represent the 50- μ L homogenate fractions. Fractions represented by orange circles were tested with marker enzymes. 81

Figure 3. MeHg burden distribution (% \pm SEM) in subcellular fractions of (a) liver (n=21) and (b) gonadal (n=24) cells. Red and pink exploded parts represent sensitive fractions.....	85
Figure 4. MeHg concentrations (ng/g dw) in (a) hepatic (n=21) and (b) gonadal (n=24) subcellular fractions of Yellow Perch. Letters denote significant differences (Tukey's HSD multiple comparisons test, $p < 0.05$). Sensitive fractions are shown in red (mitochondria) and pink (HDP).....	87
Figure 5. Relationship between MeHg concentrations (ng/g dw) in the liver and (a) MeHg in the gonads (n=44) and (b) MeHg in gonadal mitochondria (n=24). Data are log transformed. The R square and the equation of the linear regression are shown on each plot. Dashed curves represent the 95% confidence bands of the best-fit line.	89
Figure 6. Relationship between Se concentrations ($\mu\text{g/g}$ dw) in the liver and (a) Se in the gonads (n=44) and (b) Se in gonadal mitochondria (n=24). The R square and the equation of the linear regression are shown in plot (a) as the regression was significative. Dashed curves represent the 95% confidence bands of the best-fit line.....	91
Figure 7. Se:Hg molar ratios for in (a) hepatic (n=21) and (b) gonadal (n=24) subcellular fractions. The red dashed line represents a threshold of 1, above which Se is suggested to confer protection from Hg toxicity. Letters denote significant differences (Dunn's multiple comparisons test, $p < 0.05$). Sensitive fractions are shown in red (mitochondria) and pink (HDP).	93

Figure S1. Percentage (mean \pm SEM, in %, n=3) of (a) CCO (mitochondrial membrane biomarker), (b), CS (mitochondrial matrix biomarker), and (c) LDH (cytosolic biomarker) enzymatic activities in subcellular fractions of Yellow Perch liver with the most efficient protocol. Exploded parts represent the fraction in which each enzyme is located.	105
Figure S2. Percentage (mean \pm SEM, in %, n=3) of (a) CCO (mitochondrial membrane biomarker), (b), CS (mitochondrial matrix biomarker), and (c) LDH (cytosolic biomarker) enzymatic activities in subcellular fractions of Yellow Perch gonads with the most efficient protocol. Exploded parts represent the fraction in which each enzyme is located.	106
Figure S3. THg concentrations (ng/g dw) in (a) hepatic (n=21) and (b) gonadal (n=24) subcellular fractions of Yellow Perch. Letters denote significant differences (Tukey's HSD	

multiple comparisons test, $p < 0.05$). Sensitive fractions are shown in red (mitochondria) and pink (HDP).....	107
Figure S4. Relationship between MeHg concentrations (ng/g dw) in the muscle and (a) MeHg in the gonads (n=44) and (b) MeHg in gonadal mitochondria (n=24). Data are log transformed. The R square and the equation of the linear regression are shown on each plot. Dashed curves represent the 95% confidence bands of the best-fit line.	108
Figure S5. Se concentrations (ng/g dw) in (a) hepatic (n=21) and (b) gonadal (n=24) subcellular fractions of Yellow Perch. Letters denote significant differences (Tukey's HSD multiple comparisons test, $p < 0.05$). Sensitive fractions are shown in red (mitochondria) and pink (HDP).	109
Figure S6. MeHg over THg ratio (mean %MeHg \pm SEM) in (a) hepatic (n=21) and (b) gonadal (n=24) subcellular fractions of Yellow Perch. Letters denote significant differences (Dunn's multiple comparisons test, $p < 0.05$). Sensitive fractions are shown in red (mitochondria) and pink (HDP).....	110
Figure S7. Se burden distribution (% \pm SEM) in subcellular fractions of (a) liver (n=21) and (b) gonadal (n=24) cells. Red and pink exploded parts represent sensitive fractions.	111

Chapitre 3

Figure 1. (a) THg and (b) MeHg concentrations (mg/kg dw) in different Yellow Perch' organs (n=44). Letters indicate significant differences (Tukey's HSD multiple comparisons test, $p < 0.05$).	126
Figure 2. (a) THg and (b) MeHg concentrations (mg/kg dw) in Yellow Perch egg masses (n=7), newly-hatched larvae (NHL) (n=29), larvae (n=20) and juvenile (n=36). Letters indicate significant differences (Dunn's multiple comparisons test, $p < 0.05$).	129
Figure 3. Fraction of total Hg as MeHg (%MeHg) (mean \pm SEM) in (a) tissues (n=4) and (b) different parts of the life cycle of Yellow Perch (egg masses (n=7), newly-hatched larvae (NHL) (n=29), larvae (n=20) and juvenile (n=36)). Letters indicate significant differences (Dunn's multiple comparisons test, $p < 0.05$).	132
Figure 4. Se concentrations (mg/kg dw) in (a) tissues (n=44) and (b) different parts of the life cycle of Yellow Perch (egg masses (n=7), newly-hatched larvae (NHL) (n=29), larvae (n=20)	

and juvenile (n=36)). Letters indicate significant differences (Tukey's HSD multiple comparisons test, $p < 0.05$ for (a) and Dunn's multiple comparisons test, $p < 0.05$ for (b))..	134
Figure 5. Se:Hg molar ratios in (a) organs (n=44) (b) different parts of the life cycle of Yellow Perch (egg masses (n=7), newly-hatched larvae (NHL) (n=29), larvae (n=20) and juvenile (n=36)). The red dashed line represents a threshold of 1, above which Se is suggested to confer protection from Hg toxicity. Letters indicate significant differences (Dunn's multiple comparisons test, $p < 0.05$).	137
Figure 6. Principal Component Analysis (PCA) correlation biplot showing 43 gravid females (coloured points) and metal concentrations and biometric data (black arrows). Gravid females that were sampled on the north shore of LSP are represented by blue points and those sampled on the south shore by red points. The PCA biplot accounts for 79.6% of the total variation among individuals (Axis 1: 56.4% and Axis 2: 23.2%).	139
Figure S1. Map of LSP (Quebec, Canada) showing sampling sites. Gravid females were sampled from Maskinongé (Maski) on the north shore and from Baie-du-Febvre (BDF) on the south shore. Larvae and juveniles were sampled from all sites.....	147
Figure S2. (a) THg and (b) MeHg concentrations (mg/kg ww) in different Yellow Perch' organs (n=44). Letters denote significant differences (Tukey's HSD multiple comparisons test, $p < 0.05$).	148
Figure S3. (a) THg and (b) MeHg concentrations (mg/kg ww) in Yellow Perch egg masses (n=7), newly-hatched larvae (NHL) (n=29), larvae (n=20) and juvenile (n=36). Letters denote significant differences (Dunn's multiple comparisons test, $p < 0.05$).	149
Figure S4. Relationship between muscle and brain (a) THg and (b) MeHg concentrations (mg/kg ww) (n=44). The R square and the equation of the linear regression are shown on each plot ($p < 0.0001$ for both regressions). Dashed curves represent the 95% confidence bands of the best-fit line.	150
Figure S5. Frequency distribution of the total (a) mass (in g) and (b) length (in mm) of gravid Yellow Perch (n=44). The number of individuals belonging to each range of values is indicated above each histogram.....	151

Liste des abréviations

(Les caractères italiques indiquent les termes en anglais)

ADN : acide désoxyribonucléique

AMPA : *aminomethylphosphonic acid*

ANOVA : *analysis of variance*

ARLA : Agence de réglementation de la lutte antiparasitaire | *Pest Management Regulatory Agency*

BDF : Baie-du-Fèvre

C : carbone | *carbon*

CALA : *Canadian Association for Laboratory Accreditation*

CCO : *cytochrome c oxydase*

CEAEQ : Centre d'expertise en analyse environnementale du Québec

Chla : *chlorophyll a*

CIRC : Centre international de recherche sur le cancer

Cl : chlore | *chloride*

CS: *citrate synthase*

CVAFS : *cold-vapor fluorescence spectrometry*

DMA : *direct mercury analyzer*

DNA : *deoxyribonucleic acid*

ECHA : Agence européenne des produits chimiques | *European Chemicals Agency*

EDTA : *Ethylenediaminetetraacetic acid*

EFSA : *European Food Safety Authority*

EPSPS : *5-enolpyruvylshikimate-3-phosphate synthase*

GRIL: Groupe de recherche interuniversitaire en limnologie et en environnement aquatique

H : hydrogène | *hydrogen*

Hg : mercure | *mercury*

Hg(0) : mercure élémentaire

Hg(II) : mercure inorganique

HDP : *heat-denatured proteins*

HPLC : *high-performance liquid chromatography*
HSD : *honestly significant difference*
HSP : *heat-stable proteins*
IARC : *International Agency for Research on Cancer*
ICP-MS : *inductively coupled plasma mass spectrometry*
K : potassium
LC-MS : *Liquid chromatography–mass spectrometry*
LDH : *lactate dehydrogenase*
LOD : *limit of detection*
LSP : lac Saint-Pierre | *Lake Saint Pierre*
Maski : Maskinongé
MeHg : méthylmercure | *methylmercury*
MT : *metallothionein*
Na : sodium | *sodium*
O : oxygène | *oxygen*
OTU : *operational taxonomic unit*
P : phosphore | *phosphorus*
PCA : *principal component analysis*
PCoA : *principal coordinates analysis*
PICT : *pollution-induced community tolerance*
PMRA : *Pest Management Regulatory Agency*
QIIME : *Quantitative Insights Into Microbial Ecology*
rRNA : *ribosomal ribonucleic acid*
S : soufre | *sulfur*
SD : *standard deviation*
Se : sélénium | *selenium*
SEM : *standard error of the mean*
THg: mercure total | *total mercury*
YP : *Yellow Perch*

À mes parents

Remerciements

Merci à mes directeurs de thèse, Marc Amyot et Dolors Planas, de m'avoir fait confiance. Marc, merci de m'avoir accueillie dans ton laboratoire, dont les membres sont rapidement devenus ma 2^e famille. Merci pour ton support inconditionnel, pour ta disponibilité, pour ton savoir incommensurable et pour ta patience. Dolors, merci pour votre authenticité, pour votre franchise, pour les lunchs agréables au centre-ville, pour votre vécu professionnel, mais aussi personnel et pour vos connaissances précieuses sur le périphyton. Marc, Dolors, je n'aurais pas pu choisir de meilleurs modèles de rigueur et de force de caractère. Vous avez grandement contribué à façonner mon esprit scientifique, mais surtout mon esprit critique. Grâce à vous, j'entame va vie professionnelle avec un bagage précieux de savoir, de compétences et de confiance. Je vous serai éternellement reconnaissante d'avoir cru en moi et de m'avoir guidée et épaulée tout au long de mes études doctorales.

Bien que la réalisation d'un doctorat soit extrêmement enrichissante et valorisante, il va sans dire que le chemin qui mène à la ligne d'arrivée peut parfois être sinueux, voire cahoteux. Ainsi, c'est en très grande partie grâce à ma 2^e famille, le labo Amyot, que je suis présentement en train d'écrire ces lignes. Si je ressors grandi de cette expérience, c'est grâce à chacun d'entre vous. Jérémy, merci de m'avoir choisie. L'été 2016 reste l'un des plus marquants, sur tous les plans. Tu es rapidement devenu l'une des personnes les plus importantes pour moi. Merci pour ta générosité, pour ta sensibilité, pour notre complicité. Catherine, merci d'être un humain d'exception, un mentor pour tous. Merci de toujours trouver le bon mot pour me rassurer ou pour me faire rire. Merci pour ta culture pop et cosmique, merci pour les brunchs, pour le matantage, pour les manucures, pour le magasinage, pour Austin, pour les fins de semaines à Québec, pour les tacos déjeuner. Merci surtout pour ton écoute, ton empathie et pour RuPaul. Je te serai reconnaissante pour les siècles à venir. Gwyneth, merci de m'avoir accueillie si chaleureusement parmi vous. Merci pour les BBQ sur de Lorimier, pour les baleines, pour le PhD cactus, pour les soirées documentaires, pour Herman, pour Botswana (le jeu), pour Dave ☺, pour le féminisme. Merci surtout d'avoir toujours cru en moi. Maxime, merci d'avoir contribué à mon niveau (modéré) de swag. Merci pour les Dead Obies, Alaclair, Gruau, Day 'n' nite (la

bonne version), pour le Punch Club, merci pour les soirées du rock, pour ton chalet, pour les conserves de carottes et de ketchup, pour les échantillonnages de périphyton et de perchaudes, pour nos road trips, pour mes surnoms qui commencent par Crazy (sauf un) et pour les memes avec ma p'tite face d'enfant prodige. Antoine, merci d'être entré dans ma vie. Merci de m'avoir tout appris, de m'avoir redonné confiance en moi. Merci d'avoir fait un million d'aller-retours entre Québec et Montréal, merci pour les crazy mercredis, pour le chapeau de la serveuse, pour ton amitié. Kawina, merci d'être une fée, merci pour les champignons, pour nos moments de gourmandise, pour les souvenirs à Saint-Thuribe et ses environs, pour le miel, pour ta sagesse. Perrine, merci d'être toi, merci pour ta candeur, ta générosité, tes tartiflettes, tes tiramisus et ta douceur. Dominic Bélanger, merci pour ton aide indispensable, pour ton intelligence pratique et chimique, pour tes encouragements et ton écoute, et pour tes astuces au bowling. Tania, merci pour ton authenticité et pour tes chiens. Gwenola, merci pour ton aide précieuse et ton swag légendaire. Audrey, merci pour Montréal, pour Paris, pour Toronto, pour nos délires. Marie-Christine, merci pour ta fougue, ta lumière, tes talents artistiques, merci de me faire rire. Emmanuelle, amyotique d'adoption, merci pour notre équipe de feu aux commandes de l'AECBUM.

Merci à mon système de soutien, ma famille, que j'aime profondément. Au cours de ces 5 dernières années, vous m'avez vue grandir, mûrir. Vous m'avez aimée et soutenue inconditionnellement. Cette thèse, c'est grâce à vous. Marielle, tu es mon humain préféré. Merci de m'aimer comme je suis et à la folie, merci de me comprendre en profondeur, merci d'être toujours là, merci d'être inspirante, merci pour ta générosité extrême, pour tout. Papa, maman, merci d'avoir toujours été mes plus grands fans, merci de m'avoir toujours poussée vers le haut, merci pour tous les sacrifices, merci d'avoir fait en sorte que je ne manque jamais d'amour. Eric, j'ai fini ma thèse! Merci pour le télétravail, merci pour les 2 mois à Paris qui gardent une place toute spéciale dans ma tête et dans mon cœur, merci pour le plancton et le necton, merci de me faire rire comme personne, merci d'être la seule personne qui a une mémoire assez bonne pour se rappeler de choses que j'ai dites en 1994. Toi pis moi, c'est de la dynamite. Julien, merci pour les poutines, les cinémas, les livres, merci pour ta sensibilité. Mona, merci pour les sushis, pour les vacances en Floride, pour tes rêves, pour ta personnalité pétillante et rafraîchissante. Aïda, Mounir, merci d'être si fiers de moi, ça me touche énormément. Merci aux Khouzous (Jacques,

Linda, Joseph, Chantal, Jonathan) pour notre humour douteux, pour nos repas dans les escaliers et pour nos soirées Rock Band. Merci Eveline pour ta perspicacité et ton soutien.

En rafale, merci Leylha d'avoir chassé des libellules au camp Minogami il y a 16 ans et de m'avoir gardée à tes côtés depuis, merci Alice (bff) pour nos délires à imaginer la vie de perfect housewife de Marmar, merci Danny pour nos conversations intelligentes et intéressantes, merci Tatum pour ta sensibilité, merci Élisabeth pour nos soupers et ton mariage parfait, merci Joëlle pour ton écoute, ton empathie, pour ton rire contagieux et tes histoires rocambolesques, merci Georges pour ton affection et tes expressions, merci Lucie (la Bayonne) pour ta franchise et ton franc-parler tantôt inapproprié tantôt hilarant et merci Stéphanie pour mon escapade en Bretagne, pour ton grand cœur et pour nos journées d'échantillonnage sur le lac Croche (même en hiver). Cassandre, aucun mot n'est assez fort pour t'exprimer ma gratitude. Merci de m'écouter et de me rassurer, merci de me relever, de croire en moi, merci de me faire rire. Merci pour toutes tes petites et grandes surprises, pour ta générosité, merci d'affronter la vie avec moi.

Cette thèse, c'est un peu chacun d'entre vous.

“But I don't want to go among mad people,” Alice remarked.

“Oh, you can't help that,” said the Cat: “we're all mad here. I'm mad. You're mad.”

“How do you know I'm mad?” said Alice.

“You must be,” said the Cat, “or you wouldn't have come here.”

Lewis Carroll, Alice's Adventures in Wonderland

*“The ultimate answer is to use less toxic chemicals so that the public hazard from their misuse
is greatly reduced.”*

Rachel Carson, Silent Spring (1962)

Introduction

Historiquement, la perchaude (*Perca flavescens*) faisait partie intégrante de l'industrie de la pêche et de l'identité culturelle des communautés riveraines du lac Saint-Pierre, élargissement du fleuve Saint-Laurent et réserve de la biosphère de l'UNESCO. Cependant, cette espèce a connu un fort déclin depuis les années 90 et, subséquemment, un moratoire complet sur ses pêcheries a été mis en place. Ce moratoire n'a pas entraîné de retour de stocks de perchaudes. De nombreux facteurs peuvent expliquer cette incapacité de rétablissement des populations, notamment la perte d'habitat, la modification des ressources alimentaires, l'introduction d'espèces invasives et envahissantes et la dégradation de la qualité de l'eau *via* l'augmentation des apports d'éléments nutritifs, des pesticides et des nouveaux contaminants. Ainsi, les travaux conduits dans le cadre de la présente thèse avaient comme objectif principal d'évaluer l'impact potentiel de différents contaminants sur la reproduction de la perchaude. Plus précisément, le présent projet de doctorat comporte 3 axes principaux qui permettront ultimement de fournir des pistes afin de cibler les menaces chimiques qui pèsent sur la santé des perchaudes du lac Saint-Pierre, soit (1) les effets du glyphosate sur les biofilms périphytiques, (2) le potentiel de toxicité associé au transfert maternel du mercure et du sélénium chez la perchaude à l'aide d'outils de fractionnement subcellulaire et (3) la bioaccumulation du mercure et du sélénium dans les différents tissus et stades de vie précoce de la perchaude. La présente introduction se voit être une entrée en matière pour les grands concepts qui seront explorés dans chacun des chapitres. Conséquemment, à travers les prochaines pages, un portrait général de plusieurs notions clés sera dressé, du lac Saint-Pierre au fractionnement subcellulaire, en passant par la perchaude, le mercure, le sélénium et le glyphosate.

Le lac Saint-Pierre, Réserve mondiale de la Biosphère

*“You can't get drown on Lac St. Pierre
So long you stay on shore.”*

The Wreck Of The Julie Plante: A Legend Of Lac St. Pierre,
poème en dialecte de William Henry Drummond (1897)

Le tronçon fluvial du fleuve Saint-Laurent, qui s'étend sur 243 kilomètres entre Cornwall en Ontario (Canada) et l'extrémité est du lac Saint-Pierre, comporte trois lacs fluviaux, soit, d'ouest en est, les lacs Saint-François, Saint-Louis et Saint-Pierre (La Violette, 2004). Un lac fluvial peut être défini comme une étendue d'eau comprise dans un fleuve, dont la superficie est suffisamment importante pour qu'elle soit considérée comme un lac, mais dont le débit correspond à celui d'un fleuve (Mosley, 2004). Le lac Saint-Pierre (LSP), le plus grand des trois lacs fluviaux, s'étend entre les rivières Yamaska et Maskinongé jusqu'à la rivière Nicolet sur une longueur de 25.6 kilomètres et mesure 12.8 kilomètres de largeur (La Violette, 2004) (Figure 1). La superficie du LSP atteint 318 km² (Bertolo et al., 2012), en excluant l'archipel qui se situe dans son secteur en amont. Cet archipel constitue d'ailleurs le plus important du fleuve Saint-Laurent, avec un total de plus de 100 îles. En raison de sa diversité biologique impressionnante, du fait qu'il représente un refuge d'oiseaux migrateurs et qu'il inclut des aires protégées au sein de son territoire, le LSP a été désigné comme Réserve mondiale de la Biosphère par l'UNESCO en 2000. Ce titre suggère, entre autres, l'idée de vivre en harmonie avec la nature. LSP reçut également, en 1998, la désignation de site Ramsar en vertu de la Convention relative aux zones humides d'importance internationale. Cette convention a pour mission la *conservation et l'utilisation rationnelle des zones humides par des actions locales, régionales et nationales et par la coopération internationale, en tant que contribution à la réalisation du développement durable dans le monde entier* (Ramsar, 2014). Ainsi, cette nomination souligne l'importance de viser la conservation des herbiers aquatiques du LSP, soit la végétation aquatique submergée de la plaine d'inondation et du Lac en soi, qui servent d'aire de reproduction, de protection et d'alimentation pour plusieurs espèces de poissons (Bertolo et al., 2012).

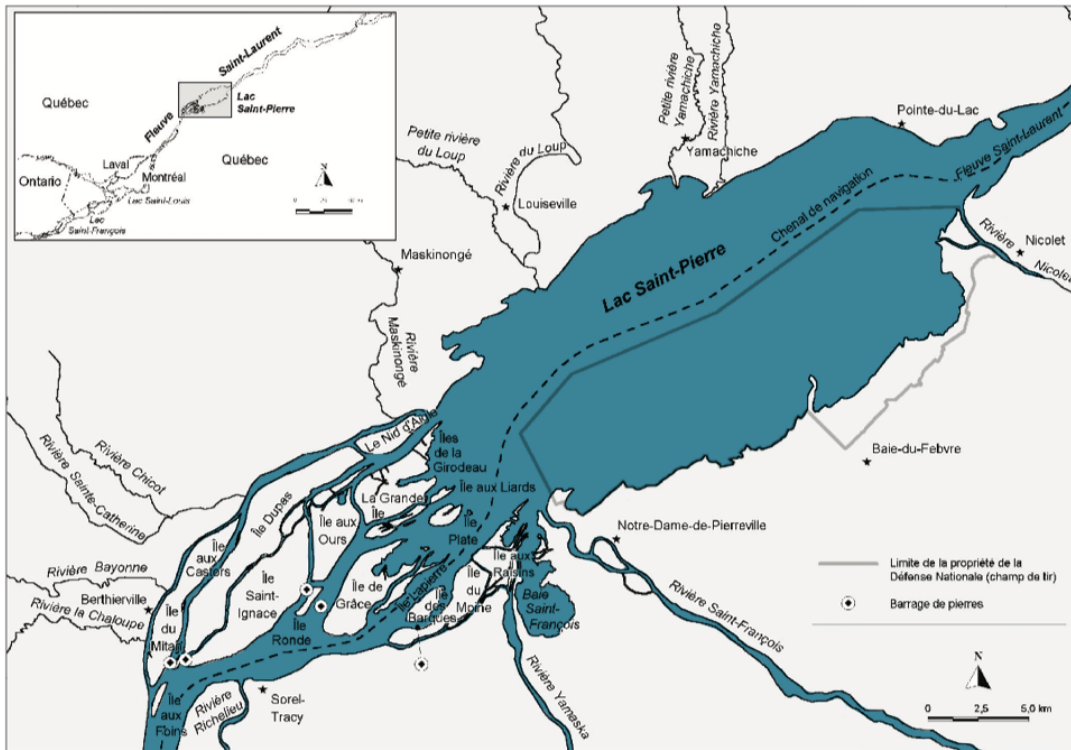


Figure 1. Le lac Saint-Pierre et son archipel en amont. Adaptée de La Violette (2004).

À l'entrée du LSP, on observe un débit moyen de 9 725 m³/s, alors que ce débit atteint 10 500 m³/s à sa sortie (La Violette, 2004). Cet accroissement de près de 8% serait dû à l'apport d'eau de plusieurs affluents. D'ouest en est, les affluents situés sur la rive sud du lac Saint-Pierre sont les rivières Richelieu, Yamaska, Saint-François et Nicolet. La masse d'eau du sud tire essentiellement son origine de l'eau de ces rivières (Bertrand et al., 2011). Ces affluents drainant des territoires agricoles, la masse d'eau associée à la rive sud est riche en nutriments, en chlorophylle *a* et en carbone organique dissous (Bertrand et al., 2011). Sur la rive nord, les affluents sont les rivières Chaloupe, Bayonne, Chicot, Maskinongé, du Loup, Petite Yamachiche et Yamachiche. Cependant, la majorité de l'eau s'écoulant le long de la rive nord origine de la rivière des Outaouais, riche en nutriments, en carbone organique dissous et en matière organique particulaire en suspension (Bertrand et al., 2011). Enfin, le chenal de navigation central du LSP tire son origine du lac Ontario et est caractérisé par des eaux dures et transparentes, ainsi que par de faibles concentrations de carbone organique dissous et de matière organique particulaire en suspension (Bertrand et al., 2011).

Avec une profondeur moyenne de 2.7 mètres, le LSP est le moins profond des trois lacs fluviaux (La Violette, 2004). Or, la profondeur de son chenal de navigation, qui sépare la masse d'eau de la rive nord de celle de la rive sud (Bertolo et al., 2012), peut atteindre 13.7 mètres (La Violette, 2004). La vitesse du courant dans ce chenal de navigation oscille entre 0.6 et 1 m/s alors qu'elle frôle à peine les 0.3 m/s dans chacune des deux masses d'eau (La Violette, 2004). Il est important de noter que les masses d'eau des rives nord et sud sont séparées de manière horizontale, en raison du chenal de navigation, par des propriétés physiques telles que la densité et le mode d'écoulement, limitant les échanges entre les deux masses (Glémet & Rodríguez, 2007). Lors de la crue printanière, 140 km² d'aire totale peut être inondée pour une période variant de 5 et 9 semaines (Bertolo et al., 2012; La Violette, 2004). La vaste étendue de sa plaine inondable représente une des principales caractéristiques du LSP et constitue également un site important pour la fraie de plusieurs poissons, dont la perchaude (*Perca flavescens*) (Bertolo et al., 2012).

La perchaude au LSP: valeur écologique et socio-économique

*“He could see the fishes swimming
Far down in the depths below him ;
See the yellow perch, the Sahwa,
Like a sunbeam in the water,”*

Hiawatha’s fishing,
poème de Henry Wadsworth Longfellow (1882)

La perchaude est exploitée commercialement au lac Saint-Pierre depuis le 19^e siècle (de la Chenelière et al., 2014). Cependant, cette exploitation était minime et ce n'est qu'à partir du début des années 1970 que la pêche commerciale et sportive à la perchaude ait connu un essor considérable (de la Chenelière et al., 2014). Ainsi, en 1986, la pêche sportive représentait déjà 25% des débarquements totaux de perchaudes, qui s'élevaient alors à 280 tonnes (Figure 2). Ces activités de pêche visant principalement les perchaudes mesurant plus de 16 centimètres, cette classe de taille démontrait des taux de mortalité annuels élevés, atteignant plus de 80% (Magnan et al., 2017). En raison de cet effort de pêche démesuré, combiné à un faible succès de

reproduction s'échelonnant sur plusieurs années successives, une rupture des stocks de perchaudes fut observée entre 1995 et 1998. Ainsi, bien que la pression de pêche demeurait inchangée, les débarquements commerciaux mesurés en 1995-1996 s'élevaient à 140 tonnes, puis à seulement 70 tonnes en 1997-1998 (de la Chenelière et al., 2014). Au cours des 15 années suivantes, certains moyens ont été employés de manière à limiter l'effort de pêche et ainsi tenter de rétablir le déclin des populations. Ces moyens incluent notamment l'imposition d'une réduction de la limite de prise, l'implantation d'une restriction de taille, une réduction de la durée de la saison de pêche, ainsi que la mise en place de quotas sur les débarquements liés à la pêche sportive et commerciale (de la Chenelière et al., 2014). Subséquemment, les autorités ont interdit de manière stricte la pêche à la perchaude au cours de sa saison de reproduction en 2008 (de la Chenelière et al., 2014). Enfin, le gouvernement du Québec a imposé, en 2012, un moratoire de 5 ans sur toute forme de pêche à la perchaude (de la Chenelière et al., 2014; Houde et al., 2014b). Cette mesure ultime a été instaurée dans l'optique de protéger les adultes reproducteurs. Or, une réévaluation de la santé des populations de perchaudes en 2016 démontre que le recrutement de jeunes perchaudes demeure déficient et que la population est vieillissante (Magnan et al., 2017). Le moratoire a donc été reconduit jusqu'en 2022. Le recrutement peut être défini comme l'abondance des individus d'âges 1+ et 2+, c'est-à-dire des individus qui amorcent leur 1^{re} et leur 2^e année de vie (Magnan et al., 2017). Afin de maintenir la viabilité d'une population de poissons soumise à une exploitation par la pêche, la production de jeunes individus est censée contrebalancer la mortalité des adultes. Or, au LSP, le recrutement des jeunes perchaudes est faible depuis 2002, limitant le rétablissement des populations, au sein desquelles prévaut une rupture des stocks depuis le milieu des années 1990. Il a été évoqué que le faible recrutement des jeunes perchaudes pourrait être dû à un retard de croissance au cours de leur première année de vie (0+), attribuable quant à lui à la diminution des ressources énergétiques nécessaires à la survie hivernale (Magnan et al., 2017).

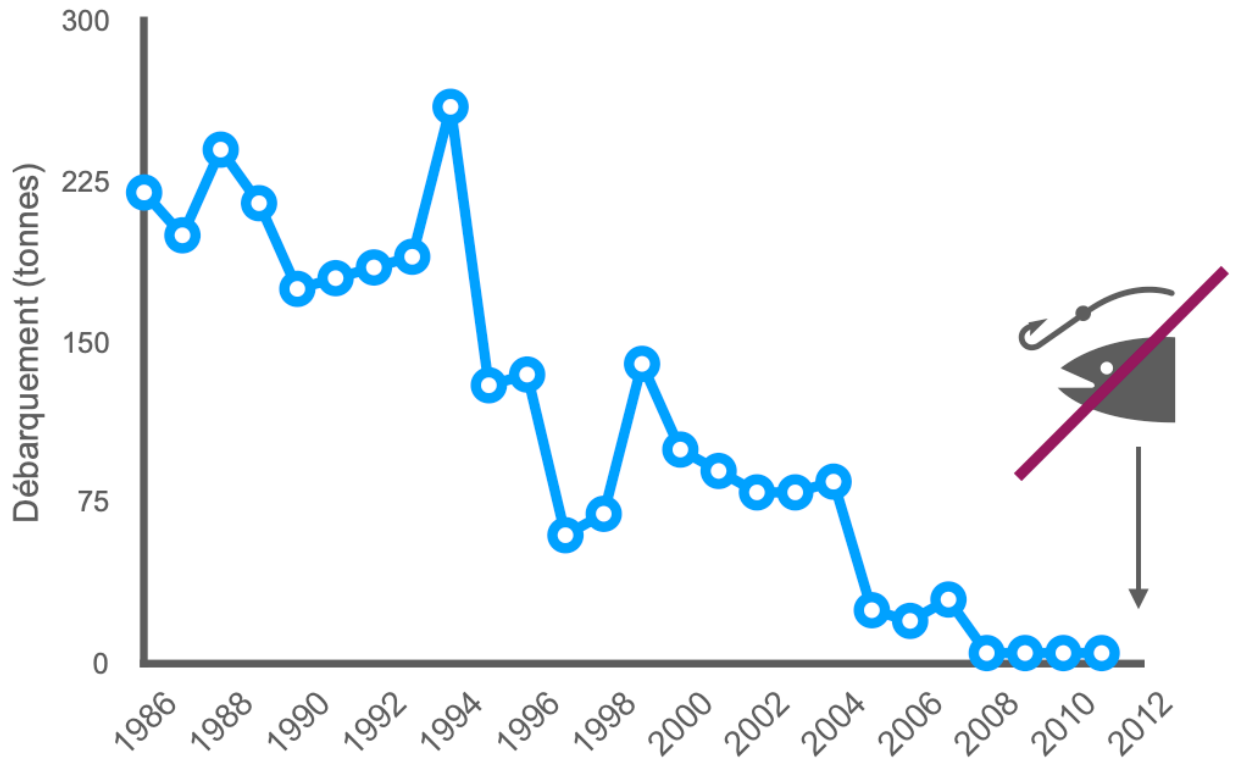


Figure 2. Débarquement commercial de perchaudes entre 1986 et 2011. Un premier moratoire de 5 ans sur toute forme de pêche a été instauré en 2012. Adaptée de Magnan et al. (2017).

Au LSP, la maturité sexuelle des femelles est atteinte à l'âge de 3 ans et ces dernières peuvent subséquemment se reproduire plusieurs fois au cours de leur vie (de la Chenelière et al., 2014). La saison de fraie a lieu au moment de la crue printanière, soit au mois d'avril (de la Chenelière et al., 2014; Paradis et al., 2014). Les perchaudes femelles présentent une préférence, au moment de la fraie, pour les habitats peu profonds se situant entre 0.3 et 1.0 mètre de profondeur et qui se réchauffent conséquemment de manière rapide (de la Chenelière et al., 2014). Les habitats sélectionnés par la perchaude sont également isolés des vents dominants et par le fait même libres de vagues (Bertolo et al., 2012). La perchaude préconise des habitats constitués soit de tapis de végétaux morts, soit d'un assemblage de végétaux morts et de tiges de macrophytes submergées (Bertolo et al., 2012). Plus précisément, ce poisson, opportuniste

au moment de la fraie, peut déposer ses œufs autant sur du gravier que sur des macrophytes ou des branches d'arbres (de la Chenelière et al., 2014). Les régions caractérisées par une végétation émergente très dense, cette dernière freinant le réchauffement de l'eau au printemps, ainsi que les zones exemptes de végétation, sont systématiquement évitées par la perchaude (Bertolo et al., 2012). Lors de la fraie, la femelle génère une masse d'œufs gélatineuse tubulaire et torsadée qui contient entre 8 000 et 45 000 œufs et qui peut atteindre 2 mètres de longueur (de la Chenelière et al., 2014). La femelle enroule cette masse autour des macrophytes submergés ou la dépose directement sur les végétaux morts présents au sol. La fécondation des œufs a lieu immédiatement au moment de la ponte (de la Chenelière et al., 2014). À la suite de l'éclosion, qui se produit entre 10 et 20 jours après la fraie, les larves débutent leur croissance dans les régions peu profondes (de la Chenelière et al., 2014). Ces habitats, caractérisés par la présence de macrophytes, permettent aux perchaudes de trouver les ressources alimentaires dont elles ont besoin en plus d'offrir une certaine protection contre les prédateurs. Au cours de leur première saison de croissance, l'alimentation des jeunes perchaudes évolue graduellement du zooplancton au mois de juin aux invertébrés benthiques associés aux macrophytes submergés à la fin de l'été (de la Chenelière et al., 2014).

Au LSP, la perchaude présente un stade larvaire pélagique et conséquemment un grand potentiel de dérive sur de longues distances (Dettmers et al., 2005; Miehls & Dettmers, 2011). Seulement quelques jours après l'éclosion en zone littorale, les larves entament une migration en milieu pélagique. Ce stade pélagique peut durer jusqu'à 40 jours (Urho, 1996; Whiteside et al., 1985). Cette longue phase pélagique pourrait potentiellement suggérer que les variables spatio-temporelles sont cruciales pour la modélisation de l'établissement des larves. Or, il semble qu'il existe une association positive entre la présence des larves et certaines variables environnementales telles que la présence de végétation aquatique, et ce, indépendamment de la structure spatiale (Bertolo et al., 2012). La distribution larvaire est donc déterminée par un processus de sélection actif de l'habitat. La dérive des larves semble ainsi ne contribuer que faiblement au patron de distribution de ces dernières. L'association positive entre les larves et la présence de végétation pourrait notamment être expliquée par l'absence de migration horizontale vers le large, par l'hypothèse d'un effet de piège dans les lits de macrophytes ou encore par la diminution de la mortalité des larves par prédation lorsqu'elles sont dissimulées dans la végétation (Bertolo et al., 2012).

Une analyse de la structure génétique des populations de perchaudes dans le fleuve Saint-Laurent démontre qu'une faible variabilité entre les individus permet tout de même de distinguer 4 populations géographiquement distinctes (Leclerc et al., 2008). Ces populations sont associées au lac Saint-François, au nord du lac Saint-Louis et au lac des Deux-Montagnes, au sud du lac Saint-Louis et au LSP jusqu'à la ville de Québec. Il semble que la présence de barrières physiques, telles que des barrages et des cascades, limite principalement le flux génétique entre les populations (Leclerc et al., 2008). L'éloignement géographique entre les populations ne semble en effet contribuer que de façon mineure à cette restriction du flux génétique. Par ailleurs, des différences au niveau des ratios d'isotopes stables et des infections parasitaires ont démontré qu'au sein du lac Saint-Pierre, l'aire d'alimentation des perchaudes ne dépasse pas 2 kilomètres (Bertrand et al., 2011). Ainsi, ces observations suggèrent que les déplacements entre les 2 masses d'eau semblent peu fréquents pour cette espèce. Il est intéressant de noter que de ces 4 populations de perchaudes, seule celle du LSP présente une situation précaire. En effet, les populations des lacs Saint-Louis et Saint-François sont considérées comme étant en santé et présentent même une forte croissance (de la Chenelière et al., 2014). Il semble donc que certaines contraintes supplémentaires pèsent sur la population du LSP. En plus d'un effort de pêche excessif ayant mené à l'effondrement des populations, la perchaude du LSP semble également affectée par la dégradation des habitats qu'elle préconise pour la croissance et la reproduction, soit les herbiers aquatiques, premiers récepteurs des eaux de ruissellement. Certaines espèces qui partagent ces habitats avec la perchaude présentent similairement certains signes de précarité dans le LSP. Ainsi, le grand brochet (*Esox lucius*), le crapet de roche (*Ambloplites rupestris*), le crapet-soleil (*Lepomis gibbosus*) et le méné à tache noire (*Notropis hudsonius*) semblent également en déclin (de la Chenelière et al., 2014).

Il importe de mentionner que l'affaiblissement des populations de perchaude au LSP peut être attribuable à plusieurs contraintes. En effet, en plus d'avoir été la cible de surpêche pendant plusieurs décennies, cette espèce fait désormais face à un problème de prédatation par le cormoran à aigrettes, ainsi qu'à une compétition pour les sites de reproduction et d'alimentation avec le gobie à taches noires, introduit dans le fleuve Saint-Laurent en 1997. Le cormoran, également une espèce envahissante, s'est quant à lui implanté au LSP au début des années 2000. L'effondrement des stocks de perchaudes ayant débuté au milieu des années 1990, ces pressions se sont donc ajoutées sur des populations déjà fragiles. On assiste également à une

transformation de la végétation aquatique et des habitats préconisés par la perchaude, au profit des cyanobactéries fixatrices d'azote. Cette perte des habitats de reproduction et d'alevinage peut être attribuable à la hausse de la superficie des champs agricoles, causant une détérioration de la plaine inondable (de la Chenelière et al., 2014).

En plus de l'importance régionale liée à la pêche commerciale et sportive à la perchaude, l'agriculture joue un rôle majeur sur le plan économique et représente la principale cause de la pollution retrouvée dans le LSP (La Violette, 2004). En effet, la majorité de l'apport de polluants dans le LSP proviendrait des affluents situés sur la rive sud, soit les rivières Saint-François, Richelieu et Yamaska, qui semblent fortement contaminées par les activités agricoles, urbaines et industrielles qui se déroulent dans leurs bassins versants (La Violette, 2004). Par exemple, 43% de la superficie totale du bassin de drainage de la rivière Yamaska est consacré à des activités agricoles (Bérubé et al., 2005). Une quantité importante d'herbicides, d'insecticides et de fongicides est donc déversée dans le LSP (Giroux, 2018). Parmi ces pesticides, le glyphosate, herbicide le plus utilisé à l'échelle mondiale, est fréquemment détecté dans l'eau du LSP (Giroux, 2015; Giroux, 2018). Par ailleurs, le glyphosate soulève actuellement une préoccupation internationale en raison de ses effets sur la santé humaine et il importe de contribuer à l'avancement des connaissances sur ses effets.

Périmyton et glyphosate, une relation toxique?

“ Filled with enthusiasm from a successfully running SIL Workshop on Hypertrophic Ecosystems, Dr. Jan Barica said to me in a jubilant voice ‘The next Växjö workshop ought to be on periphyton’. This was on the 11th of September, 1979, just outside the main entrance of Växjö College. ”

Sven Björk (1983)
Opening speech, Periphyton of Freshwater Ecosystems

Au sein de l'Union Européenne, depuis maintenant une dizaine d'années, l'homologation de nouvelles substances, dont les pesticides, est régie par le principe de précaution (Coelho, 2009). Ce type de législation est basé sur le précepte qu'une substance doit être considérée comme potentiellement nocive pour la santé humaine et pour l'environnement, jusqu'à preuve du contraire. Les pesticides sont donc interdits d'utilisation jusqu'à l'obtention

de preuves scientifiques valables justifiant leur caractère inoffensif. Or, au Canada, jusqu'en 2016, l'Agence de réglementation de la lutte antiparasitaire (ARLA) accordait des homologations conditionnelles à l'utilisation des nouveaux pesticides, lorsque les risques associés à leur usage selon les directives inscrites sur l'étiquette avaient été jugés acceptables à la suite d'une évaluation scientifique. Il importe en effet de mentionner que les étiquettes des produits pesticides sont des documents qui ont une valeur légale, contrôlés par la Loi sur les produits antiparasitaires (L.C. 2002, ch. 28). Ainsi, l'utilisation de ces substances était permise jusqu'à l'obtention de renseignements probants confirmant leur toxicité. Bien que le gouvernement canadien ait, depuis, mis fin à l'homologation conditionnelle des pesticides, le principe de précaution n'est toujours pas appliqué, soulevant des incertitudes quant à l'utilisation de certaines substances.

Le glyphosate, ingrédient actif de la formulation Roundup®, commercialisée par Monsanto, est actuellement l'herbicide le plus utilisé à l'échelle mondiale. Cet herbicide à large spectre, non-sélectif et systémique, a été classé comme étant *probablement cancérogène* en mars 2015 par le Centre international de recherche sur le cancer (CIRC), division de l'Organisation mondiale de la santé (IARC, 2015). Ce constat controversé a amené l'Autorité européenne de sécurité des aliments à publier, en novembre 2015, une revue de littérature révisée par les pairs portant sur l'évaluation des risques associés à l'utilisation du glyphosate (EFSA, 2015). La conclusion de cette étude était qu'il est improbable que le glyphosate pose un risque cancérogène pour les humains et que les éléments de preuve n'appuient pas la classification octroyée par le CIRC. L'Agence européenne des produits chimiques (ECHA) a également conclu au mois de mars 2017 que les preuves scientifiques disponibles ne répondraient pas aux critères permettant de classer le glyphosate comme cancérogène, mutagène ou toxique pour la reproduction (ECHA, 2017). Cependant, le Comité d'évaluation du risque de l'ECHA a accepté, en mars 2017, de maintenir la classification du glyphosate comme une substance causant de sérieux dommages oculaires et comme étant toxique pour la faune aquatique, causant des dommages à long terme. En avril 2017, Santé Canada a déterminé que lorsqu'employés selon les instructions du manufacturier, les produits contenant du glyphosate ne présentent aucun danger pour la santé humaine ou pour l'environnement (PMRA, 2017). Depuis, le glyphosate demeure au cœur de la controverse publique et, à la suite d'une révision de centaines d'études ayant justifié

l'approbation du glyphosate, Santé Canada maintient son approbation, du moins jusqu'à la prochaine réévaluation par l'ARLA, qui devrait avoir lieu en 2030.

Dans les champs agricoles, le glyphosate est pulvérisé directement sur le feuillage des plants, le rendant susceptible au lessivage vers les cours d'eau lors d'épisodes de précipitations. Les plantes aquatiques, et par le fait même les biofilms qui y sont associés, sont fréquemment les premiers récepteurs de ces eaux de ruissellement. Les biofilms des périphytiques, ou périphyton, sont des consortiums complexes constitués d'algues, de bactéries, de champignons et de protozoaires intégrés dans une matrice de polysaccharides qui colonisent des substrats submergés (Wetzel, 1983). Ces substrats peuvent être de nature inorganique, organique, vivante ou morte. Dans les lacs, on les retrouve à la base des réseaux trophiques. D'un point de vue physiologique, les biofilms périphytiques sont extrêmement diversifiés. Ils comprennent en effet des organismes phototrophes (cyanobactéries, diatomées, algues vertes), hétérotrophes (bactéries, champignons, amibes) et même chémoautotrophes, dont des bactéries sulfatoréductrices et méthanogènes qui procèdent à la dégradation de composés organiques. Plusieurs flux et processus biogéochimiques ont lieu au sein même des communautés périphytiques. Lors des premiers stades de formation, les biofilms sont considérés comme des systèmes ouverts présentant peu de recyclage interne de nutriments et de carbone. Les coloniseurs initiaux, autotrophes et hétérotrophes, demeurent dépendants de la disponibilité de nutriments présents dans la colonne d'eau. Dans les stades de colonisation plus avancés, des microniches sont créées et les échanges avec la colonne d'eau diminuent. Ainsi, aux stades plus avancés, les communautés sont davantage protégées des stresseurs externes et les différents niveaux trophiques interagissent, les communautés hétérotrophes devenant davantage dépendantes de la production autotrophe (Hagerhey et al., 2011). La matrice des biofilms est constituée d'eau, en grande majorité, et de substances polymériques extracellulaires (EPS). Ces EPS comprennent des hétéropolymères (glucose, galactose, arabinose, xylose), des lipides, des protéines, ainsi que de l'ADN et servent notamment de substrat de carbone pour le métabolisme bactérien (McDougald et al., 2012). La matrice procure également aux biofilms une protection contre la lumière, la dessiccation et les toxiques. En plus de représenter des producteurs primaux primordiaux dans les écosystèmes aquatiques, les biofilms sont également une source d'alimentation importante pour certains macroinvertébrés benthiques.

Le concept de *pollution-induced community tolerance* (PICT) se base sur le principe qu'un contaminant est susceptible d'exercer une pression de sélection au sein d'une communauté naturelle contaminée (Blanck, 2002). Il importe en effet de noter qu'une communauté naturelle regroupe différentes composantes présentant une sensibilité différente à un polluant donné. Par exemple, les biofilms périphytiques comportent certaines souches de cyanobactéries (*Anabaena*, *Nostoc*) qui possèdent une forme insensible de l'enzyme 5-enolpyruvylshikimate-3-phosphate synthase (EPSPS), cible directe du mode d'action du glyphosate (Forlani et al., 2008). Cette enzyme est impliquée dans la voie métabolique de biosynthèse des acides aminés aromatiques essentiels phénylalanine, tyrosine et tryptophane (Siehl, 1997). D'autres taxons de cyanobactéries (*Microcystis*, *Spirulina*), faisant également partie intégrante des biofilms périphytiques, ont la capacité de dégrader la molécule de glyphosate et de l'utiliser comme source de phosphore (Forlani et al., 2008; Lipok et al., 2007). Il importe en effet de noter que le phosphore représente 18.2% de la masse molaire totale du glyphosate. Le glyphosate aurait donc le potentiel de déstructurer les communautés périphytiques, en favorisant la croissance de certaines cyanobactéries au détriment d'algues photosynthétiques, qui sont quant à elles sensibles à l'herbicide (Pérez et al., 2007; Vera et al., 2010). Par ailleurs, *Microcystis* et *Anabaena* étant fréquemment détectées dans la composition de blooms toxiques, l'utilisation du glyphosate est d'autant plus préoccupante (Bláha et al., 2009; Chalifour et al., 2016; Yoshida et al., 2008).

Le mercure, un contaminant historique qui demeure préoccupant

“ *Mercurial poisoning became so common among the hatters in Victorian Britain that it is widely supposed that Lewis Carroll had the condition in mind when he invented the character of the Mad Hatter in Alice's Adventures in Wonderland.* ”

But did he ?
I think that the evidence is to the contrary. ”

H. A. Waldron (1983)
British Medical Journal 287: 1961

En ordre d'importance, le second déversement de polluants le plus considérable après les activités agricoles de la rive sud du LSP proviendrait du pôle industriel de Sorel-Tracy (La Violette, 2004). Ce pôle industriel comporte 4 entreprises à vocation chimique et métallurgique, contribuant notamment à l'apport de biphenyles polychlorés (BPC) et de mercure dans le lac Saint-Pierre (Kwan et al., 2003). Les rejets des stations d'épuration des eaux usées des villes de Montréal et Laval représentent également une source importante de pollution dans le lac. Le LSP constitue par ailleurs la première zone de sédimentation en aval de ces effluents (Pelletier, 2005). La station d'épuration de la ville de Laval effectue le traitement et la désinfection par ozonation des eaux depuis 1999, tandis que celle de Montréal traite les eaux usées depuis 1995, mais ne procède pas à leur désinfection (La Violette, 2004). L'ozonation permet l'élimination d'une grande partie des bactéries et des virus, en plus de la dégradation de certains contaminants émergents et de composés pharmaceutiques (Lajeunesse et al., 2013). La station d'épuration de Montréal est donc responsable du déversement dans le fleuve Saint-Laurent d'un mélange complexe de substances perfluoroalkylées (PFAs) (Houde et al., 2014b), de retardateurs de flamme halogénés (Houde et al., 2014a; Houde et al., 2014b), de métaux (Giraudo et al., 2016) et de composés pharmaceutiques (Lajeunesse et al., 2013; Lajeunesse et al., 2011).

Depuis le milieu des années 1970, on assiste à une réduction de l'apport en métaux dans le lac Saint-Pierre (Carignan et al., 1994). Cette réduction résulte notamment d'un effort accru des industries de diminution des rejets toxiques, de travaux d'assainissement des eaux usées de Montréal ainsi que de la fermeture de certaines usines situées en amont. Conséquemment, les teneurs en mercure dans les sédiments de la rive nord du lac Saint-Pierre sont passé de 0.51 µg/g en 1975 à 0.05 µg/g en 2003 (Pelletier, 2005). Dans les tissus de perchaudes, les concentrations de mercure atteignaient 0.3 mg/kg de masse humide en 1977 (carcasse entière sans la tête ni les viscères) (Sloterdijk, 1977), 0.15 mg/kg de masse humide en 1985 dans le muscle et 0.1 et 0.13 mg/kg de masse humide en 1997 dans le muscle d'individus au nord et au sud du lac, respectivement. Plus récemment, au cours de la période 2010-2014, les teneurs en mercure dans la chair de perchaude variaient entre 0.1 et 0.2 mg/kg de masse humide (Laliberté, 2016), concentrations ne dépassant pas le seuil de toxicité de 0.5 mg/kg de masse humide estimé pour le muscle des poissons d'eau douce (Dillon et al., 2010). Or, il est maintenant établi que même à de très faibles concentrations, le mercure altère le succès reproducteur des poissons (Crump & Trudeau, 2009) ainsi que leur métabolisme cellulaire (Larose et al., 2008).

Le mercure fait partie de la liste actuelle des 10 produits chimiques posant un problème majeur de santé publique, publiée par le Programme international sur la sécurité des substances chimiques de l'Organisation mondiale de la santé (IPCS, 2010). Ce contaminant a également initié l'adoption de la convention de Minamata en 2013, accord international visant à protéger l'Homme et l'environnement contre les effets du mercure. Il s'agit en effet d'un puissant neurotoxique, qui est aisément bioaccumulable et bioamplifiable dans les réseaux trophiques sous sa forme méthylée (MeHg) (Morel et al., 1998). La majorité des émissions anthropiques de mercure proviennent de la combustion du charbon ainsi que de l'extraction artisanale de l'or, à la suite desquelles il est introduit dans l'atmosphère sous forme élémentaire (Hg(0)) et inorganique (Hg(II)). Le mercure élémentaire est volatil, pouvant séjourner et voyager dans l'atmosphère sur des périodes variant de 6 mois à 2 ans avant d'être oxydé en Hg(II), qui est déposé dans les écosystèmes aquatiques. Dans ces milieux, le Hg(II) est méthylé par des bactéries sulfatoréductrices, méthanogène et ferroréductrices (Grégoire et al., 2018) avant d'être accumulé dans les organismes aquatiques, dont les poissons.

L'alimentation représente la principale voie d'exposition et de bioaccumulation du MeHg chez les poissons (Hall et al., 1997). Une fois ingéré, le mercure peut être détoxifié dans le foie *via* la séquestration par des métallothionéines (Sigel et al., 2009) ou encore accumulé dans le muscle, en raison de son affinité pour les groupements thiols (Harris et al., 2003). Il a été démontré que les poissons ont la capacité de tolérer des niveaux de mercure inférieurs à 0.5 mg/kg dans le muscle, limitant les niveaux dans le foie (Goldstein et al., 1996). Or, lorsque les concentrations musculaires dépassent 1 mg/kg, on observe généralement une augmentation des niveaux hépatiques.

Peu d'études ont, à ce jour, traité des effets du mercure sur la perchaude. Il existe une évidence de transfert maternel du MeHg chez la perchaude (Hammerschmidt et al., 1999; Niimi, 1983). Il semble en effet que le transfert de ce contaminant soit fortement influencé par la proportion de lipides présente chez la femelle ovigère ainsi que par la quantité de lipides totaux transférée aux œufs (Niimi, 1983). Bien que la quantité de mercure transférée soit relativement faible, il s'agit de la principale voie d'exposition des embryons à ce contaminant, qui peut altérer considérablement leur survie et leur développement (Hammerschmidt et al., 1999). On estime en effet que la quantité de mercure total retrouvé dans les œufs représente en moyenne 5-20% de la charge corporelle totale de la femelle ovigère (Hammerschmidt et al., 1999). De plus, la

proportion de méthylmercure et de mercure total présente dans les œufs augmente de manière proportionnelle en fonction de ces concentrations mesurées chez les perchaudes femelles (Hammerschmidt et al., 1999). La toxicité du mercure chez la perchaude a été évaluée au Kejimkujik National Park and National Historic Site (KNPNHS) en Nouvelle-Écosse, une région où les organismes présentent des taux anormalement élevés de méthylmercure (Batchelar et al., 2013a; Batchelar et al., 2013b; Graves et al., 2017). Dans un premier lieu, la santé reproductive a été évaluée (Batchelar et al., 2013b). Les mâles et les femelles sexuellement matures récoltés contenaient entre 0.28 et 0.54 mg de mercure total/kg de masse musculaire humide. Les auteurs ont évalué l'indice gonadosomatique des individus, le développement des gonades ainsi que les taux de 17β -estradiol dans le plasma des femelles. Les résultats démontrent que le mercure n'était pas corrélé de manière négative aux paramètres à l'étude et ne semblait donc pas altérer la santé reproductive de la perchaude. Conséquemment, les auteurs ont émis l'hypothèse que puisque la perchaude est reconnue comme étant une espèce particulièrement tolérante aux métaux, les individus adultes n'étaient pas sensibles aux concentrations auxquelles ils étaient exposés. Il est également possible que le mercure altère d'autres paramètres liés à la reproduction et qui n'ont pas été évalués dans cette étude, soit par exemple les patrons temporels et comportementaux liés à la fraie. Toujours dans la même région, des concentrations élevées de mercure total (THg) ont été associées à une augmentation de la taille et du nombre d'agrégats de mélanomacrophages (MA) dans le foie (Müller et al., 2015). Ces agrégats jouent le rôle de sites de détoxication, de destruction et de recyclage du matériel cellulaire endogène et exogène. L'étude de Müller et al. démontre ainsi que le mercure s'accumule dans ces cellules immunitaires, au sein desquelles aurait lieu un phénomène de phagocytose des cellules endommagées et affaiblies par le mercure. Cette prolifération de MA a également été observée par Batchelar et al. chez des perchaudes du même site (KNPNHS), en Nouvelle-Écosse, qui présentaient des concentrations de THg musculaire variant entre 0.08 et 2.13 mg/kg et des concentrations hépatiques de 0.13-6.04 mg/kg (Batchelar et al., 2013a). Enfin, Larose et al. ont noté une altération de l'activité de certaines enzymes ainsi qu'une diminution de l'indice hépatosomatique chez des perchaudes provenant de lacs de la forêt boréale (Larose et al., 2008). Les concentrations mesurées dans le foie variaient entre 0.015 et 0.294 mg/kg ww.

Le fractionnement subcellulaire, un outil qui permet de lier la bioaccumulation et la toxicité

“Exploring cells with a centrifuge”

Christian de Duve, prix Nobel de médecine en 1974

Outre les paramètres physiologiques susmentionnés, les techniques de fractionnement subcellulaire permettent également de faire un lien entre la bioaccumulation et le potentiel de toxicité d'un contaminant. Cette approche, qui repose sur une série de centrifugations successives et de variations de température, permet en effet de quantifier l'accumulation de métaux entre les fractions sensibles et les fractions dites « de détoxicification » de la cellule. Les premières expériences de fractionnement subcellulaire furent effectuées par Albert Claude en 1946. À l'aide d'une série de centrifugations différentielles, ce médecin et biologiste cellulaire belge réussit à séparer des cellules de rats et de cochons d'Inde en 3 fractions morphologiquement distinctes : (1) la fraction granulaire, qui contenait principalement des mitochondries et des granules de sécrétion, (2) la fraction des microsomes, qui contenait des éléments particulaires de taille submicroscopique et (3) la fraction du surnageant, qui comprenait essentiellement tous les éléments résiduels de petite taille. La composition chimique ainsi que l'activité de certaines enzymes furent par la suite évaluées dans chacune de ces fractions. Pour ses découvertes sur l'exploration de la cellule, Albert Claude s'est vu octroyer le prix Nobel de la médecine en 1974, conjointement avec Christian de Duve, à qui l'on doit la découverte du lysosome et du peroxysome. Il importe de noter qu'il s'agissait alors des premières recherches sur la composition de la cellule basées sur la centrifugation, puisque seules les techniques microscopiques étaient employées jusqu'alors. Par ailleurs, ce n'est qu'en 1957 que le fractionnement subcellulaire fut utilisé pour la première fois dans le but d'étudier la répartition des métaux, dans des foies de rats (Thiers & Vallee, 1957). Or, les auteurs mentionnent qu'ils ont utilisé un protocole de fractionnement publié précédemment, sans aucune modification, alors qu'il est désormais établi que l'optimisation des protocoles en fonction de l'espèce et du tissu à l'étude est nécessaire à la qualité du fractionnement (Cardon et al., 2018; Rosabal et al., 2014). L'optimisation des protocoles implique principalement la

validation de plusieurs méthodes d’homogénéisation des tissus à l’aide de l’évaluation de l’activité d’enzymes spécifiques à chaque fraction. Par exemple, à la suite de l’homogénéisation d’un tissu et de l’application d’un protocole de centrifugations successives, l’activité de la lactate déshydrogénase (LDH) sera mesurée dans le cytosol et celles de la cytochrome c oxydase (CCO) et de la citrate synthase (CS) seront mesurées dans la fraction mitochondriale. Dans le cas où une proportion importante de l’activité de la CS, enzyme de la matrice mitochondriale, est mesurée dans le cytosol, l’hypothèse d’un bris potentiel des mitochondries se doit d’être évoquée. Il est donc possible que les techniques d’homogénéisation utilisées soient trop agressives, requérant une nouvelle expérience d’optimisation. Plusieurs études publiées à ce jour sur la répartition subcellulaire des métaux ne montrent aucune trace d’optimisation, laissant sous-entendre un potentiel chevauchement des fractions. Dans ce cas, ces dernières sont définies de manière opérationnelle, et l’interprétation toxicologique de la présence de métaux se doit d’être nuancée. L’optimisation des protocoles de fractionnement subcellulaire implique également la qualité de la préservation des échantillons, la vérification de la vitesse et du temps de centrifugation en fonction du tissu et de l’organisme ainsi que la réalisation d’un bilan de masse, autant pour les enzymes que pour les métaux. Pour ce faire, la masse de chaque fraction doit impérativement être notée, de façon à pouvoir suivre une perte potentielle ou une contamination durant la procédure.

Une fois le protocole optimisé pour chaque tissu à l’étude, le fractionnement subcellulaire permet d’obtenir 6 fractions, comprenant 2 fractions dites « sensibles » (mitochondries, protéines dénaturées par la chaleur (HDP)), 2 fractions de détoxification (granules, protéines thermostables (HSP)) et 2 fractions dont la nature exacte est davantage ambiguë (débris, lysosomes/microsomes). Lorsqu’ils se retrouvent en excès dans les cellules, les métaux traces peuvent se lier physiologiquement à des molécules sensibles ou à des organelles, causant ainsi des effets délétères. Les mitochondries représentent des fractions sensibles clés, puisqu’elles sont fréquemment les cibles cellulaires principales de la toxicité métallique. En effet, il a été démontré qu’une liaison du MeHg aux mitochondries cause des malformations au niveau de leur structure ainsi qu’une perturbation de la chaîne de respiration mitochondriale chez le poisson-zèbre (Cambier et al., 2009). La fraction des HDP comportant principalement des enzymes, une proportion importante de mercure associée à cette dernière pourrait entraîner une inhibition des sélénoenzymes, impliquées dans les fonctions

antioxydantes et dans le contrôle du potentiel d’oxydoréduction. Or, les systèmes subcellulaires ont évolué afin de permettre une accumulation, une régulation ainsi qu’une immobilisation des métaux traces. Ainsi, les métallothionéines, protéines riches en cystéine retrouvées dans la fraction des HSP, assurent la séquestration et la détoxicification du mercure (Wang et al., 2012), bien que l’affinité entre le MeHg et les métallothionéines n’ait pas encore été validée. La fraction des microsomes/lysosomes se doit d’être interprétée avec prudence, puisqu’elle contient à la fois des biomolécules de détoxicification et sensibles. En effet, les lysosomes ont une fonction stockage en prévision d’une excrétion éventuelle, alors que les microsomes peuvent contenir des fragments de réticulum endoplasmique, responsable de la synthèse et du transport de protéines (Giguère et al., 2006). Une association de métaux aux microsomes est donc un indice de toxicité. La fraction des granules semble contenir des granules constitués de mercure et de sélénium (HgSe), qui représentent des produits finaux de détoxicification du mercure (Wang et al., 2012). Enfin, la fraction des débris, bien que souvent ignorée dans les études écotoxicologiques, peut contenir des noyaux, constituants importants de la cellule (Wallace & Luoma, 2003). La signification toxicologique de cette dernière fraction est donc ambiguë, puisqu’une proportion importante de métaux associée à cette dernière représente également un indice d’homogénéisation inefficace (Giguère et al., 2006).

Peu d’études traitent, à ce jour, du fractionnement subcellulaire du mercure chez les poissons (Araújo et al., 2015; Barst et al., 2016; Barst et al., 2018; Onsanit & Wang, 2011). Par ailleurs, aucune de ces études n’utilise la perchaude comme modèle ou n’évalue la distribution du mercure dans les gonades. Par exemple, chez le sébaste aux yeux jaunes (*Sebastes ruberrimus*) d’Alaska, le mercure semble préféablement associé à la fraction des débris hépatiques, et une plus grande proportion de mercure était associée aux granules qu’aux HSP (Barst et al., 2018). En comparaison, dans les foies de rougets sauvages (*Liza aurata*), les concentrations de THg mesurées dans la fraction des HSP étaient en dessous des limites de détection et les concentrations les plus élevées ont été mesurées dans la fraction des lysosomes/microsomes (Araújo et al., 2015). Ces études suggèrent que la répartition subcellulaire du mercure dépend fortement de l’espèce à l’étude ainsi que du niveau de bioaccumulation. Il importe également de noter qu’à ce jour, une seule étude traite de la spéciation du mercure (MeHg) (Peng et al., 2016) et une seule autre a considéré les effets antagonistes du sélénium (Barst et al., 2018) d’un point de vue subcellulaire.

Le sélénium: osciller entre carence et toxicité

“ All things are poison, for there is nothing without poisonous qualities. It is only the dose which makes a thing poison.”

Paraclesus, 1538

Le sélénium étant un métalloïde, il présente des propriétés propres aux métaux ainsi qu'aux non-métaux. Le sélénium est un élément du groupe 16, tout comme le soufre et l'oxygène. Ces trois derniers éléments sont donc analogues d'un point de vue chimique. Le sélénium et d'ailleurs un élément chalcophile, c'est-à-dire qu'il présente une affinité marquée pour le soufre (Goodarzi & Swaine, 1993). Les deux atomes s'associent notamment pour former du sulfure de sélénium (Se_2S_2) et des polysulfures (Adriano, 2001). En solution, le sélénium est hydrolysé pour former des oxyanions. Ainsi, contrairement au mercure qui forme des cations en milieu aqueux, le sélénium forme notamment du sélénite (SeO_3^{2-}) et du sélénate (SeO_4^{2-}) (Mason, 2013). Ces complexes oxygénés, qui sont répandus dans les sols et dans les eaux naturelles, sont caractérisés par une grande solubilité, qui augmente avec le pH (Adriano, 2001). Le sélénium élémentaire, Se^0 , est quant à lui beaucoup moins soluble. Les principaux états d'oxydation du sélénium inorganique retrouvés dans l'environnement sont (-II), (0), (+IV) et (+VI) (Mason, 2013). L'état d'oxydation majeur demeure cependant le Se^{2-} .

L'extraction des métalloïdes, dont le sélénium, à partir des réservoirs profonds dans la croûte terrestre à l'ère préindustrielle a principalement été attribuée à l'activité volcanique et aux apports hydrothermaux océaniques (Mason, 2013). Plus récemment, les activités minières et l'extraction du charbon ont exacerbé les apports de métalloïdes dans l'atmosphère et les écosystèmes aquatiques (Mason, 2013). Les sources de métalloïdes dans les eaux douces sont principalement l'érosion de la matière de surface terrestre, les apports de métalloïdes associés aux eaux souterraines et au ruissellement ainsi que le dépôt atmosphérique de métalloïdes (Mason, 2013). Pour la plupart des métalloïdes, le transport à la surface de la Terre a principalement lieu *via* la phase particulaire, soit par des solides en suspension dans les rivières et les zones côtières ainsi que par les aérosols dans l'atmosphère (Mason, 2013). Plus

particulièrement, le sélénium est suffisamment volatil pour que son transport atmosphérique se produise en phase gazeuse.

La grande majorité du sélénium d'origine anthropique provient de la combustion des combustibles fossiles, dont le charbon. À l'origine, les centrales au charbon relâchaient du sélénium sous forme de SeO_2 dans l'atmosphère (Xie et al., 2006). Le sélénium atteignait donc les cours d'eau *via* des dépôts de cendres volatiles. Depuis 2008, cependant, les centrales sont dotées de systèmes d'épuration des gaz de combustion par voie humide, modifiant la nature des rejets afin d'inclure des eaux usées d'épuration (Maher et al., 2010). Une plus faible fraction de sélénium d'origine anthropique est relâchée lors du raffinage des métaux non-ferreux, par exemple lors du raffinage électrolytique du cuivre. Le sélénium est en effet retrouvé dans les minéraux sulfureux, puisqu'il remplace partiellement les atomes de soufre. À la fin des années 1980, les principaux producteurs de sélénium *via* ce raffinage électrolytique étaient le Canada, le Japon, les États-Unis, le Mexique, la Russie, la Suisse et la Belgique (Adriano, 2001). Les émissions biologiques représentent également des sources importantes de sélénium dans l'environnement, puisque ce dernier est un élément essentiel. En effet, puisque la majorité des composés bioorganiques contenant du sélénium sont des protéines, ces dernières sont continuellement produites et excrétées par les microorganismes aquatiques (Mason, 2013).

Le sélénium présente une chimie organométallique très complexe, dans l'optique où, à l'image du Hg, il peut être méthylé. La molécule méthylée CH_3SeH et le cation CH_3Se^+ sont en effet reconnus comme étant responsables de la toxicité du sélénium (Mason, 2013). La formation de composés méthylés de sélénium est omniprésente puisque ces derniers sont produits par les bactéries et les algues. Bien que la méthylation et la déméthylation du sélénium soient peu étudiées, il a notamment été observé qu'en eau douce, des protéobactéries comme *Pseudomonas spp.* sont responsables de la méthylation du sélénium (Ranjard et al., 2003). La déméthylation du $(\text{CH}_3)_2\text{Se}$, quant à elle, a lieu en milieu anoxique et l'hypothèse que certains organismes méthanogènes utilisent ce composé pour leur croissance comme analogue à l'utilisation du DMS (diméthylsulfure) a été émise (Oremland et al., 1991).

Le cycle biogéochimique du sélénium suggère ainsi que la majorité du sélénium inorganique introduit dans l'environnement est converti en composés méthylés dans les sédiments en absence d'oxygène. Par contre, ces composés méthylés sont également produits en parallèle avec la production primaire dans la colonne d'eau. Il est donc probable que la

méthylation ayant lieu dans les sédiments soit un processus direct, contrairement aux processus qui ont lieu dans la colonne d'eau, où l'on assiste plutôt à une production de composés méthylés résultant de la décomposition de biomolécules qui contiennent du sélénium. Il a été déterminé que le pH optimal pour la biométhylation du sélénium et sa volatilisation subséquente est de 8 (Adriano, 2001). Ainsi, une augmentation du pH de 6 à 7 aurait comme effet d'augmenter de 20% la volatilisation des composés méthylés de cet élément.

Le sélénium pénètre dans l'écosystème aquatique sous la forme d'oxyanions inorganiques, soit le sélénate (+IV) et le sélénite (+VI). Une certaine quantité de sélénium organique dissous (-II) peut également se retrouver dans la colonne d'eau *via* l'activité biologique. Le cycle biogéochimique du sélénium en milieu aquatique est caractérisé par la prédominance de réactions biologiques régulées par des réactions thermodynamiques. Le sélénate et le sélénite sont ainsi pris en charge par les microorganismes, les algues et les plantes et subséquemment convertis en composés organiques de sélénium. Le sélénium est ensuite réduit biochimiquement sous la forme (-II) avant d'être ultimement incorporé dans les acides aminés tels que la sélénocystéine et la sélénométhionine. La sélénométhionine est en effet la principale forme organique de sélénium à la base des réseaux trophiques. La sélénocystéine, quant à elle, est aisément oxydable, indiquant qu'elle n'est pas stable dans le milieu. Ainsi, dans la colonne d'eau, le sélénium organique (-II) est accumulé par (1) le phytoplancton directement de l'eau, (2) le zooplancton et les invertébrés qui broutent le phytoplancton et (3) les vertébrés supérieurs qui se nourrissent de ce zooplancton. Lorsque les organismes aquatiques meurent et sédimentent, le sélénium organique qu'ils ont ingéré est oxydé par les microorganismes et remonte dans la colonne d'eau. La consommation de matière organique particulière contenant une certaine quantité de sélénium organique et inorganique est la voie d'entrée principale du sélénium dans les chaînes trophiques aquatiques.

La chimie du sélénium est importante dans l'optique où il est nécessaire aux organismes, mais peut devenir toxique lorsque présent en trop grande quantité. Cette toxicité est due au fait qu'il peut substituer le soufre dans les voies biochimiques importantes (Mason, 2013). Le sélénium est en effet un constituant des sélénoprotéines, qui ont un rôle biochimique vital. De tous les éléments qui sont nécessaires aux organismes, mais peuvent devenir toxiques à des concentrations trop élevées, le sélénium est celui qui présente le plus d'aisance à changer d'état

d'oxydation (Mason, 2013). Ainsi, de relativement petits changements dans sa concentration et dans sa spéciation peuvent avoir un impact important sur sa toxicité (Figure 3).

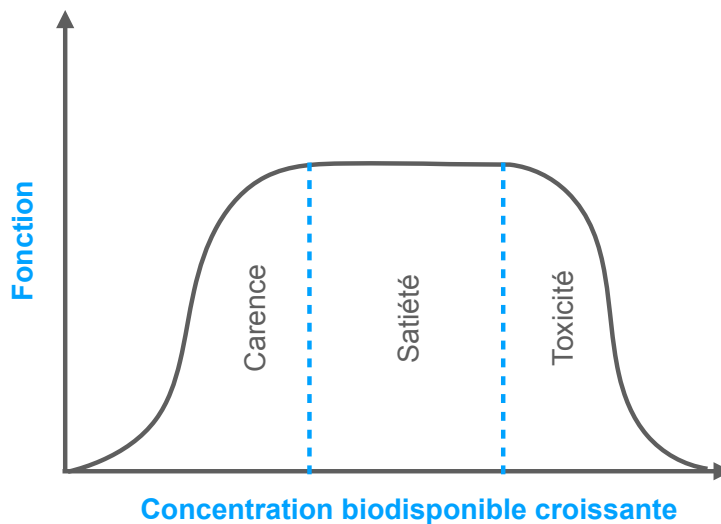


Figure 3. Courbe représentant la réponse des organismes en fonction de la concentration d'un élément trace qui est nécessaire à la survie, mais devient毒ique lorsque présent en trop grande concentration. Adaptée de Mason (2013).

Contrairement au mercure, le sélénium est nécessaire à l'activité de certaines enzymes retrouvées dans toutes les cellules des vertébrés. Cet élément peut cependant être toxique pour les organismes à de très fortes concentrations. L'ingestion de sélénium *via* les apports alimentaires est donc essentielle pour la synthèse de sélénoprotéines et de sélénoenzymes actives principalement dans les tissus nerveux (Peterson et al., 2009). Plus précisément, les sélénoenzymes régulent les processus redox intracellulaires, protègent contre le stress oxydatif pouvant affecter le système nerveux et jouent un rôle dans le métabolisme thyroïdien. Des variations dans les apports nutritifs de sélénium peuvent engendrer des variations de la concentration de sélénium dans les tissus du foie et des reins, mais ont peu d'effet sur la concentration de sélénium dans le système nerveux. Or, les mécanismes de contrôle homéostatiques ont lieu lorsqu'il y a une carence en sélénium dans le système nerveux. Ainsi, à ce moment, les tissus somatiques relâchent leurs réserves de sélénium afin de fournir un apport continu de cet élément aux tissus nerveux (Peterson et al., 2009). Il importe de mentionner qu'il existe un très faible écart entre les concentrations de sélénium engendrant des effets bénéfiques

et celles causant les effets toxiques, puisque cet élément est très faiblement présent dans l'environnement et que les concentrations requises pour les réactions vitales sont également très faibles.

Bien que les pathologies liées à une carence en sélénium soient répertoriées chez l'humain (Beck et al., 2003; Brown & Arthur, 2007; Moreno-Reyes et al., 1998; Rayman, 2000), ces effets sont beaucoup moins étudiés chez les poissons. Il semble cependant qu'une carence alimentaire en sélénium ait causé une diminution de l'activité enzymatique et une peroxydation des lipides chez le saumon de l'Atlantique (Bell et al., 1987), ainsi qu'une perturbation de la croissance chez des carpes (*Cyprinus carpio*) juvéniles (Wang et al., 2013). Le besoin d'études relatives à ces effets chez le poisson, particulièrement en milieu naturel, est cependant critique.

Les premières observations d'un antagonisme potentiel entre le mercure et le sélénium ont été publiées 1967 (Pařízek & Ošt'ádalová, 1967). Cette étude a démontré qu'en présence de sélénite de sodium, Na_2SeO_3 , les reins de rats semblaient protégés contre les effets toxiques du chlorure mercurique, HgCl_2 . En effet, les reins des rats auxquels étaient administrés du sélénite et du chlorure mercurique ne démontraient aucun dommage histologique ou de nécrose, contrairement aux rats qui avaient uniquement été exposés au chlorure mercurique. Cette étude pionnière a pavé la voie aux recherches subséquentes sur l'interaction entre le mercure et le sélénium ainsi que sur les mécanismes potentiels associés à la protection contre les effets toxiques du mercure.

Lorsqu'une quantité excessive de MeHg ou Hg^{2+} s'accumule dans la cellule, le cycle de la sélénocystéine sera interrompu (Peterson et al., 2009). La toxicité du mercure est donc notamment due au fait qu'il inhibe l'activité d'enzymes qui dépendent du sélénium et qui protègent normalement l'organisme contre le stress oxydatif. Ce dernier mécanisme est appelé *selenium sequestration mechanism of mercury toxicity* (Peterson et al., 2009) et repose sur le fait que l'inhibition des sélénoenzymes par le mercure est la cause directe des dommages oxydatifs résultant d'une intoxication au mercure. Il importe de mentionner que l'affinité de liaison du mercure et du sélénium est nettement supérieure à l'affinité entre le mercure et les groupements thiols (Spiller, 2017). Les sélénoenzymes sont donc considérées comme la cible principale des effets toxiques associés au mercure. À l'inverse, le sélénium peut également protéger l'organisme contre les effets du mercure. Cet antagonisme peut être dû à plusieurs processus, notamment *via* la séquestration intracellulaire du mercure par le sélénium. Cette

séquestration prend la forme de complexes organiques ($\text{MeHg}[\text{Cystéine}]$) ou inorganiques (HgSe) fortement insolubles dans les tissus (Peterson et al., 2009). Il a également été démontré que de faibles concentrations de sélénium ajoutées dans un lac limitaient la bioaccumulation du mercure chez la perchaude (Mailman et al., 2014). Les autres mécanismes associés au rôle du sélénium dans la réduction de la toxicité du mercure incluent (1) la favorisation de la déméthylation du MeHg , (2) la redistribution du mercure vers des organes moins sensibles, (3) la diminution de l'absorption du mercure par le tractus gastro-intestinal ainsi que (4) le rétablissement de l'activité des sélénoenzymes (Spiller, 2017).

Tant que les concentrations molaires de mercure intracellulaire demeurent plus basses que celles de sélénium dans le système nerveux, l'activité des sélénoenzymes demeure intacte. Cependant, lorsque les concentrations molaires de mercure sont supérieures à celles de sélénium, une portion du sélénium cellulaire essentiel pour la production de sélénoenzymes devient séquestrée et les symptômes de la toxicité du mercure se développent (Berry & Ralston, 2008). Ainsi, il s'agit du ratio molaire Se:Hg dans les tissus qui devient critique pour les organismes, plutôt que de la concentration en MeHg ou Hg^{2+} : lorsque le Se:Hg est plus faible que 1:1, le potentiel de toxicité du mercure est accru, alors qu'un ratio Se:Hg supérieur à 1:1 procure une certaine protection contre la toxicité du mercure. Cependant, le ratio exact conférant une protection contre les effets toxiques du mercure n'a, à ce jour, pas été déterminé. Il devient donc ardu d'interpréter la signification toxicologique de ratios élevés et variables répertoriés actuellement chez les poissons sauvages (Figure 4) (Burger & Gochfeld, 2012).

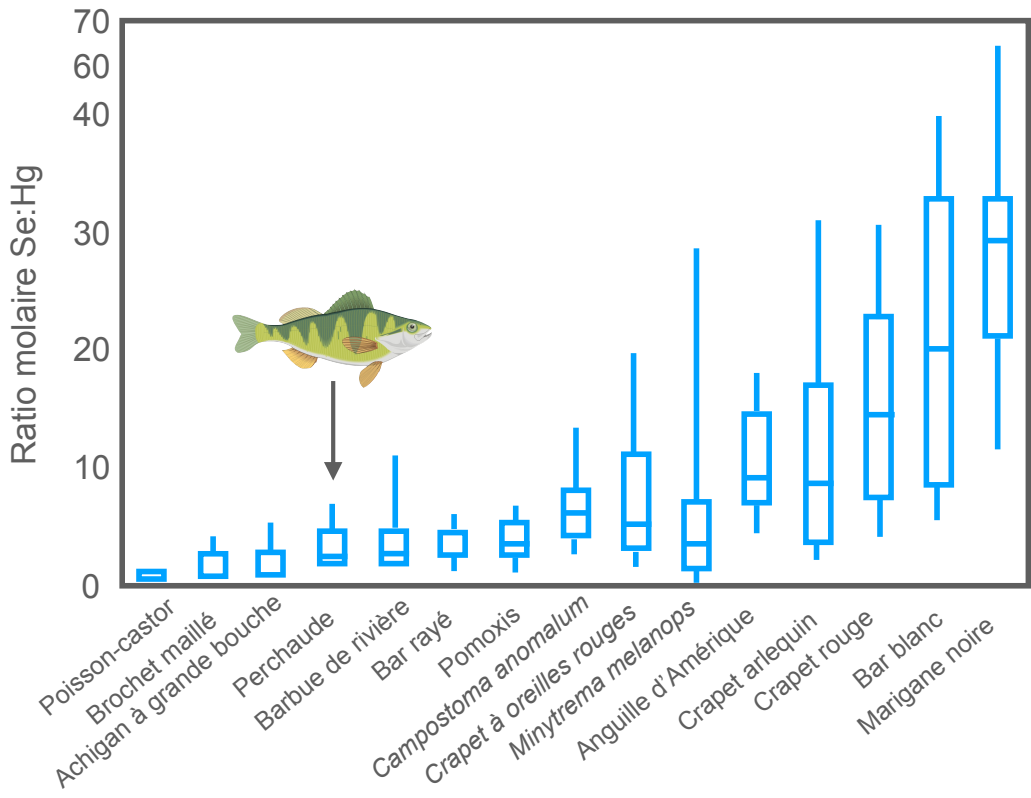


Figure 4. Ratios molaires Se:Hg mesurés dans le muscle de plusieurs espèces de poissons d'eau douce en Caroline du Sud et au Tennessee. Adaptée de Burger et Gochfeld (2013).

Cadre conceptuel et objectifs généraux de la thèse

La présente thèse s'inscrit dans le cadre d'un programme d'initiative stratégique pour l'innovation (ISI) du Fonds de recherche du Québec – Nature et technologies (FRQNT) dont l'objectif ultime vise la restauration des habitats aquatiques du LSP. Ce programme a été initié par le Groupe de recherche interuniversitaire en limnologie et en environnement aquatique (GRIL). L'exploitation des terres agricoles sur le bassin versant du LSP ainsi que les rejets industriels et des effluents d'usines d'épuration des eaux usées compromettant la qualité de l'eau de ce lac fluvial, cette dernière variable est sans contredit d'une importance capitale dans l'évaluation de l'état de santé des populations de perchaudes. L'objectif principal de la présente thèse visait ainsi à évaluer les effets directs et indirects du glyphosate, du mercure et du sélénium sur la reproduction et les stades de vie précoce de la perchaude. Le cadre conceptuel de la thèse est schématisé à la figure 5.

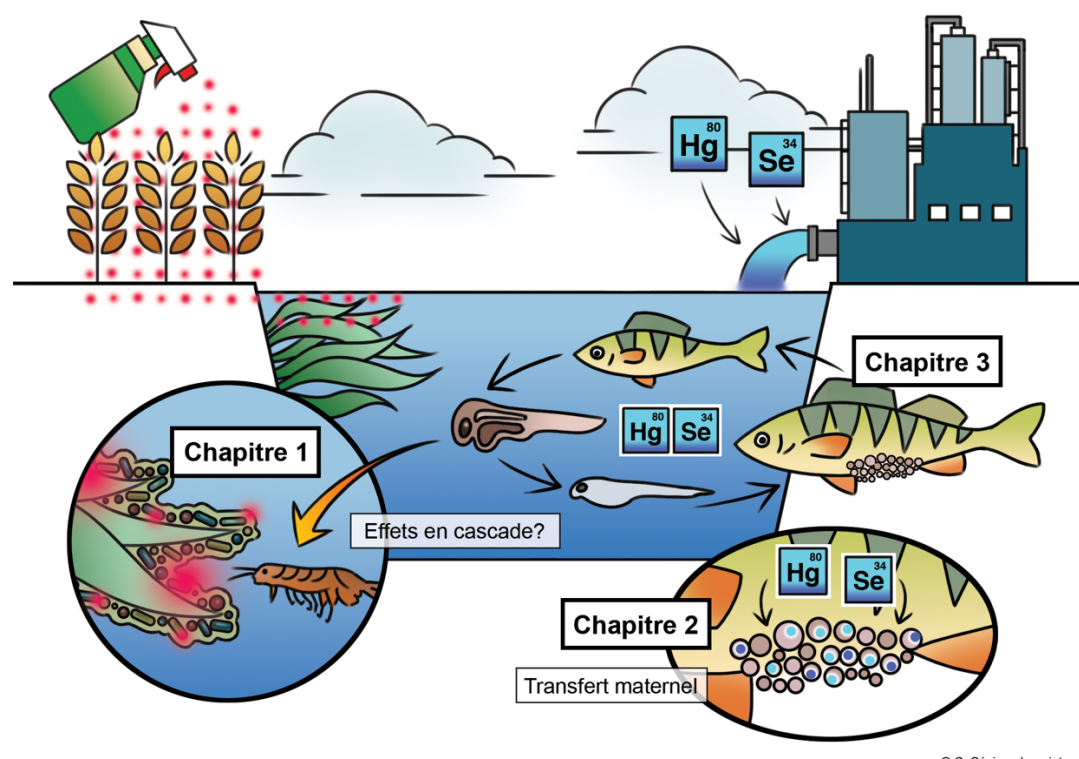


Figure 5. Cadre conceptuel de la thèse, illustrant les thèmes associés à chacun des chapitres.

L'incapacité de rétablissement des stocks de perchaudes au LSP est principalement attribuable à un recrutement déficient. Cette diminution de l'abondance des individus d'âge 1+ et 2+ connaît en effet un déclin majeur depuis le début des années 2000 (Magnan et al., 2017). Il est fort probable que ce déclin soit dû au fait que les perchaudes d'âge 0+ ne disposent pas de ressources énergétiques suffisantes de manière à atteindre la taille minimale leur permettant de survivre à l'hiver (Magnan et al., 2017). Ce retard de croissance en début de vie augmenterait ainsi considérablement la mortalité hivernale des jeunes perchaudes. Le présent projet de doctorat visait à évaluer l'hypothèse que ce faible recrutement soit en partie attribuable à l'impact direct ou indirect de la contamination chimique sur la reproduction de la perchaude. Les chapitres de la présente thèse sont donc articulés autour de cette problématique. L'agriculture intensive sur la rive sud de son bassin versant, principalement des cultures de soya et de maïs, entraîne le déversement d'une quantité importante de pesticides dans le LSP, dont le glyphosate, qui fait l'objet d'une utilisation massive. Le glyphosate étant un herbicide à large spectre non sélectif, le **Chapitre 1** visait à évaluer si cet herbicide aurait un effet toxique sur les biofilms périphytiques, ou périphyton, causant des effets en cascade jusqu'aux jeunes perchaudes. En effet, dans les champs agricoles, le glyphosate est principalement pulvérisé directement sur le feuillage des plants, le rendant susceptible au lessivage vers les cours d'eau. Les plantes aquatiques, et par le fait même les biofilms périphytiques qui y sont associés, sont fréquemment les premiers récepteurs des eaux de ces eaux de ruissellement. Plusieurs espèces de poissons, dont la perchaude, utilisent également les herbiers aquatiques comme aire de fraie. Les biofilms périphytiques étant des producteurs primaires importants, un effet néfaste du glyphosate sur ces derniers pourrait donc engendrer un effet en cascade jusqu'aux jeunes perchaudes. Afin de tester cette hypothèse, nous avons réalisé des expériences en microcosmes de manière à procéder à l'exposition de biofilms d'âge différent (2 mois, 1 an, 20 ans) à plusieurs concentrations environnementales de glyphosate et de phosphore correspondantes. La molécule de glyphosate comportant en effet 18.2% de phosphore qui peut être utilisé par certains taxons de cyanobactéries, nous voulions évaluer si cet herbicide représente une source significative de phosphore biodisponible (PO_4^{3-}). Enfin, le glyphosate étant rapidement dégradé en acide aminométhylphosphonique (AMPA) par divers processus chimiques, biologiques et physiques et ce dernier ayant pour effet d'altérer la biosynthèse de la chlorophylle, nous avons mesuré les concentrations de chl *a* dans les biofilms. Nos résultats démontrent que l'âge du périphyton

semble être le seul facteur façonnant la structure des communautés eucaryotes et cyanobactériennes, d'un point de vue génétique (Khadra et al., 2018). Cette étude est en effet la première à utiliser des amorces spécifiques aux cyanobactéries afin d'étudier la structure des communautés périphytiques ainsi que la première à utiliser des biofilms d'âge aussi différent. Nous avons également observé que le glyphosate ne semblait pas altérer la biosynthèse de la chlorophylle. Enfin, nos observations démontrent que le glyphosate relarguait du phosphore dans le milieu, mais que ce dernier n'était pas sous une forme biodisponible. Cette étude démontre ainsi que le glyphosate ne semble pas affecter négativement la structure et le métabolisme des biofilms, aux concentrations mesurées actuellement dans nos cours d'eau. Ces résultats sont également d'une importance capitale puisqu'ils soulignent l'importance de tenir compte de l'âge du périphyton dans l'évaluation des effets des pesticides.

Le mercure, à l'image du glyphosate, est un contaminant qui soulève une préoccupation d'envergure. En effet, sous sa forme méthylée, ce métal est bioaccumulé et bioamplifié dans les réseaux trophiques, menant à des effets toxiques sur la reproduction des poissons (Crump & Trudeau, 2009). Bien qu'il ait été démontré que le MeHg est transféré de la femelle ovigère à ses œufs chez la perchaude (Hammerschmidt et al., 1999; Niimi, 1983), le potentiel de toxicité associé à ce transfert, source principale d'exposition des embryons, n'a jamais été évalué. Le **Chapitre 2** traite ainsi du potentiel de toxicité associé au transfert maternel du mercure chez la perchaude à l'aide de techniques de fractionnement subcellulaire. Plus précisément, cette étude visait à évaluer (1) l'exposition des œufs de perchaudes au mercure et au sélénium à la suite d'un transfert maternel et (2) l'effet protecteur potentiel du sélénium, en calculant les ratios molaires Se:Hg. Des échantillons de foie et de gonades ont ainsi été fractionnés afin de déterminer si le mercure et le sélénium se retrouvaient préférentiellement dans des fractions sensibles (mitochondries, protéines dénaturées par la chaleur) ou dites « de détoxicification » (protéines thermostables, granules) de la cellule. La séparation des différentes composantes cellulaires a été validée par des essais enzymatiques. Les relations entre les concentrations mesurées dans le foie et celles mesurées dans les gonades ont été utilisées comme mécanisme indicateur de transfert maternel. Nos résultats ont tout d'abord appuyé l'évidence d'un transfert maternel du mercure chez la perchaude, en plus de démontrer que le mercure était transféré aux mitochondries des gonades (Khadra et al., 2019a). Puisque le MeHg a préalablement été associé à des anomalies de la structure et du métabolisme des mitochondries chez le poisson-zèbre

(*Danio rerio*) (Cambier et al., 2009; Gonzalez et al., 2005b), nos résultats soulèvent une certaine préoccupation. Nous avons également considéré l'effet antagoniste du sélénium lors du transfert maternel. Ainsi, nous avons observé que le sélénium était transféré de la femelle ovigère à ses œufs, mais pas aux mitochondries des gonades de manière significative. Or, les rapports molaires Se:Hg étaient systématiquement supérieurs à 1 dans toutes les fractions subcellulaires du foie et des gonades. Ces résultats indiquent que, bien que le mercure semble être associé aux fractions sensibles, proportionnellement davantage de sélénium s'y accumule, assurant une certaine protection.

Après avoir confirmé l'évidence d'un transfert maternel du mercure et du sélénium chez la perchaude du LSP, la suite logique de l'interprétation de ces résultats nous a amenés à évaluer la bioaccumulation de ces contaminants à tous les stades de vie de la perchaude. Les premiers stades de développement des poissons sont en effet considérés comme étant particulièrement sensibles aux contaminants organiques et inorganiques (Dillon et al., 2010; Fjeld et al., 1998; Luckenbach et al., 2001; McKim, 1977; Weber, 2006). Le **Chapitre 3** traite donc de la distribution du mercure et du sélénium dans certains organes clé (intestin, foie, muscle, gonades, cerveau) ainsi que dans les masses d'œufs, jeunes larves, larves et juvéniles de perchaudes. Les objectifs spécifiques visaient à évaluer (1) la bioaccumulation du mercure et du sélénium, (2) la proportion de THg présente sous forme de MeHg (%MeHg) et (3) les ratios molaires Se:Hg. Nos résultats démontrent que les concentrations de mercure décroissaient selon le patron suivant : muscle > foie > intestin > cerveau > gonades, alors que les concentrations de sélénium suivaient la tendance suivante : intestin > foie > gonades > cerveau > muscle (Khadra et al., 2019b). En ce qui a trait aux stades de vie, les concentrations de MeHg étaient les plus élevées chez les juvéniles, puis chez les larves, les jeunes larves et enfin dans les masses d'œufs. Les concentrations de sélénium décroissaient quant à elles selon le patron suivant : jeunes larves > masses d'œufs > larves > juvéniles. Nous avons également observé que les ratios molaires Se:Hg étaient systématiquement supérieurs à 1 dans les organes et les stades de vie de la perchaude, suggérant un potentiel de protection. Les %MeHg variaient quant à eux considérablement selon l'organe et le stade de vie à l'étude, soit, en moyenne, de 39% dans les masses d'œufs à 97% chez les larves et de 66% dans l'intestin à 85% dans le muscle. Ces dernières observations remettent en doute les résultats analytiques préalablement obtenus par Bloom en 1992, qui suggéraient que, dans le muscle de certaines espèces de poissons d'eau douce et d'eau salée,

plus de 95% du THg est présent sous forme de MeHg (Bloom, 1992). Bien que cette dernière étude inclue des valeurs de %MeHg pour la perchaude ($99 \pm 16\%$ (n=19)), il importe de spécifier que les poissons échantillonnés étaient de taille et d'âge variables, induisant un potentiel de variabilité.

Les résultats associés aux **Chapitres 1, 2 et 3** sont présentés sous forme d'articles évalués par les pairs, publiés dans des revues scientifiques. Une conclusion générale est également avancée, dans l'optique de mettre en lumière les contributions à la littérature scientifique découlant de chacun des chapitres, en plus de fournir des pistes de recherches futures et des perspectives globales liées aux retombées de cette thèse. L'**Annexe I** présente le fruit d'un concours de vulgarisation scientifique, soit une bande dessinée inspirée du **Chapitre 1** réalisée en collaboration avec l'illustrateur Martin PM. L'**Annexe II** présente les résultats issus d'analyses préliminaires qui ont permis de réaliser un aperçu de la contamination en retardateurs de flamme dans les foies et les gonades de perchaudes. Enfin, les **Annexes III et IV** contiennent des résultats supplémentaires liés, dans le cas de l'**Annexe III**, au fractionnement subcellulaire du cuivre, du cadmium, du manganèse et du fer, et dans celui de l'**Annexe IV**, à la bioaccumulation du fer, du cuivre, de l'arsenic et du sélénium dans les tissus et les stades de vie précoces de la perchaude, respectivement. L'**Annexe III** complémente ainsi les résultats du **Chapitre 2**, et l'**Annexe IV** ceux du **Chapitre 3**.



CHAPITRE 1:

Dis-moi ton âge et je te dirai qui tu es :

Le temps de colonisation du périphyton façonne la structure des
communautés soumises à une exposition au glyphosate

Age matters: Submersion period shapes community composition of lake biofilms under glyphosate stress

Melissa Khadra^a, Dolors Planas^b, Catherine Girard^c, Marc Amyot^a

^a *Groupe interuniversitaire en limnologie et en environnement aquatique (GRIL), Département de sciences biologiques, Université de Montréal, Pavillon Marie-Victorin, 90 Vincent d'Indy, Montréal QC*

^b *Groupe interuniversitaire en limnologie et en environnement aquatique (GRIL), Département de sciences biologiques, Université du Québec à Montréal, C.P. 8888, Succursale Centre-Ville, Montréal QC*

^c *Sentinelle Nord, Département de biochimie, de microbiologie et de bio-informatique, Université Laval, 1030 avenue de la Médecine, Québec QC*

Published in FACETS, 3: 934-951.

DOI: 10.1139/facets-2018-0019

Copyright © 2018 Khadra et al. This work is licensed under a Creative Commons Attribution 4.0 International License ([CC BY 4.0](#)), which permits unrestricted use, distribution, and reproduction in any medium, provided the original author(s) and source are credited.

Abstract

The phosphonate herbicide glyphosate, which is the active ingredient in the commercial formulation Roundup®, is currently the most globally used herbicide. In aquatic ecosystems, periphytic biofilms, or periphyton, are at the base of food webs and are often the first communities to be in direct contact with runoff. Microcosm experiments were conducted to assess the effects of a pulse exposure of glyphosate on community composition and chlorophyll *a* concentrations of lake biofilms at different colonization stages (2 months, 1 year, and 20 years). This is the first study that uses such contrasting submersion periods. Biofilms were exposed to either environmental levels of pure analytical grade glyphosate (6 µg/L, 65 µg/L, and 600 µg/L) or to corresponding phosphorus concentrations. Community composition was determined by deep sequencing of the 18S and 16S rRNA genes to target eukaryotes and cyanobacteria, respectively. The results showed that submersion period was the only significant contributor to community structure. However, at the taxon level, the potentially toxic genus *Anabaena* was found to increase in relative abundance. We also observed that glyphosate releases phosphorus into the surrounding water, but not in a bioavailable form. The results of this study indicate that environmental concentrations of glyphosate do not seem to impact the community composition or metabolism of lake biofilms under pulse event conditions.

Keywords Lake Biofilms; Glyphosate; Cyanobacteria; Submersion Period; Community Composition

1. Introduction

The phosphonate herbicide glyphosate, which is the active ingredient in Roundup®, is currently the most widely used herbicide in the world (Gomes et al., 2016a; Gomes et al., 2016b; Gomes et al., 2014; Vera et al., 2014; Vera et al., 2010). In 2014, worldwide glyphosate use was 825 803 tons, 90.4% of which was used in an agricultural context (Benbrook, 2016). The development of genetically modified crops designed to make them resistant to glyphosate has increased the use of the herbicide. Glyphosate is also used in urban and household settings, exacerbating its exposure potential (Benbrook, 2016).

Glyphosate is a broad spectrum, non-selective systemic herbicide (Gomes et al., 2016b; Vera et al., 2010). Its principal mode of action is the inhibition of the synthesis of the 5-enolpyruvylshikimate-3-phosphate synthase (EPSPS), an enzyme involved in the biosynthesis of the essential aromatic amino acids phenylalanine, tyrosine, and tryptophan (Gomes et al., 2014; Pérez et al., 2007). Because of its short half-life, glyphosate can be rapidly degraded by microbes to aminomethylphosphonic acid (AMPA), a metabolite that can interfere with the biosynthesis of chlorophyll (Gomes et al., 2014). Glyphosate-based herbicides are typically sprayed on seedlings in the spring but may also be applied to crops prior to harvest (Benbrook, 2016). This herbicide is, thus, subject to leaching into streams and rivers, leading to pulse exposure in aquatic organisms.

In aquatic ecosystems, periphytic biofilms, or periphyton, often contain photosynthetic organisms that contribute significantly to primary production in lakes and streams (Battin et al., 2016; Stevenson et al., 1996; Wetzel, 1983; Wetzel, 1993). They are also biogeochemical drivers of contaminant cycling, because they include phototrophic, heterotrophic, and even chemotrophic organisms (Desrosiers et al., 2006; Hamelin et al., 2011; Lazaro et al., 2013; Leclerc et al., 2015; Montuelle et al., 2010). These biofilms are a complex assemblage of living and dead bacteria, algae, and fungi embedded in a polysaccharide matrix that also includes organic and inorganic particles (Wetzel, 1983). These communities are attached to submerged surfaces such as plants, rocks, and sediments. Periphytic biofilms are often the first communities to be in direct contact with runoff. Cyanobacteria are ubiquitous members of freshwater biofilms, and certain members of this bacterial phylum have the ability to degrade glyphosate and use it as a source of phosphorus, which constitutes 18.2% of glyphosate's molecular weight

(Forlani et al., 2008; Lipok et al., 2007; Vera et al., 2010). Biofilms are one of the most significant microbial communities at the base of food webs in shallow lakes (Vadeboncoeur & Steinman, 2002). Thus, adverse effects on upper trophic levels could occur if the structure and function of these periphytic biofilms are negatively impacted by the toxic effects of glyphosate or by its use as a source of phosphorus. Glyphosate and AMPA can, therefore, alter freshwater food webs and fish stocks by affecting periphytic biofilms when they are leached into lakes and rivers.

At early colonization stages, biofilms can be seen as open systems with low levels of nutrients and carbon internal recycling. Early organisms, both autotrophs and heterotrophs, thus, remain dependent on the availability of nutrients in the water column (Hagerthey et al., 2011). At more mature colonization stages, microscopic ecological niches are created and nutrient exchanges with the water column decrease (Hagerthey et al., 2011; Wetzel, 1993). In mature biofilms, communities are, therefore, more protected from external stressors (Lozano et al., 2018; Tlili et al., 2011). This protection can be explained by the fact that as colonization proceeds, the production of extracellular polymeric substances (EPS) by algae and bacteria, including polysaccharides, might increase, forming a barrier to the surrounding water (Ivorra et al., 2000). However, little is known about the importance of the colonization stages of biofilms in lakes. Studies have also shown that some pesticides and metals can alter the function and composition of periphytic communities, based on the assumption that, within biofilms, different species show distinct levels of sensitivity to these contaminants (Lavoie et al., 2012; Schmitt-Jansen & Altenburger, 2005; Tlili et al., 2010). Even if some studies have assessed the effects of glyphosate on periphytic biofilms (Lozano et al., 2018; Pérez et al., 2007; Vera et al., 2014; Vera et al., 2010), its impact on community composition has mainly been evaluated through microscopic techniques (Lozano et al., 2018; Pérez et al., 2007; Smedbol et al., 2018; Vera et al., 2010).

The objective of this study was to identify the factors that shape the community composition of natural lake biofilms under a glyphosate pulse stress. We hypothesized that (1) mature biofilms would be less adversely impacted by glyphosate exposure because their exchanges with the water column are limited, and that (2) glyphosate exposure would shape community composition because of the varying sensitivities amongst species. To test these two hypotheses, microcosm experiments were conducted to assess the effects of glyphosate on the

community composition of natural lake periphytic biofilms grown on artificial substrates at different stages of colonization (i.e., 2 months, 1 year, and 20 years). In addition to glyphosate treatments, some biofilms were also exposed to equivalent concentrations of phosphorus to compare the amount of phosphorus potentially available for algal growth in both types of exposure. Chlorophyll *a* content was used to assess the adverse impacts of glyphosate and community composition was determined using 18S and 16S rRNA gene analysis to target eukaryotes and cyanobacteria, respectively. To our knowledge, this was the first study to use such contrasting colonization stages, hereafter referred to as biofilm age.

2. Materials and methods

2.1 Study area and sampling

Biofilms were grown *in situ* on Teflon® artificial substrates in Lake Croche (0.179 km²; 45°59'N, 74°01'W), an oligotrophic Precambrian Shield lake (Desrosiers et al., 2006; Leclerc et al., 2015; Perron et al., 2014). This lake was considered to be free from prior pesticide exposure, as it is geographically isolated from agricultural lands. Thus, biofilms were not exposed to glyphosate during colonization. Substrate setups (Fig. S1) were installed as described by Desrosiers et al. (2006) and submerged for two months (19 July 2016–11 September 2016), 1 year (20 October 2015–21 September 2016) and 20 years (1996–2016), allowing differential colonization in terms of community structure and thickness. As Teflon is an inert substrate that favours exchanges between the biofilms and their environment, the use of such artificial substrates lessens perturbations of the community, allowing it to maintain its integrity (Desrosiers et al., 2006). Substrate setups were anchored with a clay brick at 1 m depth in the littoral zone. On the day of substrate harvesting, the colonized round mesh disks (9.6 cm² surface area; 70 µm pore size) were removed from the supporting structure and kept in filtered (0.45 µm) lake water. Mesh disks and their biofilms were stored in the dark at low temperature during transport to the laboratory.

2.2 Experimental design

Three distinct pulse experiments were conducted for each different biofilm age (submersion periods of 2 months, 1 year, and 20 years). Pulse experiments were chosen over chronic exposure to mimic episodic runoff events following the application of glyphosate. For each experiment, colonized mesh disks were placed in round Pyrex® dishes (1-L capacity) filled with 600 mL of filtered (0.45 µm) lake water. Biofilms were acclimated to experimental conditions for 24 h before the addition of glyphosate or phosphorus. Biofilms were exposed to different initial concentrations of technical grade glyphosate PESTANAL® (Sigma-Aldrich, St.

Louis, Missouri, USA); 99.7% purity; CAS: 1071-83-6) or phosphorus as KH₂PO₄ (Bregnard et al., 1996) for a period of 7 d (Fig. S2). Duration of exposure was chosen given preliminary results according to which only 30% of 2.5 mg/L glyphosate remained after 48 h under the same experimental conditions (Fig. S3). We chose to directly assess the effects of the active ingredient rather than a commercial formulation, because the latter contains a mixture of additives that can alter glyphosate's toxicity (Vera et al., 2014). Treatments were performed in triplicate, for a total of 21 microcosms per experiment (Fig. S2). Experimental treatments are described in Table 1. Nominal initial concentrations of glyphosate were accurately measured in a preliminary study we conducted in 2015 under the exact same experimental conditions (Fig. S4). In a survey of Quebec streams and rivers, Giroux (2015) synchronized their sampling with the beginning of agricultural activities and the rainy season, as pesticides are subject to leaching to lakes and rivers following heavy rains. The highest glyphosate concentration they detected in an agricultural watershed was 6 µg/L. Because this concentration is much lower than most concentrations tested in the literature (Pérez et al., 2007; Smedbol et al., 2018; Vera et al., 2014; Vera et al., 2010), we chose it as our lowest glyphosate treatment level (Table 1).

Table 1. Name, nominal concentration and description of each treatment. Nominal initial concentrations of glyphosate were accurately measured in a preliminary study conducted in 2015 under the exact same experimental conditions.

Treatment	Nominal concentration	Description
Control	NA	No addition of glyphosate or phosphorus
G1	6 µg/L of glyphosate	Maximum concentration measured in the watershed of the Saint Lawrence River between 2011 and 2014 (Giroux, 2015).
G2	65 µg/L of glyphosate	Water quality guideline for the protection of aquatic wildlife in Quebec (Giroux, 2015).
G3	600 µg/L of glyphosate	100 times the maximum environmental concentration.
P1	1 µg/L of phosphorus	Concentration equivalent to the amount of phosphorus in G1.
P2	12 µg/L of phosphorus	Concentration equivalent to the amount of phosphorus in G2.
P3	110 µg/L of phosphorus	Concentration equivalent to the amount of phosphorus in G3.

Note: Nominal initial concentrations of glyphosate were accurately measured in a preliminary study we conducted in 2015 under the exact same experimental conditions.

The microcosms were randomly distributed and incubated in a growth chamber at 23 °C, which was the temperature measured in the lake when biofilms were harvested on 31 August 2016 (average pH = 7.45 and conductivity = 9.5 µS/cm²). The day:night cycle was set to 14 h:10 h, according to illumination hours on this same day. These temperature and light parameters were maintained throughout the experiments. Constant oxygenation in the microcosms was ensured using an air pump system connected to air stones. We sampled water and periphyton from the microcosms at the very beginning of the experiment (T0), and after three (T3) and 7 d (T7).

2.3 Periphyton analysis

Two mesh disks were sampled from each microcosm on T0, T3, and T7. These two disks were brushed, pooled, and suspended in filtered (0.45 µm) lake water. Following stirring and homogenization, the suspension was subsampled and several parameters were measured.

2.3.1 Chlorophyll a (Chla)

For Chla analysis, 500 µL of the periphyton suspension was filtered on GF/F glass microfibre Whatman[©] filters (Whatman International Ltd., Maidstone, England) and kept frozen (-80 °C) until extraction with hot 90% ethanol (Nusch, 1980). Extracts were kept at 4 °C overnight and absorbance values were measured before and after acidification (0.01 mL HCl 1 mol/L per 1 mL of extract) at 665 nm (A_{665}) and 750 nm (A_{750}) (Spectronic Unicam UV300 UV-Visible Spectrometer (Thermo Spectronic, Rochester, New York, USA)). Surface-normalized Chla concentrations ($\mu\text{g}\cdot\text{cm}^{-2}$) were calculated according to the following equation for each sample:

$$[\text{Chla}] = (29.5(A_b - A_a)v^*E)/(L^*S) \quad (1)$$

Where $A_b = (A_{665} - A_{750})$ before acidification, $A_a = (A_{665} - A_{750})$ after acidification, v = extraction volume (mL), E = total sample suspension volume/filtered subsample volume (L), L = spectrophotometer cell length (cm) and S = mesh disk surface that was brushed (cm^2).

2.3.2 DNA extraction and sequence analyses

Nucleic acid extraction was performed on lyophilized biofilm samples using the DNeasy Plant Mini Kit (QIAGEN, Hilden, Germany) following the manufacturer's instructions. Library preparation for 16S and 18S rRNA was done using Nextera XT (Illumina Inc., San Diego, California, USA), and next-generation sequencing was performed on an Illumina MiSeq

(Illumina Inc., San Diego, California, USA). Reads were quality checked with FastQC (Andrews, 2010), reads were filtered with FASTX-Toolkit (Gordon, 2009) and BBMap (Bushnell, 2014), and chimeras were removed with UCHIME (Edgar et al., 2011) in VSEARCH (Rognes et al., 2016). Operational taxonomic unit (OTU) picking (Greengenes version 13_8, 97% identity) was performed in QIIME (Caporaso et al., 2010). OTU tables were rarefied to 4000 and 10 000 sequences per sample for cyanobacteria-specific 16S and eukaryotic 18S, respectively. After quality filtering and rarefaction, we had 44 samples containing 916 OTUs for cyanobacteria and 49 samples containing 1920 OTUs for eukaryotes. Beta diversity analyses were performed with weighted and unweighted UniFrac (Lozupone & Knight, 2005; Lozupone et al., 2011) as a distance metric in R (RCoreTeam, 2016) using the phyloseq package (McMurdie & Holmes, 2013). UniFrac uses distances between samples on a phylogenetic tree, either accounting for the relative abundance of OTUs (weighted) or not (unweighted). Community compositions among the different submersion periods were assessed. For full sequencing and read processing methods, see the Supplementary Methods (SM.1). Sequences were submitted into the Sequence Read Archive (SRA) database (National Center for Biotechnology Information (NCBI)) (SRA accession SRP150239, BioProject PRJNA475256).

2.3.3 Essential aromatic amino acids

Aromatic amino acids (phenylalanine, tryptophan, and serine) concentrations were measured in 20-year-old biofilms exposed to glyphosate for 7 d using an Agilent 6430 triple quadrupole (QQQ)-LC-MS/MS (Santa Clara, California, USA) in a preliminary experiment we performed in 2015. For a detailed description of the analysis, refer to the Supplementary Methods (SM.2).

2.4 Water analysis

Water was sampled in each microcosm for chemical analyses on T0 (immediately after glyphosate and phosphorus additions), T3, and T7. Glyphosate degradation was only determined in herbicide-treated microcosms.

2.4.1 Glyphosate

In 2015, we conducted the same experiment but with 20-year-old periphyton exclusively. During this preliminary study, analyses of glyphosate and AMPA were conducted by a provincial government laboratory. Glyphosate and AMPA were analyzed by liquid chromatography, post-column derivation, and fluorescence detection, with a detection limit of 0.08 µg/L for glyphosate and 0.4 µg/L for AMPA (CEAEQ method MA. 403—GlyAmp 1.0 2011-03-07) (CEAEQ, 2008). In 2016, glyphosate enzyme-linked immunosorbent assay (ELISA) test kits were purchased from Abraxis LLC (Warminster, Pennsylvania, USA) and used following the manufacturer's instructions. The method detection limit (MDL) and the limit of quantification (LOQ) as defined by Abraxis were 0.05 µg/L and 0.15 µg/L, respectively. Derivatized standard and control solutions were used every 12 samples to ensure analytical quality. Although the former analytical method allowed us to measure accurate glyphosate concentrations, we used the latter to show loss patterns.

2.4.2 Phosphorus

Total phosphorus (TP), dissolved phosphorus (DP), and orthophosphate levels were analyzed by flow injection analysis (Astoria2 Analyzer, Astoria-Pacific, Clackamas, Oregon, USA). Orthophosphates represent the phosphorus species that is most readily utilized by biota (Gaffney et al., 2001). Reactive phosphorus in our experiments was, thus, measured as orthophosphates, which provide a fair estimation of the amount of phosphorus available for algal growth (Carignan & Neiff, 1992; Strickland & Parsons, 1972). We assessed (1) the amount of reactive phosphorus that was released from glyphosate degradation, and (2) whether this reactive phosphorus decreased over time as it was used by periphytic communities (deduced from decreasing concentrations over time). Water was filtered through 0.45 µm membrane filters for DP and orthophosphate analysis. TP and DP samples were analyzed after persulfate digestion in an autoclave. Orthophosphate samples were pre-acidified with 0.01 mol/L HCl (ACS grade, Fisher Scientific, Hampton, New Hampshire, USA) (Carignan & Neiff, 1992). Wash and standard solutions were used every 10 samples to ensure analytical quality.

2.5 Statistical analyses

For Chla and phosphorus results, concentrations for all treatments (Control, G1, G2, G3, P1, P2, and P3) and each sampling time (T0, T3, and T7) were compared using two-factor analysis of variance (two-way ANOVA). When required, Dunnett's or Tukey's post hoc tests were used for multiple comparisons. Multiple *t* tests were used for reactive and total dissolved phosphorus concentrations. Multiple comparisons were corrected using the Holm–Sidak method, computing adjusted *p* values. Prior to the analyses, normality and homoscedasticity were verified and data were log+1 transformed when these assumptions were not satisfied. Significance level was set at *p*<0.05. GraphPad Prism 7 (GraphPad Software Inc., La Jolla, California, USA) was used for statistical analyses.

Principal coordinate analyses (PCoA) for 16S and 18S data from UniFrac distance matrices were calculated and visualized using the phyloseq (McMurdie & Holmes, 2013) and ggplot2 (Wickham, 2009) packages in R (RCoreTeam, 2016). Sample clustering hypotheses were tested using a permutational multivariate analysis of variance (permanova, *adonis()*) in vegan (Oksanen et al., 2016), as this test has been proven to be more powerful in detecting differences in community structure even when group dispersions are heterogeneous (Anderson & Walsh, 2013). Homogeneity of dispersion among sample groups was assessed using *betadisper()* in vegan.

3. Results

3.1 Glyphosate concentrations

Biofilms of three different ages collected on artificial substrates were exposed to increasing concentrations of glyphosate. Our results showed that glyphosate concentrations in water decreased throughout all experiments by 55% to 100%, with no glyphosate remaining in the G1 series for all biofilm ages (Figs. 1a–1c). We also observed a slower relative rate of loss of glyphosate (average of 8.7% per day) at high concentrations (G3) compared with lower concentrations (G1) (average of 14.2% per day) (Figs. 1a–1c). For all three experiments, in the 65 (G2) and 600 $\mu\text{g/L}$ (G3) treatments (Figs. 1a–1c), periphyton was exposed to the herbicide throughout the experiment. The same loss pattern was observed in a preliminary experiment we conducted in 2015 with 20-year-old biofilms under the same experimental conditions and for which absolute concentrations were measured (Fig. S4). This 2015 preliminary study also confirmed that our initial concentrations were accurate, as we repeated the same glyphosate additions in 2016.

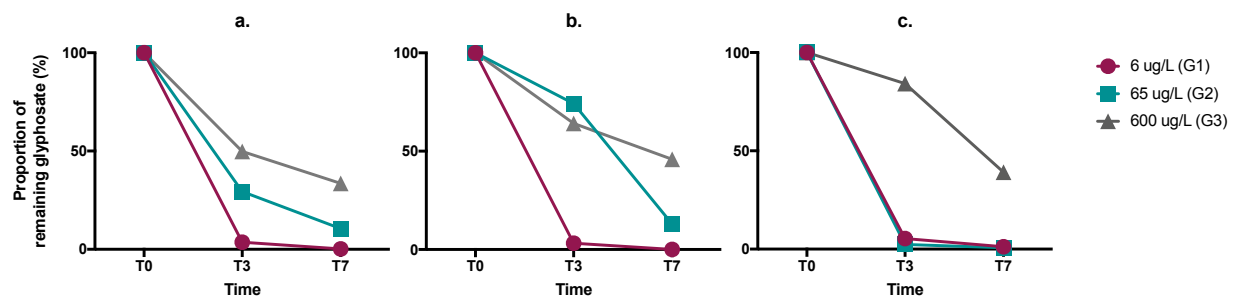


Figure 1. Proportion of remaining glyphosate in the water for each treatment over time. (a) 2-month-old periphyton, (b) 1-year-old periphyton, and (c) 20-year-old periphyton.

3.2 Dissolved and reactive phosphorus

One of our main objectives was to compare the amount of phosphorus potentially available for algal growth in the glyphosate and phosphorus treatments. Only G3 and P3 treatments were plotted (Fig. 2) because orthophosphate concentrations were often low in the other treatments. The results showed that at the beginning of the experiment (T0), shortly after phosphorus was added, the amount of reactive phosphorus was about 300 times higher in the P3 treatment than in the G3 treatment. There were no significant changes in reactive phosphorus concentrations in the G3 treatment for all three experiments. However, the decrease in reactive phosphorus was significant in the P3 treatment between T0 and T7 (t test, $p_{\text{adj}} < 0.0005$). This was also the case in the P3 treatment between T0 and T7 for the 2-month-old biofilms (t test, $p_{\text{adj}} < 0.01$) and between T0 and T3 for the 1-year-old biofilms (t test, $p_{\text{adj}} < 0.000005$) (data not shown). Dissolved phosphorus concentrations did not vary significantly in the G3 treatment, but did in the P3 treatment, between T0 and T7 (t test, $p < 0.0005$). However, the herbicide appears to release a significant amount of total dissolved phosphorus, at concentrations similar to those measured at T0 in the P3 treatment.

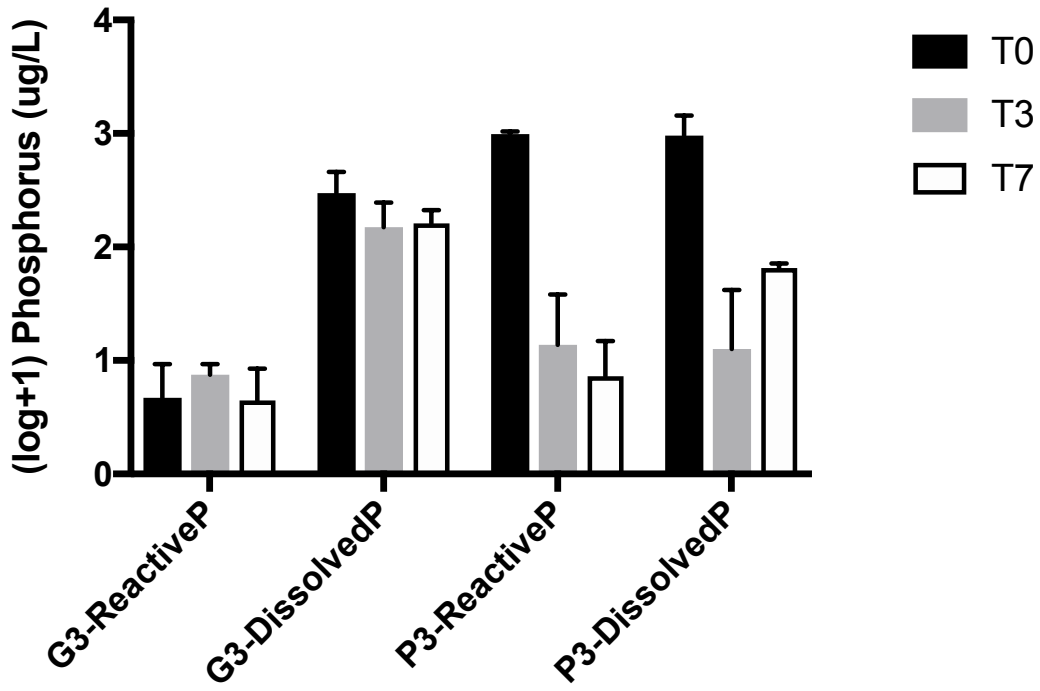


Figure 2. Reactive and total dissolved phosphorus (P) concentrations in the water throughout the experimental period for the glyphosate (G3) and P3 treatments in microcosms containing 20-year-old periphyton. Error bars represent the standard error of the mean (SEM) ($n = 3$). Data are log+1 transformed. T value is the sampling time in number of days.

3.3 Chlorophyll *a*

There was no significant decrease in Chla concentrations for all three submersion period experiments. The duration of exposure or treatment had no significant effect on Chla for 2-month-old (Fig. 3a) and 1-year-old periphyton (Fig. 3b) ($p > 0.05$) (two-way ANOVA). As shown in Fig. 3c, the effect of time was significant for the oldest biofilms (two-way ANOVA, $p < 0.0001$). However, the effect of treatment was not significant and there was no interaction between treatment and time on Chla ($p > 0.05$). For all treatments (Fig. 3c), there

was a significant increase between T0 and T3 and between T0 and T7 (Tukey's honest significant difference following two-way ANOVA) (Table S1).

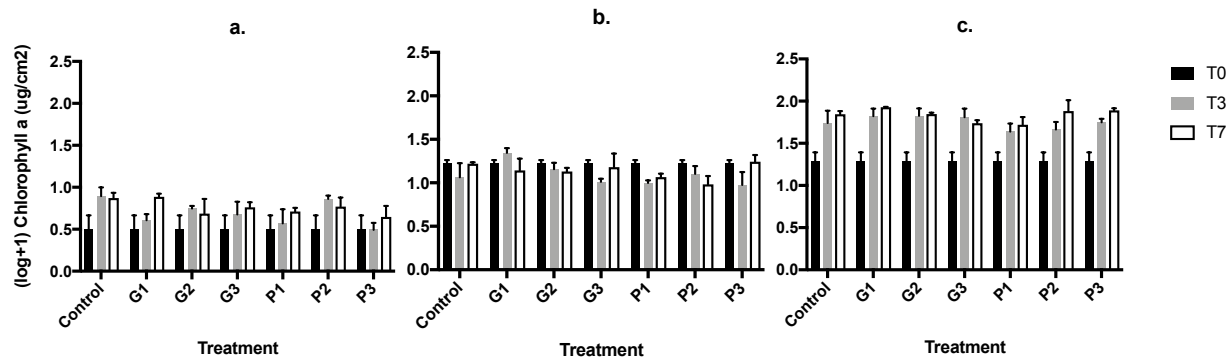


Figure 3. Impact of glyphosate (G1, G2, and G3) and phosphorus (P1, P2, and P3) on chlorophyll *a*. (a) 2-month-old periphyton, (b) 1-year-old periphyton, and (c) 20-year-old periphyton. Data are log+1 transformed. Error bars represent the standard error of the mean (SEM) ($n = 3$). T value is the sampling time in number of days.

3.4 Community composition

Using the unweighted distance metric UniFrac in beta diversity analyses, we found a significant clustering of samples by periphyton age, explaining 37% of the variation in community composition for cyanobacteria (adonis, $p = 0.001$) and 26% for eukaryotes (adonis, $p = 0.001$) (Fig. 4). Unweighted UniFrac is a presence/absence information analysis, rather than a relative abundance analysis (weighted UniFrac). We assessed both distance metrics, but cluster discrimination was sharper with unweighted UniFrac for eukaryotes (Fig. 4) (the results of the weighted UniFrac analyses are shown in Fig. S5). Multivariate dispersion was also significant for periphyton age (betadisper, $p = 0.000525$ and $p = 0.0013$ for cyanobacteria and eukaryotes, respectively), with greater dispersion within the 20-year-old samples for cyanobacteria and within the 2-month-old samples for eukaryotes. Treatment and sampling time did not significantly explain the variance in beta diversity for both weighted and unweighted analyses.

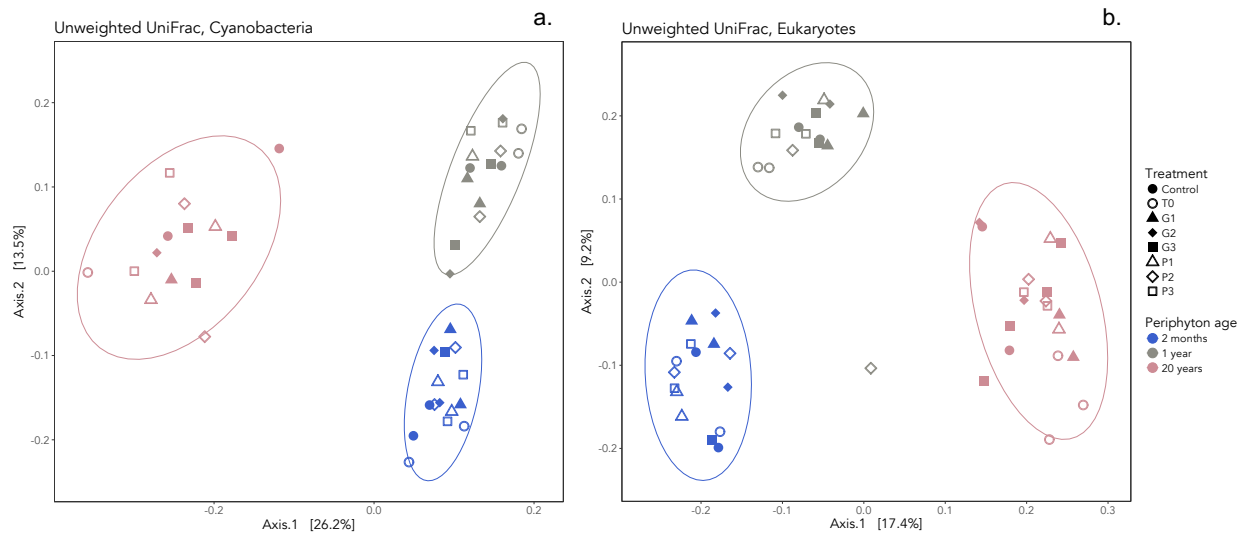


Figure 4. Principal coordinates analysis of unweighted UniFrac distances. Community composition clusters by periphyton age for (a) cyanobacteria (permanova $R^2 = 0.366, p = 0.001$) and (b) eukaryotes (permanova $R^2 = 0.248, p = 0.001$). T0, beginning of the experiment; G, glyphosate treatment; P, phosphorus treatment.

Following this community composition analysis, we assessed the relative abundance of the cyanobacterial genera *Anabaena* and *Microcystis* (Fig. 5) for control, G3, and P3 treatments throughout the experiment. This relative abundance was assessed as a fraction of the rarefied number of sequences/sample for 16S. Results show that, compared with the control and P3 treatments, the relative abundance of *Anabaena* increased in the G3 treatment between T0 and T7. In contrast, the relative abundance of *Microcystis* decreased between T0 and T3 for all three treatments and a slight increase was then observed between T3 and T7.

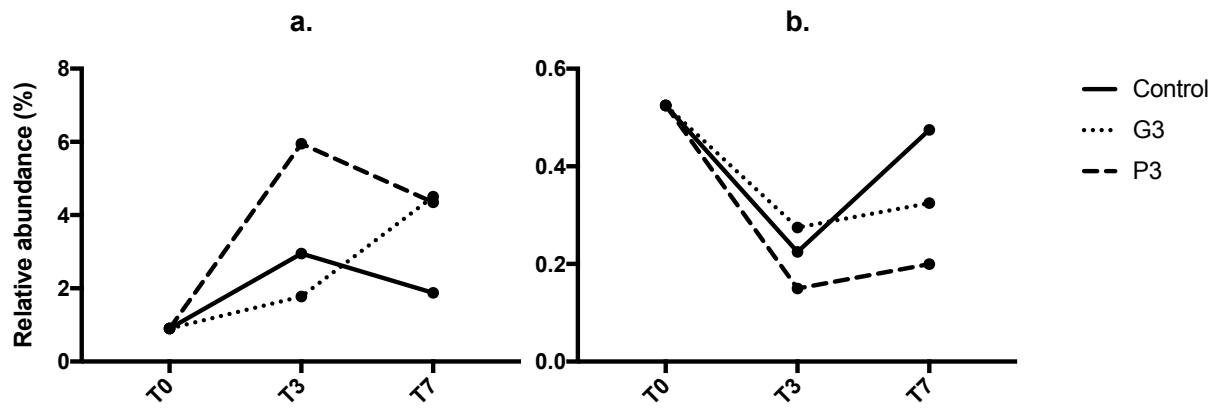


Figure 5. Relative abundance of genera (a) *Anabaena* and (b) *Microcystis* for 1-year-old periphyton in control, glyphosate (G3), and phosphorus (P3) treatments throughout the experiment ($n = 1$). T value is the sampling time in number of days.

4. Discussion

4.1 Environmentally relevant glyphosate concentrations are lost from water within 7 days under our experimental conditions

Our results showed that local environmentally relevant concentrations of glyphosate degrade entirely within 7 days, diminishing the exposure of aquatic organisms to the herbicide. This contrasts with the work of (Vera et al., 2010), who exposed periphytic communities to 8 mg/L of glyphosate and estimated a half-life of 4.2 days. This difference could be because of the fact that the latter experiment was conducted in large outdoor mesocosms with well-established bacterial communities in the water column. We attribute the observed degradation to the bacteria and fungi present in the biofilms, because glyphosate appears to be resistant to photodegradation (Aparicio et al., 2013). It is also possible that the microcosms' filtered (0.45 µm) lake water still contained bacteria that could have contributed to glyphosate degradation. Preliminary results from our 2015 experiment showed that in microcosms where periphyton was exposed to 600 µg/L, AMPA was detected at low concentrations (6–7 µg/L) at T3 and T7 (Fig. S6), implying degradation. However, the loss of glyphosate that we observed could also be due to other mechanisms such as adsorption and (or) uptake by biofilms (Bengtsson et al., 2004; Evans-White & Lamberti, 2009; Van den Brink et al., 2009). This uptake could be influenced by periphyton total biomass, which increases with submersion period, explaining differences in the loss of glyphosate in water between experiments. Even if glyphosate uptake was not directly measured, our results clearly showed that G1 and G2 initial concentrations decreased below our detection limit after 3 days in the 20-year-old biofilm experiment. Adsorption to the container walls could also explain glyphosate elimination from the water.

Our results also showed that after 7 days, biofilms from the G3 treatment were still exposed to relatively high concentrations of glyphosate. It is known that exposure of aquatic organisms to pesticides increases very rapidly following rainfall events and can reach relatively high concentrations during flood events (Tlili et al., 2008). Peruzzo et al. (2008) sampled water, sediments, and soil after glyphosate application and rain events in an agricultural area in

Argentina. The highest glyphosate concentrations in the water samples were measured right after the first significant rain event, reaching a maximum of 700 µg/L (Peruzzo et al., 2008). This level is comparable with our highest treatment, in which we measured the slowest relative rate of loss. Our experimental design, therefore, seems to accurately mimic short-term pulses following glyphosate application, suggesting that significant leaching or flooding due to heavy rains immediately following glyphosate spraying could potentially lead to significant exposure in aquatic biota. Glyphosate application frequency per season and the occurrence of heavy rain events, therefore, play a crucial role in understanding the consequences of pulse exposure on biological populations.

4.2 Glyphosate is a source of phosphorus but not in a bioavailable form

In aquatic ecosystems and soils, glyphosate is rapidly and completely degraded by microorganisms to water, carbon dioxide, and inorganic phosphate (Aparicio et al., 2013). Two main pathways were identified for glyphosate degradation, both resulting in the breakage of the molecule's C–P bond. In the first pathway, the herbicide is degraded to AMPA and glyoxylate through the activity of a glyphosate oxidoreductase. AMPA is then either directly metabolized to methylamine and orthophosphate or acetylated prior to the cleavage of the C–P bond (Forlani et al., 2008). In the second pathway, this cleavage is caused by a C–P lyase complex, leading to the release of purines and amino acids (Aparicio et al., 2013). Although the amount of total phosphorus released by glyphosate through this C–P cleavage has been reported in the literature (Gomes et al., 2016b; Lipok et al., 2007; Vera et al., 2014; Vera et al., 2010), dissolved reactive phosphorus has never been considered. Our results showed that glyphosate releases a significant amount of phosphorus into surrounding waters, but that this phosphorus does not seem to be bioavailable to biofilms. In fact, the amount of reactive phosphorus that was released while glyphosate was lost from water was low and did not decrease over time, implying that it was not used by periphytic communities.

In aquatic ecosystems, cyanobacteria play a major role in both carbon and nitrogen cycling, being the only prokaryotes capable of oxygenic photosynthesis and having the ability to fix atmospheric N₂. Some strains of cyanobacteria have also been identified to exhibit a

natural tolerance to glyphosate (Powell et al., 1991). Forlani et al. (2008) studied the ability of six strains of cyanobacteria to use glyphosate as a sole source of phosphorus. They found that four strains (*Anabaena*, *Leptolyngbya*, *Microcystis*, and *Nostoc*) out of six were able to grow on a medium that contained the herbicide as the only phosphorus source. Because they did not observe any release of inorganic phosphorus, the hypothesis that these cyanobacteria were able to hydrolyze the glyphosate molecule C–P’s bond was rejected. We observed an increase in the relative abundance of the glyphosate-resistant strain of the cyanobacterial genus *Anabaena* in comparison with the control as well as a slight increase in *Microcystis* between T3 and T7. Because we were able to detect low amounts of AMPA (Fig. S6) in our 2015 experiment under the same conditions, as well as low amounts of orthophosphates in the current study, we hypothesize that the cyanobacteria of the biofilms were able to degrade glyphosate *via* the first pathway.

Microcystis and *Anabaena* are globally detected in toxic blooms (Bláha et al., 2009; Chalifour et al., 2016; Yoshida et al., 2008), raising concern regarding the use of glyphosate, as this herbicide favours the growth of certain taxa even in the absence of bioavailable phosphorus. Vera et al. (2010) added 8 mg/L glyphosate as Roundup® to outdoor mesocosms with periphyton. After 3 d and 8 d, they measured approximately 800 µg/L TP, as this concentration did not vary significantly between the two sampling times. The input of total phosphorus through the addition of glyphosate is, therefore, fairly substantial, as was also shown by our results (Fig. S7). Vera et al. (2010) concluded that glyphosate might promote eutrophication in aquatic systems, favouring potentially toxic cyanobacterial blooms. This contradicts our results, as we found that this phosphorus input is not available to biofilms. However, it is possible that cyanobacteria could, in fact, use this phosphorus as a nutrient source, but that their number was not great enough in our biofilms. This could partially explain the absence of significative decreases in reactive and dissolved phosphorus for the G3 treatment.

4.3 Chlorophyll *a* and essential aromatic amino acid contents are not adversely impacted by glyphosate in biofilms

Because of its short half-life, glyphosate is rapidly degraded to AMPA, which is known to alter the biosynthesis of chlorophyll (Gomes et al., 2016a). Furthermore, we hypothesized that young biofilms would be more sensitive to glyphosate than mature biofilms because in older biofilms, microscopic niches are created and nutrient exchanges with the water column decrease, thus offering protection from external stressors. However, we did not observe any significant decrease in Chla content for any of the three submersion period experiments. This absence of adverse effect was also observed by Lozano et al. (2018) who exposed 60-day-old periphytic biofilms to 3 mg/L of pure glyphosate in microcosm experiments. After a colonization period of 60 days, biofilms developed a sufficiently consolidated matrix, limiting contact between the organisms and glyphosate. This latter hypothesis is consistent with our results, as our youngest biofilms were also 60 days old. It has been established that the main degradation product of glyphosate, AMPA, can alter the biosynthesis of Chla in plants (Gomes et al., 2016a; Gomes et al., 2014). To our knowledge, the adverse effects of AMPA on periphyton have yet to be explored. Preliminary results from our 2015 experiment showed that in microcosms where periphyton was exposed to 600 µg/L, AMPA was detected at low concentrations (6–7 µg/L) at T3 and T7 (Fig. S6). However, Gomes et al. (2016a) observed an adverse effect on Chla metabolism in willow plants at AMPA concentrations >3 g/L. Vera et al. (2010) and Pérez et al. (2007) also observed a decrease in Chla concentrations in periphyton exposed to 6–12 mg/L of glyphosate. These concentrations are between 10 and 100 times higher than the environmental concentrations that we tested, which might explain the absence of any observed adverse effect on Chla. Moreover, these two studies assessed the effects of the commercial formulation Roundup® rather than the active ingredient, also contrasting with our experimental design. Indeed, it has been shown that polyethoxylated tallowamine (POEA), the surfactant typically used in Roundup®, is more toxic than glyphosate itself (Struger et al., 2008).

In contrast with what we expected, we observed a significative increase in Chla for the 20-year-old periphyton, which is consistent with the work by Vera et al. (2014), who observed

an increase in Chla content in periphyton exposed to 3 mg/L glyphosate. Vera et al. (2014) tested both the active ingredient and a commercial formulation and did not detect any significant difference. Glyphosate triggered pathways for the synthesis of proteins and metabolites involved in stress response, favouring growth and Chla biosynthesis. According to Vera et al. (2014), it is also possible that the herbicide was used as a source of nutrients by some species of cyanobacteria, also stimulating growth, as shown by Forlani et al. (2008). Because the increase that we measured in the glyphosate treatments was also observed in the control, the experimental effect hypothesis cannot be excluded. However, the most significant increase we observed was between T0 and T7 in the G1 treatment (Table S1).

The principal mode of action of glyphosate is the inhibition of the synthesis of the enzyme EPSPS in plants, which is involved in the biosynthesis of the essential aromatic amino acids phenylalanine, tyrosine, and tryptophan (Gomes et al., 2014). Because this effect had never been assessed in periphytic biofilms, we measured these amino acid concentrations in 20-year-old biofilms exposed to glyphosate for 7 days in the preliminary experiment that we conducted in 2015 (SM.2). However, we did not detect any adverse effects of glyphosate on the metabolism of essential aromatic amino acids in biofilms (Fig. S8). We, therefore, infer that glyphosate might not impact the biosynthesis of amino acids at a community level, but future work should consider the effects on specific populations within the biofilms.

4.4 Microbial communities are more influenced by biofilm age than glyphosate exposure

We assessed the community composition of contrasting biofilm ages using specific primers that target cyanobacteria. Even at concentrations 100 times higher than local environmental levels, glyphosate did not significantly disrupt periphytic communities. Age, in fact, was the only factor that clearly shaped community structure, contradicting our hypothesis. However, we observed an increase in the relative abundance of *Anabaena* in the G3 treatment after 7 days compared with the control (Fig. 5). This taxon has been identified to possess a rare resistant form of the EPSPS enzyme, targeted by the mode of action of glyphosate (Forlani et al., 2008; Powell et al., 1991). In contrast, we found that the relative abundance

of *Microcystis* decreased in the G3 treatment after 3 d but increased slightly between T3 and T7. Even if this taxon does not carry the resistant form of the EPSPS enzyme, Forlani et al. (2008) found that *Microcystis* was able to grow on a medium containing glyphosate as the only phosphorus source. Although our sequencing methods do not allow us to verify the presence of the rare, resistant form of EPSPS identified by Forlani et al. (2008), we think that the increased relative abundance of *Anabaena* after 7 d in the G3 treatment compared with the control shows that it is resistant to glyphosate and favoured by the release of dissolved reactive phosphorus. The absence of a drastic temporal turnover in the community composition of our biofilms may be because of the relatively short duration of our experiments and the relatively low glyphosate levels that we tested. However, this study provides an interesting snapshot of the biological processes related to the exposure of periphytic biofilms to environmental concentrations of glyphosate under pulse event conditions.

Few studies consider the maturation stage and, hence, the stability of biofilms when assessing the effect of chemical contamination. Ivorra et al. (2000) compared the effects of metal contamination on 2- and 6-week-old biofilms. Their hypothesis was that as biofilms develop, internal cycling of materials dominates over diffusion and exchanges with the water column. Moreover, as biofilms mature, EPS production increases, limiting the penetrations of toxicants. Ivorra et al. (2000) found that older biofilms (6 weeks old) were more resistant to metal contamination than younger biofilms (2 weeks old). Guasch et al. (2004) exposed 5-week-old and 6-week-old periphytic communities from an oligotrophic stream to copper for several weeks. Contrary to their predictions, there were no differences in the physiological responses of low and high biomass biofilms exposed to copper (Guasch et al., 2004). These two studies were conducted in streams, where water velocity plays an important role in periphyton thickness and microarchitecture (Battin et al., 2016; Besemer et al., 2012), in contrast with lake biofilms. The more mature biofilms that were studied (6 weeks old) by Ivorra et al. (2000) and Guasch et al. (2004) were also significantly younger and, thus, likely thinner than the ones we exposed in our study (20 years old). Given these two major differences, it is difficult to extrapolate the results of these two studies to our own observations. We, therefore, hypothesize that, in lakes, even younger biofilms (2 months old) are characterized by a thick EPS layer that limits the penetration of glyphosate, thereby preventing its adverse effects.

5. Conclusion

Periphytic biofilms are model communities in ecotoxicological studies, as they are at the base of food webs, are important biogeochemical cyclers in streams and lakes, and are often the first communities to be in direct contact with runoff. This study assessed the effects of technical grade glyphosate on contrasting colonization stages of lake biofilms. The results showed that at levels that are currently detected in eastern Canadian rivers, glyphosate poses little risk for periphyton under pulse event conditions. In fact, no adverse effect was observed on Chla content. The herbicide was also found to release phosphorus in the water, but not in a bioavailable form, limiting uptake by biofilms. Periphyton age was the only factor shaping the community composition of biofilms, suggesting that the EPS layer produced by algae and bacteria was too thick to allow the penetration of glyphosate, even for the younger communities. Age and thickness likely caused important inter-experimental bias, and it is, therefore, critical to consider the colonization stage of biofilms before interpreting ecotoxicological effects. However, we identified an increase in the relative abundance of *Anabaena*, which has been previously found to carry a rare resistant form of the EPSPS enzyme targeted by glyphosate. This highlights the fact that some effects might be detected at a population or taxon scale, but not at a community scale. Future studies should, thus, include specific assessment of glyphosate's toxicity using biomarkers such as reactive oxygen species or enzymes. More attention should also be given to cyanobacteria, as toxic strains seem favoured by the use of the herbicide. As specific primers allowed us to monitor the presence and abundance of cyanobacteria, future studies should focus on elucidating their mechanism of resistance. In conclusion, this study represents a step towards understanding the effects of a non-selective herbicide of rising concern on lake ecosystems.

Acknowledgements

This project was financially supported by a FRQ-NT Programme d'initiatives stratégiques pour l'innovation (ISI) grant to M.A. and D.P, by an NSERC Discovery grant to M.A, and by the Canada Research Chair program to M.A. M.K. received a scholarship through the NSERC CREATE ÉcoLac training program in Lake and Fluvial Ecology. We acknowledge the Integrated Microbiome Resource (IMR) lab at Dalhousie University (Halifax, Canada) for the library preparation of 16S and 18S amplicons, sequencing, and standard bioinformatics analysis pipeline. We acknowledge the Metabolics Core Facility at McGill University (Quebec, Canada) for the amino acid analyses. We are grateful for laboratory assistance from Dominic Bélanger, Jérémie De Bonville, Antoine Caron, Marie-Christine Lafrenière, and Serge Paquet, and field assistance from Jérémie De Bonville and Maxime Leclerc. We acknowledge the staff of the Station de biologie des Laurentides (Université de Montréal) for logistical support.

Supplementary information

Supplementary methods

SM.1. 16S and 18S Amplicons

DNA Extraction and Amplicon Sequencing

Samples were disrupted with a TissueLyser LT (50 1/s oscillations for 15 minutes; QIAGEN) using approximately 100 mg of pre-sterilized glass beads (QIAGEN) per sample. Library preparation and next-generation sequencing were carried out at the Integrated Microbiome Resource at Dalhousie University, Halifax. Library preparation with Nextera XT v2 included 16S V4-V5 and 18S V4 fragments amplification and amplicons were sequenced on an Illumina MiSeq platform (V3 chemistry, 2 x 300 bp). Primers CYA359F (5'-GGG GAA TTT TCC GCA ATG GG-3') and CYA781R (equimolar mixture of CY781R(A) 5'-GAC TAC TGG GGT ATC TAA TCC CAT T-3' and CY781R(B) 5'-GAC TAC AGG GGT ATC TAA TCC CTT T-3') [22] adapted for MiSeq were used for cyanobacteria. Primers E572F (5'-CYG CGG TAA TTC CAG CTC-3') and E1009R (5'-AYG GTA TCT RAT CRT CTT YG-3'). 18S custom primers from that were used for eukaryotes are described in (Comeau et al., 2017). For 51 samples, we obtained 4 029 750 and 3 802 414 raw reads for 16S and 18S, respectively.

Sequence Processing and Analyses

FastQc (v0.11.15) (Andrews, 2010) was used to check the quality of sequenced reads. FASTX- Toolkit (v0.0.14) (Gordon, 2009) was used to remove reads that have more than a specified proportion of low-quality sites (quality score of 30 over at least 90% of the bases) (Comeau et al., 2017). Reads shorter than 400 bp were also filtered. BBMap (v35.85) (Bushnell, 2014) was then used to filter out reads that did not exactly match either the forward or reverse primer sequences. Chimeric sequences were detected and removed using the UCHIME algorithm (Edgar et al., 2011) in VSEARCH (v1.11.11) (Rognes et al., 2016) (mindiv=1.5 and

`minh=0.2`). Open reference OTU (Operational Taxonomic Unit) picking and rarefaction were performed using QIIME (Caporaso et al., 2010) (Greengenes 13_8, 97% identity). OTU tables were rarefied to 4,000 and 10,000 sequences/sample for 16S and 18S, respectively. After quality filtering and rarefaction, we had 44 samples containing 916 OTUs for 16S and 49 samples containing 1920 OTUs for 18S. To perform beta diversity analysis between samples, unweighted UniFrac and weighted UniFrac distances (Lozupone & Knight, 2005; Lozupone et al., 2011) were calculated using the phyloseq package (McMurdie & Holmes, 2013) in R software (RCoreTeam 2016).

SM.2. Amino Acids Analysis

For semi-quantitative concentration determination of amino acids, samples were injected onto an Agilent 6430 Triple Quadrupole (QQQ)-LC-MS/MS. Chromatography was achieved using a 1290 Infinity ultra-performance LC system (Agilent Technologies, Santa Clara, CA, USA) consisting of vacuum degasser, autosampler and a binary pump. Mass spectrometer was equipped with an electrospray ionization (ESI) source and samples were analyzed in positive mode. The authentic metabolite standards were purchase from Sigma-Aldrich Co. (Oakville, Ontario, Canada). Gas temperature and flow were set at 350°C and 10 l/min respectively, nebulizer pressure was set at 40 psi and capillary voltage was set at 3500V. Relative concentrations were determined from external calibration curves. Data were analyzed using MassHunter Quant (Agilent Technologies). Chromatographic separation was performed using an Intrada Amino Acid column 3 µm, 3.0×150mm (Imtakt Corp, JAPAN). The chromatographic gradient started at 100% mobile phase B (0.3% formic acid in ACN) with a 3 min gradient to 27% mobile phase A (100 mM ammonium formate in 20% ACN / 80% water) followed with a 19.5 min gradient to 100% A at a flow rate of 0.6 ml/min. This was followed by a 5.5 min hold time at 100% mobile phase A and a subsequent re-equilibration time (7 min) before next injection. For all LC/MS analyses, 5 µl of sample were injected. The column temperature was maintained at 10°C. LOD were 1.0175×10^{-12} for phenylalanine, 5.085×10^{-14} for tryptophan and 6.51×10^{-12} for tyrosine.

Supplementary tables

Table S1. Adjusted p-values associated to Tukey's multiple comparison post hoc test following a two-way ANOVA on log⁺¹ transformed chlorophyll *a* concentrations for the 20-year-old biofilms. Alpha = 0.05. Significant results are indicated in grey cells.

	T0 vs T3	T3 vs T7	T0 vs T7
Control	p<0.005**	p>0.05	p=0.0005***
G1	p<0.001***	p>0.05	p<0.0001****
G2	p<0.001***	p>0.05	p<0.001***
G3	p=0.001***	p>0.05	p<0.005**
P1	p<0.05*	p>0.05	p<0.01**
P2	p<0.05*	p>0.05	p<0.0005***
P3	p<0.005**	p>0.05	p<0.0005***

Supplementary figures

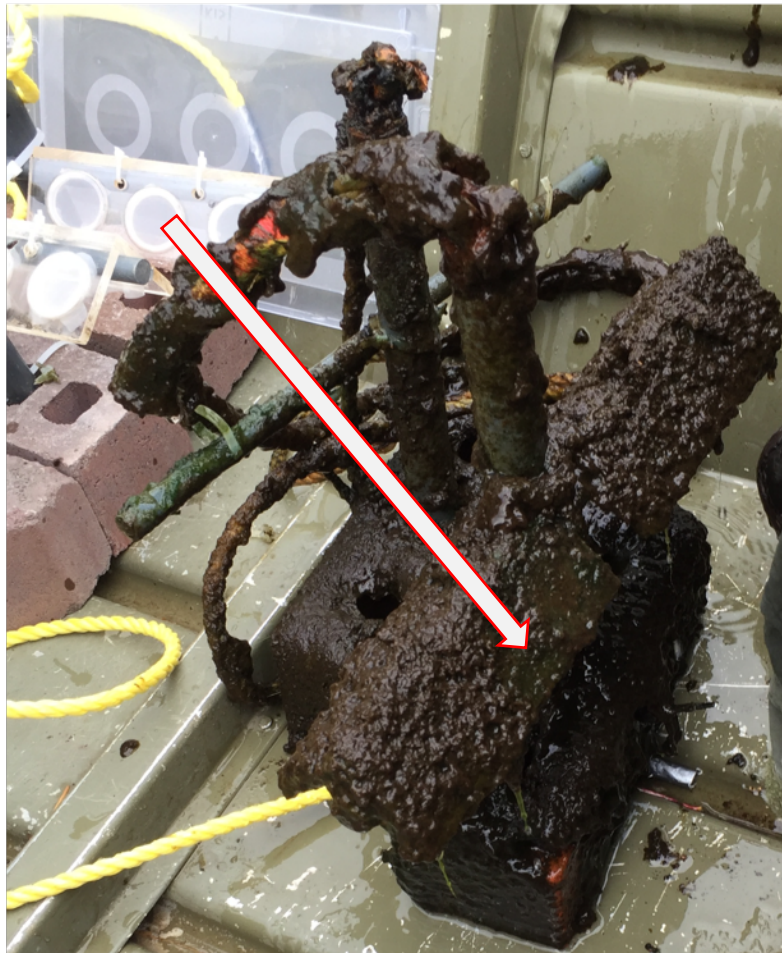


Figure S1. Picture of 20-year-old periphyton on an artificial substrate. Substrate setups are anchored with a clay brick at 1 m depth. Biofilms grow on Teflon mesh disks. Disks are installed on Plexiglas plates at a 45-degree angle. Arrow is pointing from an empty to a colonized disk. A floating rope is attached at the top to facilitate location and sampling.

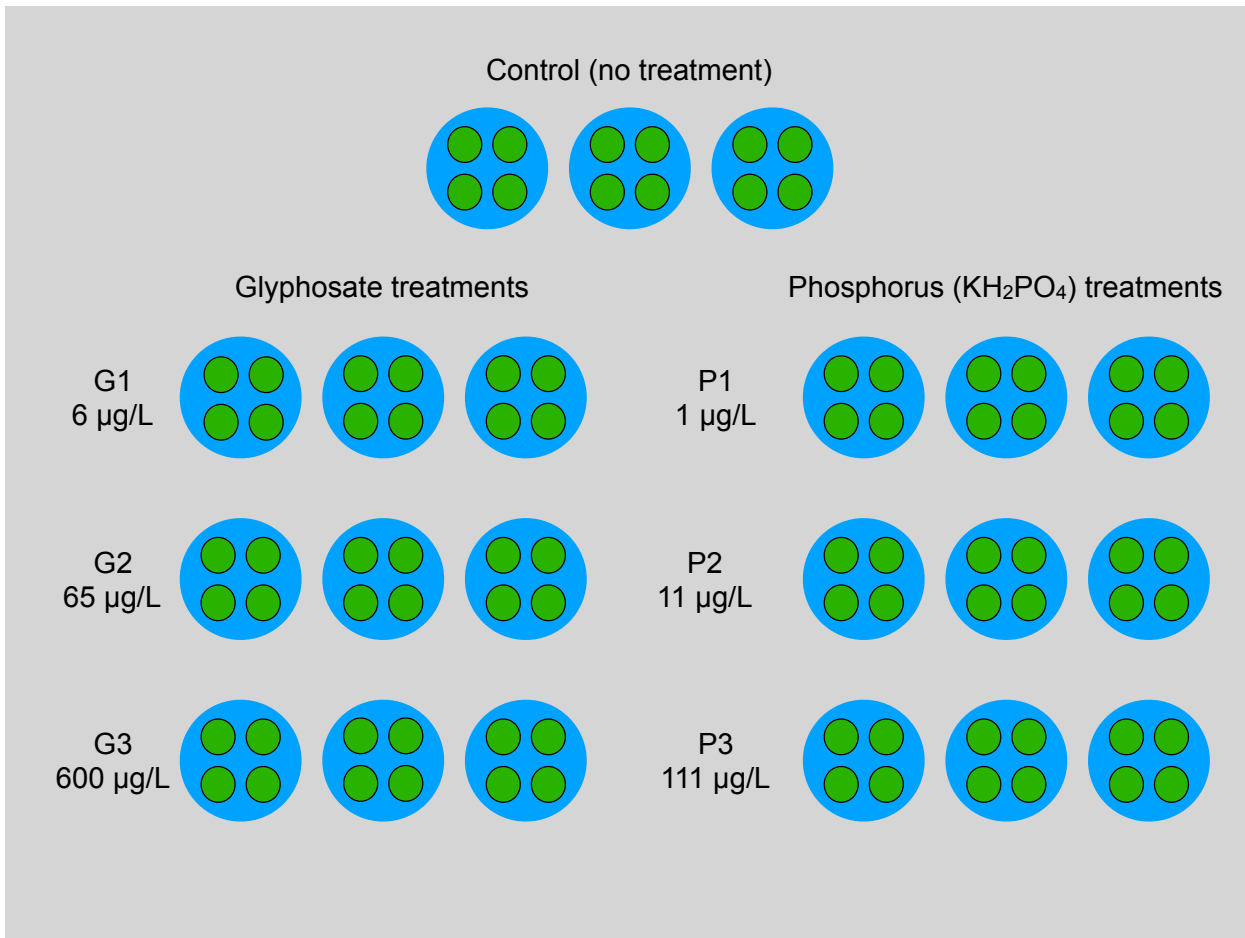


Figure S2. Experimental design. Treatments were performed in triplicate, for a total of 21 microcosms per experiment. Three experiments were conducted independently for each colonization rate. At the beginning of each experiment, 4 colonized mesh disks were placed in each Pyrex® round dish filled with filtered lake water.

Microcosms were randomly distributed in a growth chamber.

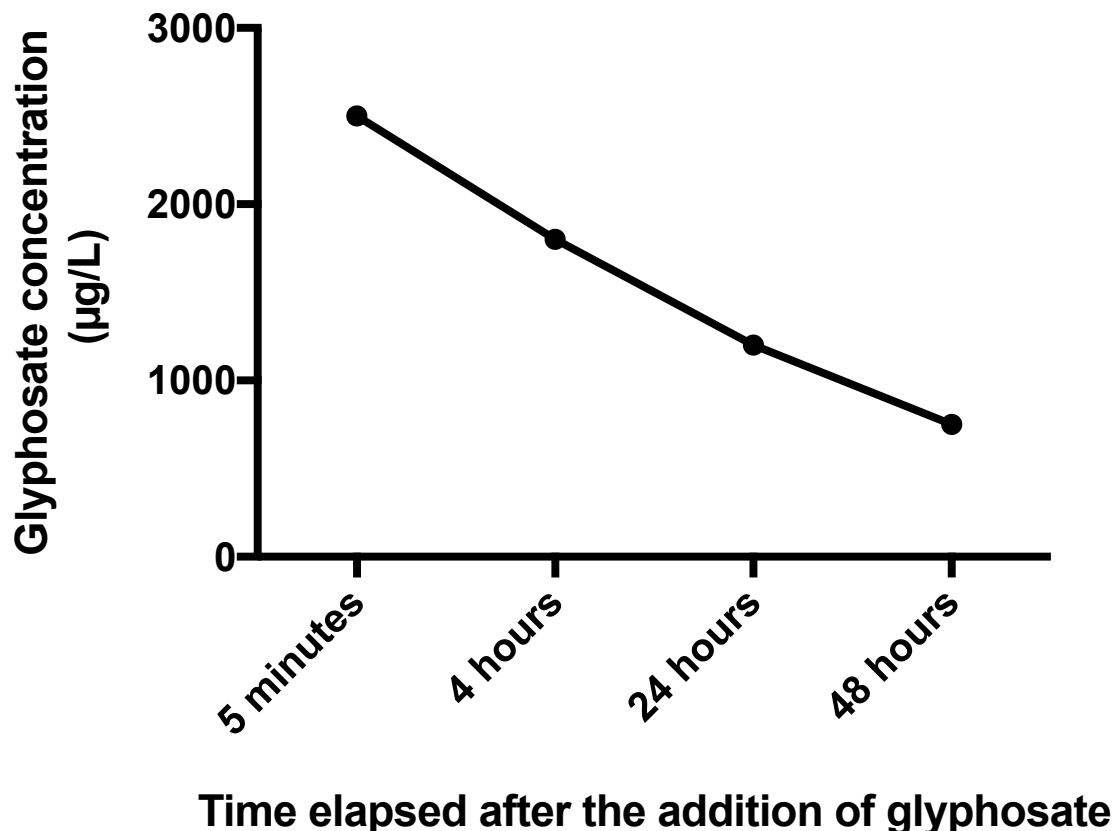


Figure S3. 48-hour monitoring of glyphosate concentrations in a preliminary test during which 2.5 mg/L of glyphosate was added under the same experimental conditions (n=1).

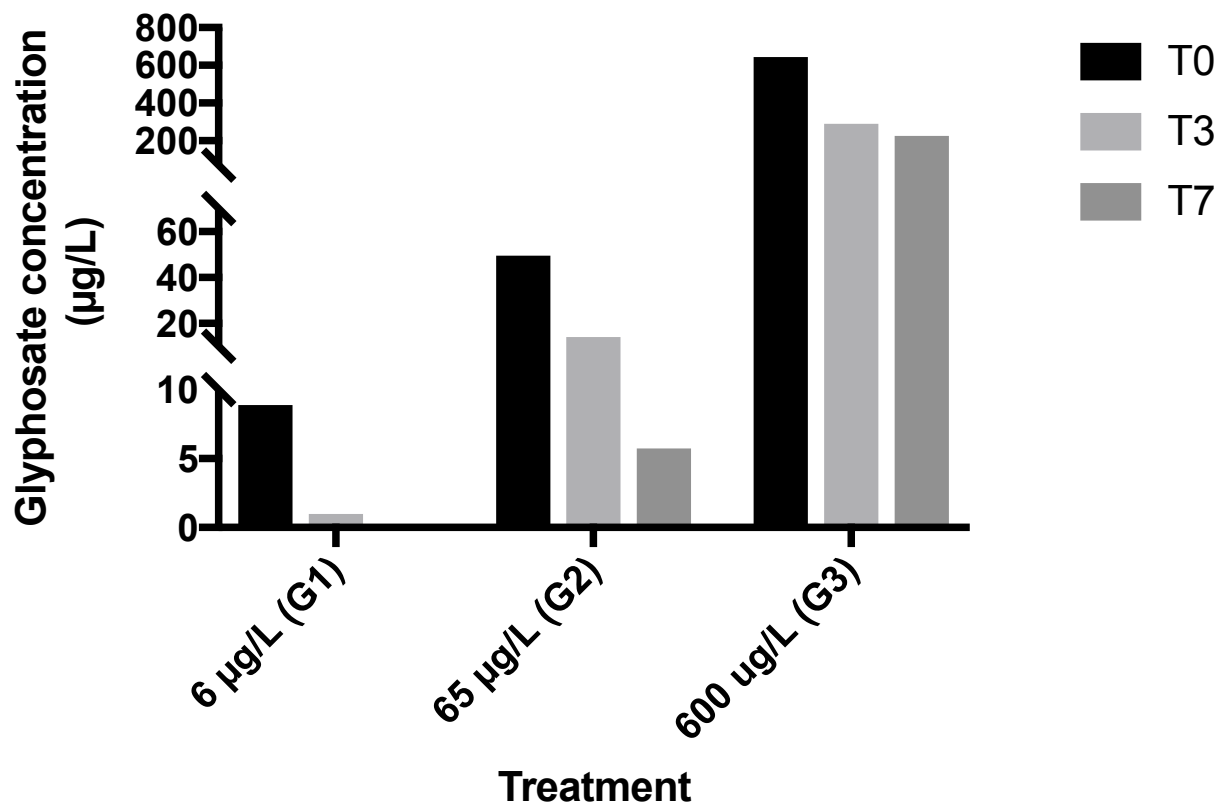


Figure S4. Glyphosate concentrations in the water of microcosms with 20-year-old biofilms exposed for 7 days in a preliminary experiment that took place in 2015 under the same experimental conditions (n=2).

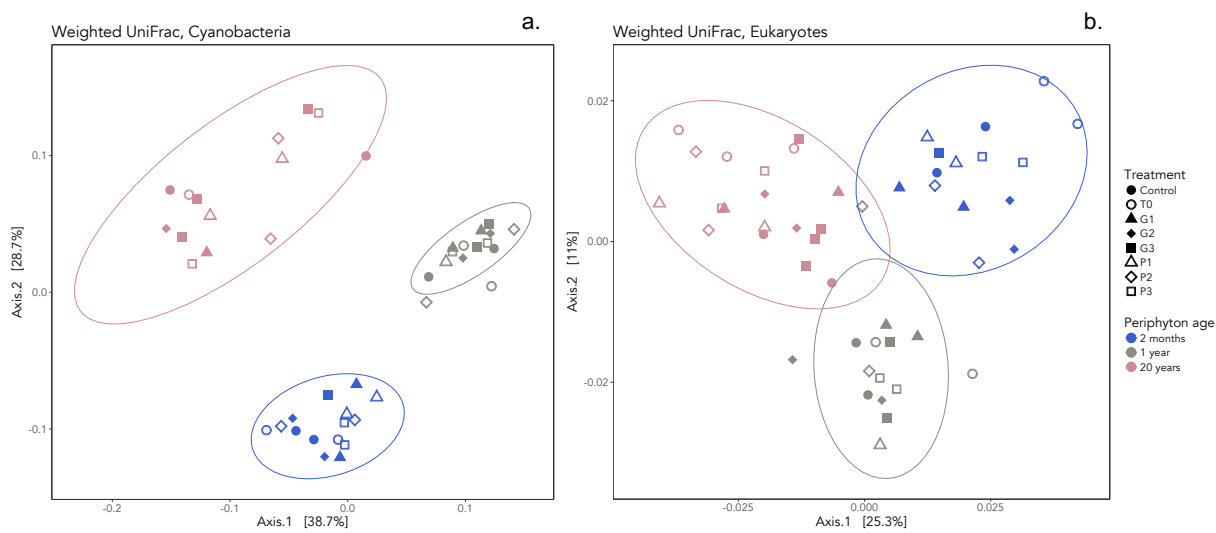


Figure S5. Principal coordinates analysis (PCoA) of weighted UniFrac distances. a. Community composition cluster by periphyton age for Cyanobacteria (Weighted UniFrac, permanova $R^2 = 0.582$, $p = 0.001$). Multivariate dispersion is significant ($p < 0.0001$). b. Community composition cluster by periphyton age for eukaryotes (Weighted UniFrac, permanova $R^2 = 0.255$, $p = 0.001$). Multivariate dispersion is not significant (betadisper, $p > 0.05$).

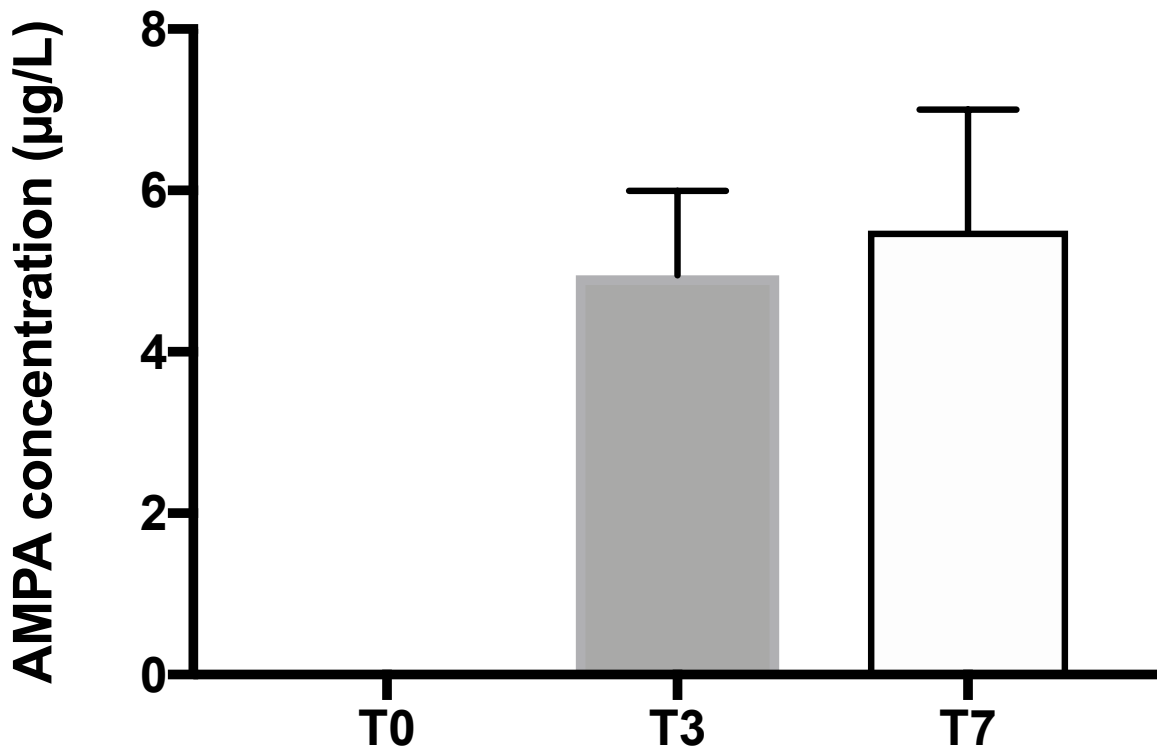


Figure S6. Aminomethylphosphonic acid (AMPA) concentrations in the water of microcosms with 20 years-old biofilms exposed to glyphosate (600 µg/L) for 7 days in a preliminary experiment that took place in 2015 under the same experimental conditions. Error bars represent standard error of the mean (SEM) (n=3). There is a significant increase between T0 and T3 (t-test, $p_{adj}<0.05$).

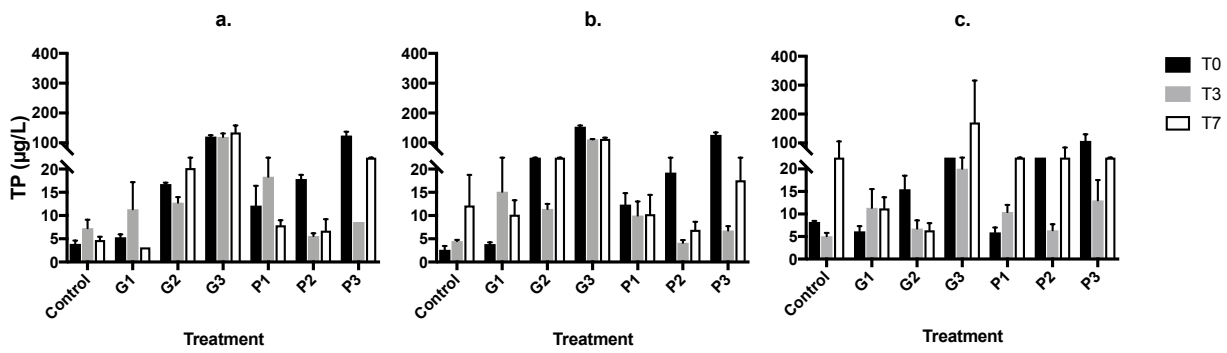


Figure S7. Total phosphorus concentrations in glyphosate (G1, G2, G3) and phosphorus (P1, P2, P3) enriched treatments throughout the experimental period. a. 2-month-old periphyton. b. 1-year-old periphyton. c. 20-year-old periphyton. Error bars show standard error of the mean (SEM) ($n=3$). While glyphosate concentrations decreased during incubations, we also noted a significant decrease in TP concentrations between T0 and T3 for the P2 treatment (t-test, adjusted $p < 0.005$), which included initial additions of phosphorus in equal amounts to the concentrations found in G2 (Fig. 2a&b). Time ($p < 0.0001$), treatment ($p < 0.0001$) and the interaction of these two factors ($p < 0.0001$) significantly explained differences in the early stages of the incubations, between T0 and T3 (multifactorial 2-way ANOVA) (Fig. 2a&b), with treatment alone explaining 68.54% of total variation. After 3 days (T3), there was a significant difference between control and all three glyphosate treatments (adjusted $p < 0.01$ for G1, $p < 0.05$ for G2 and $p = 0.0001$ for G3) (Dunnett's multiple comparisons post-hoc test). In Fig. 2c, the decrease in total phosphorus between T0 and T3 was significant for the P2 and P3 treatments (t-test $p < 0.05$). This might infer an incorporation of added phosphorus by periphyton. Time ($p < 0.0001$), treatment ($p < 0.0005$) and the interaction of the two factors ($p < 0.0001$) significantly explained differences in TP when comparing T0 to T3 (multifactorial 2-way ANOVA). Treatment explained 46.37% of total variation in TP concentrations. After 3 days (T3), we confirmed that there was a significant (adjusted $p < 0.005$) difference in TP concentrations between control and G3 treatment (Dunnett's multiple comparisons post-hoc test).

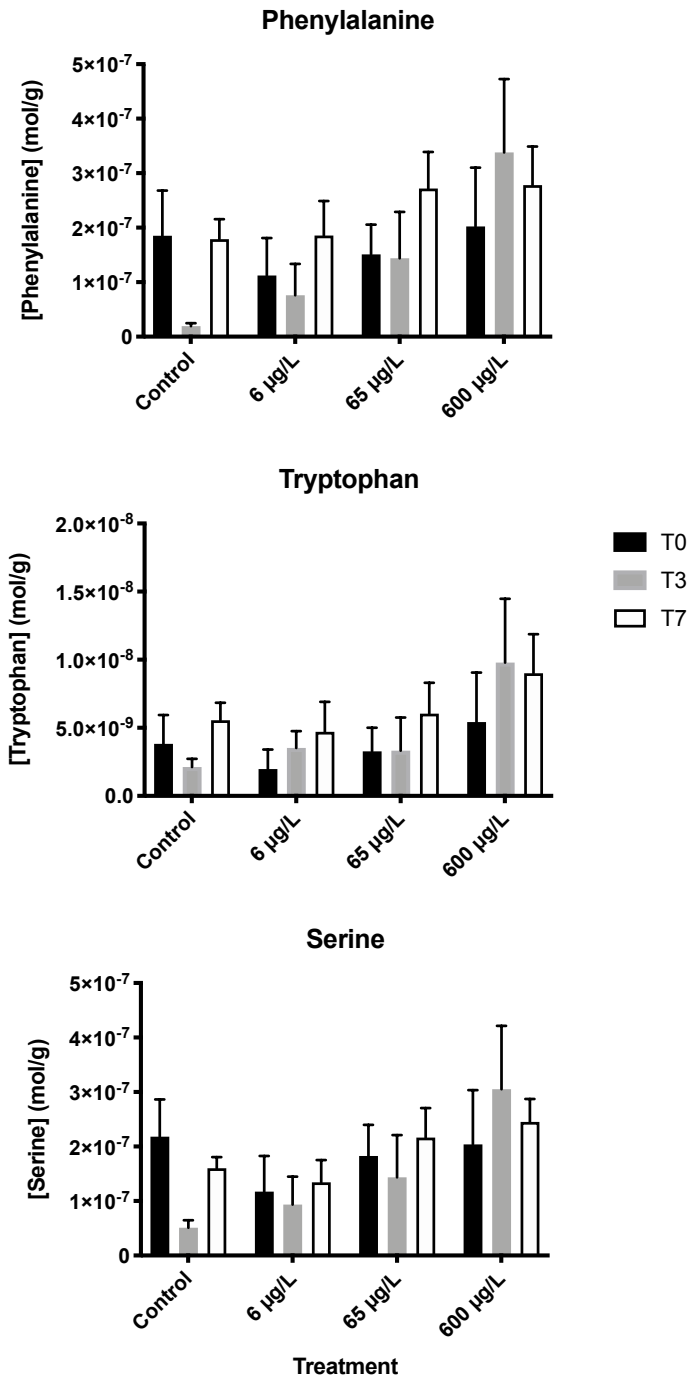


Figure S8. Aromatic amino acids concentrations in 20 years-old biofilms exposed to glyphosate for 7 days in a preliminary experiment that took place in 2015. Error bars represent standard error of the mean (SEM) ($n=3$). Neither time nor treatment had a significant effect on amino acid concentrations (2-way ANOVA, $p>0.05$).



CHAPITRE 2:

Évaluation du potentiel de toxicité associé au transfert maternel
du mercure et du sélénium chez la perchaude (*Perca*
flavescens) à l'aide d'une approche de fractionnement
subcellulaire

The fish or the egg: Maternal transfer and subcellular partitioning of mercury and selenium in Yellow Perch (*Perca flavescens*)

Melissa Khadra^a, Antoine Caron^a, Dolors Planas^b, Dominic E. Ponton^a, Maikel Rosabal^b and Marc Amyot^a

^a *Groupe interuniversitaire en limnologie et en environnement aquatique (GRIL), Département de sciences biologiques, Université de Montréal, Pavillon Marie-Victorin, 90 Vincent d'Indy, Montréal QC*

^b *Groupe interuniversitaire en limnologie et en environnement aquatique (GRIL), Département des sciences biologiques, Université du Québec à Montréal, C.P. 8888, Succursale Centre-Ville, Montréal QC*

Published in Science of the Total Environment

DOI: 10.1016/j.scitotenv.2019.04.226

Copyright © 2019 Elsevier

Abstract

Mercury (Hg) is a trace element of particular concern since it is ubiquitous in the environment and because its methylated form (MeHg) readily bioaccumulates and biomagnifies in food webs. This latter process leads to elevated Hg concentrations in fish and thus induces toxicity. Maternal transfer of bioaccumulated contaminants to offspring is a suggested mechanism of impaired reproductive success in fish. The purpose of this study was to assess the toxicity potential of Hg during maternal transfer in Yellow Perch from Lake Saint-Pierre (Quebec, Canada) using a sub-cellular partitioning approach. We also evaluated potential protective effects of selenium, as this element has been shown to alleviate Hg toxicity through sequestration. A customized subcellular partitioning protocol was used to separate liver and gonad of Yellow Perch into various subcellular fractions. Results show that, in the liver, MeHg was primarily (51%) associated to the subcellular fraction containing cytosolic enzymes. Furthermore, 23% and 15% of MeHg was found in hepatic and gonadal mitochondria, respectively, suggesting that Yellow Perch is not effectively detoxifying this metal. There was also a strong relationship ($R^2 = 0.73$) between MeHg bioaccumulation in the liver and MeHg concentrations in gonadal mitochondria, which corroborates the potential risk linked to MeHg maternal transfer. On the other hand, we also found that selenium might have a protective effect on Hg toxicity at a subcellular level. In fact, Se:Hg molar ratios in subcellular fractions were systematically above 1 in all tissues and fractions examined, which corresponds to the suggested protective threshold. This study provides the first assessment of subcellular Se:Hg molar ratios in fish. Since early developmental stages in aquatic biota are particularly sensitive to Hg, this study represents a step forward in understanding the likelihood for toxic effects in wild fish through maternal transfer.

Keywords Methylmercury; Se:Hg molar ratios; Mitochondria; Gravid females; Liver; Gonads

1. Introduction

Mercury (Hg) is a non-transition metal that exhibits a unique biogeochemical cycle. Anthropogenic activities such as mining and the combustion of fossil fuels have resulted in the increased mobilization of Hg in the environment (Mason et al., 1994). In aquatic ecosystems, inorganic Hg(II) is methylated by microbes to the toxic form methylmercury (MeHg), which can readily bioaccumulate and biomagnify in food webs (Furutani & Rudd, 1980), leading to elevated Hg concentrations in fish (Spry & Wiener, 1991). As the consumption of contaminated fish can severely impact human health (Tollefson & Cordle, 1986), Hg may also be toxic to fish themselves (Beckvar et al., 2005; Sandheinrich et al., 2011). Hg-induced reproductive health impairment in fish depends on species, state of gonadal development, route of exposure, duration of exposure, mercury speciation and concentration, and life-cycle stages (Crump & Trudeau, 2009). In fact, early-life stages of fish such as larvae, are considered particularly sensitive to organic and inorganic contaminants (Beckvar et al., 2005; Luckenbach et al., 2001; McKim, 1977; Oliveira et al., 2009). Moreover, laboratory studies showed that Hg in eggs and embryos originates primarily from maternal transfer and depends on the levels of contaminant in the diet of females during oogenesis (Hammerschmidt & Sandheinrich, 2005). In fact, female egg production involves the synthesis and incorporation of vitellogenin, a yolk protein that can transfer a portion of maternal MeHg burden to the embryo (Crump & Trudeau, 2009). Although a limited number of field studies have assessed the maternal transfer of Hg in fish (Hammerschmidt et al., 1999; Johnston et al., 2001; Niimi, 1983), there is an evidence of maternal transfer of MeHg to eggs in Yellow Perch (Hammerschmidt et al., 1999; Niimi, 1983). One way of understanding whether toxicological effects are likely to occur following metal bioaccumulation is through sub-cellular partitioning (Barst et al., 2016). This procedure relies upon differential centrifugations in order to separate the cell into metal-sensitive (cytosolic heat-denatured proteins (HDP), mitochondria) and “detoxified” (cytosolic heat-stable proteins (HSP) and peptides, granules) compartments (Wallace et al., 2003). Contaminants are then quantified in each of these fractions in order to understand how organisms cope with metal exposure (Giguère et al., 2006; Rosabal et al., 2012; Rosabal et al., 2014; Rosabal et al., 2015). In fact, in the cell, metals are sequestered by binding to proteins (e.g., metallothionein) or peptides (e.g., glutathione) or incorporated into granules. An excessive metal accumulation beyond the

capacity of those structures can lead to toxicity through interactions with organelles (e.g., mitochondria) and enzymes (HDP) (Campbell et al., 2005; Giguère et al., 2006; Wallace et al., 2003). Mitochondria represent a key sensitive fraction (Araújo et al., 2015), since it has been shown to be one of the main targets of cellular metal toxicity (Cambier et al., 2009). Thus, this fraction, as well as HDP, were used as a proxy for cellular toxicity in the present study.

Hg toxic effects to organisms have been shown to be alleviated by selenium (Se), for which Hg has a strong binding affinity (Ralston, 2008; Ralston et al., 2008; Wang et al., 2012). However, the mechanistic processes associated to Se and Hg antagonism is extremely complex (Burger et al., 2013). These processes may include the formation of insoluble, stable and inert Hg-Se complexes, leading to a reduction of Hg toxicity (Spiller, 2017). Further, as Se is required for production of selenoenzymes, a reduction of the available Se due to complexation with Hg or MeHg can lead to an alteration of function and synthesis of selenoenzymes (Wang et al., 2012). Furthermore, these enzymes are believed to be the primary target of Hg toxicity due to the high affinity and stability associated to the binding of Hg to Se (Spiller, 2017). Ralston (2008) suggested that Se:Hg molar ratios above 1 may protect against Hg toxicity, although the actual protective ratio is unclear. Since subcellular Se:Hg molar ratios in fish are unexplored, we assessed the potential protective effect of Se at a subcellular level.

A wide range of anthropogenic pressures have been threatening Lake Saint-Pierre, the largest fluvial lake within the St. Lawrence River (Canada) (Marcogliese et al., 2015), for several decades (Hudon et al., 2018). Among other impacts, water quality of Lake Saint-Pierre is compromised by industrial discharges, municipal effluents and agricultural land development in its watershed, which release a mixture composed of metals and metalloids (including Hg and Se), pesticides and contaminants of emerging concern (Bérubé et al., 2005; Giraudo et al., 2016; Giroux, 2018; Houde et al., 2014a; Houde et al., 2014b). This contamination is amplified in areas of the lake that are characterized by dense vegetation, since macrophytes favor the retention and sedimentation of suspended matter (Hudon et al., 2018). These aquatic wetlands serve as spawning grounds for several fish species, including Yellow Perch (Bertolo et al., 2012). Following a major decline in its populations since the late 1990s due to its significant commercial and sporting interest, a five-year moratorium on Yellow Perch fishing was imposed in 2012 (de la Chenelière et al., 2014). The inability of Yellow Perch populations to recover persists despite the implementation of this moratorium and it was therefore extended until 2022.

The present study tests the hypothesis that Hg contamination in Yellow Perch during their early life stages through maternal transfer may help explain this species' lack of resilience in Lake Saint-Pierre. In fact, although Hg bioaccumulation levels in Yellow Perch from Lake Saint-Pierre do not exceed toxicity thresholds (Ion et al., 1997; Laliberté, 2016), adverse behavioral effects to fish larvae were observed at very low Hg concentrations (Weber, 2006).

The adverse effects of Hg on Yellow Perch were only assessed in a limited number of field studies that were correlative in nature (Batchelar et al., 2013a; Batchelar et al., 2013b; Hammerschmidt et al., 1999; Larose et al., 2008; Müller et al., 2015; Niimi, 1983; Wiener et al., 2012). Few studies have also been carried out in order to determine the sub-cellular partitioning of Hg in fish (Araújo et al., 2015; Barst et al., 2016; Barst et al., 2018; Onsanit & Wang, 2011), none of which using Yellow Perch as a model species. These studies indicate that the intracellular Hg distribution in fish depends strongly on the species and bioaccumulation level. Thus, the specific aims of the present study were to (1) identify Hg toxicity potential using a sub-cellular partitioning approach, (2) assess Yellow Perch egg exposure to Hg and Se through maternal transfer in Lake Saint-Pierre and (3) evaluate the potential protective effect of Se through Se:Hg molar ratios.

2. Methods

2.1. Study site

The fluvial section of the St. Lawrence River extends 243 kilometers from Cornwall, Ontario to the eastern end of Lake Saint-Pierre and comprises three fluvial lakes. Lake Saint-Pierre is the largest of the three fluvial lakes, with a length of 25.6 kilometers and a width of 12.8 kilometers (La Violette, 2004). It is located downstream of major urban, agricultural and industrial areas (Hudon et al., 2018). In fact, the majority of metal and mercury inputs in Lake Saint-Pierre come from the industrial center of Sorel-Tracy (Kwan et al., 2003). With an average depth of 2.7 meters, Lake Saint-Pierre is the shallowest of the three river lakes (Paradis et al., 2014). The depth of its navigation channel, which separates the water body within the north and south water masses, can reach 13.7 meters (La Violette, 2004). It is important to point out that the water bodies on the northern and southern shores are differentiated by physical properties such as water density and flow, limiting exchanges between the two masses (Glément & Rodríguez, 2007).

2.2. Fish sampling

Gravid females were sampled from Maskinongé ($n = 24$) (Maski, $46^{\circ}19' N$, $73^{\circ}00' W$) and Baie-du-Febvre ($n = 20$) (BDF, $46^{\circ}15' N$, $72^{\circ}77' W$) (Fig. 1) in April 2016, since spawning occurs during the spring flood for Yellow Perch in Lake Saint-Pierre. Length and weight of each individual are shown in Table S1. These two bays were chosen because they represent important spawning grounds of Lake Saint-Pierre and also because the north and south shores of Lake Saint-Pierre seem to exhibit different Yellow Perch populations (Leung et al., 2011). In fact, different isotopic ratios of carbon ($\delta^{13}\text{C}$) and parasite infections showed that within Lake Saint-Pierre, Yellow Perch feeding range do not exceed 2 km, suggesting that movement between the two shores, or between two regions of the same shore of the lake are infrequent (Bertrand et al., 2011). Fish were sampled using seine nets and kept alive in aerated coolers. In the laboratory,

gravid females were decapitated and dissected. Liver, muscle, gonads, brain and digestive tract were removed for mercury and selenium analysis. Liver and gonads were first subsampled for subcellular partitioning and all tissues were then flash-frozen using liquid nitrogen and kept at -80 °C until analyses. All experiments were done in accordance with animal care guidelines at Université de Montréal, with the approval of the ethics committee (CDEA #16-023) and followed internationally recognized guidelines.

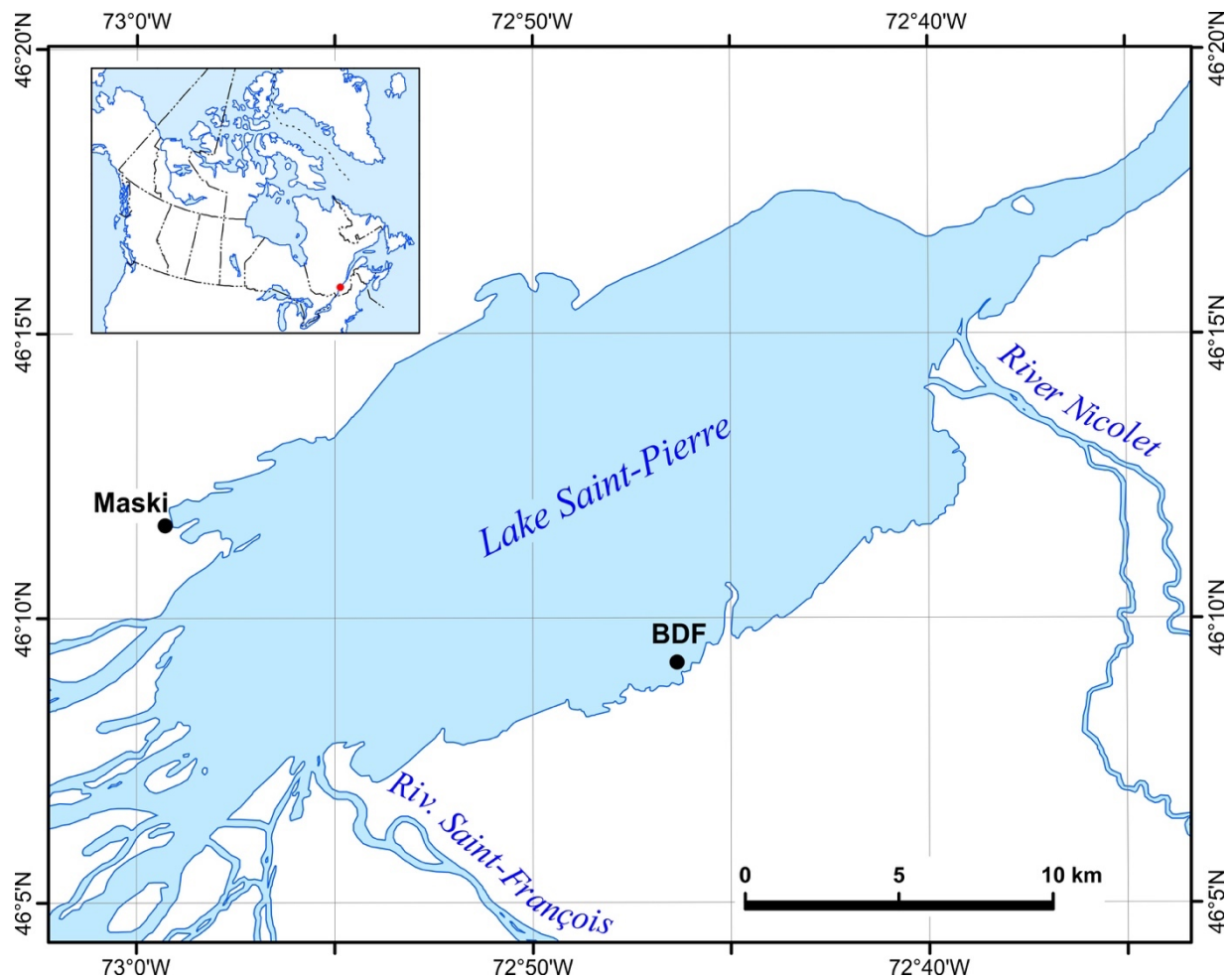


Figure 1. Map of Lake Saint-Pierre (Quebec, Canada) showing sampling sites. Gravid females were sampled from Maskinongé (Maski) on the north shore and from Baie-du-Febvre (BDF) on the south shore.

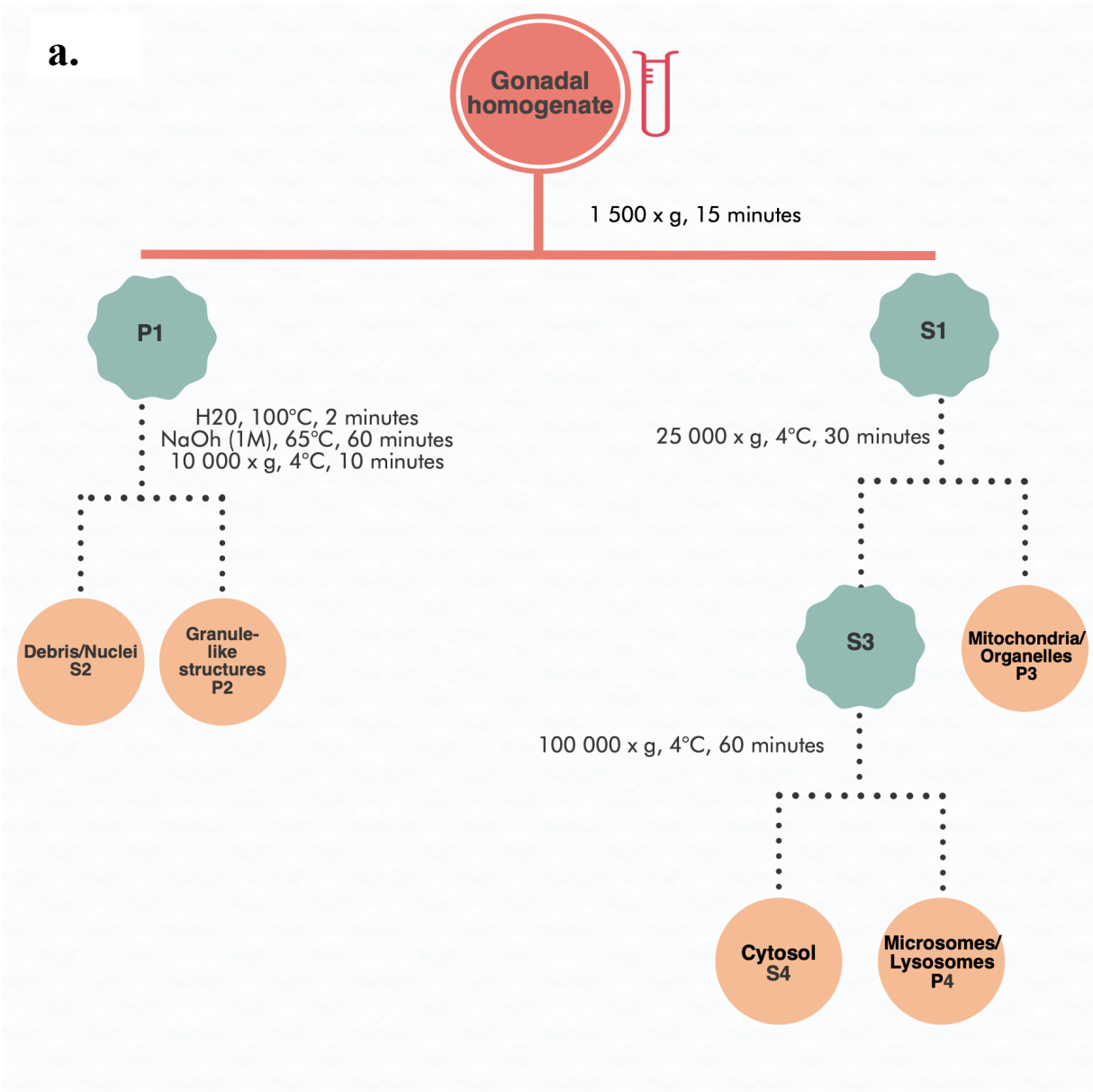
2.3. Subcellular partitioning procedure

Both gonads and liver were subjected to a subcellular partitioning approach. For each organ, a customized subcellular protocol was assessed using enzymatic biomarkers, as it is highly species-specific (Cardon et al., 2018) and organ-specific (Urien et al., 2018). The efficiency of the fractionation procedure was tested using specific enzymes expected to be present in the mitochondrial and cytosolic fractions, since no protocol validated with specific enzymes is currently available for liver and gonads of Yellow Perch. Several protocols were tested and the more efficient one was selected for each organ (Fig. S1 and S2). Subcellular fractionation is an imperfect process as it simultaneously requires plasma membrane disruption without breaking organelle membranes. In fact, partial disruption of organelle membranes causes overlapping of soluble constituents from subcellular fractions (Cardon et al., 2018). This potential overlap can be quantified by enzymatic validation, as its purpose is to assess the efficiency of subcellular fractionation methods (Rosabal et al., 2014). Enzymatic validation results are shown in Fig. S1-S2 and complete protocol is described in SM. 1. Enzymatic activities were measured according to Caron et al. (Caron et al., 2016). We provide what we consider to be an optimized customized protocol for subcellular fractionation of liver and gonads of Yellow Perch, as current protocols for Yellow Perch liver are not enzyme-validated (Campbell et al., 2005; Giguère et al., 2006; Kraemer et al., 2006).

The subcellular partitioning protocol was adapted from that given in previous studies (Wallace et al., 2003; Wallace & Luoma, 2003). Gonad samples (~200 mg) were first homogenized by disrupting the cells 12 times using a syringe with a 18G x 1 ½ needle (BD 305196 PrecisionGlide) (Prudent et al., 2013). An aliquot of 50 µL, corresponding to the homogenate fraction, was collected for element mass balance calculation. Gonadal homogenates were then subjected to the subcellular partitioning procedure (Fig. 2a). Since the gonad is a very gelatinous matrix, it was impossible to separate the cytosol in two different fractions (HSP and HDP) following the 70°C heat treatment (Fig. 2a). These protein groups are important to isolate since HSP are responsible for metal detoxification (Wang et al., 2012) and HDP play a role in the redox defense system (Spiller, 2017). Liver samples of ~150 mg were ground with a Potter-Elvehjem pestle 3 times for 2 s, with 30-s intervals between each period of grinding, in Tris

buffer solution (25 mM, pH 7.4 adjusted with HCl) at a ratio of 1:4.5 (v/v). The resulting homogenate was centrifuged at 1,500 g for 15 min at 4°C (Fig. 2b). The pellet (P1) was resuspended in Tris buffer solution (25 mM, pH 7.4) at a ratio of 1:4.5 before being disrupted with an ultrasonic probe at 40 W, 0.2 s/s for 5 s. This second homogenate (LH2) was then pooled with the supernatant (S1), mixed with a vortex, and an aliquot of 50 µL, corresponding to the homogenate fraction, was collected. This fraction (S1+LH2) was centrifuged again at 1,500 g for 15 min at 4°C. The resulting supernatant (S2) was then subjected to a centrifugation step at 25,000 g for 30 min and the pellet (P2) was separated into the Debris (S3) and Granules (P3) fractions after a NaOH digestion and a centrifugation step at 10,000 g for 10 min at 40°C. An ultracentrifugation step was performed on S4 at 100,000 g for 60 min and the pellet (P5), the lysosomal/microsomal fraction, was separated from the supernatant (S5), the cytosolic fraction, which was separated into heat-stable (S6) and heat-denatured (P6) proteins. Sensitive fractions include mitochondria and HDP, whereas detoxification fractions comprise HSP and granules. The microsomes/lysosomes fraction is difficult to interpret because it contains lysosomes, which have a storage and a detoxifying function and microsomes, which are responsible for synthesis and transport of proteins (Araújo et al., 2015). The debris fraction is generally ignored in ecotoxicological studies. However, it is relevant because it has been shown to be an indicator of efficient homogenization (Barst et al., 2018). The mass of each fraction was noted in order to monitor every step of the procedure. Mass balance calculations were carried out by comparing the total trace metal burdens, estimated from the 50-µL homogenate fractions, with burdens calculated from the sum of metals measured in each subcellular fraction (Rosabal et al., 2016). Mass balances indicated a minimum recovery of more than 80%; specifically, values were obtained in gonads for total Hg (THg) ($95\% \pm 22\%$, n=24), MeHg ($82\% \pm 25\%$, n=24) and Se ($90\% \pm 19\%$, n=24) and in liver samples for THg ($99\% \pm 10\%$, n=21), MeHg ($93\% \pm 11\%$, n=21) and Se ($96\% \pm 17\%$, n=21).

a.



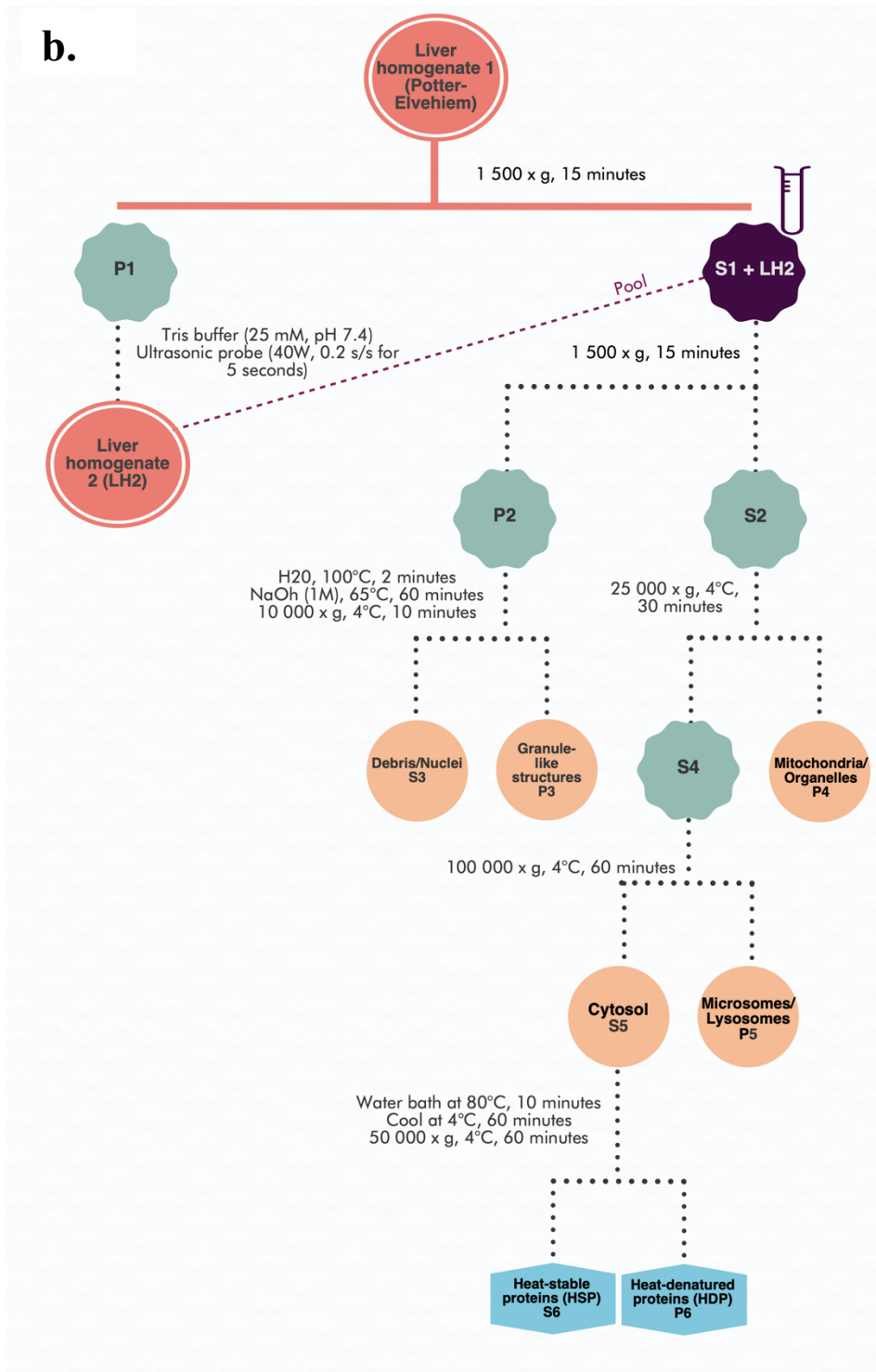


Figure 2. Schematic illustration of the subcellular partitioning procedure used to separate Yellow Perch (a) gonads and (b) liver into operationally defined fractions. Small tubes represent the 50- μ L homogenate fractions. Fractions represented by orange circles were tested with marker enzymes.

2.4. MeHg and THg Analyses

Prior to MeHg analysis, 500 µL HNO₃ OmniTrace UltraTM (MilliporeSigma) diluted three times were added to lyophilized subcellular fractions and whole-tissue samples and incubated overnight in a drying oven at 60°C. A 25-µL aliquot was used for MeHg analysis by cold-vapor fluorescence spectrometry (CVAFS) (Tekran 2700), according to U.S. EPA method 1630 (detection limit of 0.01 ng/L, calculated as three times the standard deviation (SD) of 10 blanks). New standards (0.5 ng/L) were run after each set of 10–12 samples to test for analytical stability (mean recovery 96 ± 11%, n = 48). Analyses were accepted when recovery of certified trace metal reference materials was in the certified range (152 ± 13 ng/g dw) for TORT-2 (lobster hepatopancreas, National Research Council of Canada) and the mean (±SD) recovery was 102 ± 14% (n = 39). 583 µL of a HNO₃:HCl OmniTrace UltraTM (MilliporeSigma) 1:1.8 (v/v) mix was then added to the remaining sample in a Teflon ® vial in order to restore the HNO₃:HCl 1:1 ratio. Vials were then subjected to a 3-hour cycle in an industrial pressure cooker (121°C, 15 psi) and 250 µL of Hydrogen Peroxide OPTIMA grade (Fisher Chemical) was added afterwards for an overnight digestion. Digestate volume was completed to 15 mL with Milli-Q water in 15-mL polypropylene trace metal free vials (VWR®). A 1-mL aliquot was then used for total Hg (THg) analysis using CVAFS (Tekran 2600, Tekran Instruments Corporation), following U.S. EPA method 1631 (detection limit of 0.04 ng/L, calculated as three times the SD of 10 blanks). New standards (0.5 ng/L) were run after each set of 10–12 samples to test for analytical stability (mean recovery 106 ± 8%, n = 48). THg analyses met the criteria of a Canadian Association for Laboratory Accreditation (CALA) intercalibration exercise.

2.5. Se Analyses

Se concentrations were measured by inductively coupled plasma – mass spectrometry (8900 ICP-MS Triple Quad; Agilent Technologies) on the 15-mL sample digestate. Analytical blanks and standards were added after 10 samples. Method detection limit of the ICP-MS was

0.056 µg/L for selenium. TORT-2 and DORM-2 certified biological reference materials (National Research Council Canada) were submitted to the same digestion protocol as the samples to monitor the efficiency of the digestion procedure. Recoveries (mean ± SD) were 110% ± 9% (n=40) for TORT-2 and 110% ± 28% (n=40) for DORM-2. ICP-MS analyses met the criteria of a Canadian Association for Laboratory Accreditation (CALA) intercalibration exercise.

2.6. Data Analyses

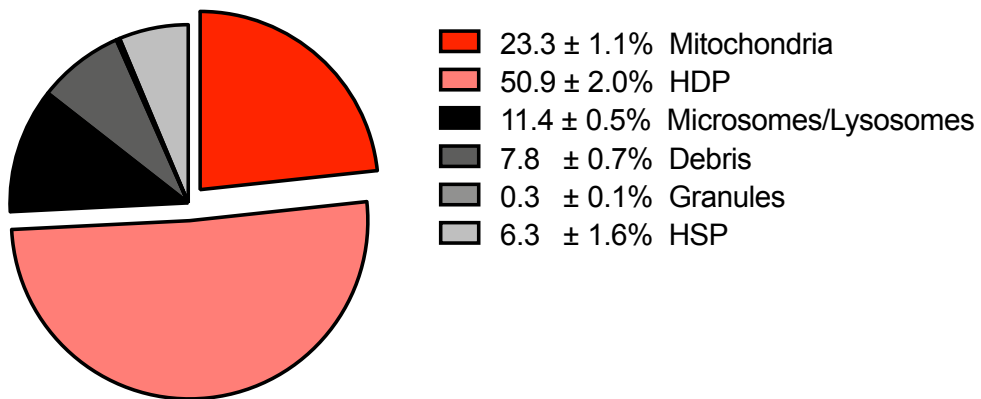
Shapiro-Wilk normality test was applied to all metal concentrations data. When required, data were log transformed prior to statistical analyses. Unpaired t-tests were performed to compare north and south metal concentrations. Since no significant differences were detected ($p > 0.05$), data from the two shores were pooled for all analyses. For organ metal subcellular distribution, pie charts were prepared using the fraction (%) of mercury burden (ng) in each subcellular fraction calculated from the sum of burdens measured in all fractions. Linear regressions between metal concentrations in females and their eggs were used as proxies for maternal transfer (Bergeron et al., 2010; Guirlet et al., 2008; Hammerschmidt et al., 1999; Hopkins et al., 2006). MeHg concentration (ng/g dw) (metal burden in a fraction/fraction weight) were represented as boxplots (median, 25th and 75th percentiles, maximum and minimum). For MeHg concentrations, one-way ANOVA with the Geisser-Greenhouse correction were applied, followed by a Tukey's multiple comparisons test, with individual variances computed for each comparison. Linear regressions were used for maternal transfer assessment. %MeHg were calculated as: $100 * [\text{MeHg}] / [\text{THg}]$. Finally, Se:Hg molar ratios were calculated on Se and THg µmol/g concentrations and represented as boxplots. Kruskal-Wallis nonparametric test followed by a Dunn's multiple comparisons test were performed on %MeHg and Se:Hg molar ratios. Significance level was set at $p < 0.05$. GraphPad Prism 7 (GraphPad Software Inc., USA) was used for statistical analyses.

3. Results

3.1. Subcellular partitioning of MeHg in liver and gonads

MeHg burden distribution in liver and gonadal cells are shown in Fig 3. Key sensitive fractions (mitochondria, HDP) are represented in red and pink exploded parts. More than 70% of MeHg is found in sensitive fractions (mitochondria and HDP) of hepatic cells (Fig. 3a). Within these fractions, there is more than twice the amount of Hg in HDP than in mitochondria, the former containing enzymes. A relatively small fraction of MeHg is bound to HSP and to debris (6-8%). Almost no MeHg was found in the granules fraction. In gonadal cells (Fig. 3b), an important amount of MeHg (44%) was found the cytosol. MeHg was equally distributed (15%) among the mitochondria and microsomes/lysosomes fractions, which are potentially sensitive compartments. As for “metal detoxified” fractions, approximately 4% of MeHg burden was found in granules of gonadal cells.

a.



b.

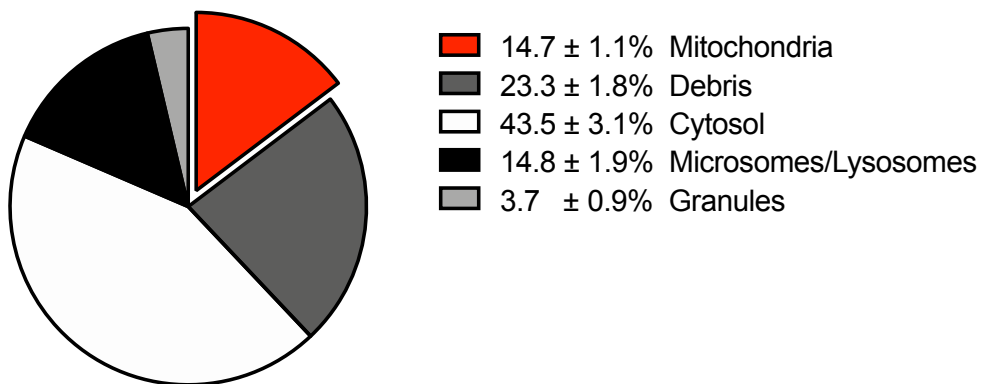


Figure 3. MeHg burden distribution (% ± SEM) in subcellular fractions of (a) liver (n=21) and (b) gonadal (n=24) cells. Red and pink exploded parts represent sensitive fractions.

3.2. MeHg concentrations in subcellular fractions

Fig. 4. presents boxplots of MeHg concentrations in subcellular fractions. THg concentrations are shown in Fig. S3. In the liver (Fig. 4a), concentrations were significantly higher in potentially sensitive fractions (mitochondria, HDP) than in metal detoxified fractions (granules, HSP). In fact, MeHg concentrations in the HDP fraction were significantly higher than all other fractions ($p_{adj} < 0.001$ for microsomes/lysosomes $p_{adj} < 0.0001$ for all other fractions). MeHg concentrations in mitochondria and in microsomes/lysosomes were also significantly higher than in the debris ($p_{adj} < 0.0001$ for both), granule ($p_{adj} < 0.0001$ for both) and HSP ($p_{adj} < 0.0001$ for both) fractions. In the gonads (Fig. 4b), mean MeHg concentrations in mitochondria (mean \pm SEM) (39.1 ± 7.4 ng/g dw) were significantly and almost 5 times higher than in debris ($p_{adj} < 0.0001$) and 2 times higher than in granules ($p_{adj} < 0.0001$). However, the highest mean concentrations were found in the cytosol (54.2 ± 12.5 ng/g dw). MeHg cytosol concentrations were significantly and 6 times higher than those measured in the debris ($p_{adj} < 0.0001$) fraction and 2.5 times higher compared to the granule ($p_{adj} < 0.0001$) fraction.

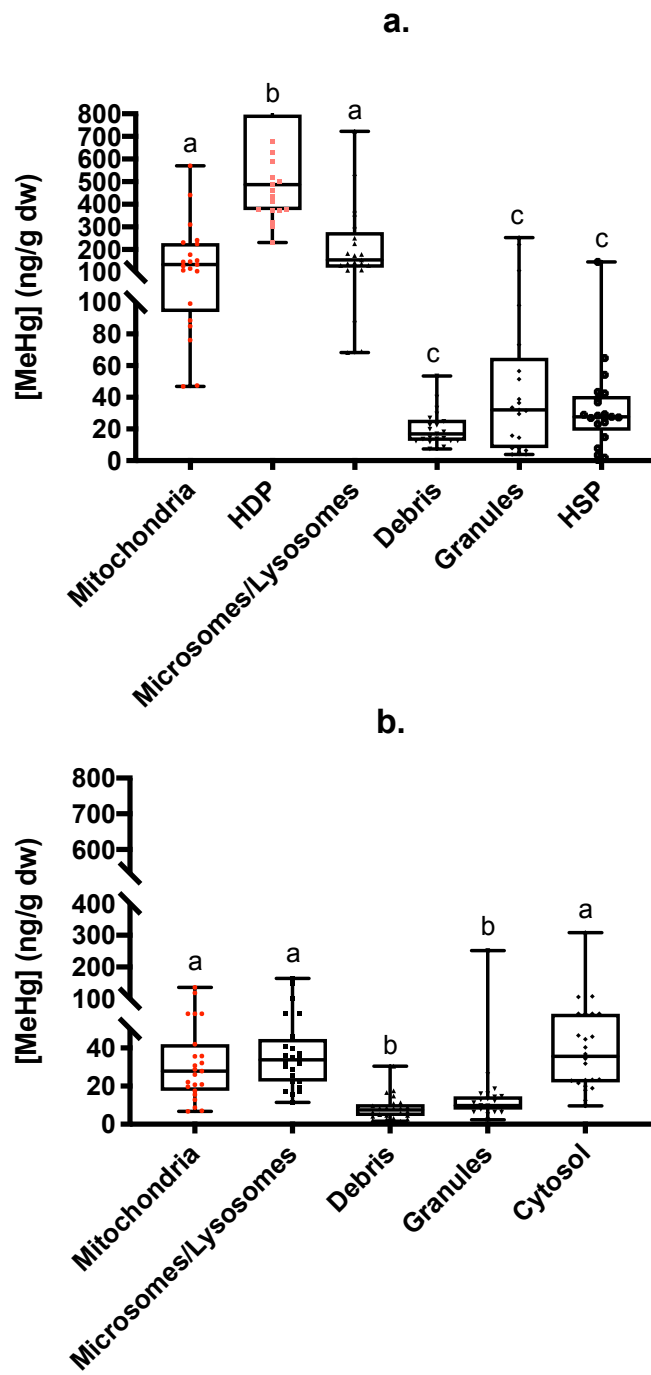


Figure 4. MeHg concentrations (ng/g dw) in (a) hepatic ($n=21$) and (b) gonadal ($n=24$) subcellular fractions of Yellow Perch. Letters denote significant differences (Tukey's HSD multiple comparisons test, $p < 0.05$). Sensitive fractions are shown in red (mitochondria) and pink (HDP).

3.3. Maternal transfer of MeHg

Simple regression models were applied to look at potential correlations between concentrations of trace elements in the eggs and in the liver of gravid Yellow Perch. In order to assess the toxicity potential of this transfer, MeHg content in gonadal mitochondria was also tested. Relationships between MeHg concentrations in the liver and MeHg in the gonads as well as gonadal mitochondria are shown in Fig. 5. Linear regressions were strongly significant both for gonadal tissue ($p < 0.0001$) (Fig. 5a) and gonadal mitochondria ($p < 0.0001$) (Fig. 5b). Linear regressions between MeHg in the muscle and gonads ($p < 0.0001$), as well as between MeHg in the muscle and gonadal mitochondria ($p < 0.0001$), are shown in SI (Fig. S4).

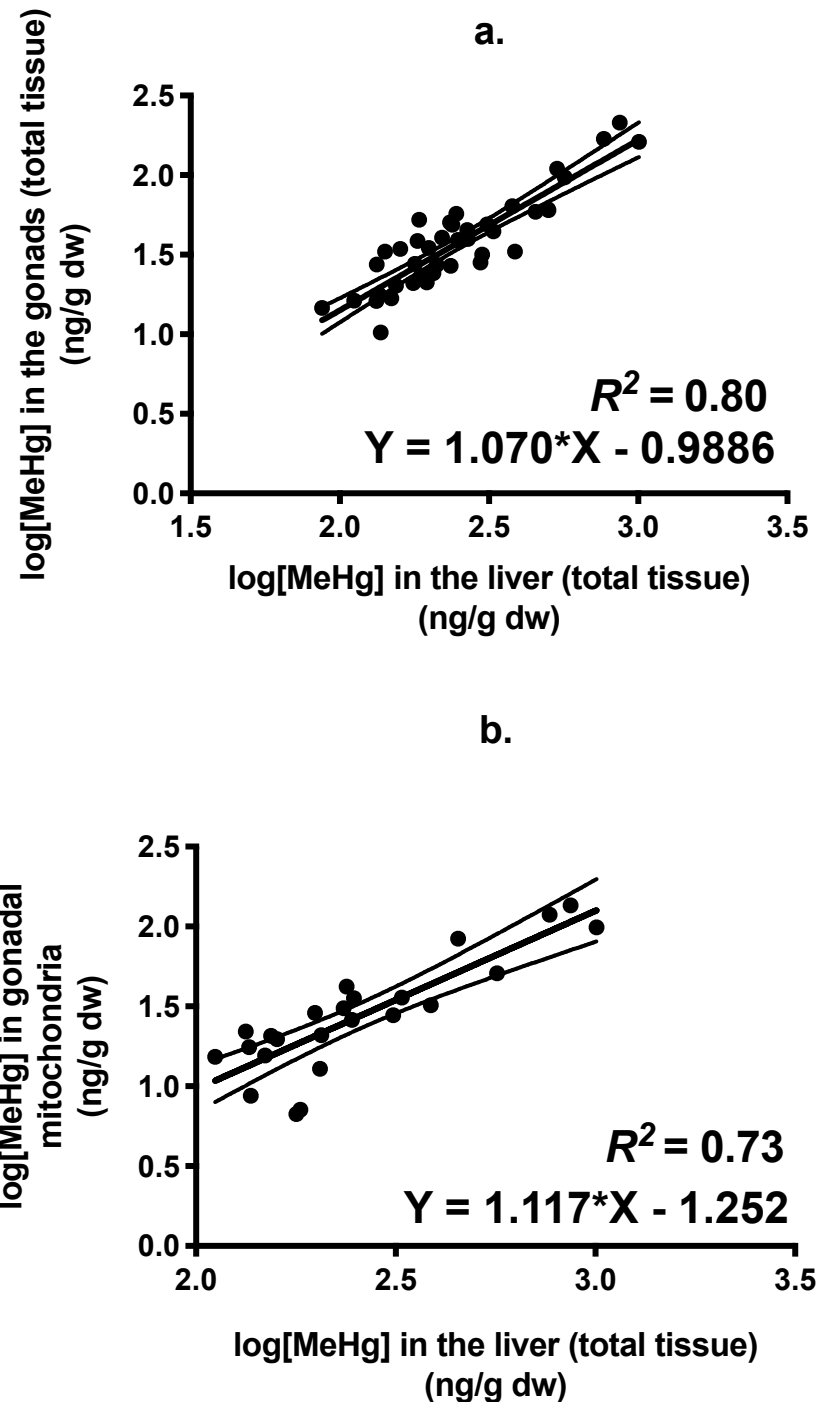


Figure 5. Relationship between MeHg concentrations (ng/g dw) in the liver and (a) MeHg in the gonads ($n=44$) and (b) MeHg in gonadal mitochondria ($n=24$). Data are log transformed. The R square and the equation of the linear regression are shown on each plot. Dashed curves represent the 95% confidence bands of the best-fit line.

3.4. Maternal transfer of Se

Since we observed a maternal transfer of MeHg in Yellow Perch, it became important to assess if Se was also transferred to eggs. Results show an evidence of maternal transfer of Se ($p < 0.0005$) (Fig. 6a) from the female liver to the eggs, but not to gonadal mitochondria ($p > 0.05$) (Fig. 6b). Se concentrations in subcellular fractions are shown in Figure S5. In the liver (Fig. S5a), these concentrations were the highest in the HDP fraction ($4.3 \pm 0.2 \text{ } \mu\text{g/g dw}$) and significantly different from microsomes/lysosomes ($p_{adj} < 0.001$), debris ($p_{adj} < 0.0001$), granule ($p_{adj} < 0.0001$) and HSP ($p_{adj} < 0.0001$) concentrations. Concentrations were also 9 times higher in the mitochondria fraction ($2.2 \pm 0.1 \text{ } \mu\text{g/g dw}$) in comparison to debris concentrations ($p_{adj} < 0.0001$). The highest individual concentration ($9.8 \text{ } \mu\text{g/g dw}$) was measured in the granule fraction. In contrast, in the gonads (Fig. S5b), the granule fractions had the second lowest mean ($0.6 \pm 0.2 \text{ } \mu\text{g/g dw}$) and the lowest individual concentration ($0.05 \text{ } \mu\text{g/g dw}$). The highest concentrations were measured in the cytosol ($1.7 \pm 0.2 \text{ } \mu\text{g/g dw}$) and were 7 times higher than in the debris fraction whereas 3 times higher than granule concentrations.

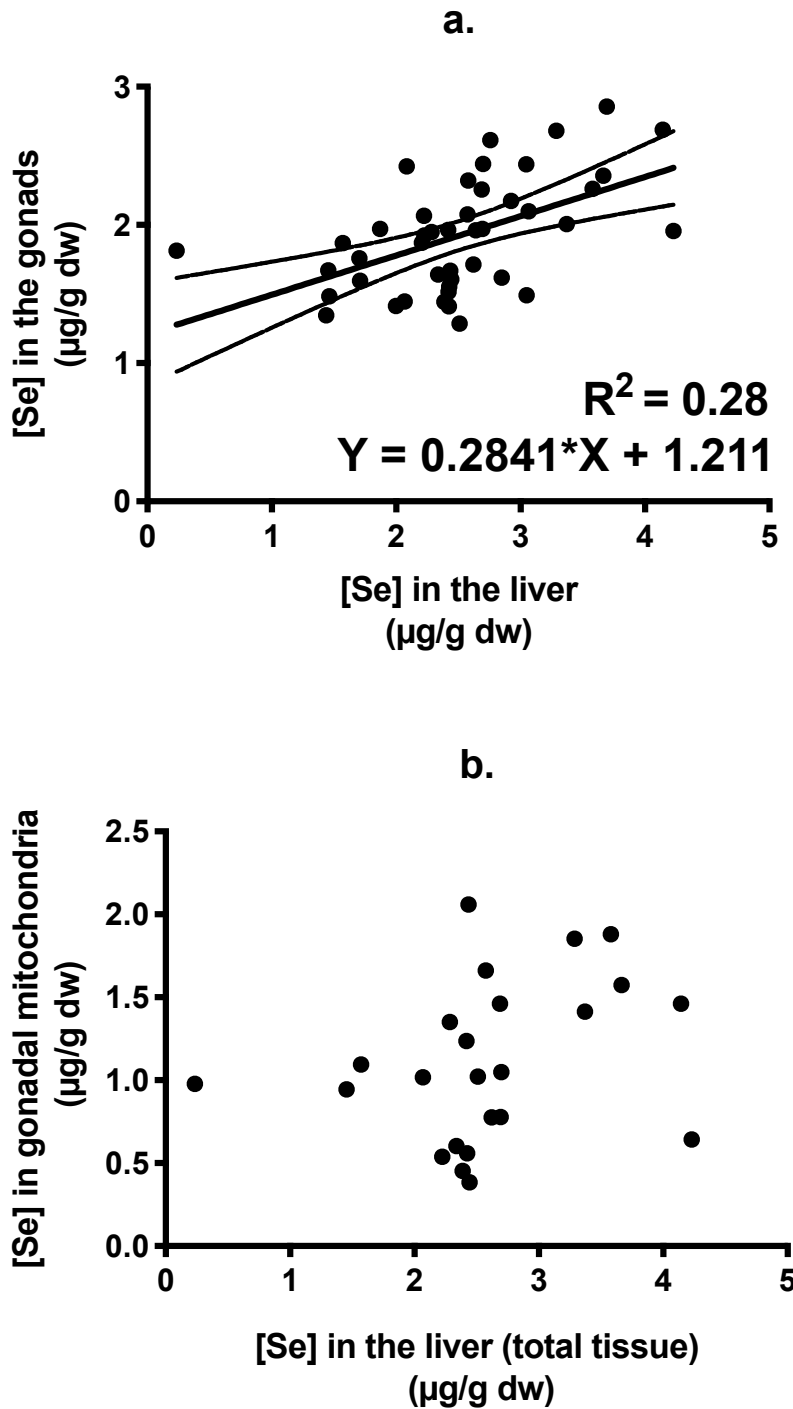


Figure 6. Relationship between Se concentrations ($\mu\text{g/g dw}$) in the liver and (a) Se in the gonads ($n=44$) and (b) Se in gonadal mitochondria ($n=24$). The R^2 square and the equation of the linear regression are shown in plot (a) as the regression was significative. Dashed curves represent the 95% confidence bands of the best-fit line.

3.5. Se:Hg molar ratios in subcellular fractions

Our results show that, in Yellow Perch from Lake Saint-Pierre, Se:Hg molar ratios in subcellular fractions are systematically above 1 (Fig. 7). In fact, in the liver (Fig. 7a), ratios ranged from 1.1 to 596 in the granule fraction. Ratios in the latter fraction were significantly higher than those measured in HDP ($p_{adj} < 0.05$). Ratios were also high in the metal detoxified HSP fraction (mean \pm SEM) (64.7 ± 9.4) and significantly different from the mitochondria ($p_{adj} < 0.01$), HDP ($p_{adj} < 0.0001$), microsomes/lysosomes ($p_{adj} < 0.0001$) and debris ($p_{adj} < 0.0001$) fractions. The lowest ratios were measured in the potentially sensitive HDP fraction (mean \pm SEM) (15.6 ± 1.7) and were significantly different from those in the granules ($p_{adj} < 0.05$) and HSP fractions ($p_{adj} < 0.0001$). In the gonads (Fig. 7b), Se:Hg molar ratios ranged from 5.0 to 251.9 in the cytosol, with the highest mean observed (103.7 ± 12.6). Cytosol ratios were significantly different than those measured in the granules ($p_{adj} = 0.0001$). The lowest ratios were measured in the granule fraction (38.1 ± 5.7) and were significantly different than the cytosolic and the mitochondrial ratios ($p_{adj} < 0.05$).

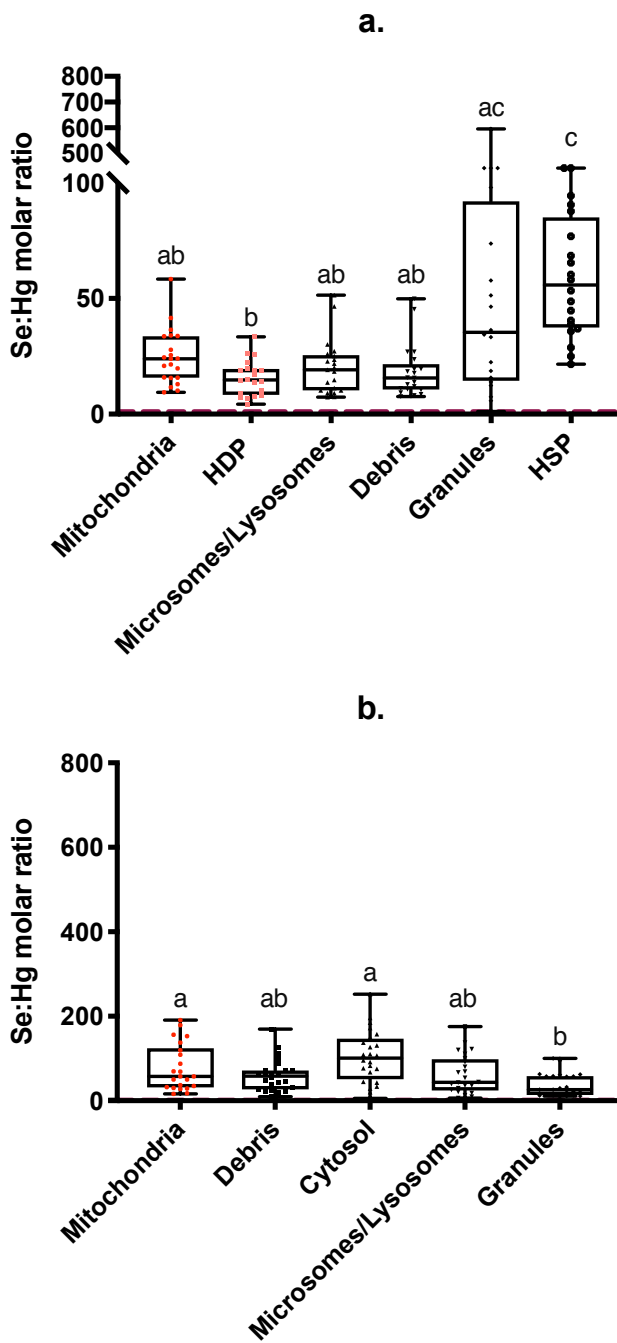


Figure 7. Se:Hg molar ratios for in (a) hepatic ($n=21$) and (b) gonadal ($n=24$) subcellular fractions. The red dashed line represents a threshold of 1, above which Se is suggested to confer protection from Hg toxicity. Letters denote significant differences (Dunn's multiple comparisons test, $p < 0.05$). Sensitive fractions are shown in red (mitochondria) and pink (HDP).

4. Discussion

4.1. Hg accumulates in sensitive fractions

Heat-stable proteins (HSP) do not seem to have a protective effect for sensitive fractions, as we found more than 70% of MeHg burden in hepatic sensitive fractions (mitochondria, HDP) in comparison to 6% in HSP and less than 1% in the granule fraction (Fig. 3a). According to the spillover effect principle, up to a certain exposure threshold, it is assumed that organisms can effectively detoxify metals through sequestration by HSP or incorporation into granules (Campbell et al., 2005). Thus, at low exposure concentrations or low internal doses, the cell is believed to cope with metal contamination and low to no accumulation of metal should be observed in sensitive fractions. However, beyond this threshold, in a contaminated lake for instance, a metal spillover to sensitive fractions should occur (Campbell et al., 2005). This phenomenon can be used as an “early-warning” indicator of metal toxicity (Campbell et al., 2005). Although this model has been studied and validated in the laboratory for cadmium and copper (Jenkins & Mason, 1998; Sanders & Jenkins, 1984), it was not observed in Hg chronically exposed wild populations (Araújo et al., 2015). This could be explained by the fact that under low chronic environmental exposure conditions, fish adapt through trade-offs between the presumably high energetic cost of activating detoxification mechanisms and the cost of allowing metals to accumulate in sensitive fractions (Campbell et al., 2005). As a result, metals progressively accumulate simultaneously in detoxification and sensitive fractions without compromising individual reproduction, growth and survival (Campbell et al., 2005). Accordingly, our results do not support the occurrence of a spillover effect. This can be related to the low level of contamination of Yellow Perch in Lake Saint-Pierre, as 0.06 and 0.009 mg/kg ww of MeHg were measured in the liver and in the gonad whole tissues, respectively. In comparison, Araújo et al. (2015) also measured a low median of 0.05 mg/kg ww THg in wild mullet (*Liza aurata*) livers from a non-contaminated reference site in Portugal. The authors also found low proportions of THg in the HSP and granules fractions in livers of wild mullets, questioning the spillover theory and supporting our results. It was suggested by Araújo et al. that the Hg concentrations that they measured were below the physiological threshold that is

believed to activate the production of metallothionein in *Liza aurata* (Mieiro et al., 2011). However, this threshold is not known for Yellow Perch.

Our results show that about 23% of MeHg was found in hepatic mitochondria and 15% in gonadal mitochondria. Cambier et al. (2009) exposed zebrafish to environmental levels of dietary MeHg in order to assess the effects on mitochondrial structure and function. Binding of MeHg to mitochondria led to structural abnormalities and disturbance of the respiratory mitochondrial chain and the mitochondrial protein synthesis in fish muscle. Since we observed a significant proportion of MeHg in hepatic and gonadal mitochondria, the hypothesis of the occurrence of these latter effects in Yellow Perch cannot be excluded. Few studies have focused on the sub-cellular partitioning of Hg in fish (Araújo et al., 2015; Barst et al., 2016; Barst et al., 2018). Barst et al. (2018) found a greater proportion of Hg in the granule fraction compared to HSP in Yelloweye Rockfish livers, and discussed the accumulation of HgSe granules, which are an end-product of MeHg detoxification (Wang et al., 2012). The production of these granules is not likely to be significant in our study, since only 0.32% of the cellular MeHg burden was found in the hepatic granules fraction. An important proportion of MeHg was also found in gonadal debris. Although this fraction is usually considered to be an indicator of efficient homogenization, it might accumulate nuclei (Barst et al., 2018). The toxicological significance of the debris fraction thus remains ambiguous (Barst et al., 2018).

In terms of concentrations, hepatic HDP had the highest MeHg levels, potentially causing toxicity to the redox defense system through enzymatic impairment (Barst et al., 2018). The HDP fraction contains enzymes and other non-enzymatic proteins (Wallace et al., 2003). All animals also possess selenium-dependent enzymes that are essential to antioxidant and redox control functions (Berry & Ralston, 2008). Due to the fact that Hg binds to Se with high affinity (Berry & Ralston, 2008; Burger & Gochfeld, 2013; Wang et al., 2012), it was shown that Hg and MeHg are irreversible selenoenzymes inhibitors through the impairment of selenoprotein form and function (Carvalho et al., 2008; Watanabe et al., 1999). Since more than 50% of MeHg was found in the HDP fraction of Yellow Perch liver cells (Fig. 3a), the interaction between the latter metal and selenoenzymes might cause a diminution of the available pool of selenoenzymes which are crucial because of their physiological role (Spiller, 2017).

We also found high MeHg concentrations in the hepatic microsomes/lysosomes fraction (Fig. 4a). This fraction is difficult to interpret because it also contains lysosomes, which have a

storage and a detoxifying function (Araújo et al., 2015). On the other hand, microsomes might include fragmented endoplasmic reticulum, which is responsible for synthesis and transport of proteins (Araújo et al., 2015). Binding of MeHg to this fraction might therefore also induce toxicity.

Since MeHg is known to readily bioaccumulate and bioamplify in biota and also to impact cellular energy metabolism (Cambier et al., 2009), the assessment of its binding to sensitive fractions is crucial. However, subcellular MeHg in fish has been assessed in only one study (Peng et al., 2016), as THg is usually measured in subcellular partitioning studies (Araújo et al., 2015; Barst et al., 2016; Barst et al., 2018). Peng et al. (2016) assessed the subcellular partitioning of THg and MeHg in wild rabbitfish from a low contaminated site in China. In this region, they measured THg concentrations in fish muscle ranging from 0.5 to 34 ng/g ww. In contrast, we measured THg levels up to three orders of magnitude higher (108-656 ng/g ww) in Yellow Perch muscle. Moreover, the authors did not report Hg concentrations in all subcellular fractions, also limiting the potential for comparison. However, Peng et al. suggested that metallothionein-like proteins and granules play an important role in MeHg sequestration in the livers of Rabbitfish. Our results do not support this hypothesis, as the lowest MeHg concentrations were found in granules and HSP in Yellow Perch. Since MeHg in subcellular fractions is scarcely explored, we also measured the proportion of MeHg in comparison to THg (%MeHg) in hepatic and gonadal fractions (Fig. S6). Our results show an important variability in proportion of MeHg across fractions. For instance, in the liver (Fig. S6a), there was a significantly lower proportion of MeHg in the granule fraction in comparison to its proportion in HDP, microsomes/lysosomes, debris and HSP. Furthermore, the lowest values were measured in the granule fraction for both organs (42% in the liver and 47% in the gonads) and the highest proportions were found in hepatic microsomes/lysosomes (79%) and in gonadal mitochondria (74%), raising concern because of MeHg toxicity potential.

4.2. MeHg is maternally transferred to gonadal mitochondria

Vitellogenin is a substrate for developing eggs that is produced in the liver of female fish (Drevnick & Sandheinrich, 2003) that may transfer MeHg to developing embryos (Crump & Trudeau, 2009). As a result, we used linear regressions between MeHg concentrations in the liver and eggs of Yellow Perch as proxies for maternal transfer. Our results suggest an evidence of maternal transfer of MeHg in Yellow Perch, which has been assessed in two studies (Hammerschmidt et al., 1999; Niimi, 1983). Hammerschmidt et al. (1999) found a strong relationship ($R^2 = 0.87$) between MeHg in eggs and carcass of Yellow Perch of four seepage lakes in Wisconsin. The authors discussed that even if the amount of mercury that is transferred from the gravid female to her eggs is relatively low (5-20% of the total carcass burden), maternal transfer is the principal exposure path of embryos. Survival and development of young perch could therefore be altered by this maternal transfer. Niimi (1983) also found an evidence of maternal transfer of mercury in Yellow Perch. Factors such as the fraction of lipids in the fish and the amount of total lipids deposited in the eggs significantly influenced mercury transfer. The present study is the first to use subcellular partitioning as a proxy for assessing the toxicity potential linked to maternal transfer. To our knowledge, little is known about the toxicity of MeHg to fish mitochondria and this toxicity has exclusively been assessed experimentally (Cambier et al., 2009; Gonzalez et al., 2005b). Similarly to Cambier et al. (2009), Gonzalez et al. (2005) found that dietary MeHg impacted mitochondrial metabolism and induced the production of reactive oxygen species in zebrafish muscle. While we have not directly measure biomarkers of toxicity and since the previously cited studies did not report mitochondrial MeHg concentrations, it becomes difficult to conclude on possible reproductive impairment *via* damage to gonadal mitochondria energy metabolism in Yellow Perch. Thus, while we confirm the presence of MeHg in the mitochondrial fraction of Yellow Perch gonads through maternal transfer, further enzymatic analyses are needed.

4.3. Selenium is maternally transferred to eggs and might confer protection from Hg toxicity at a subcellular level

Se is an essential micronutrient that is readily transferable from mother to egg in fish and amphibians (Hopkins et al., 2006; Saiki et al., 2004). Despite Se's essential and antioxydant properties to animals including Yellow Perch (Ponton et al., 2016), high concentrations can cause deformities to fish embryos (Lemly, 1993b). We found an evidence of maternal transfer of Se in Yellow Perch of Lake Saint-Pierre, supported by a strong relation between concentration in eggs and concentrations accumulated in female liver. This process was previously observed between fish muscle and eggs (Janz et al., 2010). However, since it was shown that Se is transferred from the liver to gonads through yolk proteins incorporation during oogenesis (Janz et al., 2010), we used the liver instead of the muscle as a proxy for maternal transfer. This maternal transfer has been linked to offspring deformities, reproductive teratogenesis and larval mortality (Janz et al., 2014). A recent study (Covington et al., 2018) assessed the toxicity potential of maternal transfer of Se in wild brown trout. Results showed a strong linear relationship ($R^2 = 0.85$) between egg and whole-body Se. Although the authors did not observe reduced hatching success, they did detect larval deformities and mortality. However, the toxicity threshold that they derived for embryos ($21.1\text{--}22.1 \mu\text{g/g dw Se}$) is far above the concentrations that we measured in gonads ($1.9 \pm 0.06 \mu\text{g/g dw}$). Furthermore, Lemly (1993a) set biological effects thresholds for the health and reproductive success of freshwater fish of $10 \mu\text{g/g dw}$ for gonads, which is 10 times higher than the present concentrations. A more recent assessment of Se reproductive toxicity suggests that this threshold varies between 17 and $24 \mu\text{g/g dw Se}$ in fish gonads (Janz et al., 2010), which is even higher than the former. Since Se is an essential antioxidant (Janz et al., 2014), we hypothesize that, in Yellow Perch from Lake Saint-Pierre, this element is incorporated into embryonic proteins such as selenoamino acids (Janz et al., 2014).

Since we found that Hg and Se are both maternally transferred in Yellow Perch, we assessed their potential antagonism in hepatic and gonadal subcellular fractions. This study provides an interesting snapshot of the potential protective effect of Se at a subcellular level, as these ratios were systematically above 1. Thus, our results indicate that Se might decrease the

toxicity of Hg. Due to the high affinity of Hg for Se, the latter has been suggested to sequester MeHg in vertebrates, reducing its binding availability to essential proteins (Ralston, 2008; Ralston et al., 2008; Wang et al., 2012). It was shown that these two elements form mercury selenide detoxification complexes that can be found in the granules fraction (Ikemoto et al., 2004). Accordingly, the highest ratios that we measured were found in hepatic granules. Ikemoto et al. (2004) measured Se:Hg molar ratios in subcellular fractions of marine birds and mammals. In Dall's porpoises, that mainly feed on fish, ratios were also above 1, averaging 2.3 in nuclei, lysosomes and mitochondria, 2.4 in microsomes/lysosomes and 2.3 in the cytosol (Ikemoto et al., 2004). Authors discussed that the accumulation of Hg in the animals was low (3.8 mg/kg ww in the liver). In comparison, our results show that Yellow Perch THg concentrations in the liver averaged 0.09 mg/kg ww, which are about 42 times lower. We therefore hypothesize that because of these low Hg bioaccumulation levels in Yellow Perch, most Hg is sequestered by Se, reducing Hg toxicity. It is also possible that Se limits Hg bioaccumulation in Yellow Perch, leading to the low Hg levels that we measured (Mailman et al., 2014). Further mechanistic studies are needed to identify the process involved in the interaction between Se and Hg, as it is inconsistent among field studies (Stewart et al., 2010).

We also found (Fig. S7) that Se was preferably bound to HDP in hepatic cells. This is consistent with the fact that in vertebrates, Se is mainly stored as selenomethionine (Janz et al., 2014), a compound that should be heat-denatured in contrast to the active Se form selenocysteine found in the HSP fraction (Barst et al., 2018; Ponton et al., 2016). It was also suggested that Se preference for the HDP fraction is due to its biochemical role in enzymes (Barst et al., 2018). Urien et al. (2018) assessed the subcellular partitioning of Se in gonads of wild white suckers from a mining region and they observed that in gonadal cells, Se was preferentially associated to the HDP fraction. Since we could not separate the cytosol into the HDP and the HSP fractions in gonads, it becomes difficult to extrapolate our results to these latter findings. Because of the major proportion of Se in hepatic sensitive fractions (HDP, mitochondria), we hypothesize that in the liver of Yellow Perch, Se detoxification is limited. This might be observed because selenium concentrations are below the liver biological effects threshold of 12 µg/g dw for the health of freshwater fish (Lemly, 1993a).

In comparison to other studies, the liver (2.5 ± 0.1 µg/g dw) and gonad (1.92 ± 0.06 µg/g dw) Se concentrations that we reported are low. In fact, Urien et al. (2018) measured Se

concentrations of 2.4 µg/g dw in the liver and 2.1 µg/g dw in the gonads of wild White Suckers from a reference site, in comparison to 33.5 µg/g dw in the liver and 28.4 µg/g dw in the gonads of fish from a contaminated site. Our results are therefore closer to the levels measured in the former, uncontaminated site. Ponton et al. (2016) also measured Se concentration up to 15 times higher (38.5 µg/g dw) than our results in liver of Yellow Perch from highly contaminated mining sites. Lastly, Barst et al. (2018) also detected high Se concentrations in liver of Alaskan Yelloweye Rockfish, ranging from 10.8 to 32.9 µg/g dw. The hypothesis of a Se deficiency in Yellow Perch from Lake Saint-Pierre is thus worth mentioning, as it can lead to reduced enzymatic activity and tissue peroxidation in adults (Bell et al., 1987) and delayed growth in juvenile fish (Wang et al., 2013). In fact, Bell et al. (1987) observed adverse Se deficiency effects in Atlantic Salmon fed with a 0.017 mg Se/kg diet, with corresponding liver concentrations of 0.082 µg/g dw. In comparison to this study, the Se concentrations that we measured in the liver of Yellow Perch are higher, questioning the deficiency hypothesis. In sum, the comparison with published data leads us to conclude that it is unlikely that Se is toxic or deficient in Yellow Perch from Lake Saint-Pierre. Rather, we hypothesize that Se is present at levels providing protection from Hg. A thorough assessment of Se deficiency endpoints in fish is needed as related studies are scarce.

5. Conclusion

In aquatic ecosystems, Hg is a contaminant of particular concern, as it is methylated by microbes to the toxic form methylmercury (MeHg), which can readily bioaccumulate and biomagnify in food webs. The present study aimed to assess the toxicity potential of MeHg during maternal transfer in Yellow Perch using an enzyme-validated subcellular partitioning approach. The potential protective effect of selenium was also evaluated. Results showed that MeHg was preferably found in sensitive fractions (mitochondria, HDP) of hepatic cells, indicating that heat-stable proteins might fail to protect mitochondria and enzymes from Hg toxicity. This could lead to harmful effects, since MeHg was shown to cause structural abnormalities to mitochondria as well as inhibition of cellular energy metabolism in previous studies (Cambier et al., 2009; Gonzalez et al., 2005b). Our results also suggest an evidence of maternal transfer of MeHg and Se from gravid females to their eggs. MeHg was also found to be transferred to gonadal mitochondria, implying a toxicity potential. On the other hand, we found that Se:Hg subcellular molar ratios were systematically above 1, indicating a potential protective effect of Se through Hg sequestration. We conclude that although the presence of MeHg in sensitive fractions could lead to adverse effects, proportionally more Se accumulate in cellular fractions than Hg. These results demonstrate the importance of exploring the protective role of Se in fish early-life stages, since they are commonly considered as being particularly sensitive to organic and inorganic contaminants. Accordingly, further studies should focus on specific biomarker analyses in order to validate that high Se:Hg molar ratios are indicators of protection against Hg toxicity. In sum, this study provides an interesting snapshot of the subcellular processes related to Hg contamination in Yellow Perch from Lake Saint-Pierre.

Acknowledgements

This project was financially supported by a FRQ-NT Programme d'initiatives stratégiques pour l'innovation (ISI) grant to M.A. and D.P, by an NSERC Discovery grant to M.A, and by the Canada Research Chair program to M.A.. M.K. received a scholarship through the NSERC CREATE ÉcoLac training program in Lake and Fluvial Ecology. The authors would like to acknowledge Marco Boutin at Natural Resources Canada (Québec, Canada) for the map. We acknowledge Philippe Brodeur, Nicolas Auclair and Rémi Bacon (ministère des Forêts, de la Faune des Parcs du Québec) and local commercial fishermen during fish sampling. We acknowledge laboratory assistance from Dominic Bélanger, Jérémy De Bonville and Gwenola Capelle, and field assistance from Jérémy De Bonville, Maxime Leclerc, Lucie Baillon, Valérie René and Alexandre Arscott-Gauvin. We acknowledge the staff at Pourvoirie Roger Gladu (Saint-Ignace-de-Loyola, Québec) for accommodation and field equipment.

Supplementary Material

Supplementary table

Table S1. Length and weight of each gravid female that was sampled on the North shore (Maski) and on the south shore (BDF) of Lake Saint-Pierre.

Sample	Sampling site	Total length (mm)	Total weight (g)
1	Maski	302	508
2	Maski	271	364
3	Maski	215	148
4	Maski	205	79
5	Maski	285	360
6	Maski	190	100
7	Maski	265	273
8	Maski	240	205
9	Maski	210	118
10	Maski	190	85
11	Maski	247	245
12	Maski	255	255
13	Maski	222	165
14	Maski	151	45
15	Maski	221	175
16	Maski	195	101
17	Maski	213	163
18	Maski	212	133
19	Maski	167	62
20	Maski	196	109
21	Maski	191	82
22	Maski	170	70
23	Maski	292	448
24	Maski	232	175
1	BDF	201	118
2	BDF	233	190
3	BDF	198	110
4	BDF	250	256

5	BDF	251	215
6	BDF	301	384
7	BDF	204	110
8	BDF	235	185
9	BDF	270	327
10	BDF	272	320
11	BDF	254	211
12	BDF	210	131
13	BDF	340	613
14	BDF	305	470
15	BDF	272	303
16	BDF	273	296
17	BDF	194	104
18	BDF	262	264
19	BDF	206	130
20	BDF	223	161
Average ± SD		233.9 ±41.9	212.9 ± 131.1

Supplementary figures

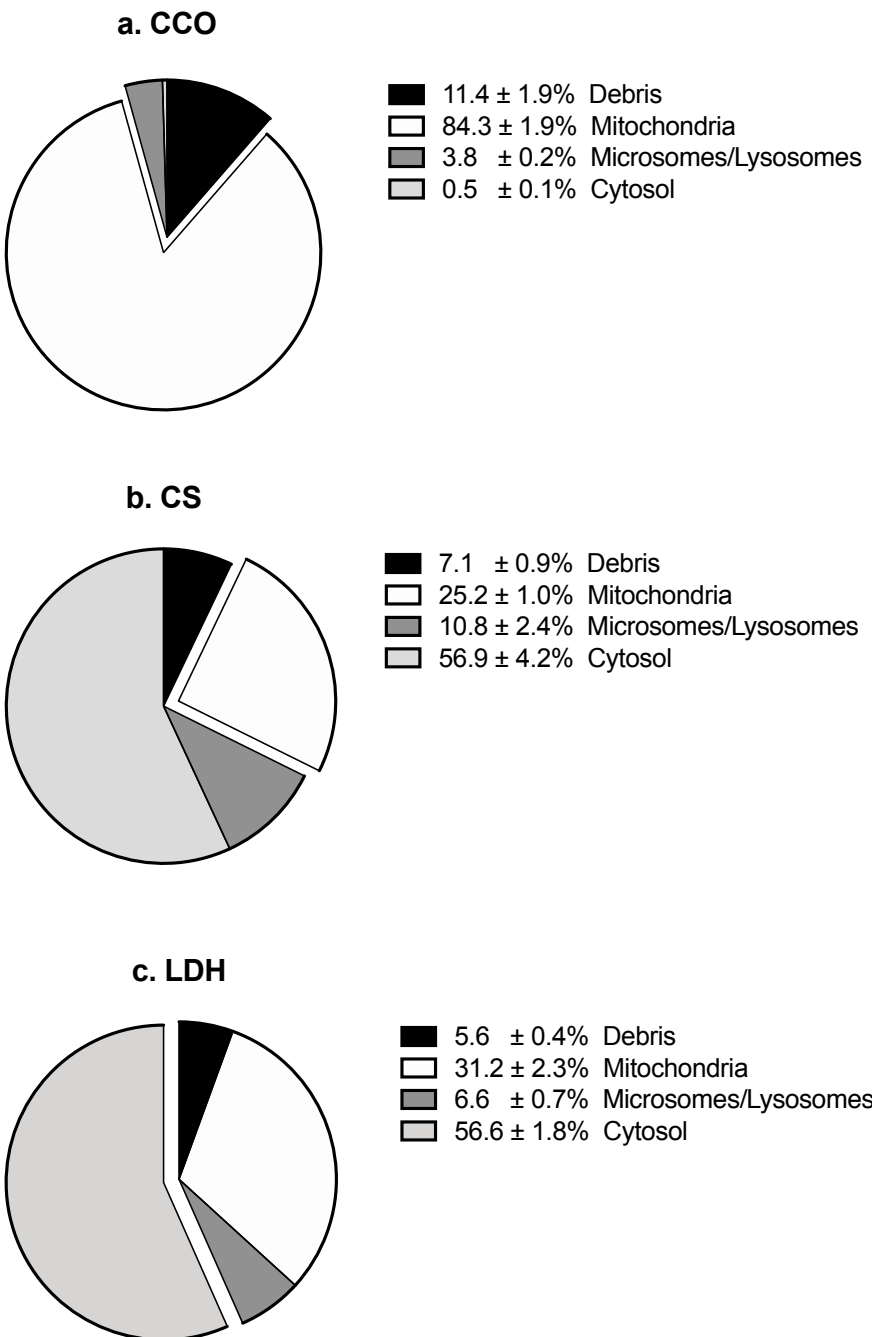
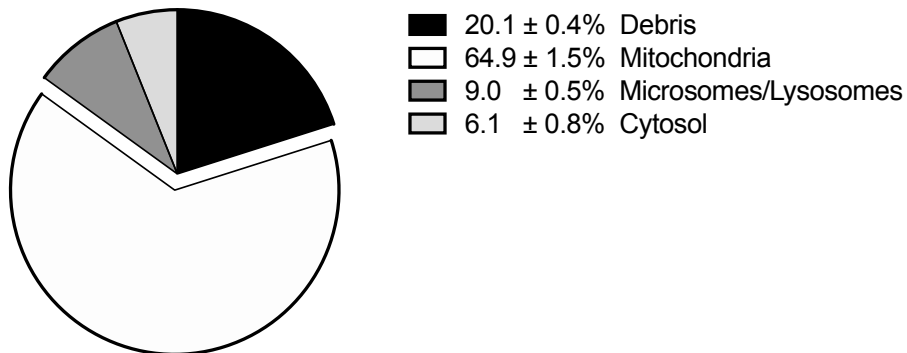
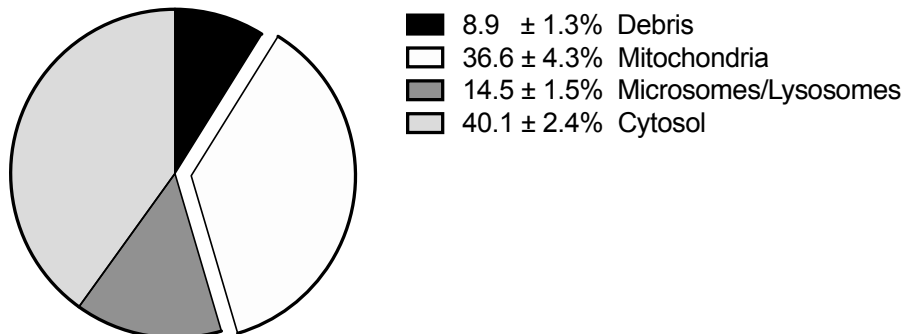


Figure S1. Percentage (mean \pm SEM, in %, n=3) of (a) CCO (mitochondrial membrane biomarker), (b), CS (mitochondrial matrix biomarker), and (c) LDH (cytosolic biomarker) enzymatic activities in subcellular fractions of Yellow Perch liver with the most efficient protocol. Exploded parts represent the fraction in which each enzyme is located.

a. CCO



b. CS



c. LDH

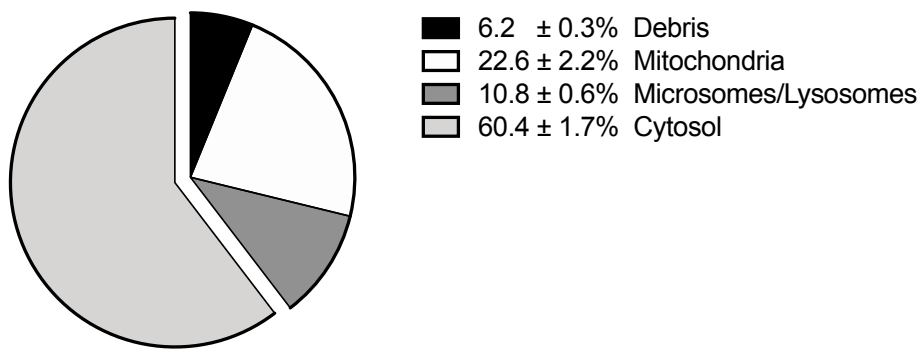


Figure S2. Percentage (mean ± SEM, in %, n=3) of (a) CCO (mitochondrial membrane biomarker), (b), CS (mitochondrial matrix biomarker), and (c) LDH (cytosolic biomarker) enzymatic activities in subcellular fractions of Yellow Perch gonads with the most efficient protocol. Exploded parts represent the fraction in which each enzyme is located.

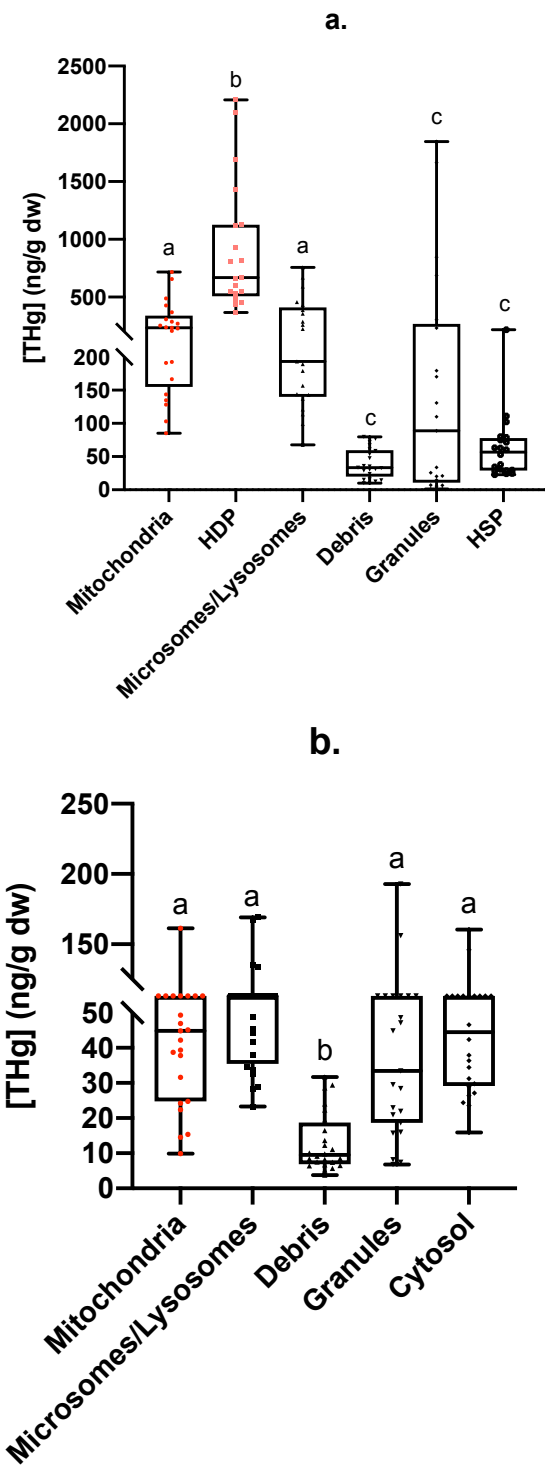


Figure S3. THg concentrations (ng/g dw) in (a) hepatic ($n=21$) and (b) gonadal ($n=24$) subcellular fractions of Yellow Perch. Letters denote significant differences (Tukey's HSD multiple comparisons test, $p < 0.05$). Sensitive fractions are shown in red (mitochondria) and pink (HDP).

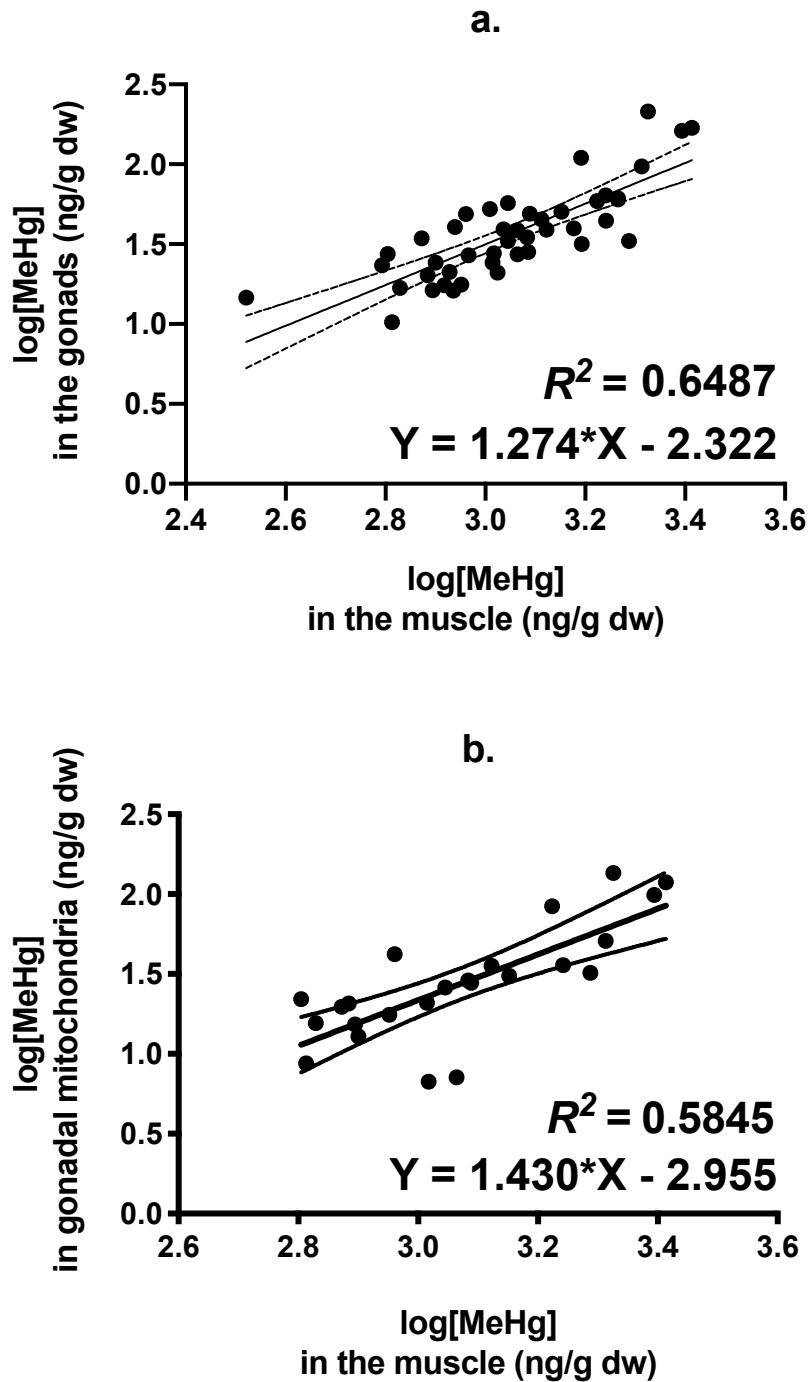


Figure S4. Relationship between MeHg concentrations (ng/g dw) in the muscle and (a) MeHg in the gonads ($n=44$) and (b) MeHg in gonadal mitochondria ($n=24$). Data are log transformed. The R^2 square and the equation of the linear regression are shown on each plot. Dashed curves represent the 95% confidence bands of the best-fit line.

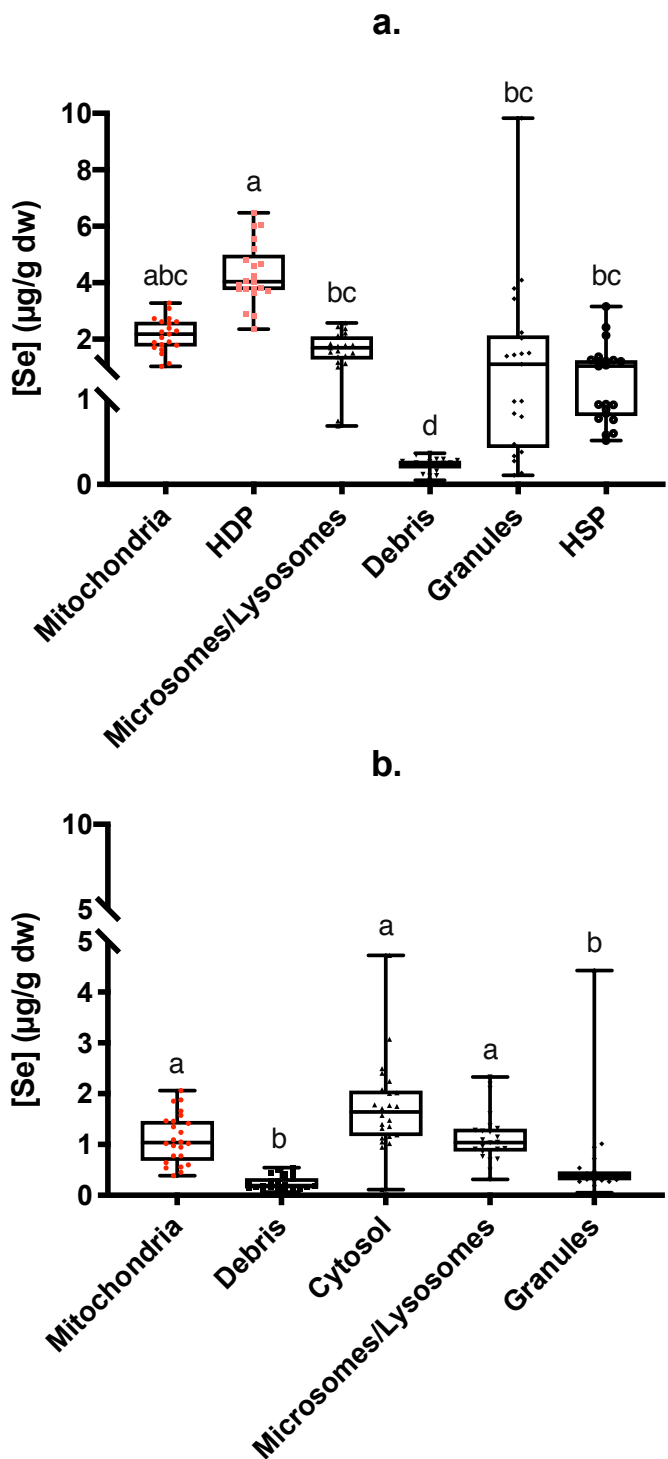


Figure S5. Se concentrations (ng/g dw) in (a) hepatic ($n=21$) and (b) gonadal ($n=24$) subcellular fractions of Yellow Perch. Letters denote significant differences (Tukey's HSD multiple comparisons test, $p < 0.05$). Sensitive fractions are shown in red (mitochondria) and pink (HDP).

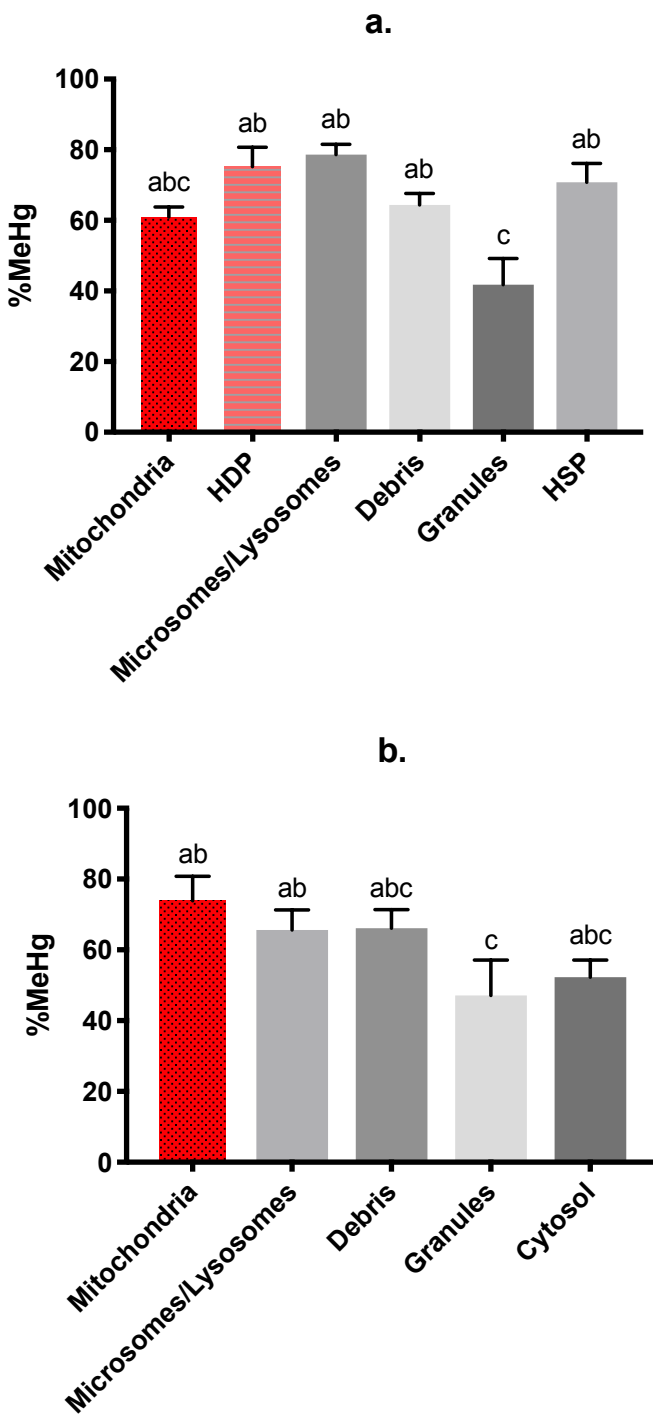


Figure S6. MeHg over THg ratio (mean %MeHg \pm SEM) in (a) hepatic ($n=21$) and (b) gonadal ($n=24$) subcellular fractions of Yellow Perch. Letters denote significant differences (Dunn's multiple comparisons test, $p < 0.05$). Sensitive fractions are shown in red (mitochondria) and pink (HDP).

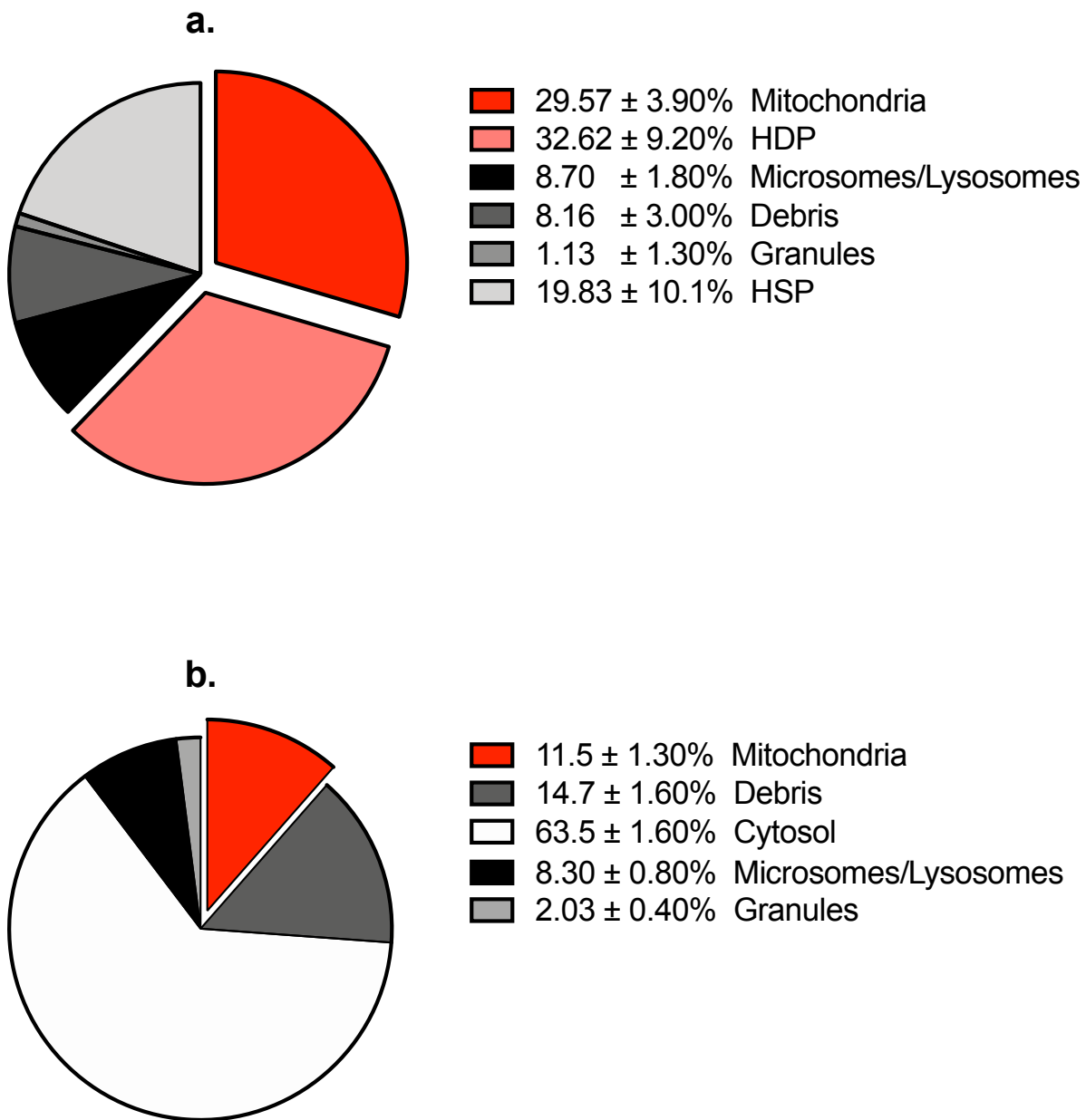


Figure S7. Se burden distribution (% \pm SEM) in subcellular fractions of (a) liver (n=21) and (b) gonadal (n=24) cells. Red and pink exploded parts represent sensitive fractions.

Supplementary methods

SM. 1. Efficiency of the subcellular fractionation procedure / enzymatic analyses

The efficiency of the fractionation procedure was tested using specific enzymes expected to be present in the mitochondrial and cytosolic fractions. Activities were measured according to Caron et al. (2016) (Caron et al., 2016). Enzyme reactions were performed in triplicate in 96-well microplates (BRANDplates ® -PureGrade™S-). The enzymatic activities were assessed by spectrophotometry with a Mithras LB940 (Berthold Technologies) and expressed as units (IU) of enzyme activity per mg of wet weight tissue (IU or mIU mg⁻¹).

In order to solubilize membranes before initiating the enzymatic assays, lysis buffer (pH 7.5) containing 1% Triton™ X-100 (Sigma Aldrich), 20 mM HEPES H7006 (Sigma Aldrich) and 1 mM EDTA E9884 (Sigma Aldrich) was added to each pellet (debris, mitochondria and lysosome/microsome) and was then mixed by vortex agitation.

Citrate synthase (CS; EC 2.3.3.1)

Citrate synthase (CS) is a mitochondrial biomarker located in the mitochondrial matrix. In each well, 10 µL of each subcellular fraction was mixed with 170 µL of a reaction solution composed of phosphate buffer (1 mM, pH 8), Tris T1503 (110 mM; Sigma Aldrich), acetyl coenzyme A (0.2 mM; Sigma Aldrich) and 2-nitro-benzoic acid (0.11 mM; DTNB D8130; Sigma Aldrich). After a 2-min period, a first measurement was taken at 412 nm over 7 min in order to set the baseline. Then, 20 µL of oxaloacetate substrate solution (1.5 mM, 98%, Sigma Aldrich; prepared with the reaction solution) was added, initiating the enzymatic reaction. The formation of DTNB-SH, assessed by measuring the increase in absorbance at 412 nm over 7 min, enabled the determination of CS activity. An extinction coefficient of 13.6 mM⁻¹ cm⁻¹ was used to calculate CS activity expressed as the formation of 1 µmol of DTNB-SH min⁻¹ mg⁻¹ at pH 8.0 and 25°C.

Cytochrome c oxidase (CCO; EC 1.9.3.1)

Cytochrome c oxidase (CCO) is a mitochondrial enzymatic biomarker located in the mitochondrial membrane. The enzymatic reaction was started by mixing in the wells 10 µL of each subcellular fraction with 190 µL of a reaction solution composed of a phosphate buffer (0.1 M, pH 7) and the substrate cytochrome C (0.07 mM, >95%, Sigma Aldrich) previously reduced by adding sodium dithionite (>85%, Sigma Aldrich) in aerated condition. For the reference sample, the 10 µL of subcellular fraction was replaced by 10 µL of K₃Fe(CN)₆ (>99%, Sigma Aldrich). The oxidation of 1 µmol of ferrocytochrome C by CCO, monitored by measuring the decrease in absorbance at 550 nm over 7 min, enabled the determination of CCO activity. An extinction coefficient of 18.5 mM⁻¹ cm⁻¹ was used to calculate CCO activity expressed as the oxidation of 1 µmol of ferrocytochrome C min⁻¹ mg⁻¹ at pH 7.0 and 25°C.

Lactate dehydrogenase (LDH; EC 1.1.1.27)

Lactate dehydrogenase (LDH) is a cytosolic biomarker. In each well, 10 µL of each subcellular fraction was mixed with 170 µL of a reaction solution composed of a phosphate buffer (0.1 M, pH 7) and reduced nicotinamide adenine dinucleotide (0.16 mM, 98%, β-NADH, Sigma Aldrich). After a 2-min period of rest, a first measure was taken at 340 nm over 7 min in order to set the baseline. Then, 20 µL of a pyruvate substrate solution (10 mM, 99%, Sigma Aldrich; prepared with the reaction solution) was added, initiating the enzymatic reaction. The oxidation of NADH to NAD⁺ accompanying the reduction of pyruvate to lactate was monitored by measuring the decrease in absorbance at 340 nm for 7 min and enabled the determination of LDH activity. An extinction coefficient of 6.22 mM⁻¹ cm⁻¹ was used to calculate LDH activity expressed as the oxidation of 1 µmol of NADH min⁻¹ mg⁻¹ at pH 7.0 and 25°C.

SM.2. Efficiency of the subcellular fractionation procedure

In the liver (Fig. S1), more than 80% of CCO and 25% of CS activities were measured in the mitochondria fraction. We considered that separation of fractions was acceptable, even if some mitochondrial matrix was detected in the cytosol (about 57%). We also considered that

cell disruption was acceptable since less than 12% of the CCO and CS activities were measured in the debris fraction and more than 50% of the LDH activity was detected in the cytosol. In the gonads (Fig. S2), about 65% of CCO and 37% if CS activities were measured in the mitochondria fraction. We also observed a leakage of the mitochondrial matrix during cell fractionation, since 40% of CS activity was detected in the cytosol. Since this leaking is inevitable (Cardon et al., 2018; Rosabal et al., 2014), separation of fractions was considered acceptable. Cell disruption was also deemed successful, as more than 60% of LDH activity was measured in the cytosol. We acknowledge that our mitochondrial fraction consists mainly of mitochondrial membrane and that a fraction of the mitochondrial matrix is present in the cytosol.



CHAPITRE 3:

Distribution du mercure et du sélénium dans différents tissus et
stades de vie de la perchaude (*Perca flavescens*) au lac Saint-

Pierre

**Mercury and selenium distribution in key tissues and early life stages of Yellow Perch
(*Perca flavescens*)**

Melissa Khadra^a, Dolors Planas^b, Philippe Brodeur^c and Marc Amyot^a

^a Groupe interuniversitaire en limnologie et en environnement aquatique (GRIL), Département de sciences biologiques, Université de Montréal, Pavillon Marie-Victorin, 90 Vincent d'Indy, Montréal QC

^b Groupe interuniversitaire en limnologie et en environnement aquatique (GRIL), Département de sciences biologiques, Université du Québec à Montréal, C.P. 8888, Succursale Centre-Ville, Montréal QC

^c Ministère des Forêts, de la Faune et des Parcs, Direction de la gestion de la faune de la Mauricie et du Centre-du-Québec, 100 rue Laviolette, Trois-Rivières QC

Published in Environmental Pollution

DOI : 10.1016/j.envpol.2019.112963

Copyright © 2019 Elsevier Ltd.

Abstract

Whereas early life stages are usually considered as particularly sensitive to both organic and inorganic contaminants, field studies assessing contaminant bioaccumulation in these stages are scarce. Selenium (Se) is thought to counteract Hg toxic effects when it is found at Se:Hg molar ratios above 1. However, the variation of this ratio in key fish tissues of different early life stages is mostly unknown. The present study therefore aimed to assess Hg and Se content in gravid female tissues (gonads, muscle, liver, gut, and brain) and different life stages (egg masses, newly hatched larvae (NHL), larvae and juvenile) of Yellow Perch (YP) in a large fluvial lake (Lake Saint-Pierre, Québec, Canada). Se:Hg molar ratios were measured for each compartment in order to fill associated knowledge gaps. Total Hg (THg) and methylmercury (MeHg) concentration varied between tissue according to the following trend: Muscle > Liver > Gut > Brain > Gonads. During YP early life stages, MeHg values increased according to an ontogenetic pattern (mg/kg dw) (mean \pm SEM): Egg masses (0.01 ± 0.002) < NHL (0.015 ± 0.001) < Larvae (0.14 ± 0.01) < Juveniles (0.18 ± 0.01). Se concentrations in different YP tissues showed the following trend (mg/kg dw) (mean \pm SEM): Gut (3.6 ± 0.1) > Liver (2.5 ± 0.1) > Gonads (1.92 ± 0.06) > Brain (1.26 ± 0.03) > Muscle (1.23 ± 0.06). In YP early life stages, Se concentrations were highest in NHL (3.0 ± 0.2), and then decreased as follows: Egg masses (2.8 ± 0.1) > Larvae (1.37 ± 0.04) > Juveniles (0.93 ± 0.05). Se:Hg molar ratios varied considerably and were systematically above 1. This is the first study to simultaneously report Hg and Se bioaccumulation through fish life cycle.

Keywords: mercury; selenium; Yellow Perch; gravid females; early life stages

1. Introduction

Mercury (Hg) is listed as one of the 10 chemicals of major public health concern according to the World Health Organization (WHO), through the International Programme on Chemical Safety (IPCS) (IPCS, 2010). In aquatic ecosystems, microbes convert inorganic Hg to methylmercury (MeHg), a toxic form that is bioaccumulated and biomagnified within aquatic food chains (Mason et al., 2000). As a result, all aquatic organisms, including fish, contain at least traces of MeHg (Ralston et al., 2008), and this methylated compound was found to be dominant in fish tissue (Bloom, 1992). Although it was first assumed that more than 95% of the THg detected in fish muscle was MeHg (Bloom, 1992), this proportion was recently found to increase as fish age and grow, and to vary among species and tissues (Lescord et al., 2018). In addition to being a potent neurotoxin to human consumers (Clarkson & Magos, 2006), MeHg is also highly toxic to fish themselves (Beckvar et al., 2005; Sandheinrich et al., 2011) and may lead to reproductive impairment (Crump & Trudeau, 2009). Dietary MeHg uptake is believed to contribute primarily to Hg accumulation in adult fish (Hall et al., 1997), whereas accumulation of Hg in eggs and embryos originates primarily from maternal transfer (Hammerschmidt et al., 1999; Johnston et al., 2001; Niimi, 1983).

Early developmental stages of fish, namely embryo-larval and early juvenile stages, have been shown to be particularly sensitive to contaminants (Dillon et al., 2010; Fjeld et al., 1998; Luckenbach et al., 2001; McKim, 1977; Weber, 2006). Furthermore, studies using bioenergetics models have demonstrated the importance of integrating ontogenetic parameters in order to better assess contaminant bioaccumulation patterns (Ng et al., 2008; Ng & Gray, 2009). Despite the ecotoxicological significance of early life stages, there is a lack of data on contaminant bioaccumulation, in particular for Hg, in different compartments of fish life cycle. In fact, Beckvar et al. (2005) identified a tissue Hg concentration of 0.02 mg/kg wet weight (ww) in early life stages below which adverse effects were unlikely. However, this threshold was based on a single laboratory study (Matta et al., 2001), urging the need for field toxicity studies on early development stages. Similarly, to our knowledge, only one study reported MeHg as a fraction of total Hg in fish larvae from natural environments (Belzile et al., 2006).

Once assimilated, MeHg can be detoxified or transported to tissues and organs (Peng et al., 2016). It was reported that Hg concentrations are higher in fish muscle than in liver tissue

when whole-body levels are low and that this ratio is reversed at high exposure (Goldstein et al., 1996). Besides muscle and liver tissues, Hg is also often detected in the brain and gonads (Cizdziel et al., 2003; Goldstein et al., 1996; Peng et al., 2016). It is important to understand the dynamics of Hg in fish through the assessment of its bioaccumulation in key tissues particularly since (1) the liver plays a role in detoxification processes (Goldstein et al., 1996), (2) the brain is a target organ for MeHg toxicity (Spry & Wiener, 1991) and (3) the gonads mature into developing embryos (Hammerschmidt et al., 1999). Although some studies have taken into account the distribution of Hg in fish tissues from different aquatic ecosystems (Cizdziel et al., 2003; Kwaśniak & Falkowska, 2012; Mieiro et al., 2011), the determination of the tissue-specific proportion of Hg as MeHg is scarcely explored (Lescord et al., 2018).

Selenium (Se) is an essential micronutrient that is also readily transferable from gravid female into egg in fish (Covington et al., 2018; Saiki et al., 2004), causing deformities to embryos (Lemly, 1993b) as well as larval deformities and mortality at high concentrations (Covington et al., 2018). Se is also known to counteract Hg toxicity because of the high binding affinities between the two elements (Ralston et al., 2008). Thus, when Se:Hg molar ratios exceed a 1:1 stoichiometry (Ralston, 2008), Se is believed to offset Hg accumulation and enhance its elimination (Amlund et al., 2015; Bjerregaard et al., 2011). This protective effect of Se was observed in mammals, birds and fish and reported Se:Hg molar ratios often exceed 1 in fish muscle from natural populations (Belzile et al., 2006; Burger et al., 2013; Cuvin-Aralar & Furness, 1991; Ralston et al., 2008). Despite its importance, the assessment of Se:Hg molar ratios is not systematically taken into account in Hg ecotoxicological studies (Berry & Ralston, 2008). More specifically, there is a lack of data on Se:Hg molar ratios in wild freshwater fish tissues and developmental stages.

Yellow Perch (YP) (*Perca flavescens*) was previously shown to be tolerant to metal contamination (Couture et al., 2008; Eaton et al., 1992). Furthermore, as this species is often dominant in highly contaminated lakes, it can be used as a bioindicator (Couture & Rajotte, 2003). On the other hand, YP was found to be adversely impacted by environmental levels of Hg in some recent field studies (Batchelar et al., 2013a; Larose et al., 2008; Müller et al., 2015). These effects include physiology and cellular metabolism impairment as well as oxidative stress. There is also an evidence of maternal transfer of Hg in YP, leading to an exposure to embryos and potentially reducing hatching success (Hammerschmidt et al., 1999; Niimi, 1983). YP

populations in Lake Saint-Pierre (LSP), the largest fluvial lake of the St. Lawrence River (Canada), are undergoing a major decline that is mainly characterized by poor recruitment (Magnan et al., 2017). Water quality and fish habitat in LSP are heavily affected by inputs of nutrient and chemical pollution from tributaries which drain agricultural watersheds, from municipal effluents and from industrial discharges (Houde et al., 2014b; Hudon et al., 2018). As a result of this low recruitment, a five-year moratorium on sport and commercial fisheries was imposed in 2012 on this commercially important species. Despite the implementation of this moratorium, the inability to restore YP populations appears to persist and it was therefore extended until 2022 (Magnan et al., 2017).

We previously showed evidence of maternal transfer of Hg and Se in YP from LSP (Khadra et al., 2019a), potentially exposing embryos to toxic effects. We therefore used YP as a model species to fill some knowledge gaps on (1) the biodistribution of Se and Hg, (2) the proportion of THg as MeHg (%MeHg) and (3) the Se:Hg molar ratios, in key tissues and different stages of the early YP life cycle. In order to better understand bioaccumulation trends, we analyzed THg, MeHg and Se in key tissues, egg masses and early life stages of YP from LSP. We chose this approach as Hg is bioaccumulative and its toxicity on reproductive and development processes will therefore likely be a function of the accumulated concentrations in key tissues and early life cycle compartments. Furthermore, in order to assess whether YP populations in LSP are at risk of deleterious effects, THg, MeHg and Se concentrations were compared to published tissue-residue toxicity thresholds (Dillon et al., 2010; Holm et al., 2005; Matta et al., 2001).

Because of the application of pollution reduction plans linked to industrial processes upstream of LSP, metal inputs have been greatly reduced during the last decades (Carignan et al., 1994; Caron & Lucotte, 2008). We therefore hypothesized that Hg and Se would be detected in YP tissues and early life stages but that they would not exceed toxicity thresholds established for fish. We also made the assumption that %MeHg would follow an ontogenetic pattern due to a shift in YP diet from zooplankton to benthic invertebrates. Finally, we hypothesized that Se:Hg molar ratios would vary greatly between tissues and across life stages as these ratios were shown to differ considerably within (Belzile et al., 2006) and among fish species (Burger & Gochfeld, 2013).

2. Material and methods

2.1 Study site

The fluvial section of the St. Lawrence River comprises three fluvial lakes, which are, from west to east, Lakes Saint-François, Saint-Louis and Saint-Pierre (La Violette, 2004). Lake Saint-Pierre (LSP) is the largest, covering an area of 318 km². In LSP, a navigation channel separates the water body into the northern and southern water masses, which exhibit contrasting physico-chemical characteristics (Frenette et al., 2003; Paradis et al., 2014). The majority of mercury and selenium inputs in LSP come from chemical and metallurgical industries located on the south shore (Kwan et al., 2003) and from upstream sources.

2.2 Fish sampling

Gravid YP were sampled from Maskinongé Bay (Maski) on the north shore (46°19' N, 73°00' W) and Baie-du-Fèvre (BDF) on the south shore (46°15' N, 72°77' W) (Fig. S1), representing important spawning grounds of LSP. Gravid females were sampled using fyke nets in mid-April 2016 and were kept alive in aerated coolers. In the laboratory, fish were measured, weighed, beheaded and dissected. Liver, muscle, gonads, brain and digestive tract (gut) were removed for Hg and Se analysis. Liver and gonads were weighed. Organs were flash frozen using liquid nitrogen and kept at -80°C until analysis. Egg masses were collected in the field with a dip net at the edge of an agricultural land in LSP (Berthierville, 46°08'29" N, 73°16'37" O) at the end of April 2016. Some of these egg masses were brought back to the laboratory and kept in oxygenated lake water until hatching. Newly hatched larvae (NHL) were flash frozen and kept at -80°C until analysis. Larvae and juveniles were sampled at 4 stations on the north shore and 5 stations on the south shore of LSP (Fig. S1) using push-nets and seine nets in May and August 2016, respectively. Water samples were also collected at all stations. Water samples for dissolved MeHg and Se analyses were pumped through acid-washed Teflon tubing with a peristaltic pump, after the apparatus was flushed with site water for 5 min. Samples were stored

in acid-cleaned amber glass bottles. Water samples were filtered (pore size 0.45 µm) using a peristaltic pump, acid-cleaned Teflon tubing and a GWV high capacity in-line groundwater sampling capsule (Pall Corporation) and preserved with ultrapure hydrochloric acid to 0.4% final concentration until laboratory analysis. Fish were flash frozen directly on the field and kept at -80°C until analysis. All experiments were done in accordance with animal care guidelines from Université de Montréal, with the approval of the ethics committee (CDEA #16-023) following internationally recognized guidelines.

2.3 MeHg, THg and Se analyses

Prior to metal analyses, gravid female tissues, egg masses, NHL, larvae, and juveniles were lyophilized. To ensure adequate biomass for all required analyses, 5 to 10 NHL and larvae of similar size within a sampling site were pooled. All tissue and juvenile samples represented individual fish. Lyophilized samples were homogenized using a glass rod. The resulting dried and ground tissues were used in the following analyses.

For MeHg analyses, fish samples were extracted overnight in 5 mL of 4 M HNO₃ (Fisher Scientific, ACS-pur) at 60°C. A 25 µL aliquot was used for MeHg analysis by cold-vapor atomic fluorescence spectrometer (CVAFS) (Tekran 2700, Tekran Instruments Corporation), according to U.S. EPA method 1630 (detection limit of 0.01 ng/L, calculated as three times the standard deviation (SD) of 10 blanks). Aqueous MeHg concentrations were also determined following U.S. EPA method 1630, by acid-distillation to remove matrix interferences, derivatization by aqueous-phase ethylation, purging on Tenax (Tenax Corporation) and separation by gas chromatography, before detection with a Tekran 2700 CVAFS. New standards (0.5 ng/L) were run after each set of 10–12 samples to test for analytical stability. Analyses were accepted when recovery of certified trace metal reference materials was in the certified range (152 ± 13 ng/g) for TORT-2 lobster hepatopancreas, National Research Council of Canada), and the mean (\pm SD) recovery was $107 \pm 14\%$ (n = 29).

THg concentrations were determined by direct mercury analyzer (DMA-80, Milestone Inc.), in which samples were combusted at 750°C and mercury vapors were retained on a gold

trap for analysis by cold vapor atomic absorption spectrometry (CVAAS). Detection limit was 0.05 ng THg/sample. The certified reference material TORT-2 (lobster hepatopancreas, National Research Council, Canada) (mean recovery $110 \pm 7\%$, n=44) was used for quality control.

Prior to Se analysis, 500 µL of HNO₃:HCl OmniTrace Ultra™ (Millipore Sigma) 1:1 mix was added to freeze-dried samples in Teflon ® vials. Vials were then subjected to a 3-hour cycle in an industrial pressure cooker (121 °C, 15 psi) and 250 µL of hydrogen peroxide OPTIMA grade (Fisher Chemical) was added afterwards for an overnight digestion. Digestate volume was completed to 15 mL with Milli-Q water in 15-mL polypropylene trace metal free vials (VWR®). Water samples were analyzed without any preparation. Se concentrations were measured by inductively coupled plasma – mass spectrometry (8900 ICP-MS Triple Quad; Agilent Technologies). Analytical blanks and standards were added after 10 samples. Method detection limit (limit of detection, LOD, µg/L) of the ICP-MS was 0.056 for selenium. TORT-2 and DORM-2 certified biological reference materials (National Research Council Canada) were submitted to the same digestion protocol as the samples to monitor the efficiency of the digestion procedure. Recoveries (mean ± SD) averaged $103\% \pm 5\%$ (n=18) for TORT-2 and $103\% \pm 9\%$ (n=18) for DORM-2. ICP-MS analyses met the criteria of a Canadian Association for Laboratory Accreditation (CALA) intercalibration exercise.

2.4 Statistical analyses

Shapiro-Wilk normality test was applied to all metal concentrations data. When required, data were log-transformed prior to statistical analyses. Unpaired t-tests were performed to compare metal concentrations of tissues and different life stages between the north and south shores. Since no significant difference was detected ($p > 0.05$), data from the two shores were pooled for all analyses. Furthermore, we did not detect any significant difference in MeHg water concentrations between the north and south shores ($p > 0.05$) (Table S1). Metal concentrations (mg/kg dry weight (dw)) in YP organs and different stages of its early life cycle were represented as boxplots (median, 25th and 75th percentiles, maximum and minimum). Wet weight (ww) concentrations are shown in SI. In order to detect differences among tissue concentrations, one-

way ANOVA were applied, followed by a Tukey's multiple comparisons test, with individual variances computed for each comparison. For the different early stages of the YP life cycle, Kruskal-Wallis nonparametric test was performed, followed by a Dunn's multiple comparisons test. The fraction of THg as MeHg (%MeHg) was calculated as: $100 * [\text{MeHg}] / [\text{THg}]$ and plotted as histograms (mean \pm SEM) for all tissues and early life stages. Finally, Se:Hg molar ratios (dw) were calculated for all organs and for the different early stages of the life cycle and represented as boxplots. Kruskal-Wallis nonparametric test followed by a Dunn's multiple comparisons test were performed on %MeHg and on Se:Hg molar ratios. GraphPad Prism 8 (GraphPad Software Inc., USA) was used for the previously described statistical analyses.

A principal component analysis (PCA) was used to explore the relationships between different biometric measurements and Hg and Se concentrations in the different tissues of gravid females. PCA was performed using the vegan package in R (RCoreTeam, 2016) on log normalized (mg/kg dw), centered and scaled data (n=43). Scaling=2 was used to preserve the correlations amongst descriptors. The length of an arrow represents how well the parameter explains the distribution of the data and the angle between the arrows are representative of the degree of correlation between descriptors ($R^2 \approx \cos(\text{angle})$) (Legendre & Legendre, 1998).

3. Results and discussion

3.1 Biodistribution of THg and MeHg in tissues of gravid YP

THg and MeHg concentrations in YP gonads, brain, gut, liver and muscle are shown in Fig. 1. For both mercury species, values showed the following trend: Muscle > Liver > Gut > Brain > Gonads. THg concentrations ranged from (mean \pm SEM) 0.061 ± 0.007 in gonads to 1.47 ± 0.09 mg/kg dw in the muscle. MeHg content varied from 0.048 ± 0.006 in gonads to 1.23 ± 0.08 mg/kg dw in muscle. For both Hg species, concentrations in gonads and muscle were significantly different than all other tissues. Adjusted *p*-values associated to Tukey's multiple comparison post hoc test are shown in Table S2. MeHg concentrations in muscle were 4 and 26 times higher than those measured in liver and in gonads, respectively. THg and MeHg concentrations in brain and gut were not significantly different and were 4.5 and 5 times higher than in gonads. The same decreasing pattern between the different tissues were noted for wet weight (ww) concentrations (Fig. S2).

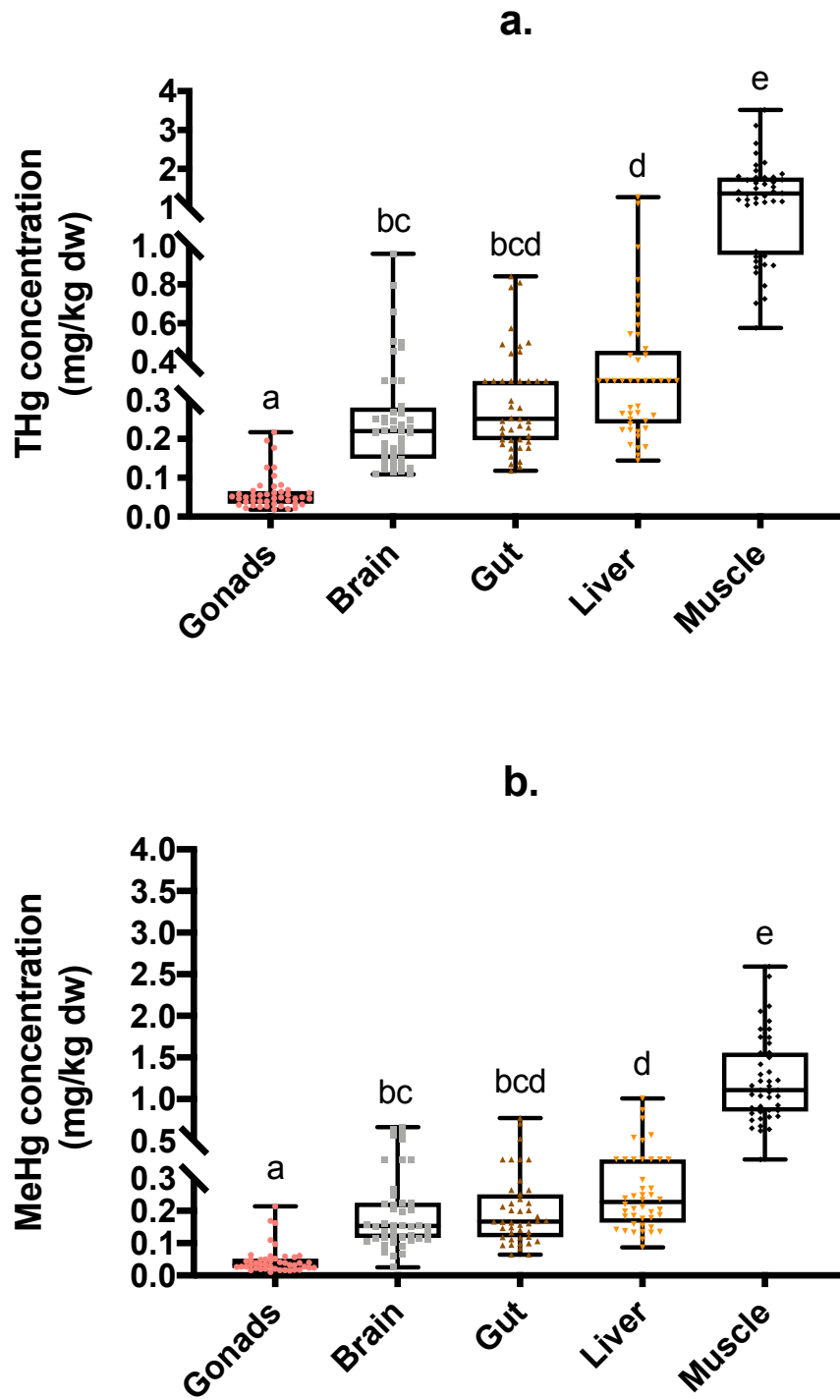


Figure 1. (a) THg and (b) MeHg concentrations (mg/kg dw) in different Yellow Perch' organs (n=44). Letters indicate significant differences (Tukey's HSD multiple comparisons test, $p < 0.05$).

Our results indicate that the highest Hg concentrations were found in the muscle of YP. Dillon et al. (2010) estimated a lowest observable adverse effect level (LOAEL) of 0.5 mg/kg ww in adult fish muscle through a compilation of several fish toxicology studies. Since only two individuals exceeded this threshold in the present study (Fig. S2), we can hypothesize a low exposure to Hg, suggesting that adult individuals are not likely to show cellular or reproductive damage (Sandheinrich et al., 2011). In order of importance, the second highest Hg concentrations were measured in the liver, with a liver:muscle ratio averaging 0.3 for THg and 0.2 for MeHg. It was previously shown that when Hg in muscle or whole-body concentrations are low (less than approximately 0.5 mg/kg ww), Hg concentrations measured in the muscle are usually about twice those found in the liver (Goldstein et al., 1996). In fact, it was hypothesized that fish can tolerate low concentrations of Hg (less than 0.5 mg/kg ww). However, when muscle concentrations exceed approximately 1.0 mg/kg ww, Hg is redistributed from the muscle, thereby increasing the concentrations in the liver (Cizdziel et al., 2003; Goldstein et al., 1996). Our results therefore suggest that YP from LSP are exposed to low concentrations of Hg, as the average muscle concentrations did not exceed 0.5 mg/kg ww. We measured MeHg concentrations in liver ranging from 0.019 to 0.219 mg/kg ww (Table S3), which are consistent with Larose et al. (2008) who measured levels ranging from 0.015 to 0.294 mg/kg ww in YP liver from lakes of the boreal forest. These low concentrations were linked to adverse effects on YP physiology and cellular metabolism (Larose et al., 2008). In order of importance, the highest Hg concentrations were measured in the gut. However, this tissue is usually not taken into account in Hg tissue distribution freshwater field studies. We therefore hypothesize that high concentrations in gut are due to the fact that diet is the main route of MeHg exposure in fish (Hall et al., 1997).

It was shown that high MeHg concentrations in fish brain tissue may lead to neurotoxic effects and oxidative stress (Gonzalez et al., 2005a; Graves et al., 2017). In fact, Graves et al. (2017) observed these adverse effects in YP from a Hg hotspot in Nova Scotia (Canada) with brain concentrations ranging from 0.28 to 2.13 mg/kg ww, which are 10-fold higher than the concentrations that were measured in the present study (Table S3). On the other hand, Cizdziel et al. (2003) measured an average of 0.08 mg/kg ww in striped bass brain tissue from Lake Mead, which is comparable to our results (mean of 0.05 mg/kg ww). However, the toxicity

potential of these levels was not discussed. The authors (Cizdziel et al., 2003) also found a direct correlation between brain and muscle concentrations, which was also observed in several catfish species by Bastos et al. (2015). We also observed that MeHg and THg concentrations in YP muscle are strong predictors of brain concentrations (Fig. S4). As Hg has been found to disrupt the hypothalamic and pituitary function in fish at concentrations as low as 0.07 mg/kg ww in brain tissue (reviewed in Crump and Trudeau (2009)), the prediction of brain concentrations through muscle tissue content may be a useful tool in field ecotoxicological studies (Bastos et al., 2015).

Gonads had the lowest Hg concentrations of all analyzed tissues, which is consistent with Cizdziel et al. (2003) who observed a pattern of decreasing concentrations of muscle > liver > gonad in Largemouth Bass (*Micropterus salmoides*) and Bluegill (*Lepomis macrochirus*) from Lake Mead. Hammerschmidt et al. (1999) assessed the Hg content in eggs and carcasses of YP from seepage lakes in Wisconsin and egg concentrations ranged from 0.01 to 0.25 mg/kg ww (concentrations were converted assuming that water content averaged 85% in the eggs). Although the concentrations measured in YP gonads from LSP approximated the lower limit of the latter range (Table S3), the toxicological significance of this Hg content was not discussed by the authors, as the associated literature is scarce (Hammerschmidt et al., 1999).

3.2 Bioaccumulation of THg and MeHg at different YP life stages

THg and MeHg concentrations in YP egg masses, NHL, larvae and juveniles are shown in Fig. 2. For THg (Fig. 2a), values showed the following trend: Juveniles > Larvae > Egg masses > NHL. THg content ranged from (mean \pm SEM) 0.030 ± 0.002 in NHL to 0.200 ± 0.011 mg/kg dw in juveniles. THg concentrations in juveniles were 159, 131 and 3 times higher than those measured in NHL ($p_{adj} < 0.0001$), egg masses ($p_{adj} < 0.0001$) and larvae ($p_{adj} > 0.05$), respectively. For MeHg (Fig. 2b), values increased according to an ontogenetic pattern: Egg masses < NHL < Larvae < Juveniles. MeHg content ranged from (mean \pm SEM) 0.012 ± 0.002 in egg masses to 0.184 ± 0.009 mg/kg dw in juveniles. MeHg concentrations measured in juveniles were 15 and 12 times higher than in egg masses and NHL, respectively ($p_{adj} < 0.0001$)

. THg and MeHg concentrations in NHL and egg masses did not differ significantly, nor did juveniles and larvae concentrations ($p > 0.05$). The same decreasing patterns between the different life stages were noted for wet weight (ww) concentrations (Fig. S3).

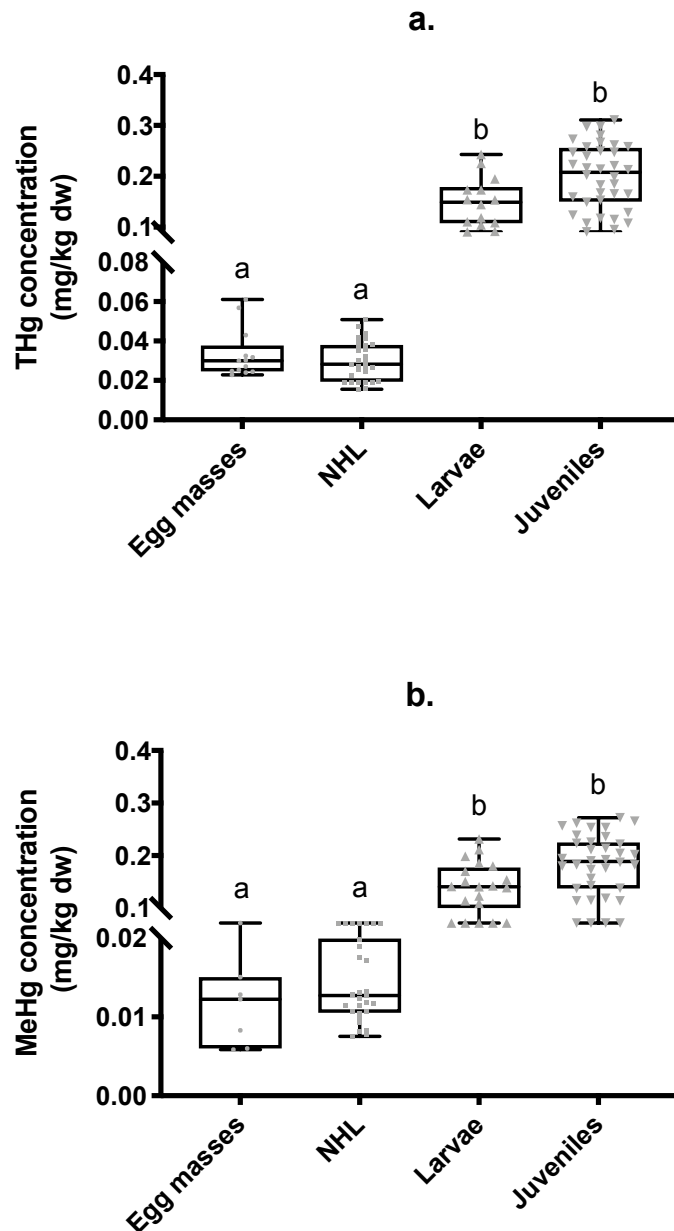


Figure 2. (a) THg and (b) MeHg concentrations (mg/kg dw) in Yellow Perch egg masses (n=7), newly-hatched larvae (NHL) (n=29), larvae (n=20) and juvenile (n=36). Letters indicate significant differences (Dunn's multiple comparisons test, $p < 0.05$).

YP in LSP are currently undergoing a decline in populations that is mainly characterized by poor recruitment (Magnan et al., 2017). Thus, one of our objectives was to assess the fate of Hg throughout the first year of this species' life cycle. We previously confirmed that this contaminant was maternally transferred to embryos (Khadra et al., 2019a), potentially reducing hatching success (Hammerschmidt et al., 1999; Kihlström et al., 1971). The ontogenetic pattern in MeHg bioaccumulation that we observed could be mainly explained by the shift from endogenous to exogenous feeding in YP larvae, since it has been shown that MeHg bioaccumulates in fish primarily through dietary uptake (Hall et al., 1997; Spry & Wiener, 1991). Hg bioaccumulation in egg masses can occur via maternal transfer as well as bioconcentration of waterborne Hg, supporting the low concentrations that we observed (Latif et al., 2001). Exogenous feeding in YP then starts at the larval stage, when YP length reaches 9 mm and their mouth is fully differentiated and in terminal position (Spanovskaya & Grygorash, 1977). Therefore, NHL survival depends on yolk sac utilization efficiency and on the amount of endogenous nutrient stores (Rust, 2002). Larvae feed on zooplankton for 30 to 40 days until they become juveniles with fully differentiated stomachs, at which point they start to eat primarily benthic invertebrates (Byström et al., 2003). Since MeHg is biomagnified up trophic chains, food source can help explain why juveniles present 12 times more MeHg than NHL. In fact, a previously published stable isotope analysis confirmed a slight increase in trophic position between 0+ and 1+ YP in LSP, highlighting the dietary shift from zooplankton to macroinvertebrates (Bertrand et al., 2011).

Since embryo-larval and early juvenile stages are particularly sensitive to organic and inorganic contaminants (Luckenbach et al., 2001; McKim, 1977; Oliveira et al., 2009), Beckvar et al. (2005) suggested a Hg toxicity threshold for early life stages of 0.02 mg/kg ww, which is 10 times more protective than the adult and fully developed juvenile threshold of 0.2 mg/kg ww. Our results show that Hg concentrations in egg masses and NHL are below the toxicity threshold, whereas 17% of individuals at larval stage are above it, indicating a potential toxicity. This protective concentration was in fact associated to reduced fertilization success in Mummichog (*Fundulus heteroclitus*) in a previous study (Matta et al., 2001). Juveniles are, however, far below the toxicity threshold for adult fish, but above the threshold for early life stages. A more recent tissue-residue toxicity study highlighted the scarcity of published data on

laboratory and field toxicity studies on fish early-life stages (Dillon et al., 2010). Nevertheless, using a mercury dose-response curve, the authors established that fish early life stages (eggs, NHL, larvae) that showed no injury had a median tissue concentration of 0.05 mg/kg ww. Since the highest THg concentration that we measured in larvae was 0.02 mg/kg ww (Fig. S3), adverse effects are unlikely to occur at the larval stage in the LSP YP population. It is somehow relevant to point out that behavioural effects, namely predator escape, were adversely impacted in zebrafish larvae at similar low tissue concentrations (0.0007-0.015 mg/kg ww) in a laboratory study (Weber, 2006). However, embryos were exposed to Hg²⁺, underlining the importance of considering the toxic and bioaccumulated form MeHg.

3.3 Differences in %MeHg among key tissues and early life stages

The percentages of MeHg (%MeHg) in different YP tissues and stages of early life cycle are shown in Fig. 3. In YP tissues (Fig. 3a), the lowest %MeHg (mean ± SEM) (66.4 ± 2.0) were measured in the gut, whereas the highest were measured in the muscle (84.5 ± 1.9). %MeHg in the muscle were significantly higher than those observed in the gut ($p_{adj} < 0.0001$), in the liver ($p_{adj} < 0.0001$) and in the gonads ($p_{adj} = 0.001$). %MeHg values showed the following trend: Muscle > Brain > Gonads > Liver > Gut. In the different stages of YP early life cycle (Fig. 3b), the lowest %MeHg (mean ± SEM) (39.4 ± 6.0) were measured in the egg masses, whereas the highest values were found in larvae (97.0 ± 1.9). %MeHg did not follow an ontogenetic pattern, as values showed the following trend: Larvae > Juveniles > NHL > Egg masses. %MeHg in larvae was significantly higher than in egg masses ($p_{adj} < 0.0001$) and NHL ($p_{adj} < 0.0001$), but not in juveniles ($p > 0.05$).

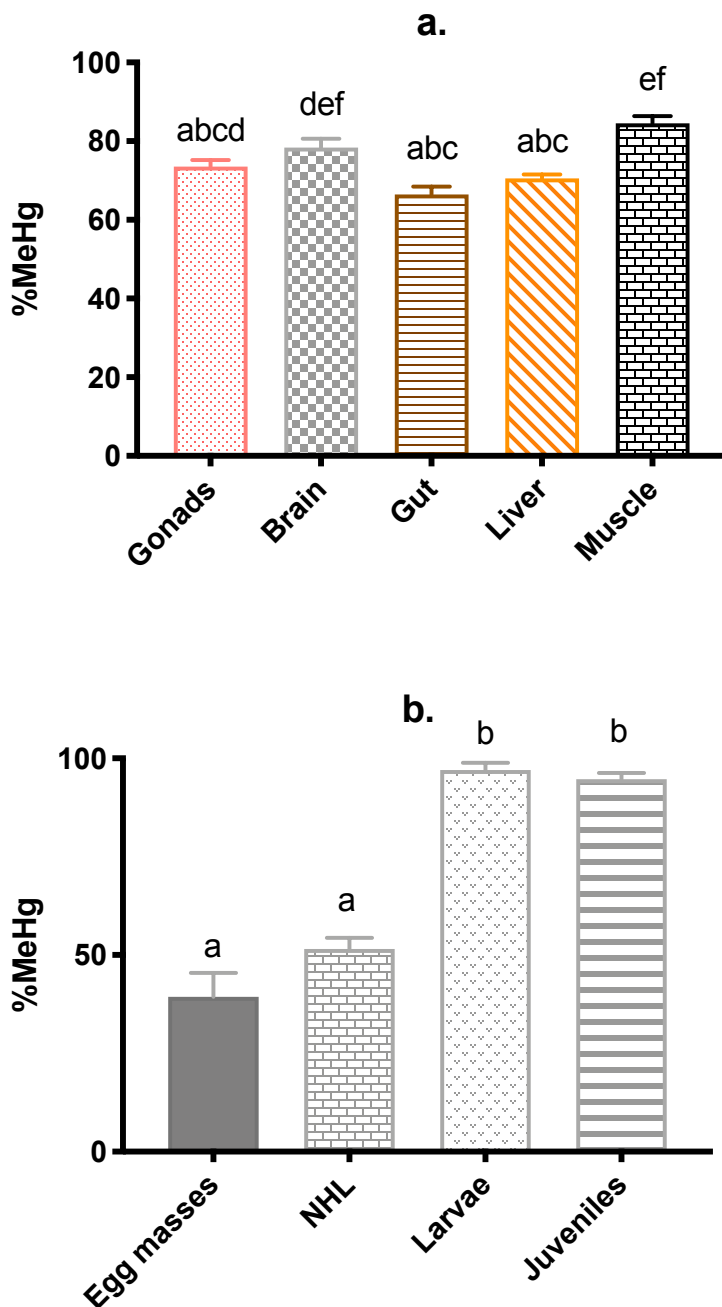


Figure 3. Fraction of total Hg as MeHg (%MeHg) (mean \pm SEM) in (a) tissues ($n=4$) and (b) different parts of the life cycle of Yellow Perch (egg masses ($n=7$), newly-hatched larvae (NHL) ($n=29$), larvae ($n=20$) and juvenile ($n=36$)). Letters indicate significant differences (Dunn's multiple comparisons test, $p < 0.05$).

It was previously reported that more than 95% of THg in fish muscle was MeHg (Bloom, 1992). However, it was recently shown that the percentage of MeHg is both species- and tissue-specific and that it also varies with age and body size (Lescord et al., 2018). In fact, Lescord et al. (2018) assessed the %MeHg in several fish species from lakes in Ontario (Canada). The authors found an average of 83.5% in fish muscle, which is consistent with our results. The preferential accumulation of MeHg in fish muscle can be due to its binding affinity to sulphydryl groups in protein (Harris et al., 2003). Our results also show that almost 100% of THg is found as MeHg in larvae and juveniles, whereas only reaching 50% in NHL. This observation could be attributed to the initiation of MeHg accumulation through zooplankton ingestion in fully differentiated larvae. The %MeHg in fish early life stages is scarcely explored. Belzile et al. (2006) assessed the %MeHg in several organisms including YP larvae (less than 40 days old) in lakes located at an increasing distance from metal smelters, and therefore Se deposition, in Ontario (Canada). They found an average of 62% in YP larvae, whereas we measured an average of 97% in the same life compartment from LSP. These differences could be due to the fact that the high Se deposition from smelters could have reduced Hg methylation rates (Jackson, 1991). The authors (Belzile et al., 2006) also observed an increase in %MeHg along the food chain, a pattern that was also somewhat apparent in our results, as egg masses and NHL as a group had significantly lower %MeHg than larvae and juveniles, also as a group. It therefore seems that the relative proportion of MeHg to THg increases during early YP development, most likely due to a dietary shift in YP larvae (Hall et al., 1997). These findings reinforce the importance of systematically measuring the proportion of MeHg instead of relying on the assumption of 95%.

3.4 Biodistribution of Se in key tissues and early life stages

Se concentrations in different YP tissues and early life stages are shown in Fig. 4. Se concentrations in YP tissues showed the following trend: Gut > Liver > Gonads > Brain > Muscle (Fig. 4a). Concentrations in the gut (mean \pm SEM) (3.56 ± 0.14 mg/kg dw) were almost three times higher than muscle (1.23 ± 0.06 mg/kg dw) ($p_{adj} < 0.0001$) and brain (1.26 ± 0.03 mg/kg dw) ($p_{adj} < 0.0001$) concentrations. Muscle and brain Se concentrations did not differ significantly ($p > 0.05$) and averaged 1 mg/kg dw. Egg masses and NHL had significantly higher

Se concentrations than larvae and juveniles ($p_{adj} < 0.0001$). (Fig. 4b). Juveniles showed the lowest Se concentrations (mean \pm SEM) (0.93 ± 0.05 mg/kg dw). Se concentrations in NHL were three times higher than juveniles ($p_{adj} < 0.0001$). Se concentrations in egg masses and NHL did not differ significantly ($p > 0.05$).

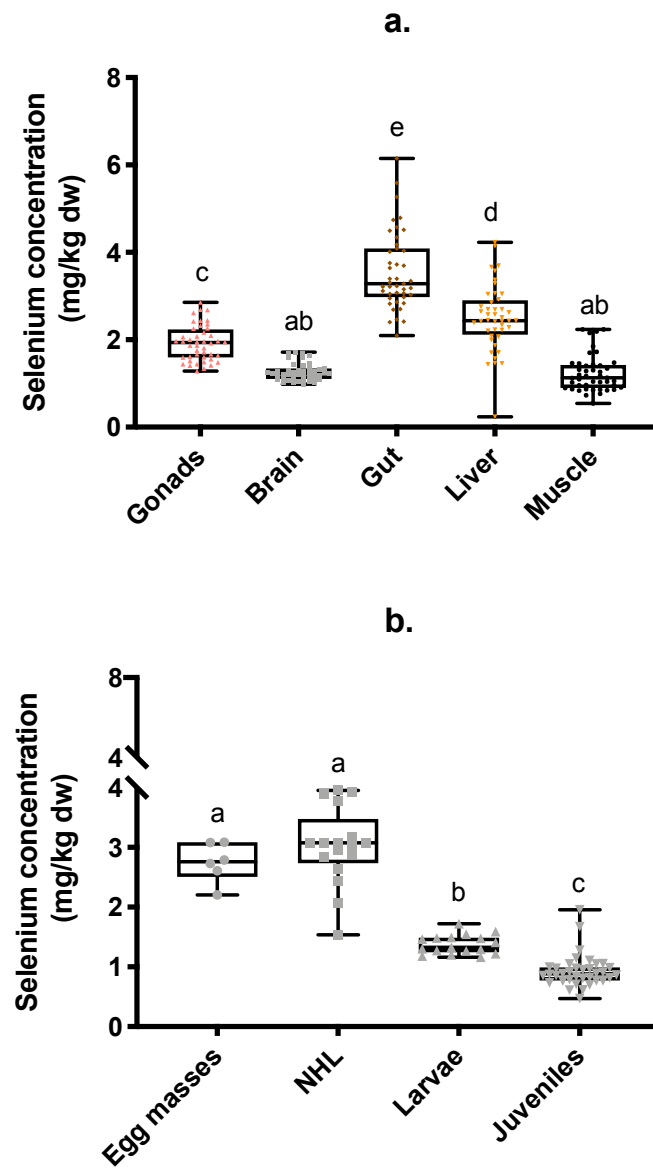


Figure 4. Se concentrations (mg/kg dw) in (a) tissues (n=44) and (b) different parts of the life cycle of Yellow Perch (egg masses (n=7), newly-hatched larvae (NHL) (n=29), larvae (n=20) and juvenile (n=36)). Letters indicate significant differences (Tukey's HSD multiple comparisons test, $p < 0.05$ for (a) and Dunn's multiple comparisons test, $p < 0.05$ for (b)).

As Se was preferably accumulated in the gut, we hypothesize that diet is a significant source of this metal for YP in LSP. It was in fact shown that organic forms of Se are readily bioaccumulated in fish following dietary exposure (Lemly, 1997). Lemly set biological effects thresholds for the health and reproductive success of freshwater fish of 8, 12 and 10 µg/g dw for the muscle, liver and eggs, respectively (Lemly, 1993a). These thresholds were based on a compilation of numerous laboratory and field ecotoxicological studies. The concentrations that we measured did not exceed these guidelines, as the highest individual Se concentration was found in the gut and reached 6.15 µg/g dw. A more recent study also stated that when egg Se concentrations reached 8-10 µg/g dw, skeletal deformities, craniofacial defects and edema could occur in rainbow trout larvae (Holm et al., 2005). However, the highest individual Se concentration that we measured in YP gonads reached 2.86 µg/g dw. Rather, the Se gonad content reported here (1.92 ± 0.06 µg/g dw) approximated the concentrations that Kennedy et al. (2000) measured in cutthroat trout eggs from a reference site (4.6 ± 1.8 µg/g dw) in British Columbia (Canada). Similarly, the authors measured Se concentrations of 8.2 ± 3.3 µg/g dw in the liver and 2.4 ± 0.8 µg/g dw in the muscle of trout from the reference site, with a decreasing pattern of liver > gonads > muscle, which is similar to the pattern presented here. The authors discussed that the distribution of Se in tissues might depend on tissue-specific lipid content (Kennedy et al., 2000). However, we found a decreasing pattern of gonads (4.4 ± 0.4 %) > liver (3.9 ± 1.0 %) > muscle (1.2 ± 0.2 %) for the total lipid proportion. Therefore, the lowest Se concentrations are linked to the lowest lipid content. At high concentrations, Se is also known to cause teratogenic deformities in fish embryos following maternal transfer (Lemly, 1997). However, it was observed that larval whole-body concentrations of 30-40 µg/g dw caused 80% deformities in centrarchids (Lemly, 1997), which are far above the average of 1.4 µg/g dw that we measured in YP larvae. These low larval concentrations could be attributed to the fact that in the yolk, Se is incorporated into the lipovitellin and phosvitin platelets, which are assimilated by the developing larval fish (Holm et al., 2005). Therefore, it is only after Se has been assimilated, if it is found in sufficient concentrations, that bioaccumulation and toxic effects begin to occur. On the other hand, Se dietary deficiency was shown to cause growth disturbance in juvenile carp (Wang et al., 2013). However, Se deficiency in fish is, to this day, not well understood, urging the need for further assessment of this pathology, particularly within natural

populations. Thus, our data provides some information on the tissues and early life stages that are more likely to develop Se deficiency symptoms, considering the fact that Hg antagonism could accentuate these adverse effects.

3.5 Se:Hg molar ratios in tissues and early life stages

Se:Hg molar ratios in YP tissues and different early stages are shown in Fig. 5. Results show that all ratios were systematically above one, except for two muscle samples, both exhibiting ratios of 0.9. In YP tissues (Fig. 5a), the highest values were measured in the gonads (mean \pm SEM) (112 ± 10) and the lowest values were measured in the muscle (2.5 ± 0.2). Muscle, gut and gonadal Se:Hg molar ratios were significantly different from all other tissues. Brain ratios were 6 times higher than muscle ratios. In the different stages of YP early life cycle (Fig. 5b), the highest Se:Hg ratios were measured in NHL (299 ± 28) and the lowest values were found in juveniles (14 ± 1). Ratios measured in NHL were significantly higher than in larvae ($p_{adj} < 0.005$) and in juveniles ($p_{adj} < 0.0001$). The ratios measured in juveniles were significantly lower than all other stages of early life cycle.

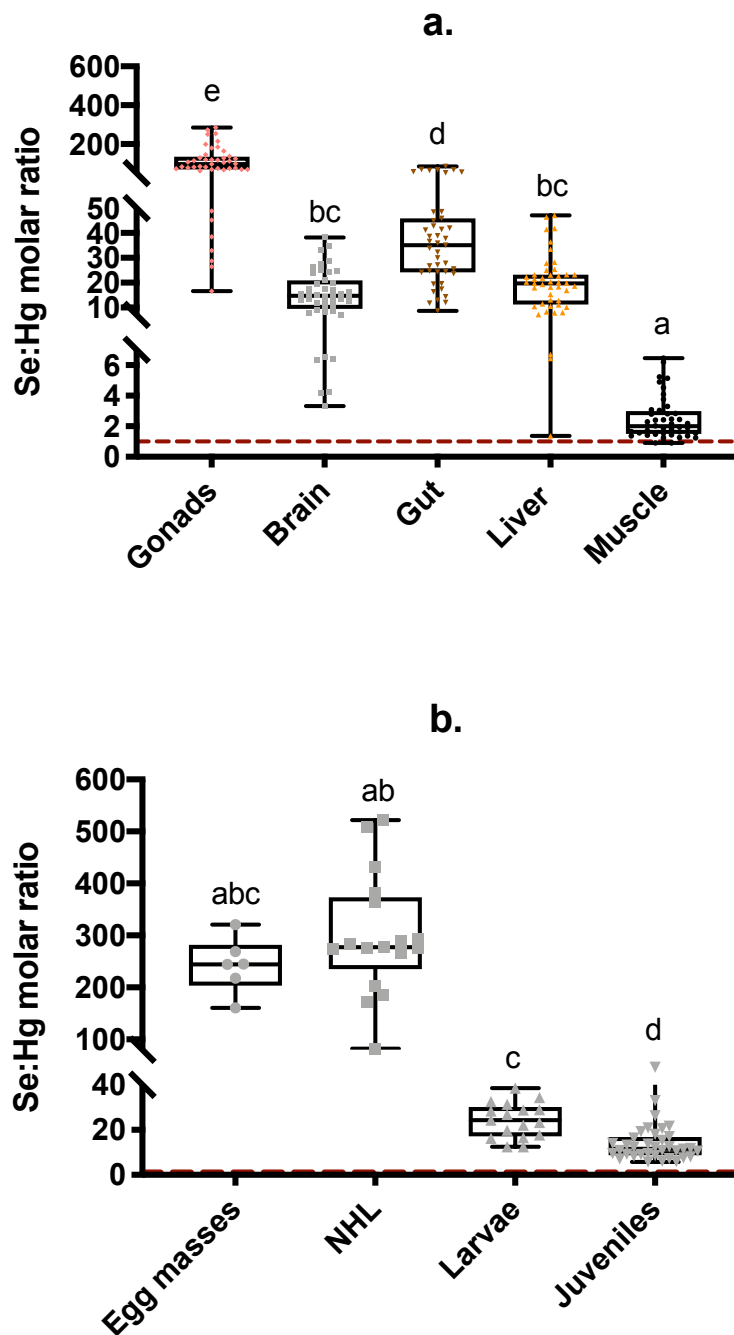


Figure 5. Se:Hg molar ratios in (a) organs ($n=44$) (b) different parts of the life cycle of Yellow Perch (egg masses ($n=7$), newly-hatched larvae (NHL) ($n=29$), larvae ($n=20$) and juvenile ($n=36$)). The red dashed line represents a threshold of 1, above which Se is suggested to confer protection from Hg toxicity. Letters indicate significant differences (Dunn's multiple comparisons test, $p < 0.05$).

It is now acknowledged that Se moderates Hg toxicity through sequestration, thus reducing its bioavailability (Peterson et al., 2009; Ralston et al., 2008). Furthermore, it has been suggested that it is not the concentration of (Me)Hg present in an organism that is critical, but rather the molar ratio of Hg relative to Se in the tissues (Peterson et al., 2009). Accordingly, although the exact protective ratio is not known, a Se:Hg molar ratio approaching or exceeding 1:1 could protect fish from Hg adverse effects (Deng et al., 2008; Scheuhammer et al., 2015). However, the protective effect of this ratio for different fish tissues is unclear (Burger et al., 2013). Burger et al. (2013) measured Se:Hg molar ratios in different tissues (brain, muscle, liver, kidney) of Bluefish from the New Jersey Atlantic coast. For all tissues, ratios were greater than 1. The lowest values were measured in the muscle and averaged 3, which is consistent with our results. Elevated Se:Hg molar ratio values suggest that proportionally more Se accumulates in tissues than Hg, increasing Se protective effects (Burger et al., 2013). Literature on Se:Hg molar ratios in fish early life stages is scarce. Belzile et al. (2006) assessed the Se:MeHg molar ratios in YP from several lakes located at an increasing distance from metal smelters, causing important Se deposition, in Sudbury (Canada). They found an average of 437 for larvae and 820 for adults (whole-body), which contrast with our lower ratios, mainly because of the difference in Se inputs between the 2 regions. While these results are consistent with the fact that we measured ratios that systematically exceeded the 1:1 threshold, they mainly highlight the need to establish an accurate ratio. In fact, the range between 1 and 820 is wide and it is currently unclear if such high values are toxicologically significant.

3.6 Correlation between biometric data and metal concentrations

The PCA biplot accounted for 79.6% of the total variation among individuals (Axis 1: 56.4% and Axis 2: 23.2%) (Fig. 6). Based on the PCA scores, gonad weight and gonad MeHg concentrations were the most important variables in explaining axis 1. On the other hand, gonad mass and YP mass were strongly associated with the construction of axis 2. Based on the angles between descriptors, MeHg concentrations in all tissues are strongly positively correlated to one another. The strongest correlation is observed between gut and gonads. MeHg and Se concentrations are also strongly positively correlated in the muscle and in the liver, but not in

the brain or in the gut. In the gonads, MeHg and Se concentrations are negatively correlated. Brain Se concentrations are also negatively correlated to biometric measurements, whereas muscle and gut Se concentrations are positively correlated to the latter descriptors. There is little correlation between MeHg concentrations and biometric data.

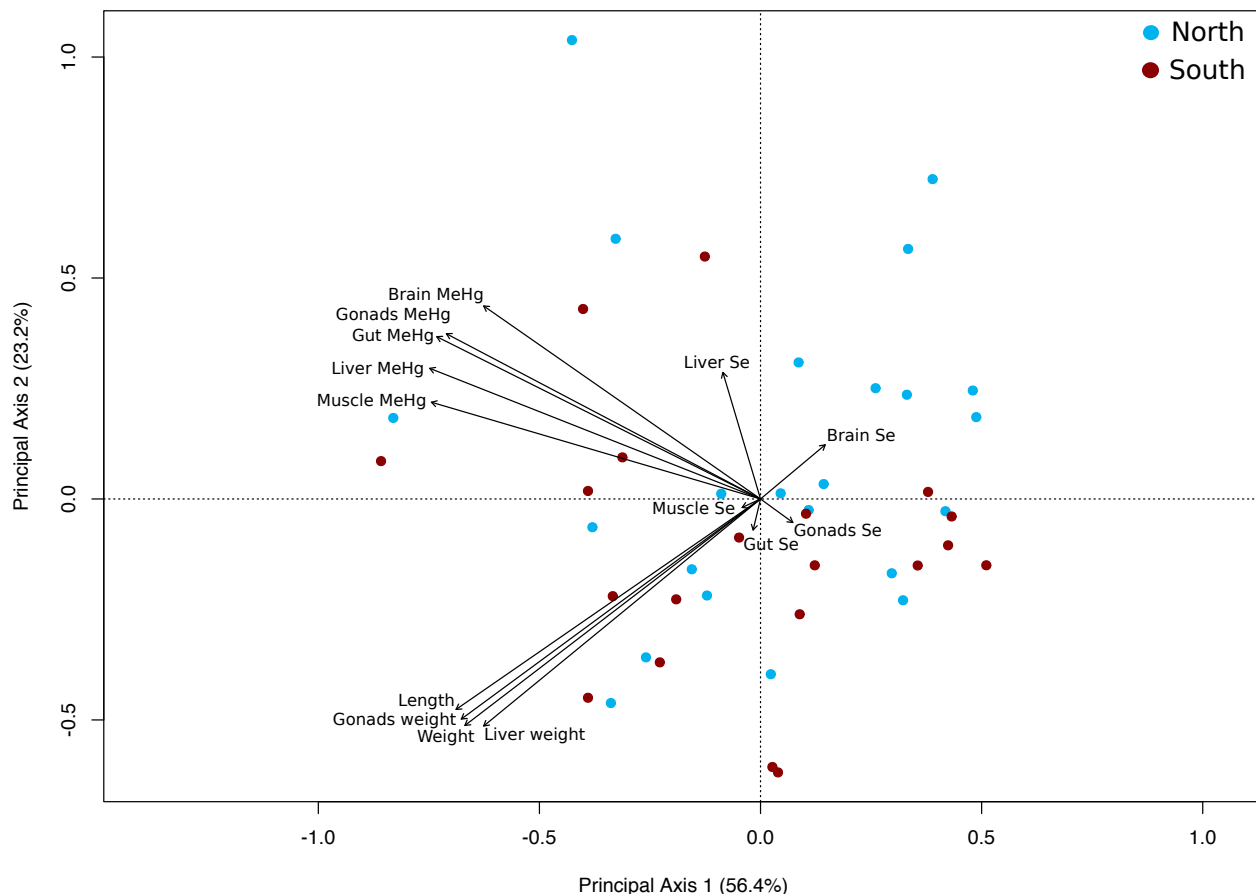


Figure 6. Principal Component Analysis (PCA) correlation biplot showing 43 gravid females (coloured points) and metal concentrations and biometric data (black arrows). Gravid females that were sampled on the north shore of LSP are represented by blue points and those sampled on the south shore by red points. The PCA biplot accounts for 79.6% of the total variation among individuals (Axis 1: 56.4% and Axis 2: 23.2%).

The main conclusion that can be drawn from the PCA is that MeHg concentrations in different tissues are strongly and positively correlated to one another. The analysis of the correlation between tissues can be used to assess the uptake, retention and elimination of contaminants (Cizdziel et al., 2003; Peng et al., 2016). Accordingly, it appears that the strongest correlation in MeHg tissue concentrations prevails between gut and gonads, implying that diet is an important source of MeHg during gonadal development (Pyle et al., 2005). These results validate the laboratory-assessed finding that maternal diet during oogenesis is the main source of MeHg in Fathead Minnow (*Pimephales promelas*) embryos (Hammerschmidt & Sandheinrich, 2005). It was later shown that both female tissues and maternal diet during oogenesis are important sources of MeHg in Sheepshead Minnows (*Cyprinodon variegatus*) (Stefansson et al., 2014).

The link between fish size and Hg concentrations is well documented (Cizdziel et al., 2002; Driscoll et al., 1995; Huckabee et al., 1979), and was also observed in LSP (Ion et al., 1997). Our results suggest an absence of correlation between these variables. Our hypothesis is that the herein gravid YP size range was relatively limited (Fig. S4), a phenomenon that was previously noted (Alonso et al., 2000; Ion et al., 1997). It is also possible that because Hg levels in YP from LSP are low, the relationship between size and Hg may not hold (Burger & Gochfeld, 2011). Finally, the fact that all individuals were gravid females could have led to a length-weight relationship bias (Le Cren, 1951).

Our results also show that the only intra-tissue negative correlation between MeHg and Se concentrations was observed in gonads, suggesting the antagonistic influence of Se on Hg accumulation (Pyle et al., 2005). This is also consistent with the fact that gonads had the highest Se:Hg molar ratio values (Fig. 5), potentially protecting embryos from Hg toxic effects.

Finally, PCA biplot suggests that the correlation between Se concentrations in different tissues is inconsistent. Se was previously shown to be readily transferred maternally in fish (Covington et al., 2018; Saiki et al., 2004). Furthermore, Coyle et al. found that Se concentrations in Bluegill gonads were related to dietary exposure (Coyle et al., 1993). This is consistent with our results, as gut and gonad Se concentrations seem positively correlated. However, the absence of correlation between the other tissues could be attributed to the fact that we observed a narrower gradient for Se concentrations than for MeHg concentrations (Table S3). Our results also show that muscle and gut Se concentrations are positively correlated to

biometric measurements. Lima et al. (2005) found a positive correlation between Se whole-body concentrations and weight for *Hoplias malabaricus*, a freshwater fish species from the Amazon region (Brazil) (Lima et al., 2005). However, differences in Se concentrations according to fish size is not well studied (Burger & Gochfeld, 2011). We hypothesize that as bigger fish are usually older, they thus hold a history of metal accumulation (Gochfeld et al., 2012).

4. Conclusions

The present study aimed to investigate the bioaccumulation of Hg and Se in key tissues and early life stages of YP. Results show that MeHg concentrations increased following an ontogenetic pattern and that nearly 100% of THg was present as the toxic form MeHg in larvae and juveniles. We also found that Hg bioaccumulation was potentially compensated by Se accumulation, as Se:Hg molar ratios were systematically above 1. The present data provides important information that fills previously reported knowledge gaps on Hg and Se bioaccumulation in wild fish early life cycle, as this is the first study to take into account all early development stages. Further studies should include specific endpoints such as hatching success, larval survival and growth as well as larval deformities in order to link Hg bioaccumulation to the ongoing YP recruitment failure in LSP. It is also critical to explore Se deficiency in fish.

Acknowledgements

This project was financially supported by a FRQ-NT Programme d’initiatives stratégiques pour l’innovation (ISI) grant to M.A. and D.P, by an NSERC Discovery grant to M.A, and by the Canada Research Chair program to M.A.. M.K. received a scholarship through the NSERC CREATE ÉcoLac training program in Lake and Fluvial Ecology. The authors would like to acknowledge the contribution of Marco Boutin at Natural Resources Canada (Quebec, Canada) for the map. We thank Nicolas Auclair and Rémi Bacon (ministère des Forêts, de la Faune et des Parcs du Québec) and local commercial fishermen during fish sampling. We acknowledge laboratory assistance from Dominic Bélanger, Antoine Caron, Jérémie De Bonville and Gwenola Capelle, and field assistance from Jérémie De Bonville, Maikel Rosabal, Maxime Leclerc, Lucie Baillon, Valérie René and Alexandre Arscott-Gauvin. We thank the staff at Pourvoirie Roger Gladu (Saint-Ignace-de-Loyola, Québec) for accommodation and field equipment.

Supplementary Material

Supplementary tables

Table S1. MeHg (n=3) and Se (n=1) concentrations in water samples from all sampling stations (mapped in Fig. S1).

	MeHg (ng/L) (\pm SEM)	Se (ng/L)
Maski	0.295 \pm 0.001	129
BDF	0.117 \pm 0.002	104
27	0.073 \pm 0.004	109
97	0.053 \pm 0.015	214
122	0.212 \pm 0.005	119
125	0.156 \pm 0.004	128
174	0.105 \pm 0.002	131
201	0.062 \pm 0.002	142
190	0.064 \pm 0.004	124

Table S2. Adjusted p-values associated to Tukey's multiple comparison post hoc test following a two-way ANOVA on *log* transformed THg and MeHg dry weight tissue concentrations. Alpha = 0.05. Significant results are indicated in grey cells.

	THg, adjusted p-values	MeHg, adjusted p-values
Gonads vs. Brain	< 0.0001****	< 0.0001****
Gonads vs. Gut	< 0.0001****	< 0.0001****
Gonads vs. Liver	< 0.0001****	< 0.0001****
Gonads vs. Muscle	< 0.0001****	< 0.0001****
Brain vs. Gut	> 0.05	> 0.05
Brain vs. Liver	< 0.005**	< 0.05*
Brain vs. Muscle	< 0.0001****	< 0.0001****
Gut vs. Liver	> 0.05	> 0.05
Gut vs. Muscle	<0.0001****	<0.0001****
Liver vs. Muscle	<0.0001****	<0.0001****

Table S3. Comparison table for descriptive statistics related to MeHg, THg and Se concentrations in gonads, brain, gut, liver and muscle of gravid Yellow Perch (n=44).

	Minimum	Maximum	Average	Standard error	Max:Min
MeHg-gonads (mg/kg ww)	0.002	0.039	0.009	0.001	20.8
MeHg-brain (mg/kg ww)	0.005	0.133	0.042	0.004	26.1
MeHg-gut (mg/kg ww)	0.013	0.155	0.043	0.005	11.9
MeHg-liver (mg/kg ww)	0.019	0.219	0.063	0.007	11.5
MeHg-muscle (mg/kg ww)	0.062	0.483	0.229	0.014	7.81
THg-gonads (mg/kg ww)	0.003	0.040	0.011	0.001	11.8
THg-brain (mg/kg ww)	0.022	0.1916	0.054	0.006	8.77
THg-gut (mg/kg ww)	0.024	0.1684	0.063	0.005	7.10
THg-liver (mg/kg ww)	0.031	0.2782	0.088	0.008	8.85
THg-muscle (mg/kg ww)	0.108	0.656	0.274	0.018	6.10
Se-gonads ($\mu\text{g/g dw}$)	1.29	2.86	1.92	2.51	2.22
Se-brain ($\mu\text{g/g dw}$)	0.986	1.72	1.26	0.029	1.74
Se-gut ($\mu\text{g/g dw}$)	2.097	6.15	3.56	0.135	2.93
Se-liver ($\mu\text{g/g dw}$)	0.2351	4.23	2.51	0.114	18.0
Se-muscle ($\mu\text{g/g dw}$)	0.543	2.24	1.23	0.063	4.12

Supplementary figures

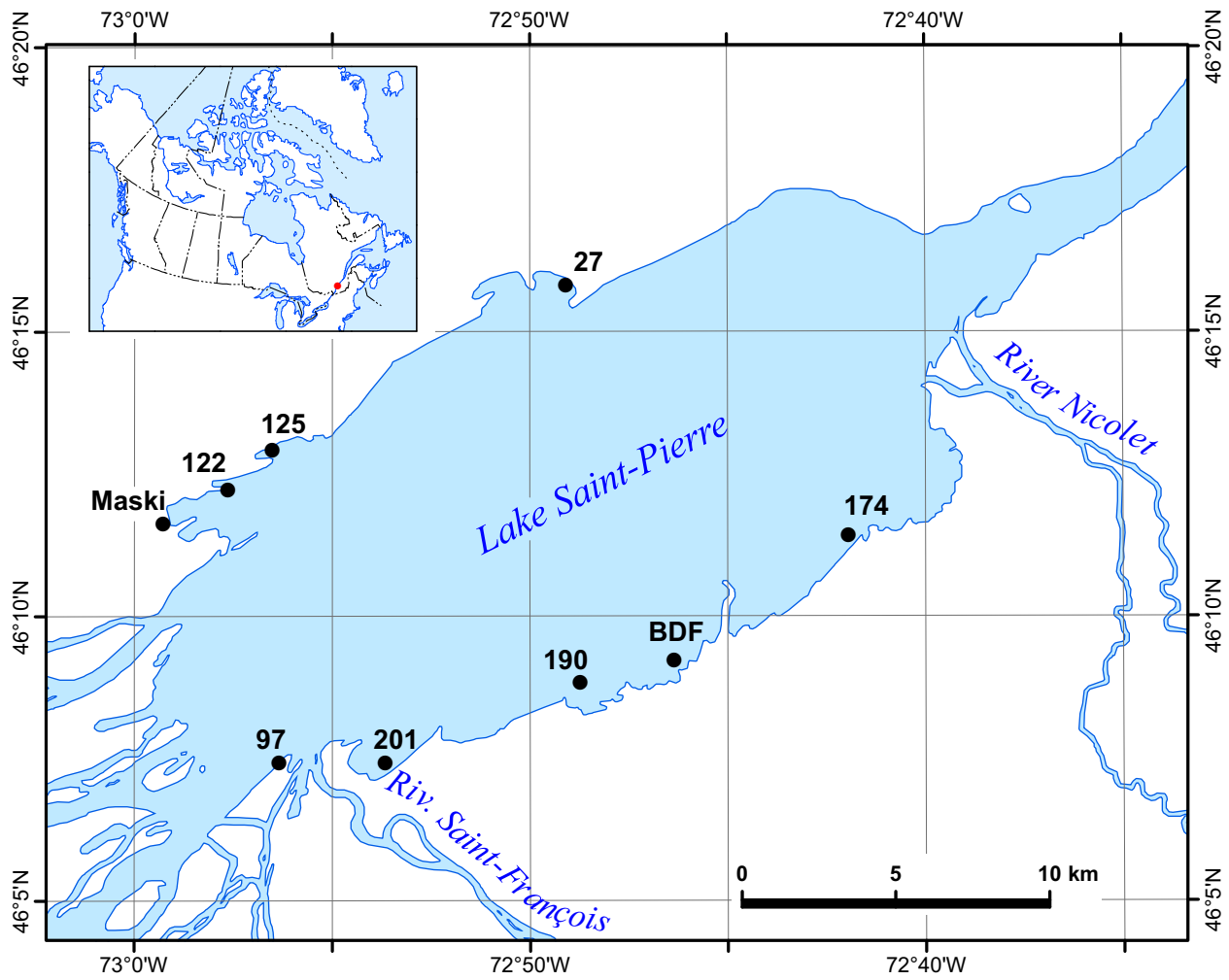


Figure S1. Map of LSP (Quebec, Canada) showing sampling sites. Gravid females were sampled from Maskinongé (Maski) on the north shore and from Baie-du-Febvre (BDF) on the south shore. Larvae and juveniles were sampled from all sites.

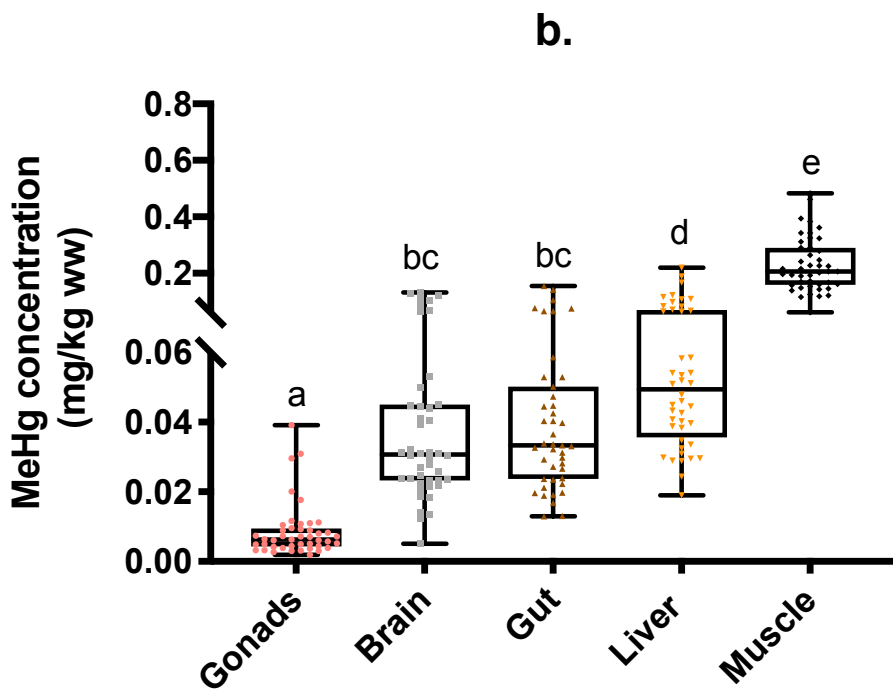
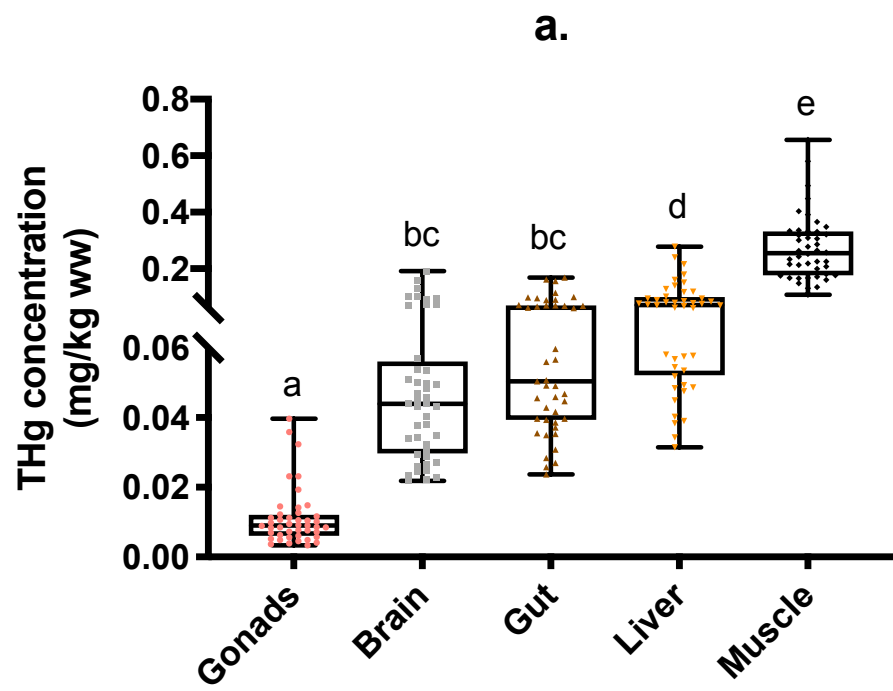


Figure S2. (a) THg and (b) MeHg concentrations (mg/kg ww) in different Yellow Perch' organs (n=44). Letters denote significant differences (Tukey's HSD multiple comparisons test, $p < 0.05$).

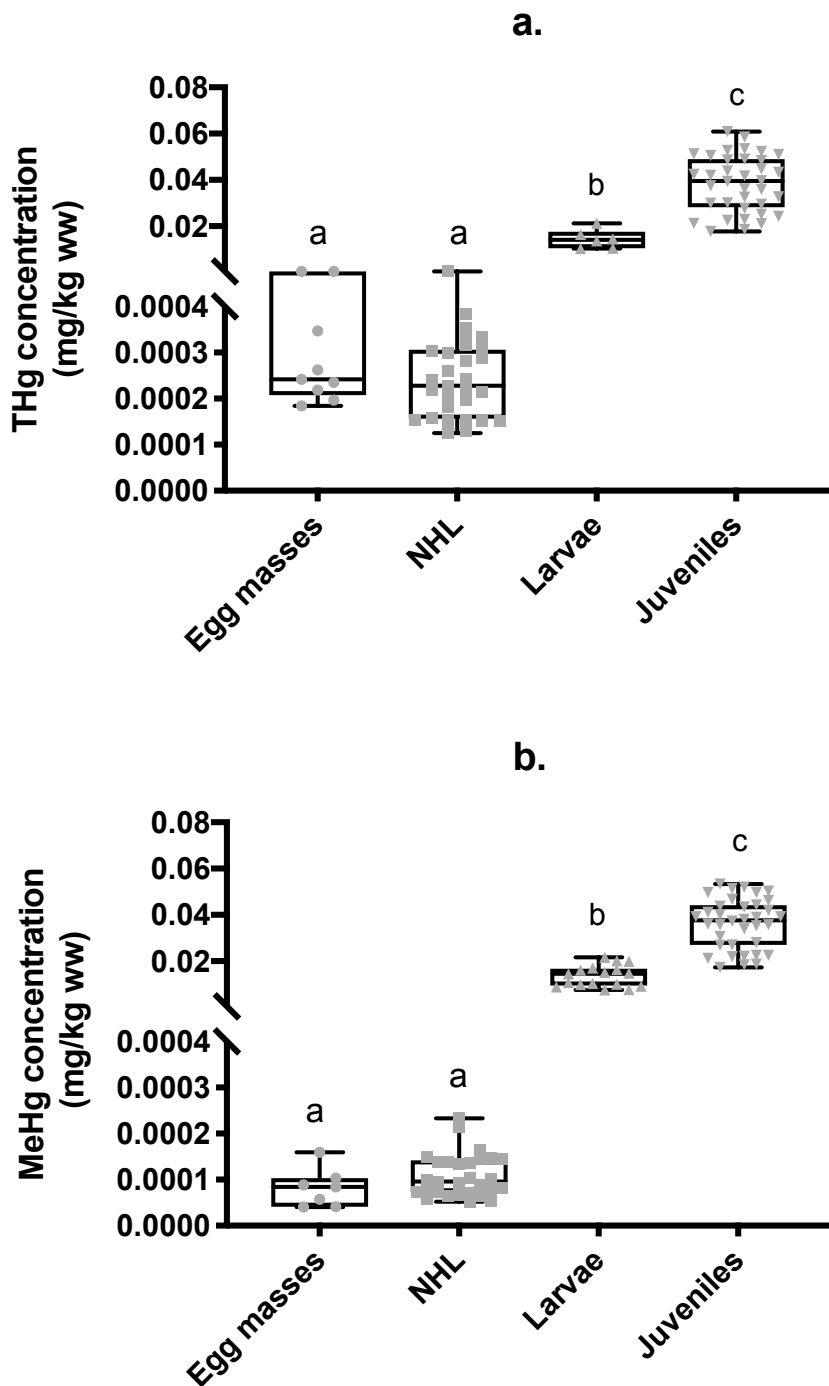


Figure S3. (a) THg and (b) MeHg concentrations (mg/kg ww) in Yellow Perch egg masses (n=7), newly-hatched larvae (NHL) (n=29), larvae (n=20) and juvenile (n=36). Letters denote significant differences (Dunn's multiple comparisons test, $p < 0.05$).

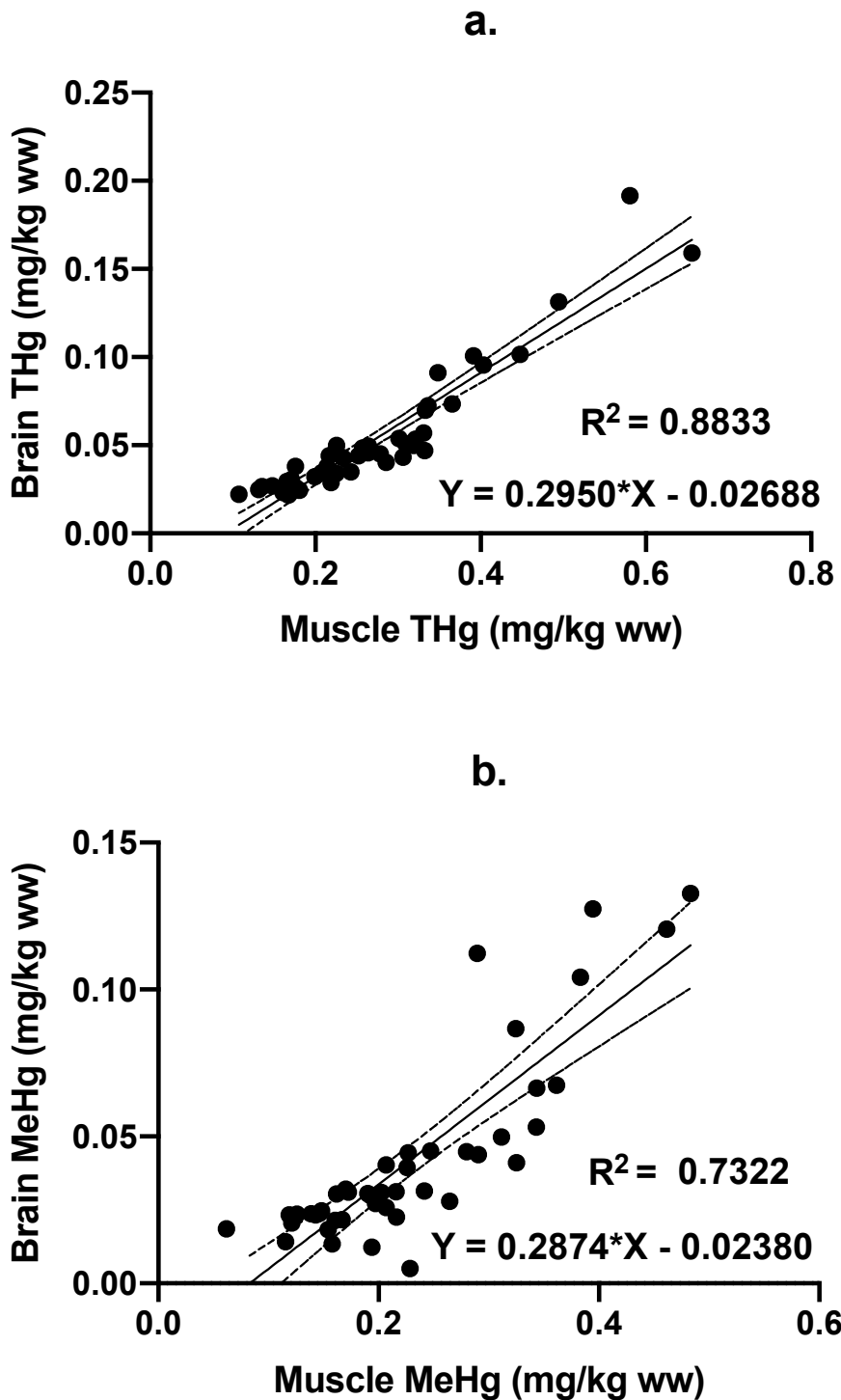
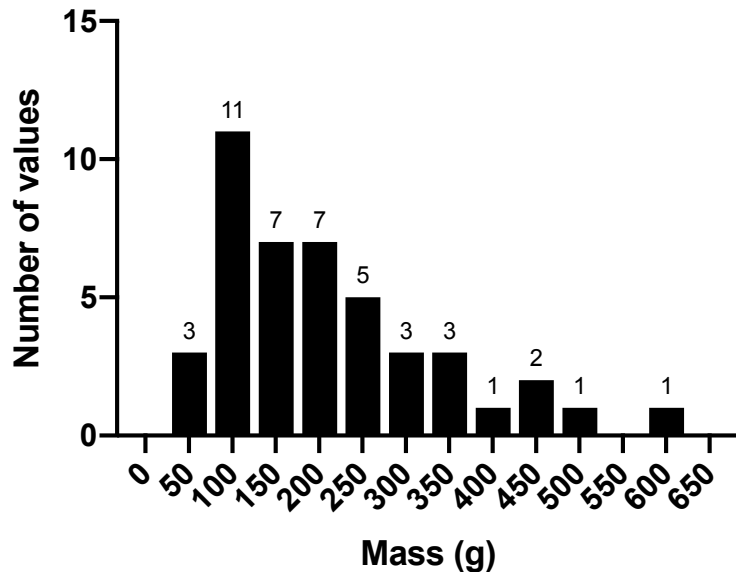


Figure S4. Relationship between muscle and brain (a) THg and (b) MeHg concentrations (mg/kg ww) ($n=44$). The R^2 square and the equation of the linear regression are shown on each plot ($p < 0.0001$ for both regressions). Dashed curves represent the 95% confidence bands of the best-fit line.

a.



b.

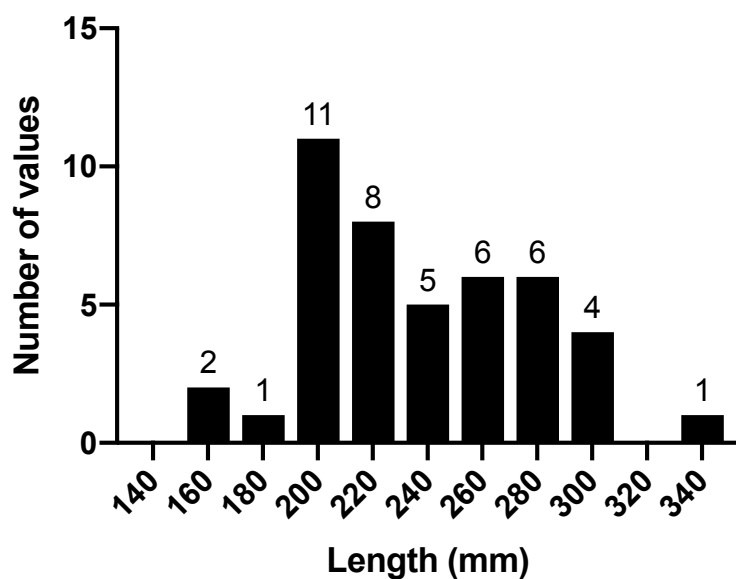


Figure S5. Frequency distribution of the total (a) mass (in g) and (b) length (in mm) of gravid Yellow Perch ($n=44$). The number of individuals belonging to each range of values is indicated above each histogram.

Conclusion

La présente thèse avait comme objectif principal d'évaluer le rôle de la contamination chimique dans le déclin des populations de perchaudes au lac Saint-Pierre (LSP). Cette incapacité de rétablissement se traduit par un recrutement déficient, laissant sous-entendre une mortalité accrue des jeunes individus lors de leur premier hiver (Magnan et al., 2017). Les travaux de recherche menés dans le cadre de ce doctorat visaient par conséquent à évaluer les effets indirects du glyphosate sur la qualité des ressources à la base des réseaux trophiques en plus des effets directs du mercure, hautement bioaccumulable et bioamplifiable, sur la reproduction et les stades de vie précoce de la perchaude. Ainsi, par l'entremise de cette thèse, j'ai fourni des pistes de réponses aux questions suivantes :

1. Le glyphosate, aux concentrations retrouvées actuellement dans l'environnement, influence-t-il la composition des communautés de périphyton, source d'alimentation des invertébrés dont se nourrissent les jeunes perchaudes? **(Chapitre 1)**
2. Le mercure et le sélénium sont-ils transférés de la femelle ovigère à ses œufs chez la perchaude? Et si oui, ce transfert maternel est-il associé à un potentiel de toxicité? **(Chapitre 2)**
3. Comment le mercure et le sélénium sont-ils distribués dans les organes et les différents stades de vie de la perchaude? **(Chapitre 3)**

Les prochaines sections soulignent les principales contributions à la littérature scientifique associées à chaque chapitre. Des pistes de recherche futures sont également proposées, ainsi qu'une mise en perspective des retombées découlant du travail accompli.

Biofilms périphytiques et pesticides

L'agriculture intensive qui se déroule dans le bassin versant du LSP, notamment sur la rive sud, engendre ainsi le lessivage plus ou moins important de pesticides, dont du glyphosate, dans les tributaires. Les herbicides à base de glyphosate sont en effet parmi les plus utilisés à

l'échelle mondiale. Dans les champs agricoles, ces herbicides sont pulvérisés directement sur le feuillage des plants, rendant le glyphosate susceptible au lessivage vers les cours d'eau. Dans les lacs, les plantes aquatiques et les biofilms périphytiques sont fréquemment les premiers récepteurs de ces eaux de ruissellement. Le **Chapitre 1** visait donc à examiner si le glyphosate aurait le potentiel de modifier les communautés périphytiques à la base des réseaux trophiques menant aux jeunes perchaudes. Les principales contributions à la littérature associées à ce chapitre sont (1) l'utilisation de biofilms périphytiques d'âge contrastant, soit 2 mois, 1 an et 20 ans, (2) le suivi temporel des communautés cyanobactériennes par séquençage d'ARN ribosomal à l'aide d'amorces spécifiques et (3) l'exposition à des concentrations environnementales de glyphosate. Ainsi, cette première étude canadienne traitant des effets du glyphosate sur le périphyton suggère que seul l'âge du périphyton semblait influencer la composition taxonomique des communautés. Or, une augmentation de l'abondance relative de certaines cyanobactéries toxiques (*Anabaena*) résistantes à l'herbicide a également été observée en fonction du temps. Ces dernières étant communément dominantes dans les blooms toxiques, l'utilisation du glyphosate soulève une préoccupation d'intérêt public. Cette étude fournit ainsi un aperçu novateur des processus biologiques liés à l'exposition des biofilms à des concentrations environnementales de glyphosate. Par ailleurs, puisque cet herbicide se retrouve au cœur d'une spirale médiatique en raison de ses propriétés cancérigènes, il est impératif de contribuer à l'avancement des connaissances sur ses effets. Le caractère opportun des retombées de cette étude a ainsi été mis en valeur dans le cadre d'un concours de vulgarisation scientifique, au terme duquel j'ai eu l'opportunité de collaborer avec un illustrateur afin de créer une bande dessinée illustrant mes travaux de recherche (**Annexe I**).

Le **Chapitre 1** pave la voie à plusieurs avenues de recherche associée aux effets du glyphosate sur le périphyton. Dans un premier temps, alors que nous avions choisi d'exposer du périphyton provenant d'un milieu vierge, il pourrait être intéressant de comparer les résultats que nous avons obtenus avec ceux qui émergeraient d'expériences réalisées avec du périphyton indigène au LSP. De cette manière, il deviendrait possible d'établir un niveau basal de l'activité métabolique et physiologique de biofilms soumis à une exposition chronique à un mélange complexe de contaminants. En second lieu, il serait intéressant d'évaluer les effets distincts de l'ingrédient actif (glyphosate) et du produit de dégradation principal de ce dernier, l'acide aminométhylphosphonique (AMPA). Présentant une courte demi-vie, le glyphosate est

rapidement dégradé en AMPA par divers processus chimiques, biologiques et physiques (Van Eerd et al., 2003). Ainsi, alors que le mode d'action principal du glyphosate réside dans le fait qu'il inhibe la synthèse de la 5-enolpyruvyl-shikimate-3-phosphate synthase (EPSPS) (Siehl, 1997), une enzyme impliquée dans la biosynthèse de trois acides aminés, soit la phénylalanine, la tyrosine et le tryptophane, l'AMPA semble quant à lui responsable de l'inhibition de la biosynthèse de la chlorophylle (Reddy et al., 2004). En effet, les plantes traitées à l'AMPA semblent présenter des faibles teneurs en acides aminés glycine, sérine et glutamate (Serra et al., 2013). La glycine et la sérine étant impliquées dans la biosynthèse de l'acide δ-aminolévulinique (ALA), un produit intermédiaire de la biosynthèse de la chlorophylle, l'AMPA semble altérer ce dernier processus. De plus, il a été suggéré qu'en raison de certaines similarités moléculaires entre l'AMPA et la glycine, ces deux composés entrent en compétition pour les sites actifs des enzymes impliqués dans la biosynthèse de la chlorophylle (Serra et al., 2013). Ces mécanismes demeurent cependant inexplorés chez les biofilms périphytiques. En effet, bien qu'une étude ait démontré que l'AMPA ne semble pas altérer les paramètres photosynthétiques et l'activité d'enzymes antioxydantes du périphyton soumis à une exposition aiguë (Bonnineau et al., 2012), il serait intéressant d'évaluer les effets chroniques d'une exposition à l'AMPA sur la biosynthèse de la glycine, la sérine et le glutamate.

Il serait également primordial de distinguer les effets du glyphosate et ceux de ses principales formulations commerciales, telles que le Roundup®, puisque ce sont ces dernières qui sont appliquées dans les champs. Or, cette approche comporte certaines limites, puisque la totalité des ingrédients de ce type de formulation est rarement connue. Il devient alors ardu d'attribuer les effets observés à une substance précise. Par exemple, une étude a été réalisée dans le but de comparer les effets du glyphosate pur et d'une formulation commerciale, le Glifosato Atanor®, sur le contenu en pigment des communautés périphytiques (Vera et al., 2014). La concentration testée était de 3 mg/L de glyphosate pour les deux types de contaminants. Une augmentation significative des concentrations de chlorophylle *a* et *b* et des carotènes a été observée pour les deux types d'herbicides après 2 jours d'exposition. Ces résultats impliquent que ces herbicides ont possiblement fourni une source supplémentaire de nutriments à une partie de la communauté. Une autre hypothèse possible est que ces herbicides ont favorisé la production de protéines et de métabolites en réponse au stress, induisant une augmentation de la croissance. Or, les auteurs ont spécifié que la composition des surfactants présents dans le

Glifosato Atanor® est inconnue, rendant ardue l'extrapolation des résultats obtenus. On sait cependant que le surfactant utilisé dans le Roundup® est le polyoxyéthylène amine (POEA), substance qui présente une toxicité aiguë et chronique exacerbée envers certains amphibiens (Struger et al., 2008) et macroinvertébrés (Brausch & Smith, 2007), en comparaison au glyphosate. Les effets du POEA sur les biofilms périphytiques sont cependant inconnus, à ce jour. L'idéal serait ainsi d'effectuer une expérience en mésocosmes extérieurs, afin d'augmenter le réalisme environnemental, dans lesquels on placerait des substrats artificiels permettant la colonisation du périphyton (Vera et al., 2010). En plus du traitement contrôle, des concentrations environnementales de glyphosate pur, Roundup® et POEA seraient ajoutées dans des mésocosmes distincts. Les paramètres biologiques et physiologiques à considérer devront inclure la bioaccumulation et la dégradation des différents contaminants par les biofilms, le dosage des acides aminés ciblés par le glyphosate (tyrosine, phénylalanine, tryptophane) et ceux ciblés par l'AMPA (glycine, sérine, glutamate) ainsi que le suivi taxonomique des communautés par des techniques microscopiques et génomiques. Des analyses de transcriptomique permettraient en effet de cibler la présence du gène responsable de la résistance de l'enzyme EPSPS, cible du mode d'action du glyphosate et qui est présente chez certains taxons de cyanobactéries (Forlani et al., 2008).

Enfin, il est évident qu'il serait impératif d'évaluer les effets des deux autres herbicides les plus utilisés dans le bassin versant du LSP, soit l'atrazine et le métolachlore, sur les biofilms périphytiques. Des effets de l'atrazine sur la photosynthèse, la croissance, la concentration de chlorophylle ainsi que la biomasse ont été répertoriés chez les producteurs primaires aquatiques (Guasch et al., 1997). Le métolachlore, quant à lui, semble causer une altération du métabolisme des acides gras chez les algues (Couderchet et al., 1999).

Fractionnement subcellulaire et transfert maternel

Les activités industrielles et urbaines qui prennent place en amont engendrent quant à elles un rejet de métaux dans le LSP. Bien que les apports de mercure aient diminué depuis quelques décennies dans le fleuve Saint-Laurent, ce contaminant est hautement bioaccumulable

et bioamplifiable dans les réseaux trophiques en plus de causer des effets toxiques sur la reproduction des poissons à de très faibles concentrations (Crump & Trudeau, 2009). Par ailleurs, il a été démontré que le transfert maternel du mercure chez les poissons représente la principale voie d'exposition des embryons (Hammerschmidt & Sandheinrich, 2005; Hammerschmidt et al., 1999). Le **Chapitre 2** visait donc à confirmer l'évidence d'un transfert maternel du Hg chez la perchaude en plus d'y associer un certain potentiel de toxicité grâce à des techniques de fractionnement subcellulaire. Nos résultats suggèrent un transfert maternel du mercure de la femelle ovigère à ses œufs ainsi qu'aux mitochondries des gonades, fractions sensibles de la cellule. De plus, les ratios molaires Se:Hg étaient systématiquement supérieurs à 1 dans toutes les fractions subcellulaires hépatiques et gonadiques, réduisant potentiellement les effets toxiques du mercure. Les résultats novateurs associés à cette étude viennent ainsi combler d'importantes lacunes, soit principalement (1) l'emploi d'essais enzymatiques afin d'élaborer des protocoles optimisés de fractionnement subcellulaire pour le foie et les gonades de perchaudes, (2) l'utilisation de la perchaude comme organisme modèle afin d'évaluer le fractionnement subcellulaire du Hg et du Se, (3) l'établissement d'un lien entre le fractionnement subcellulaire et le transfert maternel ainsi que (4) la détermination des ratios molaires Se:Hg dans les fractions subcellulaires des gonades et du foie.

Bien que les essais enzymatiques représentent une méthode assez efficace dans l'optique de la validation de la séparation des fractions subcellulaires (Cardon et al., 2018; Rosabal et al., 2014), il serait intéressant de commencer à utiliser des techniques de protéomique, ces dernières étant plus précises. La protéomique permet en effet l'analyse complète de toutes les protéines exprimées dans un type de cellule ou dans un tissu particulier d'une espèce (Malécot et al., 2009). La méthode d'électrophorèse en 2 dimensions (2D) permet ainsi l'étude de centaines de protéines en une seule expérience (Fey & Larsen, 2001). L'optimisation des protocoles de fractionnement constituerait donc en l'identification de la présence et de l'expression de certaines protéines spécifiques à chaque fraction. Par exemple, pour la fraction mitochondriale du foie, il serait intéressant de valider la présence de la prohibitine, l'ATP synthase ou de l'aldéhyde déshydrogénase 2 (Malécot et al., 2009). Une inhibition de l'expression de ces 3 protéines a également été associée à un stress oxydatif (Malécot et al., 2009), fournissant de précieuses informations quant aux effets d'une exposition aux contaminants. Pour les protéines du cytosol, il serait bien entendu crucial de combiner les techniques de transcriptomique avec

celles de protéomique afin d'identifier et d'évaluer l'expression de la métallothionéine (Hogstrand et al., 2002).

Il serait également important d'évaluer le transfert maternel de certains contaminants organiques émergents tels que les retardateurs de flamme halogénés (HFR) dont l'occurrence dans les écosystèmes est ubiquitaire. Les effets néfastes des retardateurs de flamme sur la faune ont largement été étudiés. En effet, des impacts sur le système immunitaire, reproducteur et endocrinien ont été observés chez les poissons, les reptiles, les oiseaux et les mammifères (Darnerud, 2003). Il importe de mentionner que ces contaminants ont été détectés dans les tissus de perchaudes du fleuve Saint-Laurent (Houde et al., 2014a). Par ailleurs, certaines zones du nord du LSP présentent, dans les sédiments, des concentrations très élevées de retardateurs de flamme polybromés, qui proviendraient de l'effluent de l'usine d'épuration des eaux usées de Montréal (Pelletier & Rondeau, 2013). Ce sont donc des composés d'intérêt qu'il importe d'inclure dans le cadre d'un projet découlant de la continuité du **Chapitre 2**. Par exemple, les polybromodiphényléthers (PBDE) sont des composés ignifuges retrouvés dans les appareils électroniques et électriques, dans les meubles rembourrés, les textiles et les automobiles, notamment (Houde et al., 2014a). Ils sont hautement persistants, bioaccumulables et toxiques. Or, les PBDE ne sont plus considérés comme étant émergents et leur utilisation est restreinte depuis 2006 au Canada (Pelletier & Rondeau, 2013). Ces composés ont donc graduellement été remplacés par retardateurs de flamme halogénés tels que le déchlorane plus (DP), le decabromodiphenylethane (DBDPE), le pentabromoethylbenzene (PBEB) et l'hexabromobenzene (HBB) (Houde et al., 2014a).

Lors d'une étude préliminaire qui mériterait d'être reconduite de manière approfondie, nous avons évalué le ratio entre les concentrations mesurées dans les œufs et celles mesurées dans le muscle de 5 femelles ovigères (**Annexe II**). On note tout d'abord que ces ratios varient considérablement entre les différents congénères. Une étude similaire réalisée sur le transfert maternel du composé BDE-47 chez une espèce de poisson marin (*Oryzias melastigma*) suggère que lorsque le ratio œufs:muscle ne diffère pas significativement de 1, le dépôt des contaminants dans les œufs est dû à un partitionnement des lipides entre la femelle et les œufs plutôt qu'à un dépôt actif (van de Merwe et al., 2011). Si, au contraire, le dépôt des contaminants se fait de façon active par la mère, le ratio sera supérieur à 1. Selon nos résultats (**Annexe II**), il semble que le BDE-17, le BDE-49, le BDE-100, le BDE-99, le BDE-153 et le BDE-154 soient déposés

activement dans les œufs par la femelle, puisqu'ils présentent un ratio œufs: muscle supérieur à un. Les prochaines études devraient notamment inclure l'évaluation des effets des congénères transférés sur le développement embryonnaire.

Il a été démontré que les BFR se lient aux lipoprotéines qui sont déposées dans le jaune d'œuf lors de la vitellogenèse chez la Dorade Royale (*Sparus aurata*) (Serrano et al., 2008). Ainsi, une autre avenue de recherche intéressante serait d'élucider les processus mécanistiques liés au transfert maternel des retardateurs de flamme chez la perchaude. Pour ce faire, il faudrait procéder à l'isolation des différents types de lipoprotéines (VLDL, LDL, VHDL, HDL) du plasma des perchaudes par ultracentrifugation de densité (Salvador et al., 2007). Les concentrations de HFR seraient ensuite déterminées dans chacune de ces fractions lipoprotéiniques par chromatographie en phase gazeuse couplée à la spectrométrie de masse des ions négatifs à capture d'électrons (GC/MS-ECNI) de manière à évaluer à laquelle de celles-ci les différents congénères se lient de manière préférentielle. Une étude similaire a été réalisée par Ungerer et Thomas (1996) dans le but d'évaluer la liaison du DDT aux lipoprotéines du plasma ainsi que leur accumulation dans les gonades chez un poisson marin (*Micropogonias undulatus*). Les auteurs ont noté que le DDT, composé extrêmement lipophile, se lie surtout aux lipoprotéines de très faible densité (VLDL), riches en triglycérides non polaires (Ungerer & Thomas, 1996).

Par ailleurs, en plus de ces expériences sur le transfert maternel, il serait pertinent de mesurer les retardateurs de flamme dans les fractions subcellulaires, puisque le fractionnement subcellulaire des contaminants organiques chez les poissons demeure, à ce jour, inexploré. Afin de comparer la distribution subcellulaire de certains métaux traces chez la perchaude du LSP avec des perchaudes provenant d'autres lacs davantage contaminés (Campbell et al., 2005; Campbell et al., 2008; Giguère et al., 2006), il serait également pertinent d'y mesurer le cadmium, le cuivre, l'argent et le nickel. De cette manière, il deviendrait possible de comparer les stratégies de détoxication chez les perchaudes exposées à un gradient de contamination. En effet, le nickel et le cadmium semblent avoir un effet sur le métabolisme du rétinol chez la perchaude, en plus de causer un stress oxydatif (Defo et al., 2012). Le rétinol, métabolite de la vitamine A, est essentiel pour la croissance, la reproduction et le développement embryonnaire. Une forte bioaccumulation du cuivre, de l'argent et du cadmium dans les foies de perchaudes du LSP a également été associée à de faibles indices de condition ainsi qu'à des lésions

hépatiques (Giraudo et al., 2016). Nous avons débuté ce travail en évaluant la distribution subcellulaire du cuivre, du cadmium, du manganèse et du fer dans les foies de perchaudes (**Annexe III**). Le cuivre et le cadmium semblent davantage associés à la fraction des HSP, qui contient des protéines de détoxication telles que les métallothionéines. Conséquemment, il serait approprié d'utiliser des techniques de chromatographie d'exclusion de taille couplées à de la spectrométrie de masse à plasma inductif (SEC-ICP-MS) afin d'identifier à quelles biomolécules cytosoliques se lient les différents métaux (Caron et al., 2017). Le manganèse et le fer, éléments essentiels, mais devenant toxiques à de hautes concentrations, semblent quant à eux associés préférablement aux fractions sensibles.

Il va sans dire qu'il faudrait également procéder au fractionnement subcellulaire des différents tissus (muscle, foie, gonades, cerveau, intestin) et stades de vie de la perchaude (masses d'œufs, jeunes larves, larves, juvéniles), de manière à établir un pont entre les résultats de bioaccumulation obtenus au **Chapitre 3** et leur potentiel de toxicité. Ces expériences représentent un travail assez considérable d'optimisation des techniques pour chacun des compartiments à l'étude, à l'aide d'essais enzymatiques ou de techniques de protéomique. Les résultats seraient cependant extrêmement novateurs, puisqu'à ce jour, aucune étude n'a traité du fractionnement subcellulaire des stades larvaires de poissons. Puisque ces derniers sont considérés comme étant particulièrement sensibles aux contaminants organiques et inorganiques, il deviendrait possible d'évaluer si cette sensibilité serait due en partie à une accumulation du Hg dans les mitochondries ou les protéines sensibles, indiquant des capacités de détoxicification moins développées. En plus du Hg, il serait également intéressant de mesurer les concentrations en métaux traces (Cd, As, Fe, Mn, Cu, Ni, Zn) ainsi qu'en contaminants organiques (HFR) dans les fractions subcellulaires des différents compartiments.

Bioaccumulation des contaminants organiques et inorganiques

Après avoir confirmé l'évidence d'un transfert maternel du mercure et du sélénium chez la perchaude, nous tenions à réaliser un suivi ontogénique et tissulaire de la contamination. Le **Chapitre 3** visait donc à évaluer la distribution du mercure et du sélénium dans plusieurs tissus

et stades précoces du cycle de vie de la perchaude. Les résultats associés à ce chapitre démontrent tout d'abord que près de 100% du mercure total était présent sous forme de MeHg dans les larves et les juvéniles. Il semble également que les concentrations de MeHg mesurées dans l'intestin étaient préférablement accumulées dans les gonades. Enfin, les ratios molaires Se:Hg étaient supérieurs à 1 dans tous les tissus et stades de vie de la perchaude, suggérant proportionnellement davantage de sélénium était accumulé que de mercure. Les principales contributions de ce volet à la littérature scientifique sont (1) l'utilisation de tous les stades de vie précoces de la perchaude, qui sont considérés comme étant particulièrement sensibles aux contaminants organiques et inorganiques, (2) la prise en compte de l'antagonisme entre le mercure et le sélénium et (3) l'établissement de données récentes liées à la contamination de la perchaude au LSP. Le **Chapitre 3** découle d'un travail préliminaire qui visait la réalisation d'un aperçu de la contamination en contaminants organiques et inorganiques dans les tissus de perchaudes au LSP et l'identification des contaminants à risque. Les prochains paragraphes traitent ainsi de certains résultats que nous avons obtenus en lien avec la bioaccumulation de pesticides, de BPC, de composés pharmaceutiques et de retardateurs de flamme dans certains tissus de perchaudes. Ces analyses pavent la voie à de nouvelles avenues de recherche découlant de la présente thèse.

Dans un premier temps, nous avions évalué la bioaccumulation de certains pesticides organiques chez la perchaude sur un nombre restreint d'échantillons de foies de perchaudes grâce à plusieurs collaborateurs. Ainsi, l'atrazine et les insecticides pyréthrinoïdes ont été mesurés, mais n'ont pas été détectés dans nos échantillons. L'atrazine, l'un des herbicides les plus utilisés à l'échelle mondiale, est fréquemment détecté dans les rivières du Québec irriguant des zones de cultures de soya et de maïs dans le bassin versant du LSP (Giroux, 2015; Giroux, 2018). Puisque de faibles concentrations d'atrazine semblent causer une diminution de la production d'œufs chez le méné à tête de boule (*Pimephales promelas*) via une perturbation endocrine (Tillitt et al., 2010), il serait crucial d'approfondir ses effets chez la perchaude.

Les biphenyles polychlorés (BPC) ont également été mesurés dans nos échantillons de foies de perchaudes (Σ BPC = 10.6 mg/kg ww, n=2). Ainsi, bien que l'importation, la fabrication et la vente des BPC aient été interdites en 1977 au Canada et malgré le fait que les concentrations de BPC aient diminué de 90% dans les sédiments du LSP depuis la fin des années 1970 (Pelletier, 2005), il serait pertinent d'approfondir ce volet. Les BPC et leurs dérivés (dioxines,

furanes) sont en effet très persistants dans l'environnement, hautement toxiques et bioamplifiables dans les réseaux trophiques (Gandhi et al., 2019; Masset et al., 2019).

La carbamazépine, un médicament utilisé pour traiter certains types de crises convulsives, est parfois utilisée comme traceur d'effluents municipaux (Lajeunesse et al., 2013). En effet, les rejets des usines d'épuration des eaux usées sont responsables du déversement de la majorité des composés pharmaceutiques actifs dans les environnements aquatiques (Lajeunesse et al., 2013). La carbamazépine n'a pas été détectée dans nos échantillons de foies de perchaudes.

Le déchlorane plus (DP), le BEHTBP, le OBIND et le DBDPE sont des retardateurs de flamme émergents ayant été inclus dans la liste de Howard et Muir des produits chimiques préoccupants présentant un fort potentiel de persistance et de bioaccumulation (Howard & Muir, 2011). Houde et al. ont dressé le portrait de la présence de retardateurs de flamme bromés et de déchloranés dans des échantillons de plusieurs espèces de poissons, dont la perchaude, échantillonnés autour de l'île de Montréal (Houde et al., 2014a). Le composé DEC 604 CB était le déchlorane prédominant dans les échantillons de poissons du fleuve Saint-Laurent. Son taux élevé de chloration et ses propriétés chimiques lui procurent en effet un potentiel très élevé de persistance et de bioaccumulation. Les composés PBEB et BDE-209 présentaient également un fort potentiel de bioaccumulation, le BDE-209 en raison de sa bromination complète (Houde et al., 2014a). Enfin, les auteurs ont observé que les congénères dominants dans les échantillons d'homogénats de perchaudes étaient le BDE-47, le BDE-99 et le BDE-1002. Le BDE-47 étant un produit de dégradation des retardateurs de flamme présentant un fort taux de bromination en plus d'être un constituant majeur des formulations commerciales utilisées à l'échelle mondiale, il est régulièrement détecté dans les échantillons de poissons analysés en Europe, en Asie et en Amérique du Nord (Houde et al., 2014a).

Nous avons ainsi mesuré certains congénères de retardateurs de flamme et comparé les concentrations obtenues aux recommandations fédérales pour la qualité de l'environnement (RFQE) (**Annexe II**). Les organes ciblés étaient les gonades et le foie, puisque ce sont les tissus présentant la plus grande fraction lipidique (2.87% en moyenne pour les gonades et 8.97% en moyenne dans le foie), les retardateurs de flamme étant hautement lipophiles (Houde et al., 2014a). Les concentrations mesurées dans les échantillons de gonades et de foie dépassaient les recommandations établies pour les congénères BDE-99 et BDE-100. Il importe de noter que

lorsque les concentrations mesurées sont inférieures aux RFQE, les risques liés aux effets toxiques des PBDE sont faibles. Or, un dépassement des RFQE n’implique pas nécessairement que les organismes seront exposés à des effets nocifs. Il serait cependant pertinent de se pencher sur la bioaccumulation des BDE-99 et BDE-100 chez la perchaude du LSP dans tous les organes et les stades de vie.

La suite logique du **Chapitre 3**, en plus de poursuivre les études préliminaires que nous avons entamées en augmentant l’effectif ainsi que les gradients spatio-temporels, consiste à mesurer des paramètres physiologiques spécifiques à la contamination. Par exemple, en lien avec la contamination en métaux inorganiques, il serait intéressant d’évaluer le stress oxydatif chez les perchaudes ainsi que la peroxydation des lipides. Pour ce faire, nous pourrions mesurer les niveaux de glutathion et de substances réactives à l’acide thiobarbiturique, respectivement (Ponton et al., 2016). En ce qui a trait aux retardateurs de flamme, qui sont des perturbateurs endocriniens, nous pourrions évaluer l’activité estrogénique, la production d’œufs, la mortalité des larves ainsi que les malformations et le retard de développement chez les embryons (Kuiper et al., 2007). Pour ce faire, il faudrait exposer des poissons en laboratoire à des concentrations environnementales de certains congénères de retardateurs de flamme et évaluer les effets sur plusieurs stades de vie.

Perspectives

Bien qu’il soit ardu d’établir un lien direct entre le déclin des populations de perchaudes et la contamination chimique qui prévaut au LSP en raison des effets combinés de toutes les autres contraintes biotiques et anthropiques, cette thèse démontre que les jeunes perchaudes sont à risque de développer des effets toxiques liés à une exposition à plusieurs substances nocives. Ces effets néfastes pourraient avoir une incidence sur la survie et la croissance des jeunes de l’année. Ainsi, malgré que plusieurs aspects demeurent à explorer, j’ai contribué à l’avancement des connaissances sur l’utilisation des pesticides (**Chapitre 1**), sur le fractionnement subcellulaire (**Chapitre 2**) ainsi que sur la bioaccumulation du mercure et du sélénium (**Chapitre 3**). La contamination chimique a donc un rôle à jouer dans l’incapacité de

rétablissement des populations de perchaudes, bien qu'il soit maintenant bien établi que ce déclin est multifactoriel. Les résultats associés à cette thèse permettront d'informer la communauté scientifique ainsi que les élus sur les effets néfastes qu'entraîne l'utilisation des pesticides de synthèse et les rejets industriels sur la santé environnementale. Dans une optique plus large, j'aimerais pouvoir sensibiliser les décideurs et leaders d'opinion aux effets des polluants sur l'enjeu de la qualité de l'eau du fleuve Saint-Laurent. En ce sens, le fait que mon projet fasse partie intégrante d'un programme d'*Initiatives Stratégiques pour l'Innovation* du FRQNT permet un partenariat étroit avec le ministère du Développement Durable, de l'Environnement, de la Faune et des Parcs (MDDEP). Ainsi, en collaboration avec les scientifiques du Ministère et les autres chercheurs impliqués dans ce programme, une diffusion des résultats et un transfert des connaissances seront assurés *via* la publication de documents synthèses et l'organisation d'ateliers de consultation et de prises de décision.

La problématique des niveaux de contamination dans le fleuve Saint-Laurent a été soulevée au début des années 70. Dès lors, on se préoccupe de la qualité de l'eau potable et des impacts de la pollution chimique sur les activités récréatives et économiques ainsi que sur la santé des écosystèmes du Fleuve. C'est par la suite un peu plus tard, soit en 1988, que le Plan d'action Saint-Laurent commence à prendre forme. Ce plan d'action résulte d'une collaboration entre plusieurs acteurs gouvernementaux, organismes sans but lucratif et industries dans l'optique de diminuer l'apport de produits toxiques dans le Fleuve. L'évaluation des retombées de cet accord révèle qu'au LSP en 2014, les teneurs en PBDE et en mercure étaient jugées « non préoccupantes » et suivaient une tendance « à la baisse » pour le doré jaune et le grand brochet. Or, pour le meunier noir, les concentrations en PBDE et en BPC étaient « à surveiller » (Laliberté, 2016). Bien que ces résultats soient encourageants, il n'en demeure pas moins qu'il faut maintenant faire face aux nouvelles menaces chimiques, soit les contaminants émergents.

Il importe tout d'abord de distinguer les contaminants émergents des contaminants d'intérêt émergent. Ainsi, les contaminants émergents sont des contaminants qui ont fait leur apparition récemment, alors que les contaminants d'intérêt émergents sont des produits chimiques ou naturels, ou encore des matériaux, manufacturés ou fabriqués par l'homme, qui ont récemment été découverts ou qui sont présumés présents dans divers compartiments de l'environnement et dont la toxicité ou la persistance sont susceptibles de modifier considérablement le métabolisme d'un être vivant. On peut distinguer trois types de

contaminants d'intérêt émergent, soit (1) des contaminants émergents proprement dits, nouveaux composés ou molécules inconnus auparavant ou récemment parus dans la littérature scientifique, (2) des contaminants connus pour lesquels les problèmes de contamination de l'environnement n'étaient pas préalablement appréhendés, et (3) d'anciens contaminants pour lesquels de nouvelles informations viennent bousculer notre compréhension des risques environnementaux et de la santé humaine (Sauvé & Desrosiers, 2014). L'idéal serait ainsi de concentrer les prochaines recherches axées sur la contamination de la perchaude au LSP sur ces contaminants d'intérêt émergent. Ces derniers incluent notamment les nanoparticules de plastique qui peuvent être transférées de la mère à ses œufs chez les poissons (Pitt et al., 2018), les retardateurs de flamme halogénés, les produits pharmaceutiques incluant les hormones synthétiques qui induisent une féminisation chez les poissons (Kidd et al., 2007), les cyanotoxines et les nouveaux pesticides. Parmi ces derniers, on soupçonne le chlorantraniliprole (CAP) d'être une alternative prometteuse aux insecticides néonicotinoïdes en raison de sa faible toxicité envers les abeilles. Les effets du CAP sur les poissons sont cependant peu documentés (Clasen et al., 2018) et il importe d'élargir le spectre des connaissances sur ses effets sur les taxons non ciblés en prévision d'une augmentation de son utilisation.

À l'ère où certains agronomes dénoncent une surutilisation des engrains et des pesticides au Québec, il est inévitable de trouver des solutions alternatives à l'utilisation des pesticides. Parmi ces solutions, une compagnie québécoise, Phytodata, a réussi à remplacer l'insecticide chlorpyrifos par des mouches roses stériles afin d'enrayer les populations nuisibles de mouches à l'oignon (Gerbet, 2018). Les mâles rendus stériles par radiations et colorés en rose afin de faciliter leur dénombrement s'accouplent avec les femelles indigènes, qui produisent des œufs non féconds. L'efficacité de cette technique de biocontrôle est comparable à celle liée à l'utilisation du chlorpyrifos, limitant le besoin d'utiliser ce dernier. Du côté des solutions alternatives aux herbicides, la compagnie anglaise Weedingtech Ltd a développé un herbicide combinant l'eau, la chaleur et Foamstream®, une mousse naturelle constituée d'huiles végétales et de sucres (UE, 2014). Une fois pulvérisé sur les plantes nuisibles, cet herbicide les élimine de manière entièrement naturelle et sécuritaire pour les écosystèmes.

À mon sens, la présente thèse permet d'apporter une vision innovatrice à l'enjeu actuel qui concerne les impacts de la pollution chimique diffuse sur les écosystèmes. Ainsi, ce n'est qu'en combinant des efforts de réduction des apports en polluants avec le développement de

nouvelles technologies alternatives aux pesticides que nous réussirons à limiter les dégâts causés par la contamination sur les écosystèmes. En attendant, il importe de redoubler d'efforts afin de mieux comprendre les effets des contaminants, autant les « anciens » polluants persistants que ceux d'intérêt émergent, sur les différents acteurs des réseaux trophiques.

Petit poisson deviendra grand, à condition que chacun y mette du sien.

Bibliographie

- Adriano, D. C. (2001). *Trace Elements in Terrestrial Environments: Biochemistry, Bioavailability and Risks of Metals, 2nd Edition*. New York, NY: Springer-Verlag.
- Alonso, D., Pineda, P., Olivero, J., González, H., & Campos, N. (2000). Mercury levels in muscle of two fish species and sediments from the Cartagena Bay and the Ciénaga Grande de Santa Marta, Colombia. *Environmental Pollution*, 109(1), 157-163. doi: [https://doi.org/10.1016/S0269-7491\(99\)00225-0](https://doi.org/10.1016/S0269-7491(99)00225-0)
- Amlund, H., Lundebye, A. K., Boyle, D., & Ellingsen, S. (2015). Dietary selenomethionine influences the accumulation and depuration of dietary methylmercury in zebrafish (*Danio rerio*). *Aquatic Toxicology*, 158, 211-217. doi: <https://doi.org/10.1016/j.aquatox.2014.11.010>
- Anderson, M. J., & Walsh, D. C. I. (2013). PERMANOVA, ANOSIM, and the mantel test in the face of heterogeneous dispersions: What null hypothesis are you testing? . *Ecological Monographs*, 83(4), 557-574. doi: <https://doi.org/10.1890/12-2010.1>.
- Andrews, S. (2010). *FastQC a quality-control tool for high-throughput sequence data*. Retrieved from <http://www.bioinformatics.babraham.ac.uk/projects/fastqc/>
- Aparicio, V. C., De Geronimo, E., Marino, D., Primost, J., Carriquiriborde, P., & Costa, J. L. (2013). Environmental fate of glyphosate and aminomethylphosphonic acid in surface waters and soil of agricultural basins. *Chemosphere*, 93(9), 1866-1873. doi: <https://doi.org/10.1016/j.chemosphere.2013.06.041>
- Araújo, O., Pereira, P., Cesario, R., Pacheco, M., & Raimundo, J. (2015). The sub-cellular fate of mercury in the liver of wild mullets (*Liza aurata*)--Contribution to the understanding of metal-induced cellular toxicity. *Marine Pollution Bulletin*, 95(1), 412-418. doi: <https://doi.org/10.1016/j.marpolbul.2015.03.036>
- Barst, B. D., Rosabal, M., Campbell, P. G. C., Muir, D. G. C., Wang, X., Kock, G., & Drevnick, P. E. (2016). Subcellular distribution of trace elements and liver histology of landlocked Arctic char (*Salvelinus alpinus*) sampled along a mercury contamination gradient. *Environmental Pollution*, 212, 574-583. doi: <https://doi.org/10.1016/j.envpol.2016.03.003>

- Barst, B. D., Rosabal, M., Drevnick, P. E., Campbell, P. G. C., & Basu, N. (2018). Subcellular distributions of trace elements (Cd, Pb, As, Hg, Se) in the livers of Alaskan yelloweye rockfish (*Sebastodes ruberrimus*). *Environmental Pollution*, 242(Pt A), 63-72. doi: <https://doi.org/10.1016/j.envpol.2018.06.077>
- Bastos, W. R., Dorea, J. G., Bernardi, J. V. E., Lauthartte, L. C., Mussy, M. H., Hauser, M., Doria, C., & Malm, O. (2015). Mercury in muscle and brain of catfish from the Madeira river, Amazon, Brazil. *Ecotoxicology and Environmental Safety*, 118, 90-97. doi: <https://doi.org/10.1016/j.ecoenv.2015.04.015>
- Batchelar, K. L., Kidd, K. A., Drevnick, P. E., Munkittrick, K. R., Burgess, N. M., Roberts, A. P., & Smith, J. D. (2013a). Evidence of impaired health in yellow perch (*Perca flavescens*) from a biological mercury hotspot in northeastern North America. *Environmental Toxicology and Chemistry*, 32(3), 627-637. doi: <https://doi.org/10.1002/etc.2099>
- Batchelar, K. L., Kidd, K. A., Munkittrick, K. R., Drevnick, P. E., & Burgess, N. M. (2013b). Reproductive health of yellow perch (*Perca flavescens*) from a biological mercury hotspot in Nova Scotia, Canada. *Science of The Total Environment*, 454-455, 319-327. doi: <https://doi.org/10.1016/j.scitotenv.2013.03.020>
- Battin, T. J., Besemer, K., Bengtsson, M. M., Romani, A. M., & Packmann, A. I. (2016). The ecology and biogeochemistry of stream biofilms. *Nature Reviews Microbiology*, 14(4), 251-263. doi: <https://doi.org/10.1038/nrmicro.2016.15>
- Beck, M. A., Levander, O. A., & Handy, J. (2003). Selenium Deficiency and Viral Infection. *The Journal of Nutrition*, 133(5), 1463S–1467S. doi: <https://doi.org/10.1093/jn/133.5.1463S>
- Beckvar, N., Dillon, T. M., & Read, L. B. (2005). Approaches for linking whole-body fish tissue residues of mercury or DDT to biological effects thresholds. *Environmental Toxicology and Chemistry*, 24(8), 2094-2105. doi: <https://doi.org/10.1897/04-284R.1>
- Bell, J. G., Cowey, C. B., Adron, J. W., & Pirie, B. J. S. (1987). Some effects of selenium deficiency on enzyme activities and indices of tissue peroxidation in Atlantic salmon parr (*Salmo salar*). *Aquaculture*, 65(1), 43-54. doi: [https://doi.org/10.1016/0044-8486\(87\)90269-9](https://doi.org/10.1016/0044-8486(87)90269-9)

- Belzile, N., Chen, Y.-W., Gunn, J. M., Tong, J., Alarie, Y., Delonchamp, T., & Lang, C.-Y. (2006). The effect of selenium on mercury assimilation by freshwater organisms. *Canadian Journal of Fisheries and Aquatic Sciences*, 63(1), 1-10. doi: <https://doi.org/10.1139/f05-202>
- Benbrook, C. M. (2016). Trends in glyphosate herbicide use in the United States and globally. *Environmental Sciences Europe*, 28(1), 3. doi: <https://doi.org/10.1186/s12302-016-0070-0>
- Bengtsson, G., Hansson, L.-A., & Montenegro, K. (2004). Reduced grazing rates in *Daphnia pulex* caused by contaminants: implications for trophic cascades. *Environmental Toxicology and Chemistry*, 23(11), 2641-2648. doi: <https://doi.org/10.1897/03-432>
- Bergeron, C. M., Bodinof, C. M., Unrine, J. M., & Hopkins, W. A. (2010). Bioaccumulation and maternal transfer of mercury and selenium in amphibians. *Environmental Toxicology and Chemistry*, 29(4), 989-997. doi: <https://doi.org/10.1002/etc.125>
- Berry, M. J., & Ralston, N. V. (2008). Mercury toxicity and the mitigating role of selenium. *Ecohealth*, 5(4), 456-459. doi: <https://doi.org/10.1007/s10393-008-0204-y>
- Bertolo, A., Blanchet, F. G., Magnan, P., Brodeur, P., Mingelbier, M., & Legendre, P. (2012). Inferring processes from spatial patterns: the role of directional and non-directional forces in shaping fish larvae distribution in a freshwater lake system. *PLoS One*, 7(11), e50239. doi: <https://doi.org/10.1371/journal.pone.0050239>
- Bertrand, M., Cabana, G., Marcogliese, D. J., & Magnan, P. (2011). Estimating the feeding range of a mobile consumer in a river-flood plain system using delta(13)C gradients and parasites. *Journal of Animal Ecology*, 80(6), 1313-1323. doi: <https://doi.org/10.1111/j.1365-2656.2011.01861.x>
- Bérubé, V. E., Boily, M. H., DeBlois, C., Dassylva, N., & Spear, P. A. (2005). Plasma retinoid profile in bullfrogs, *Rana catesbeiana*, in relation to agricultural intensity of sub-watersheds in the Yamaska River drainage basin, Quebec, Canada. *Aquatic Toxicology*, 71(2), 109-120. doi: <https://doi.org/10.1016/j.aquatox.2004.https://doi.org/10.018>
- Besemer, K., Peter, H., Logue, J. B., Langenheder, S., Lindstrom, E. S., Tranvik, L. J., & Battin, T. J. (2012). Unraveling assembly of stream biofilm communities. *The ISME Journal*, 6(8), 1459-1468. doi: <https://doi.org/10.1038/ismej.2011.205>

- Bjerregaard, P., Fjordside, S., Hansen, M. G., & Petrova, M. B. (2011). Dietary selenium reduces retention of methyl mercury in freshwater fish. *Environmental Science & Technology*, 45(22), 9793-9798. doi: <https://doi.org/10.1021/es202565g>
- Bláha, L., Babica, P., & Maršálek, B. (2009). Toxins produced in cyanobacterial water blooms - toxicity and risks. *Interdisciplinary Toxicology*, 2(2), 36-41. doi: <https://doi.org/10.2478/v10102-009-0006-2>
- Blanck, H. (2002). A Critical Review of Procedures and Approaches Used for Assessing Pollution-Induced Community Tolerance (PICT) in Biotic Communities. *Human and Ecological Risk Assessment: An International Journal*, 8(5), 1003-1034. doi: <https://doi.org/10.1080/1080-700291905792>
- Bloom, N. S. (1992). On the Chemical Form of Mercury in Edible Fish and Marine Invertebrate Tissue. *Canadian Journal of Fisheries and Aquatic Sciences*, 49(5), 1010-1017. doi: <https://doi.org/10.1139/f92-113>
- Bonnineau, C., Sague, I. G., Urrea, G., & Guasch, H. (2012). Light history modulates antioxidant and photosynthetic responses of biofilms to both natural (light) and chemical (herbicides) stressors. *Ecotoxicology*, 21(4), 1208-1224. doi: <https://doi.org/10.1007/s10646-012-0876-5>
- Brausch, J. M., & Smith, P. N. (2007). Toxicity of three polyethoxylated tallowamine surfactant formulations to laboratory and field collected fairy shrimp, *Thamnocephalus platyurus*. *Archives of Environmental Contamination and Toxicology*, 52(2), 217-221. doi: <https://doi.org/10.1007/s00244-006-0151-y>
- Bregnard, T., Höhener, P., Häner, A., & Zeyer, J. (1996). Degradation of weathered diesel fuel by microorganisms from a contaminated aquifer in aerobic and anaerobic microcosms. *Environmental Toxicology and Chemistry*, 15(3), 299-307. doi: <https://doi.org/10.1002/etc.5620150312>
- Brown, K. M., & Arthur, J. R. (2007). Selenium, selenoproteins and human health: a review. *Public Health Nutrition*, 4(2b). doi: <https://doi.org/10.1079/phn2001143>
- Burger, J., & Gochfeld, M. (2011). Mercury and selenium levels in 19 species of saltwater fish from New Jersey as a function of species, size, and season. *Science of The Total Environment*, 409(8), 1418-1429. doi: <https://doi.org/10.1016/j.scitotenv.2010.12.034>

- Burger, J., & Gochfeld, M. (2012). Selenium and mercury molar ratios in saltwater fish from New Jersey: individual and species variability complicate use in human health fish consumption advisories. *Environmental Research*, 114, 12-23. doi: <https://doi.org/10.1016/j.envres.2012.02.004>
- Burger, J., & Gochfeld, M. (2013). Selenium/mercury molar ratios in freshwater, marine, and commercial fish from the USA: variation, risk, and health management. *Reviews on Environmental Health*, 28(2-3), 129-143. doi: <https://doi.org/10.1515/reveh-2013-0010>
- Burger, J., Jeitner, C., Donio, M., Pittfield, T., & Gochfeld, M. (2013). Mercury and selenium levels, and selenium:mercury molar ratios of brain, muscle and other tissues in bluefish (*Pomatomus saltatrix*) from New Jersey, USA. *Science of The Total Environment*, 443, 278-286. doi: <https://doi.org/10.1016/j.scitotenv.2012.https://doi.org/10.040>
- Bushnell, B. (2014, Sep 19). *BBMap: a fast, accurate, splice-aware aligner*. [2012/09/20]. Retrieved from <https://www.osti.gov/servlets/purl/1241166>
- Byström, P., Persson, L., Wahlström, E., & Westman, E. (2003). Size- and Density-Dependent Habitat Use in Predators: Consequences for Habitat Shifts in Young Fish. *Journal of Animal Ecology*, 72(1). doi: <https://doi.org/10.1046/j.1365-2656.2003.00681.x>
- Cambier, S., Benard, G., Mesmer-Dudons, N., Gonzalez, P., Rossignol, R., Brethes, D., & Bourdineaud, J. P. (2009). At environmental doses, dietary methylmercury inhibits mitochondrial energy metabolism in skeletal muscles of the zebra fish (*Danio rerio*). *International Journal of Biochemistry & Cell Biology*, 41(4), 791-799. doi: <https://doi.org/10.1016/j.biocel.2008.08.008>
- Campbell, P. G., Giguere, A., Bonneris, E., & Hare, L. (2005). Cadmium-handling strategies in two chronically exposed indigenous freshwater organisms--the yellow perch (*Perca flavescens*) and the floater mollusc (*Pyganodon grandis*). *Aquatic Toxicology*, 72(1-2), 83-97. doi: <https://doi.org/10.1016/j.aquatox.2004.11.023>
- Campbell, P. G. C., Kraemer, L. D., Giguère, A., Hare, L., & Hontela, A. (2008). Subcellular Distribution of Cadmium and Nickel in Chronically Exposed Wild Fish: Inferences Regarding Metal Detoxification Strategies and Implications for Setting Water Quality Guidelines for Dissolved Metals. *Human and Ecological Risk Assessment: An International Journal*, 14(2), 290-316. doi: <https://doi.org/10.1080/10807030801935009>

- Caporaso, J. G., Kuczynski, J., Stombaugh, J., Bittinger, K., Bushman, F. D., Costello, E. K., Fierer, N., Peña, A. G., Goodrich, J. K., Gordon, J. I., Huttley, G. A., Kelley, S. T., Knights, D., Koenig, J. E., Ley, R. E., Lozupone, C. A., McDonald, D., Muegge, B. D., Pirrung, M., Reeder, J., Sevinsky, J. R., Turnbaugh, P. J., Walters, W. A., Widmann, J., Yatsunenko, T., Zaneveld, J., & Knight, R. (2010). QIIME allows analysis of high-throughput community sequencing data. *Nature Methods*, 7(5), 335-336. doi: <https://doi.org/10.1038/nmeth.f.303>.
- Cardon, P.-Y., Caron, A., Rosabal, M., Fortin, C., & Amyot, M. (2018). Enzymatic validation of species-specific protocols for metal subcellular fractionation in freshwater animals. *Limnology and Oceanography: Methods*, 16(9), 537-555. doi: <https://doi.org/10.1002/lom3.10265>
- Carignan, R., Lorrain, S., & Lum, K. (1994). A 50-yr Record of Pollution by Nutrients, Trace Metals, and Organic Chemicals in the St Lawrence River. *Canadian Journal of Fisheries and Aquatic Sciences*, 51(5), 1088-1100. doi: <https://doi.org/10.1139/f94-108>
- Carignan, R., & Neiff, J. J. (1992). Nutrient dynamics in the floodplain ponds of the Paraná River (Argentina) dominated by the water hyacinth *Eichhornia crassipes*. *Biogeochemistry*, 17, 85-121. doi: <https://doi.org/10.1007/bf00002642>
- Caron, A., Pannetier, P., Rosabal, M., Budzinski, H., Lauzent, M., Labadie, P., Nasri, B., Pierron, F., Baudrimont, M., & Couture, P. (2016). Organic and inorganic contamination impacts on metabolic capacities in American and European yellow eels. *Canadian Journal of Fisheries and Aquatic Sciences*, 73(10), 1557-1566. doi: <https://doi.org/10.1139/cjfas-2015-0473>
- Caron, A., Rosabal, M., Drevet, O., Couture, P., & Campbell, P. G. C. (2017). Binding of trace elements (Ag, Cd, Co, Cu, Ni, and Tl) to cytosolic biomolecules in livers of juvenile yellow perch (*Perca flavescens*) collected from lakes representing metal contamination gradients. *Environmental Toxicology and Chemistry*, 37(2), 576-586. doi: <https://doi.org/10.1002/etc.3998>
- Caron, S., & Lucotte, M. (2008). Regional and Seasonal Inputs of Mercury into Lake St. Pierre (St. Lawrence River), a Major Commercial and Sports Fisheries in Canada. *Water, Air, and Soil Pollution*, 195(1-4), 85-97. doi: <https://doi.org/10.1007/s11270-008-9729-5>

- Carvalho, C. M., Chew, E. H., Hashemy, S. I., Lu, J., & Holmgren, A. (2008). Inhibition of the human thioredoxin system. A molecular mechanism of mercury toxicity. *Journal of Biological Chemistry*, 283(18), 11913-11923. doi: <https://doi.org/10.1074/jbc.M710133200>
- CEAEQ. (2008). *Détermination du glyphosate et de l'AMPA dans les eaux: dosage par chromatographie en phase liquide; dérivation post-colonne et détection en fluorescence. MA. 403—GlyAmp 1.0, Rév. 3.* Quebec, Canada: Ministère du Développement durable, de l'Environnement et des Parcs du Québec Retrieved from <http://www.ceaeq.gouv.qc.ca/methodes/pdf/MA403GlyAmp10.pdf>.
- Chalifour, A., LeBlanc, A., Sleno, L., & Juneau, P. (2016). Sensitivity of *Scenedesmus obliquus* and *Microcystis aeruginosa* to atrazine: Effects of acclimation and mixed cultures, and their removal ability. *Ecotoxicology*, 25(10), 1822-1831. doi: <https://doi.org/10.1007/s10646-016-1728-5>
- Cizdziel, J., Hinnens, T., Cross, C., & Pollard, J. (2003). Distribution of mercury in the tissues of five species of freshwater fish from Lake Mead, USA. *Journal of Environmental Monitoring*, 5(5). doi: <https://doi.org/10.1039/b307641p>
- Cizdziel, J. V., Hinnens, T. A., Pollard, J. E., Heithmar, E. M., & Cross, C. L. (2002). Mercury concentrations in fish from Lake Mead, USA, related to fish size, condition, trophic level, location, and consumption risk. *Archives of Environmental Contamination and Toxicology*, 43(3), 309-317. doi: <https://doi.org/10.1007/s00244-002-1191-6>
- Clarkson, T. W., & Magos, L. (2006). The toxicology of mercury and its chemical compounds. *Critical Reviews in Toxicology*, 36(8), 609-662. doi: <https://doi.org/10.1080/10408440600845619>
- Clasen, B., Loro, V. L., Murussi, C. R., Tiecher, T. L., Moraes, B., & Zanella, R. (2018). Bioaccumulation and oxidative stress caused by pesticides in *Cyprinus carpio* reared in a rice-fish system. *Science of The Total Environment*, 626, 737-743. doi: <https://doi.org/10.1016/j.scitotenv.2018.01.154>
- Coelho, S. (2009). Agriculture. European pesticide rules promote resistance, researchers warn. *Science*, 323(5913), 450. doi: <https://doi.org/10.1126/science.323.5913.450>

- Comeau, A. M., Douglas, G. M., & Langille, M. G. (2017). Microbiome helper: A custom and streamlined workflow for microbiome research. *mSystems*, 2(1). doi: <https://doi.org/10.1128/mSystems.00127-16>
- Couderchet, M., Schmalfuß, J., & Böger, P. (1999). A specific and sensitive assay to quantify the herbicidal activity of chloroacetamides. *Pest Management Science*, 52(4), 381-387. doi: [https://doi.org/10.1002/\(SICI\)1096-9063\(199804\)52:4<381::AID-PS735>3.0.CO;2-8](https://doi.org/10.1002/(SICI)1096-9063(199804)52:4<381::AID-PS735>3.0.CO;2-8)
- Couture, P., Busby, P., Gauthier, C., Rajotte, J., & Pyle, G. (2008). Seasonal and Regional Variations of Metal Contamination and Condition Indicators in Yellow Perch (*Perca flavescens*) along Two Polymetallic Gradients. I. Factors Influencing Tissue Metal Concentrations. *Human and Ecological Risk Assessment: An International Journal*, 14(1), 97-125. doi: <https://doi.org/10.1080/10807030701790330>
- Couture, P., & Rajotte, J. W. (2003). Morphometric and metabolic indicators of metal stress in wild yellow perch (*Perca flavescens*) from Sudbury, Ontario: A review. *Journal of Environmental Monitoring*, 5(2), 216-221. doi: <https://doi.org/10.1039/b210338a>
- Covington, S. M., Naddy, R. B., Prouty, A. L., Werner, S. A., & Lewis, M. D. (2018). Effects of in situ selenium exposure and maternal transfer on survival and deformities of brown trout (*Salmo trutta*) fry. *Environmental Toxicology and Chemistry*, 37(5), 1396-1408. doi: <https://doi.org/10.1002/etc.4086>
- Coyle, J. J., Buckler, D. R., Ingersoll, C. G., Fairchild, J. F., & May, T. W. (1993). Effect of dietary selenium on the reproductive success of bluegills (*Lepomis macrochirus*). *Environmental Toxicology and Chemistry*, 12(3), 551-565. doi: <https://doi.org/10.1002/etc.5620120315>
- Crump, K. L., & Trudeau, V. L. (2009). Mercury-induced reproductive impairment in fish. *Environmental Toxicology and Chemistry*, 28(5), 895-907. doi: <https://doi.org/10.1897/08-151.1>
- Cuvin-Aralar, M. L. A., & Furness, R. W. (1991). Mercury and selenium interaction: A review. *Ecotoxicology and Environmental Safety*, 21(3), 348-364. doi: [https://doi.org/10.1016/0147-6513\(91\)90074-Y](https://doi.org/10.1016/0147-6513(91)90074-Y)
- Darnerud, P. (2003). Toxic effects of brominated flame retardants in man and in wildlife. *Environment International*, 29(6), 841-853. doi: [https://doi.org/10.1016/s0160-4120\(03\)00107-7](https://doi.org/10.1016/s0160-4120(03)00107-7)

- de la Chenelière, V., Brodeur, P., & Mingelbier, M. (2014). Restauration des habitats du lac Saint-Pierre: un prérequis au rétablissement de la perchaude. *Le Naturaliste Canadien*, 138(2), 50-62
- Defo, M. A., Pierron, F., Spear, P. A., Bernatchez, L., Campbell, P. G., & Couture, P. (2012). Evidence for metabolic imbalance of vitamin A2 in wild fish chronically exposed to metals. *Ecotoxicology and Environmental Safety*, 85, 88-95. doi: <https://doi.org/10.1016/j.ecoenv.2012.08.017>
- Deng, D. F., Teh, F. C., & Teh, S. J. (2008). Effect of dietary methylmercury and selenomethionine on Sacramento splittail larvae. *Science of The Total Environment*, 407(1), 197-203. doi: <https://doi.org/10.1016/j.scitotenv.2008.08.028>
- Desrosiers, M., Planas, D., & Mucci, A. (2006). Mercury methylation in the epilithon of boreal shield aquatic ecosystems. . *Environmental Science & Technology*, 40(5), 1540-1546. doi: <https://doi.org/10.1021/es0508828>
- Dettmers, J. M., Janssen, J., Pientka, B., Fulford, R. S., & Jude, D. J. (2005). Evidence across multiple scales for offshore transport of yellow perch (*Perca flavescens*) larvae in Lake Michigan. *Canadian Journal of Fisheries and Aquatic Sciences*, 62(12), 2683-2693. doi: <https://doi.org/10.1139/f05-173>
- Dillon, T., Beckvar, N., & Kern, J. (2010). Residue-based mercury dose-response in fish: an analysis using lethality-equivalent test endpoints. *Environmental Toxicology and Chemistry*, 29(11), 2559-2565. doi: <https://doi.org/10.1002/etc.314>
- Drevnick, P. E., & Sandheinrich, M. B. (2003). Effects of dietary methylmercury on reproductive endocrinology of fathead minnows. *Environmental Science & Technology*, 37(19), 4390–4396. doi: <https://doi.org/10.1021/es034252m>
- Driscoll, C. T., Blette, V., Yan, C., Schofield, C. L., Munson, R., & Holsapple, J. (1995). The role of dissolved organic carbon in the chemistry and bioavailability of mercury in remote Adirondack lakes. *Water, Air, and Soil Pollution*, 80, 499-508. doi: <https://doi.org/10.1021/es00052a003>,
- Eaton, J. G., Swenson, W. A., McCormick, J. H., Simonson, T. D., & Jensen, K. M. (1992). A Field and Laboratory Investigation of Acid Effects on Largemouth Bass, Rock Bass, Black Crappie, and Yellow Perch. *Transactions of the American Fisheries Society*,

121(5), 644-658. doi: [https://doi.org/10.1577/1548-8659\(1992\)121<0644:Afalio>2.3.Co;2](https://doi.org/10.1577/1548-8659(1992)121<0644:Afalio>2.3.Co;2)

ECHA. (2017). Glyphosate not classified as a carcinogen by ECHA. Helsinki, Finland: European Chemicals Agency.

Edgar, R. C., Haas, B. J., Clemente, J. C., Quince, C., & Knight, R. (2011). UCHIME improves sensitivity and speed of chimera detection. *Bioinformatics*, *27*(16), 2194-2200. doi: <https://doi.org/10.1093/bioinformatics/btr381>

EFSA. (2015). Conclusion on the peer review of the pesticide risk assessment of the active substance glyphosate (Vol. 13, pp. 4302). Parma, Italy: European Food Safety Authority Journal.

Evans-White, M. A., & Lamberti, G. A. (2009). Direct and indirect effects of a potential aquatic contaminant on grazer-algae interactions. *Environmental Toxicology and Chemistry*, *28*(2), 418-426. doi: <https://doi.org/10.1897/07-586.1>

Fey, S. J., & Larsen, P. M. (2001). 2D or not 2D. *Current Opinion in Chemical Biology*, *5*(1), 26-33. doi: [https://doi.org/10.1016/S1367-5931\(00\)00167-8](https://doi.org/10.1016/S1367-5931(00)00167-8)

Fjeld, E., Haugen, T. O., & Vøllestad, L. A. (1998). Permanent impairment in the feeding behavior of grayling (*Thymallus thymallus*) exposed to methylmercury during embryogenesis. *Science of The Total Environment*, *213*(1-3), 247-254. doi: [https://doi.org/10.1016/S0048-9697\(98\)00097-7](https://doi.org/10.1016/S0048-9697(98)00097-7)

Forlani, G., Pavan, M., Gramek, M., Kafarski, P., & Lipok, J. (2008). Biochemical bases for a widespread tolerance of cyanobacteria to the phosphonate herbicide glyphosate. *Plant and Cell Physiology*, *49*(3), 443-456. doi: <https://doi.org/10.1093/pcp/pcn021>

Frenette, J.-J., Arts, M. T., & Morin, J. (2003). Spectral gradients of downwelling light in a fluvial lake (Lake Saint-Pierre, St-Lawrence River). *Aquatic Ecology*, *37*, 77-85. doi: <https://doi.org/10.1023/A:1022133530244>

Furutani, A., & Rudd, J. W. M. (1980). Measurement of mercury methylation in lake water and sediment samples. *Applied and Environmental Microbiology*, *40*(4), 770-776

Gaffney, A. M., Markov, S. A., & Gunasekaran, M. (2001). Utilization of Cyanobacteria in photobioreactors for orthophosphate removal from water. *Applied Biochemistry and Biotechnology*, *91*(1-9), 185-193. doi: <https://doi.org/10.1385/abab>

- Gandhi, N., Gewurtz, S. B., Drouillard, K. G., Kolic, T., MacPherson, K., Reiner, E. J., & Bhavsar, S. P. (2019). Dioxins in Great Lakes fish: Past, present and implications for future monitoring. *Chemosphere*, 222, 479-488. doi: <https://doi.org/10.1016/j.chemosphere.2018.12.139>
- Gerbet, T. (2018). Cet agriculteur élimine les pesticides grâce à une solution surprenante, *Radio-Canada*. Retrieved from <https://ici.radio-canada.ca/nouvelle/1101870/agriculture-pesticides-quebec-insecticides-oignons-mouche-solution>
- Giguère, A., Campbell, P. G., Hare, L., & Couture, P. (2006). Sub-cellular partitioning of cadmium, copper, nickel and zinc in indigenous yellow perch (*Perca flavescens*) sampled along a polymetallic gradient. *Aquatic Toxicology*, 77(2), 178-189. doi: <https://doi.org/10.1016/j.aquatox.2005.12.001>
- Giraudo, M., Bruneau, A., Gendron, A. D., Brodeur, P., Pilote, M., Marcogliese, D. J., Gagnon, C., & Houde, M. (2016). Integrated spatial health assessment of yellow perch (*Perca flavescens*) populations from the St. Lawrence River, Quebec, Canada) part A: physiological parameters and pathogen assessment. *Environmental Science and Pollution Research (international)*, 23(18), 18073-18084. doi: <https://doi.org/10.1007/s11356-016-7002-9>
- Giroux, I. (2015). *Présence de pesticides dans l'eau au Québec: Portrait et tendances dans les zones de maïs et de soya - 2011 à 2014.* (ISBN 978-2-550-73603-5). Québec: ministère du Développement durable, de l'Environnement et de la Lutte contre les changements climatiques Retrieved from <http://www.mddelcc.gouv.qc.ca/eau/flrivlac/pesticides.htm>
- Giroux, I. (2018). *État de situation sur la présence de pesticides au lac Saint-Pierre.* Québec: ministère du Développement durable, de l'Environnement et de la Lutte contre les changements climatiques Retrieved from www.mddelcc.gouv.qc.ca/eau/lac-st-pierre/etat-presence-pesticides.pdf.
- Glémet, H., & Rodríguez, M. A. (2007). Short-term growth (RNA/DNA ratio) of yellow perch (*Perca flavescens*) in relation to environmental influences and spatio-temporal variation in a shallow fluvial lake. *Canadian Journal of Fisheries and Aquatic Sciences*, 64(12), 1646-1655. doi: <https://doi.org/10.1139/f07-126>

- Gochfeld, M., Burger, J., Jeitner, C., Donio, M., & Pittfield, T. (2012). Seasonal, locational and size variations in mercury and selenium levels in striped bass (*Morone saxatilis*) from New Jersey. *Environmental Research*, 112, 8-19. doi: <https://doi.org/10.1016/j.envres.2011.12.007>
- Goldstein, R. M., Brigham, M. E., & Stauffer, J. C. (1996). Comparison of mercury concentrations in liver, muscle, whole bodies, and composites of fish from the Red river of the North. *Canadian Journal of Fisheries and Aquatic Sciences*, 53, 244-252. doi: <https://doi.org/10.1139/f95-203>
- Gomes, M. P., Le Manac'h, S. G., Maccario, S., Labrecque, M., Lucotte, M., & Juneau, P. (2016a). Differential effects of glyphosate and aminomethylphosphonic acid (AMPA) on photosynthesis and chlorophyll metabolism in willow plants. *Pesticide Biochemistry and Physiology*, 130, 65-70. doi: <https://doi.org/10.1016/j.pestbp.2015.11.010>
- Gomes, M. P., Le Manac'h, S. G., Moingt, M., Smedbol, E., Paquet, S., Labrecque, M., Lucotte, M., & Juneau, P. (2016b). Impact of phosphate on glyphosate uptake and toxicity in willow. *Journal of Hazardous Materials*, 304, 269-279. doi: <https://doi.org/10.1016/j.jhazmat.2015.10.043>
- Gomes, M. P., Smedbol, E., Chalifour, A., Henault-Ethier, L., Labrecque, M., Lepage, L., Lucotte, M., & Juneau, P. (2014). Alteration of plant physiology by glyphosate and its by-product aminomethylphosphonic acid: An overview. *Journal of Experimental Botany*, 65(17), 4691-4703. doi: <https://doi.org/10.1093/jxb/eru269>
- Gonzalez, P., Dominique, Y., Massabuau, J. C., Boudou, A., & Bourdineaud, J. P. (2005a). Comparative Effects of Dietary Methylmercury on Gene Expression in Liver, Skeletal Muscle, and Brain of the Zebrafish (*Danio rerio*). *Environmental Science & Technology*, 39(11), 3972–3980. doi: <https://doi.org/10.1021/es0483490>
- Gonzalez, P., Dominique, Y., Massabuau, J. C., Boudou, A., & Bourdineaud, J. P. (2005b). Comparative effects of dietary methylmercury on gene expression in liver, skeletal muscle, and brain of the zebrafish (*Danio rerio*). *Environmental Science & Technology*, 39(11), 3972-3980. doi: <https://doi.org/10.1021/es0483490>

- Goodarzi, F., & Swaine, D. J. (1993). Chalcophile elements in western Canadian coals. *International Journal of Coal Geology*, 24(1-4), 281-292 doi:
[https://doi.org/10.1016/0166-5162\(93\)90015-3](https://doi.org/10.1016/0166-5162(93)90015-3)
- Gordon, A. (2009). *FASTX-Toolkit: FASTQ/A short-reads pre-processing tools*. Retrieved from http://hannonlab.cshl.edu/fastx_toolkit/.
- Graves, S. D., Kidd, K. A., Batchelor, K. L., Cowie, A. M., O'Driscoll, N. J., & Martyniuk, C. J. (2017). Response of oxidative stress transcripts in the brain of wild yellow perch (*Perca flavescens*) exposed to an environmental gradient of methylmercury. *Comparative Biochemistry and Physiology Part C: Toxicology & Pharmacology*, 192, 50-58. doi: <https://doi.org/10.1016/j.cbpc.2016.12.005>
- Grégoire, D. S., Poulain, A. J., & Ivanova, E. P. (2018). Shining light on recent advances in microbial mercury cycling. *Facets*, 3(1), 858-879. doi: <https://doi.org/10.1139/facets-2018-0015>
- Guasch, H., Muñoz, I., Rosés, N., & Sabater, S. (1997). Changes in atrazine toxicity throughout succession of stream periphyton communities. *Journal of Applied Phycology*, 9(2), 137–146. doi: <https://doi.org/10.1023/A:1007970211549>
- Guasch, H., Navarro, E., Serra, A., & Sabater, S. (2004). Phosphate limitation influences the sensitivity to copper in periphytic algae. *Freshwater Biology*, 49, 463-473. doi: <https://doi.org/10.1111/j.1365-2427.2004.01196.x>
- Guirlet, E., Das, K., & Girondot, M. (2008). Maternal transfer of trace elements in leatherback turtles (*Dermochelys coriacea*) of French Guiana. *Aquatic Toxicology*, 88(4), 267-276. doi: <https://doi.org/10.1016/j.aquatox.2008.05.004>
- Hagerthey, S. E., Bellinger, B. J., Wheeler, K., Gantar, M., & Gaiser, E. (2011). Everglades periphyton: A biogeochemical perspective. *Critical Reviews in Environmental Science and Technology*, 41(sup1), 309-343. doi: <https://doi.org/10.1080/10643389.2010.531218>
- Hall, B. D., Bodaly, R. A., Fudge, R. J. P., Rudd, J. W. M., & Rosenberg, D. M. (1997). Food as the dominant pathway of methylmercury uptake by fish. *Water, Air, and Soil Pollution*, 100(1-2), 13–24. doi: <https://doi.org/10.1023/A:1018071406537>

- Hamelin, S., Amyot, M., Barkay, T., Wang, Y., & Planas, D. (2011). Methanogens: principal methylators of mercury in lake periphyton. *Environmental Science & Technology*, 45(18), 7693-7700. doi: <https://doi.org/10.1021/es2010072>
- Hammerschmidt, C. R., & Sandheinrich, M. B. (2005). Maternal diet during oogenesis is the major source of methylmercury in fish embryos. *Environmental Science & Technology*, 39(10), 3580–3584. doi: <https://doi.org/10.1021/es0486263>
- Hammerschmidt, C. R., Wiener, J. G., Frazier, B. E., & Rada, R. G. (1999). Methylmercury Content of Eggs in Yellow Perch Related to Maternal Exposure in Four Wisconsin Lakes. *Environmental Science & Technology*, 33(7), 999-1003. doi: <https://doi.org/10.1021/es980948h>
- Harris, H. H., Pickering, I. J., & George, G. N. (2003). The chemical form of mercury in fish. *Science*, 301(5637), 1203. doi: <https://doi.org/10.1126/science.1085941>
- Hogstrand, C., Balesaria, S., & N.Glover, C. (2002). Application of genomics and proteomics for study of the integrated response to zinc exposure in a non-model fish species, the rainbow trout. *Comparative Biochemistry and Physiology Part B: Biochemistry and Molecular Biology*, 133(4), 523-535. doi: [https://doi.org/10.1016/S1096-4959\(02\)00125-2](https://doi.org/10.1016/S1096-4959(02)00125-2)
- Holm, J., Palace, V., Siwik, P., Sterling, G., Evans, R., Baron, C., Werner, J., & Wautier, K. (2005). Developmental effects of bioaccumulated selenium in eggs and larvae of two salmonid species. *Environmental Toxicology and Chemistry*, 24(9), 2373-2381. doi: <https://doi.org/10.1897/04-402R1.1>
- Hopkins, W. A., DuRant, S. E., Staub, B. P., Rowe, C. L., & Jackson, B. P. (2006). Reproduction, Embryonic Development, and Maternal Transfer of Contaminants in the Amphibian *Gastrophryne carolinensis*. *Environmental Health Perspectives*, 114(5), 661-666. doi: <https://doi.org/10.1289/ehp.8457>
- Houde, M., Berryman, D., de Lafontaine, Y., & Verreault, J. (2014a). Novel brominated flame retardants and dechloranes in three fish species from the St. Lawrence River, Canada. *Science of The Total Environment*, 479-480, 48-56. doi: <https://doi.org/10.1016/j.scitotenv.2014.01.105>
- Houde, M., Giraudo, M., Douville, M., Bougas, B., Couture, P., De Silva, A. O., Spencer, C., Lair, S., Verreault, J., Bernatchez, L., & Gagnon, C. (2014b). A multi-level biological

- approach to evaluate impacts of a major municipal effluent in wild St. Lawrence River yellow perch (*Perca flavescens*). *Science of The Total Environment*, 497-498, 307-318. doi: <https://doi.org/10.1016/j.scitotenv.2014.07.059>
- Howard, P. H., & Muir, D. C. (2011). Identifying new persistent and bioaccumulative organics among chemicals in commerce II: pharmaceuticals. *Environmental Science & Technology*, 45(16), 6938-6946. doi: <https://doi.org/10.1021/es201196x>
- Huckabee, J. W., Elwood, J. W., & Hildebrand, S. G. (1979). Accumulation of mercury in freshwater biota *Biogeochemistry of mercury in the environment*. (pp. 199-216). New York: Elsevier/North-Holland Biomedical Press.
- Hudon, C., Jean, M., & Létourneau, G. (2018). Temporal (1970–2016) changes in human pressures and wetland response in the St. Lawrence River (Québec, Canada). *Science of The Total Environment*, 643, 1137-1151. doi: <https://doi.org/10.1016/j.scitotenv.2018.06.080>
- IARC. (2015). IARC Monographs Volume 112: Evaluation of Five Organophosphate Insecticides and Herbicides. Lyon, France: International Agency for Research on Cancer.
- Ikemoto, T., Kunito, T., Tanaka, H., Baba, N., Miyazaki, N., & Tanabe, S. (2004). Detoxification mechanism of heavy metals in marine mammals and seabirds: interaction of selenium with mercury, silver, copper, zinc, and cadmium in liver. *Archives of Environmental Contamination and Toxicology*, 47(3), 402-413. doi: <https://doi.org/10.1007/s00244-004-3188-9>
- Ion, J., Lafontaine, Y. d., Dumont, P., & Lapierre, L. (1997). Contaminant levels in St. Lawrence River yellow perch (*Perca flavescens*): spatial variation and implications for monitoring. *Canadian Journal of Fisheries and Aquatic Sciences*, 54(12), 2930-2946. doi: <https://doi.org/10.1139/f97-198>
- IPCS. (2010). Action is needed on chemicals of major public health concern. Geneva, Switzerland: International Programme on Chemical Safety, World Health Organization.
- Ivorra, N., Bremer, S., Guasch, H., Kraak, M. H. S., & Admiraal, W. (2000). Differences in the sensitivity of benthic microalgae to Zn and Cd regarding biofilm development and exposure history. *Environmental Toxicology and Chemistry*, 19(5), 1332-1339. doi: <https://doi.org/10.1002/etc.5620190516>.

Jackson, T. A. (1991). Effects of heavy metals and selenium on mercury methylation and other microbial activities in freshwater sediments. In J.-P. Vernet (Ed.), *Heavy metals in the environment* (pp. 191-217). Amsterdam, The Netherlands.: Elsevier Science Publishers B.V.

Janz, D. M., DeForest, D. K., Brooks, M. L., Chapman, P. M., Gilron, G., Hoff, D., Hopkins, W. A., McIntyre, D. O., Mebane, C. A., Palace, V. P., Skorupa, J. P., & Wayland, M. (2010). Selenium Toxicity to Aquatic Organisms. In P. M. Chapman, W. J. Adams, M. L. Brooks, C. G. Delos, S. N. Luoma, W. A. Maher, H. M. Ohlendorf, T. S. Presser & D. P. Shaw (Eds.), *Ecological Assessment of Selenium in the Aquatic Environment* (pp. 141-231). Pensacola, Florida: Society of Environmental Toxicology and Chemistry (SETAC) and CRC Press.

Janz, D. M., Liber, K., Pickering, I. J., Wiramanaden, C. I., Weech, S. A., Gallego-Gallegos, M., Driessnack, M. K., Franz, E. D., Goertzen, M. M., Phibbs, J., Tse, J. J., Himbeault, K. T., Robertson, E. L., Burnett-Seidel, C., England, K., & Gent, A. (2014). Integrative assessment of selenium speciation, biogeochemistry, and distribution in a northern coldwater ecosystem. *Integrated Environmental Assessment and Management*, 10(4), 543-554. doi: <https://doi.org/10.1002/ieam.1560>

Jenkins, K. D., & Mason, A. Z. (1998). Relationships between subcellular distributions of cadmium and perturbations in reproduction in the polychaete *Neanthes arenaceodentata*. *Aquatic Toxicology*, 12(3), 229-244. doi: [https://doi.org/10.1016/0166-445X\(88\)90025-2](https://doi.org/10.1016/0166-445X(88)90025-2)

Johnston, T. A., Bodaly, R. A., Latif, M. A., Fudge, R. J. P., & Strange, N. E. (2001). Intra- and interpopulation variability in maternal transfer of mercury to eggs of walleye (*Stizostedion vitreum*). *Aquatic Toxicology*, 52(1), 73-85. doi: [https://doi.org/10.1016/S0166-445X\(00\)00129-6](https://doi.org/10.1016/S0166-445X(00)00129-6)

Kennedy, C. J., McDonald, L. E., Loveridge, R., & Strosher, M. M. (2000). The effect of bioaccumulated selenium on mortalities and deformities in the eggs, larvae, and fry of a wild population of cutthroat trout (*Oncorhynchus clarki lewisi*). *Archives of Environmental Contamination and Toxicology*, 39(1), 46-52

Khadra, M., Caron, A., Planas, D., Ponton, D. E., Rosabal, M., & Amyot, M. (2019a). The fish or the egg: Maternal transfer and subcellular partitioning of mercury and selenium in

- Yellow Perch (*Perca flavescens*). *Science of The Total Environment*, 675, 604-614.
doi: <https://doi.org/10.1016/j.scitotenv.2019.04.226>
- Khadra, M., Planas, D., Brodeur, P., & Amyot, M. (2019b). Mercury and selenium distribution in key tissues and early life stages of Yellow Perch (*Perca flavescens*). *Environmental Pollution*, 254(Pt A), 112963. doi: <https://doi.org/10.1016/j.envpol.2019.112963>
- Khadra, M., Planas, D., Girard, C., & Amyot, M. (2018). Age matters: Submersion period shapes community composition of lake biofilms under glyphosate stress. *Facets*, 3, 934-951. doi: <https://doi.org/10.1139/facets-2018-0019>
- Kidd, K. A., Blanchfield, P. J., Mills, K. H., Palace, V. P., Evans, R. E., Lazorchak, J. M., & Flick, R. W. (2007). Collapse of a fish population after exposure to a synthetic estrogen. *Proceedings of the National Academy of Sciences of the United States of America*, 104(21), 8897-8901. doi: <https://doi.org/10.1073/pnas.0609568104>
- Kihlström, J. E., C.Lundberg, & L.Hulth. (1971). Number of eggs and young produced by zebrafishes (*Brachydanio rerio*, Ham.-Buch.) spawning in water containing small amounts of phenylmercuric acetate. *Environmental Research*, 4(4), 355-359. doi: [https://doi.org/10.1016/0013-9351\(71\)90034-X](https://doi.org/10.1016/0013-9351(71)90034-X)
- Kraemer, L. D., Campbell, P. G., & Hare, L. (2006). Seasonal variations in hepatic Cd and Cu concentrations and in the sub-cellular distribution of these metals in juvenile yellow perch (*Perca flavescens*). *Environmental Pollution*, 142(2), 313-325. doi: <https://doi.org/10.1016/j.envpol.2005.https://doi.org/10.004>
- Kuiper, R. V., van den Brandhof, E. J., Leonards, P. E., van der Ven, L. T., Wester, P. W., & Vos, J. G. (2007). Toxicity of tetrabromobisphenol A (TBBPA) in zebrafish (*Danio rerio*) in a partial life-cycle test. *Archives of Toxicology*, 81(1), 1-9. doi: <https://doi.org/10.1007/s00204-006-0117-x>
- Kwan, K. H. M., Chan, H. M., & Lafontaine, Y. D. (2003). Metal Contamination in Zebra Mussels (*Dreissena polymorpha*) Along the st. Lawrence River. *Environmental Monitoring and Assessment*, 88(1-3), 193-219. doi: <https://doi.org/10.1023/A:1025517007605>
- Kwaśniak, J., & Falkowska, L. (2012). Mercury distribution in muscles and internal organs of the juvenile and adult Baltic cod (*Gadus morrhua callarias* Linnaeus, 1758).

Oceanological and Hydrobiological Studies, 41(2). doi:

<https://doi.org/10.2478/s13545-012-0018-y>

La Violette, N. (2004). Les lacs fluviaux du Saint-Laurent: Hydrologie et modifications humaines. *Le Naturaliste Canadien*, 128(1), 98-104

Lajeunesse, A., Blais, M., Barbeau, B., Sauve, S., & Gagnon, C. (2013). Ozone oxidation of antidepressants in wastewater -Treatment evaluation and characterization of new by-products by LC-QToFMS. *Chemistry Central journal*, 7(1), 15. doi:
<https://doi.org/10.1186/1752-153X-7-15>

Lajeunesse, A., Gagnon, C., Gagne, F., Louis, S., Cejka, P., & Sauve, S. (2011). Distribution of antidepressants and their metabolites in brook trout exposed to municipal wastewaters before and after ozone treatment--evidence of biological effects.

Chemosphere, 83(4), 564-571. doi: <https://doi.org/10.1016/j.chemosphere.2010.12.026>

Laliberté, D. (2016). *La contamination des poissons d'eau douce par les toxiques - 3e édition*. (ISBN 978-2-550-75595-1 (PDF)). Québec: Ministère du Développement durable, de l'Environnement et de la Lutte contre les changements climatiques, Direction générale du suivi de l'état de l'environnement.

Larose, C., Canuel, R., Lucotte, M., & Di Giulio, R. T. (2008). Toxicological effects of methylmercury on walleye (*Sander vitreus*) and perch (*Perca flavescens*) from lakes of the boreal forest. *Comparative Biochemistry and Physiology C-Toxicology & Pharmacology*, 147(2), 139-149. doi: <https://doi.org/10.1016/j.cbpc.2007.09.002>

Latif, M. A., Bodaly, R. A., Johnston, T. A., & Fudge, R. J. P. (2001). Effects of environmental and maternally derived methylmercury on the embryonic and larval stages of walleye (*Stizostedion vitreum*). *Environmental Pollution*, 111(1), 139-148. doi: [https://doi.org/10.1016/S0269-7491\(99\)00330-9](https://doi.org/10.1016/S0269-7491(99)00330-9)

Lavoie, I., Lavoie, M., & Fortin, C. (2012). A mine of information: Benthic algal communities as biomonitor of metal contamination from abandoned tailings. *Science of The Total Environment*, 425, 231-241. doi: <https://doi.org/10.1016/j.scitotenv.2012.02.057>

Lazaro, W. L., Guimaraes, J. R., Ignacio, A. R., Da Silva, C. J., & Diez, S. (2013). Cyanobacteria enhance methylmercury production: A hypothesis tested in the periphyton of two lakes in the Pantanal floodplain, Brazil. *Science of The Total Environment*, 456-457, 231-238. doi: <https://doi.org/10.1016/j.scitotenv.2013.03.022>

- Le Cren, E. D. (1951). The Length-Weight Relationship and Seasonal Cycle in Gonad Weight and Condition in the Perch (*Perca fluviatilis*). *Journal of Animal Ecology*, 20(2), 201-219. doi: <https://doi.org/10.2307/1540>
- Leclerc, E., Mailhot, Y., Mingelbier, M., & Bernatchez, L. (2008). The landscape genetics of yellow perch (*Perca flavescens*) in a large fluvial ecosystem. *Molecular Ecology*, 17(7), 1702-1717. doi: <https://doi.org/10.1111/j.1365-294X.2008.03710.x>
- Leclerc, M., Planas, D., & Amyot, M. (2015). Relationship between extracellular low-molecular-weight thiols and mercury species in natural lake periphytic biofilms. *Environmental Science & Technology*, 49(13), 7709-7716. doi: <https://doi.org/10.1021/es505952x>
- Legendre, P., & Legendre, L. (1998). *Numerical Ecology, Volume 24, (Developments in Environmental Modelling)*. Amsterdam, The Netherlands: Elsevier Science.
- Lemly, A. D. (1993a). Guidelines for evaluating selenium data from aquatic monitoring and assessment studies. *Environmental Monitoring and Assessment*, 28, 83-100. doi: <https://doi.org/10.1007/BF00547213>
- Lemly, A. D. (1993b). Teratogenic effects of selenium in natural populations of fresh water fish. *Ecotoxicology and Environmental Safety*, 26(2), 181-204. doi: <https://doi.org/10.1006/eesa.1993.1049>
- Lemly, A. D. (1997). A Teratogenic Deformity Index for Evaluating Impacts of Selenium on Fish Populations. *Ecotoxicology and Environmental Safety*, 37(3), 259-266. doi: <https://doi.org/10.1006/eesa.1997.1554>
- Lescord, G. L., Johnston, T. A., Branfireun, B. A., & Gunn, J. M. (2018). Percentage of methylmercury in the muscle tissue of freshwater fish varies with body size and age and among species. *Environmental Toxicology and Chemistry*, 37(10), 2682-2691. doi: <https://doi.org/10.1002/etc.4233>
- Leung, C., Magnan, P., & Angers, B. (2011). Genetic Evidence for Sympatric Populations of Yellow Perch (*Perca flavescens*) in Lake Saint-Pierre (Canada): the Crucial First Step in Developing a Fishery Management Plan. *Journal of Aquaculture Research & Development*, 01(S6). doi: <https://doi.org/10.4172/2155-9546.S6-001>
- Lima, A. P., Sarkis, J. E., Shihomatsu, H. M., & Muller, R. C. (2005). Mercury and selenium concentrations in fish samples from Cachoeira do PiriaMunicipality, ParaState, Brazil.

Environmental Research, 97(3), 236-244. doi:

<https://doi.org/10.1016/j.envres.2004.05.005>

Lipok, J., Owsiak, T., Mlynarz, P., Forlani, G., & Kafarski, P. (2007). Phosphorus NMR as a tool to study mineralization of organophosphonates—The ability of *Spirulina* spp. to degrade glyphosate. *Enzyme and Microbial Technology*, 41(3), 286-291. doi:
<https://doi.org/10.1016/j.enzmictec.2007.02.004>

Lozano, V. L., Vinocur, A., Sabio y García, C. A., Allende, L., Cristos, D. S., Rojas, D., Wolansky, M., & Pizarro, H. (2018). Effects of glyphosate and 2,4-D mixture on freshwater phytoplankton and periphyton communities: a microcosms approach. *Ecotoxicology and Environmental Safety*, 148, 1010-1019. doi:
<https://doi.org/10.1016/j.ecoenv.2017.12.006>

Lozupone, C., & Knight, R. (2005). UniFrac: A new phylogenetic method for comparing microbial communities. *Applied and Environmental Microbiology*, 71(12), 8228-8235. doi: <https://doi.org/10.1128/AEM.71.12.8228-8235.2005>

Lozupone, C., Lladser, M. E., Knights, D., Stombaugh, J., & Knight, R. (2011). UniFrac: An effective distance metric for microbial community comparison. *The ISME Journal*, 5(2), 169-172. doi: <https://doi.org/10.1038/ismej.2010.133>

Luckenbach, T., Kilian, M., Triebeskorn, R., & Oberemm, A. (2001). Fish early life stage tests as a tool to assess embryotoxic potentials in small streams. *Journal of Aquatic Ecosystem Stress and Recovery*, 8(3-4), 355–370. doi:
<https://doi.org/10.1023/A:1012976809450>

Magnan, P., Brodeur, P., Paquin, E., Vachon, N., Paradis, Y., Dumont, P., & Mailhot, Y. (2017). *État du stock de perchaudes du lac Saint-Pierre en 2016. Comité scientifique sur la gestion de la perchaude du lac Saint-Pierre. Chaire de recherche du Canada en écologie des eaux douces*. Retrieved from Université du Québec à Trois-Rivières et ministère des Forêts, de la Faune et des Parcs.

Maher, W. A., Roach, A., Doblin, M., Fan, T., Foster, S., Garrett, R., Möller, G., Oram, L., & Wallschläger, D. (2010). Environmental Sources, Speciation, and Partitioning of Selenium. In P. M. Chapman, W. J. Adams, M. L. Brooks, C. G. Delos, S. N. Luoma, W. A. Maher, H. M. Ohlendorf, T. S. Presser & D. P. Shaw (Eds.), *Ecological*

Assessment of Selenium in the Aquatic Environment (pp. 47-92). Pensacola, Florida: Society of Environmental Toxicology and Chemistry (SETAC) and CRC Press.

Mailman, M., Bodaly, R. A., Paterson, M. J., Thompson, S., & Flett, R. J. (2014). Low-level experimental selenite additions decrease mercury in aquatic food chains and fish muscle but increase selenium in fish gonads. *Archives of Environmental Contamination and Toxicology*, 66(1), 32-40. doi: <https://doi.org/10.1007/s00244-013-9950-0>

Malécot, M., Mezhoud, K., Marie, A., Praseuth, D., Puiseux-Dao, S., & Edery, M. (2009). Proteomic study of the effects of microcystin-LR on organelle and membrane proteins in medaka fish liver. *Aquatic Toxicology*, 94(2), 153-161. doi: <https://doi.org/10.1016/j.aquatox.2009.06.012>

Marcogliese, D. J., Blaise, C., Cyr, D., de Lafontaine, Y., Fournier, M., Gagne, F., Gagnon, C., & Hudon, C. (2015). Effects of a major municipal effluent on the St. Lawrence River: A case study. *Ambio*, 44(4), 257-274. doi: <https://doi.org/10.1007/s13280-014-0577-9>

Mason, R. P. (2013). *Trace Metals in Aquatic Systems*. Hoboken, NJ: Wiley-Blackwell.

Mason, R. P., Fitzgerald, W. F., & Morel, F. M. M. (1994). The biogeochemical cycling of elemental mercury: Anthropogenic influences. *Geochimica et Cosmochimica Acta*, 58(15), 3191-3198. doi: [https://doi.org/10.1016/0016-7037\(94\)90046-9](https://doi.org/10.1016/0016-7037(94)90046-9)

Mason, R. P., Laporte, J., & Andres, S. (2000). Factors controlling the bioaccumulation of mercury, methylmercury, arsenic, selenium, and cadmium by freshwater invertebrates and fish. *Archives of Environmental Contamination and Toxicology*, 38(3), 283-297. doi: <https://doi.org/10.1007/s002449910038>

Masset, T., Frossard, V., Perga, M. E., Cottin, N., Piot, C., Cachera, S., & Naffrechoux, E. (2019). Trophic position and individual feeding habits as drivers of differential PCB bioaccumulation in fish populations. *Science of The Total Environment*, 674, 472-481. doi: <https://doi.org/10.1016/j.scitotenv.2019.04.196>

Matta, M. B., Linse, J., Cairncross, C., Francendese, L., & Kocan, R. M. (2001). Reproductive and transgenerational effects of methylmercury or Aroclor 1268 on *Fundulus heteroclitus*. *Environmental Toxicology and Chemistry*, 20(2), 327-335. doi: <https://doi.org/10.1002/etc.5620200213>

- McDougald, D., Rice, S. A., Barraud, N., Steinberg, P. D., & Kjelleberg, S. (2012). Should we stay or should we go: mechanisms and ecological consequences for biofilm dispersal. *Nature Reviews Microbiology*, 10(1), 39-50. doi: <https://doi.org/10.1038/nrmicro2695>
- McKim, J. M. (1977). Evaluation of tests with early life stages of fish for predicting long-term toxicity. *Journal of the Fisheries Research Board of Canada*, 34(8), 1148-1154. doi: <https://doi.org/10.1139/f77-172>
- McMurdie, P. J., & Holmes, S. (2013). phyloseq: An R package for reproducible interactive analysis and graphics of microbiome census data. *PLoS One*, 8(4), e61217. doi: <https://doi.org/10.1371/journal.pone.0061217>
- Miehls, S. M., & Dettmers, J. M. (2011). Factors Influencing Habitat Shifts of Age-0 Yellow Perch in Southwestern Lake Michigan. *Transactions of the American Fisheries Society*, 140(5), 1317-1329. doi: <https://doi.org/10.1080/00028487.2011.620484>
- Mieiro, C. L., Bervoets, L., Joosen, S., Blust, R., Duarte, A. C., Pereira, M. E., & Pacheco, M. (2011). Metallothioneins failed to reflect mercury external levels of exposure and bioaccumulation in marine fish--considerations on tissue and species specific responses. *Chemosphere*, 85(1), 114-121. doi: <https://doi.org/10.1016/j.chemosphere.2011.05.034>
- Montuelle, B., Dorigo, U., Bérard, A., Volat, B., Bouchez, A., Tlili, A., Gouy, V., & Pesce, S. (2010). The periphyton as a multimetric bioindicator for assessing the impact of land use on rivers: An overview of the Ardières-Morcille experimental watershed (France). *Hydrobiologia*, 657(1), 123-141. doi: <https://doi.org/10.1007/s10750-010-0105-2>
- Morel, F. M. M., Kraepiel, A. M. L., & Amyot, M. (1998). The chemical cycle and bioaccumulation of mercury. *Annual Review of Ecology and Systematics*, 29, 543-566. doi: <https://doi.org/10.1146/annurev.ecolsys.29.1.543>
- Moreno-Reyes, R., Suetens, C., Mathieu, F., Begaux, F., Zhu, D., Rivera, M. T., Boelaert, M., Nève, J., Perlmutter, N., & Vanderpas, J. (1998). Kashin–Beck Osteoarthropathy in Rural Tibet in Relation to Selenium and Iodine Status. *The New England Journal of Medicine*, 339, 112-1120. doi: <https://doi.org/10.1056/NEJM199810153391604>
- Mosley, P. (2004). Geomorphology and hydrology of lakes. In J. Harding, P. Mosley, C. Pearson & B. Sorrell (Eds.), *Freshwaters of New Zealand* Wellington, New Zealand: NZ Hydrological Society and NZ Limnological Society.

- Müller, A. K., Brinkmann, M., Baumann, L., Stoffel, M. H., Segner, H., Kidd, K. A., & Hollert, H. (2015). Morphological alterations in the liver of yellow perch (*Perca flavescens*) from a biological mercury hotspot. *Environmental Science and Pollution Research (international)*, 22(22), 17330-17342. doi: <https://doi.org/10.1007/s11356-015-4177-4>
- Ng, C. A., Berg, M. B., Jude, D. J., Janssen, J., Charlebois, P. M., Amaral, L. A. N., & Gray, K. A. (2008). Chemical amplification in an invaded food web: Seasonality and ontogeny in a high-biomass, low-diversity ecosystem. *Environmental Toxicology and Chemistry*, 27(10), 2186-2195. doi: <https://doi.org/10.1897/07-636.1>
- Ng, C. A., & Gray, K. A. (2009). Tracking bioaccumulation in aquatic organisms: A dynamic model integrating life history characteristics and environmental change. *Ecological Modelling*, 220(9-10), 1266-1273. doi: <https://doi.org/10.1016/j.ecolmodel.2009.02.007>
- Niimi, A. J. (1983). Biological and toxicological effects of environmental contaminants in fish and their eggs. *Canadian Journal of Fisheries and Aquatic Sciences*, 40, 306-312
- Nusch, E. A. (1980). Comparison of different methods for chlorophyll and phaeopigment determination. *Archiv für Hydrobiologie–Beiheft Ergebnisse der Limnologie*, 14, 14-36
- Oksanen, J., Blanchet, F. G., Friendly, M., Kindt, R., Legendre, P., Mcglinn, D., Peter, R., Hara, R. B. O., Simpson, G. L., Solymos, P., Stevens, H. H., Szoecs, E., & Wagner, H. (2016). vegan: Community Ecology Package. Retrieved from <https://cran.r-project.org/package=vegan>
- Oliveira, R., Domingues, I., Koppe Grisolia, C., & Soares, A. M. (2009). Effects of triclosan on zebrafish early-life stages and adults. *Environmental Science and Pollution Research (international)*, 16(6), 679-688. doi: <https://doi.org/10.1007/s11356-009-0119-3>
- Onsanit, S., & Wang, W. X. (2011). Sequestration of total and methyl mercury in different subcellular pools in marine caged fish. *Journal of Hazardous Materials*, 198, 113-122. doi: <https://doi.org/10.1016/j.jhazmat.2011.https://doi.org/10.020>
- Oremland, R. S., Culbertson, C. W., & Winfrey, M. R. (1991). Methylmercury Decomposition in Sediments and Bacterial Cultures: Involvement of Methanogens and Sulfate

Reducers in Oxidative Demethylation. *Applied and Environmental Microbiology*, 57(1), 130-137

Paradis, Y., Bertolo, A., Mingelbier, M., Brodeur, P., & Magnan, P. (2014). What controls distribution of larval and juvenile yellow perch? The role of habitat characteristics and spatial processes in a large, shallow lake. *Journal of Great Lakes Research*, 40(1), 172-178. doi: <https://doi.org/10.1016/j.jglr.2013.12.001>

Pařízek, J., & Ošťádalová, I. (1967). The protective effect of small amounts of selenite in sublimate intoxication. *Experientia*, 23(2), 142–143. doi: <https://doi.org/10.1007/BF02135970>

Pelletier, M. (2005). *La contamination des sédiments par les toxiques-le lac Saint-Pierre: dernière halte avant l'estuaire*. Environnement Canada.

Pelletier, M., & Rondeau, M. (2013). *Les polybromodiphényléthers (PBDE) dans les matières en suspension et les sédiments du fleuve Saint-Laurent*. Quebec, Canada: Environnement Canada, Direction des sciences et de la technologie de l'eau.

Peng, X., Liu, F., & Wang, W. X. (2016). Organ-specific accumulation, transportation, and elimination of methylmercury and inorganic mercury in a low Hg accumulating fish. *Environmental Toxicology and Chemistry*, 35(8), 2074-2083. doi: <https://doi.org/10.1002/etc.3363>

Pérez, G. L., Torremorell, A., Mugni, H., Rodriguez, P., Vera, M. S., Naschimento, M. D., Allende, L., Bustingorry, J., Escaray, R., Ferraro, M., Izaguirre, I., Pizarro, H., Bonetto, C., Morris, D. P., & Zagarese, H. (2007). Effects of the herbicide Roundup on freshwater microbial communities: A mesocosm study. *Ecological Applications*, 17(8), 2310-2322. doi: <https://doi.org/10.1890/07-0499.1>

Perron, T., Chetelat, J., Gunn, J., Beisner, B. E., & Amyot, M. (2014). Effects of experimental thermocline and oxycline deepening on methylmercury bioaccumulation in a Canadian shield lake. *Environmental Science & Technology*, 48(5), 2626-2634. doi: <https://doi.org/10.1021/es404839t>

Peruzzo, P. J., Porta, A. A., & Ronco, A. E. (2008). Levels of glyphosate in surface waters, sediments and soils associated with direct sowing soybean cultivation in north pampasic region of Argentina. *Environmental Pollution*, 156(1), 61-66. doi: <https://doi.org/10.1016/j.envpol.2008.01.015>

- Peterson, S. A., Ralston, N. V. C., Whanger, P. D., Oldfield, J. E., & Mosher, W. D. (2009). Selenium and Mercury Interactions with Emphasis on Fish Tissue. *Environmental Bioindicators*, 4(4), 318-334. doi: <https://doi.org/10.1080/15555270903358428>
- Pitt, J. A., Trevisan, R., Massarsky, A., Kozal, J. S., Levin, E. D., & Di Giulio, R. T. (2018). Maternal transfer of nanoplastics to offspring in zebrafish (*Danio rerio*): A case study with nanopolystyrene. *Science of The Total Environment*, 643, 324-334. doi: <https://doi.org/10.1016/j.scitotenv.2018.06.186>
- PMRA. (2017). Re-evaluation Decision RVD2017-01, Glyphosate. Ottawa, Canada: Pest Management Regulatory Agency, Health Canada.
- Ponton, D. E., Caron, A., Hare, L., & Campbell, P. G. C. (2016). Hepatic oxidative stress and metal subcellular partitioning are affected by selenium exposure in wild yellow perch (*Perca flavescens*). *Environmental Pollution*, 214, 608-617. doi: <https://doi.org/10.1016/j.envpol.2016.04.051>
- Powell, H. A., Kerby, N. W., & Rowell, P. (1991). Natural tolerance of Cyanobacteria to the herbicide glyphosate. *New Phytologist*, 119, 421-426. doi: <https://doi.org/10.1111/j.1469-8137.1991.tb00042.x>
- Prudent, J., Popgeorgiev, N., Bonneau, B., & Gillet, G. (2013). Subcellular fractionation of zebrafish embryos and mitochondrial calcium uptake application. *Protocol Exchange*. doi: <https://doi.org/10.1038/protex.2013.073>
- Pyle, G. G., Rajotte, J. W., & Couture, P. (2005). Effects of industrial metals on wild fish populations along a metal contamination gradient. *Ecotoxicology and Environmental Safety*, 61(3), 287-312. doi: <https://doi.org/10.1016/j.ecoenv.2004.09.003>
- Ralston, N. V. (2008). Selenium health benefit values as seafood safety criteria. *Ecohealth*, 5(4), 442-455. doi: <https://doi.org/10.1007/s10393-008-0202-0>
- Ralston, N. V., Ralston, C. R., Blackwell, J. L., 3rd, & Raymond, L. J. (2008). Dietary and tissue selenium in relation to methylmercury toxicity. *Neurotoxicology*, 29(5), 802-811. doi: <https://doi.org/10.1016/j.neuro.2008.07.007>
- Ramsar. (2014). *La Convention de Ramsar et sa mission*. Retrieved from <https://www.ramsar.org/fr/a-propos/la-convention-de-ramsar-et-sa-mission>
- Ranjard, L., Nazaret, S., & Cournoyer, B. (2003). Freshwater Bacteria Can Methylate Selenium through the Thiopurine Methyltransferase Pathway. *Applied and*

Environmental Microbiology, 69(7), 3784-3790. doi:

<https://doi.org/10.1128/aem.69.7.3784-3790.2003>

Rayman, M. P. (2000). The importance of selenium to human health. *The Lancet*, 356(9225), 233-241. doi: [https://doi.org/10.1016/s0140-6736\(00\)02490-9](https://doi.org/10.1016/s0140-6736(00)02490-9)

RCoreTeam. (2016). *R: A language and environment for statistical computing*. Retrieved from <https://cran.r-project.org>

Reddy, K. N., Rimando, A. M., & Duke, S. O. (2004). Aminomethylphosphonic Acid, a Metabolite of Glyphosate, Causes Injury in Glyphosate-Treated, Glyphosate-Resistant Soybean. *Journal of Agricultural and Food Chemistry*, 52(16), 5139–5143. doi: <https://doi.org/10.1021/jf049605v>

Rognes, T., Flouri, T., Nichols, B., Quince, C., & Mahe, F. (2016). VSEARCH: a versatile open source tool for metagenomics. *PeerJ*, 4, e2584. doi: <https://doi.org/10.7717/peerj.2584>

Rosabal, M., Hare, L., & Campbell, P. G. C. (2012). Subcellular metal partitioning in larvae of the insect *Chaoborus* collected along an environmental metal exposure gradient (Cd, Cu, Ni and Zn). *Aquatic Toxicology*, 120-121, 67-78. doi: <https://doi.org/10.1016/j.aquatox.2012.05.001>

Rosabal, M., Hare, L., & Campbell, P. G. C. (2014). Assessment of a subcellular metal partitioning protocol for aquatic invertebrates: preservation, homogenization, and subcellular fractionation. *Limnology and Oceanography: Methods*, 12(7), 507-518. doi: <https://doi.org/10.4319/lom.2014.12.507>

Rosabal, M., Mounicou, S., Hare, L., & Campbell, P. G. (2016). Metal (Ag, Cd, Cu, Ni, Tl, and Zn) Binding to Cytosolic Biomolecules in Field-Collected Larvae of the Insect *Chaoborus*. *Environmental Science & Technology*, 50(6), 3247-3255. doi: <https://doi.org/10.1021/acs.est.5b05961>

Rosabal, M., Pierron, F., Couture, P., Baudrimont, M., Hare, L., & Campbell, P. G. (2015). Subcellular partitioning of non-essential trace metals (Ag, As, Cd, Ni, Pb, and Tl) in livers of American (*Anguilla rostrata*) and European (*Anguilla anguilla*) yellow eels. *Aquatic Toxicology*, 160, 128-141. doi: <https://doi.org/10.1016/j.aquatox.2015.01.011>

Rust, M. B. (2002). Nutritional Physiology *Fish Nutrition (Third Edition)* (pp. 367-452).

U.S.A.: Academic Press.

- Saiki, M. K., Martin, B. A., & May, T. W. (2004). Reproductive status of western mosquitofish inhabiting selenium-contaminated waters in the Grassland water district, Merced county, California. *Archives of Environmental Contamination and Toxicology*, 47(3), 363-369. doi: <https://doi.org/10.1007/s00244-004-2051-3>
- Salvador, A. M., Alonso-Damián, A., Choubert, G., & Milicua, J. C. G. (2007). Effect of Soybean Phospholipids on Canthaxanthin Lipoproteins Transport, Digestibility, and Deposition in Rainbow Trout (*Oncorhynchus mykiss*) Muscle. *Journal of Agricultural and Food Chemistry*, 55(22), 9202–9207. doi: <https://doi.org/10.1021/jf070145q>
- Sanders, B. M., & Jenkins, K. D. (1984). Relationships between free cupric ion concentrations in sea water and copper metabolism and growth in crab larvae. *Biological Bulletin*, 167(3), 704-712. doi: <https://doi.org/10.2307/1541421>
- Sandheinrich, M. B., Bhavsar, S. P., Bodaly, R. A., Drevnick, P. E., & Paul, E. A. (2011). Ecological risk of methylmercury to piscivorous fish of the Great Lakes region. *Ecotoxicology*, 20(7), 1577-1587. doi: <https://doi.org/10.1007/s10646-011-0712-3>
- Sauvé, S., & Desrosiers, M. (2014). A review of what is an emerging contaminant. *Chemistry Central journal*, 8(1), 15. doi: <https://doi.org/10.1186/1752-153X-8-15>
- Scheuhammer, A., Braune, B., Chan, H. M., Frouin, H., Krey, A., Letcher, R., Loseto, L., Noel, M., Ostertag, S., Ross, P., & Wayland, M. (2015). Recent progress on our understanding of the biological effects of mercury in fish and wildlife in the Canadian Arctic. *Science of The Total Environment*, 509-510, 91-103. doi: <https://doi.org/10.1016/j.scitotenv.2014.05.142>
- Schmitt-Jansen, M., & Altenburger, R. (2005). Toxic effects of isoproturon on periphyton communities – a microcosm study. *Estuarine, Coastal and Shelf Science*, 62(3), 539-545. doi: <https://doi.org/10.1016/j.ecss.2004.09.016>
- Serra, A. A., Nuttens, A., Larvor, V., Renault, D., Couee, I., Sulmon, C., & Gouesbet, G. (2013). Low environmentally relevant levels of bioactive xenobiotics and associated degradation products cause cryptic perturbations of metabolism and molecular stress responses in *Arabidopsis thaliana*. *Journal of Experimental Botany*, 64(10), 2753-2766. doi: <https://doi.org/10.1093/jxb/ert119>

- Serrano, R., Blanes, M. A., & Lopez, F. J. (2008). Maternal transfer of organochlorine compounds to oocytes in wild and farmed gilthead sea bream (*Sparus aurata*). *Chemosphere*, 70(4), 561-566. doi: <https://doi.org/10.1016/j.chemosphere.2007.07.011>
- Siehl, D. L. (1997). Inhibitors of EPSP synthase, glutamine synthetase and histidine synthesis. In R. M. Roe, J. D. Burton & R. J. Kuhr (Eds.), *Herbicide Activity: Toxicology, Biochemistry and Molecular Biology* (pp. 37-67). Amsterdam, The Netherlands: IOS Press.
- Sigel, A., Sigel, H., & Sigel, R. K. O. (2009). *Metallothioneins and Related Chelators*: Walter de Gruyter GmbH & Co KG.
- Sloterdijk, H. (1977). *Accumulation des métaux lourds et des composés organochlorés dans la chair des poissons du fleuve Saint-Laurent*. Québec, Canada. Retrieved from Ministère du Tourisme de la Chasse et de la Pêche du Québec, Comité d'étude sur le fleuve Saint-Laurent.
- Smedbol, E., Gomes, M. P., Paquet, S., Labrecque, M., Lepage, L., Lucotte, M., & Juneau, P. (2018). Effects of low concentrations of glyphosate-based herbicide factor 540((R)) on an agricultural stream freshwater phytoplankton community. *Chemosphere*, 192, 133-141. doi: <https://doi.org/10.1016/j.chemosphere.2017.11.028>
- Spanovskaya, V. D., & Grygorash, V. A. (1977). Development and Food of Age-0 Eurasian Perch (*Perca fluviatilis*) in Reservoirs near Moscow, USSR. *Journal of the Fisheries Research Board of Canada*, 34(10), 1551-1558. doi: <https://doi.org/10.1139/f77-218>
- Spiller, H. A. (2017). Rethinking mercury: the role of selenium in the pathophysiology of mercury toxicity. *Clinical Toxicology*, 56(5), 313-326. doi: <https://doi.org/10.1080/15563650.2017.1400555>
- Spry, D. J., & Wiener, J. G. (1991). Metal bioavailability and toxicity to fish in low-alkalinity lakes: A critical review. *Environmental Pollution*, 71(2-4), 243-304. doi: [https://doi.org/10.1016/0269-7491\(91\)90034-T](https://doi.org/10.1016/0269-7491(91)90034-T)
- Stefansson, E. S., Heyes, A., & Rowe, C. L. (2014). Tracing maternal transfer of methylmercury in the sheepshead minnow (*Cyprinodon variegatus*) with an enriched mercury stable isotope. *Environmental Science & Technology*, 48(3), 1957-1963. doi: <https://doi.org/10.1021/es404325c>

- Stevenson, R. J., Bothwell, M. L., & Lowe, R. L. (1996). *Algal Ecology: Freshwater Benthic Ecosystems*. San Diego, CA: Academic Press.
- Stewart, R., Grosell, M., Buchwalter, D., Fisher, N. S., Luoma, S., Mathews, T., Orr, P., & Wang, W.-X. (2010). Bioaccumulation and Trophic Transfer of Selenium. In P. M. Chapman, W. J. Adams, M. L. Brooks, C. G. Delos, S. N. Luoma, W. A. Maher, H. M. Ohlendorf, T. S. Presser & D. P. Shaw (Eds.), *Ecological Assessment of Selenium in the Aquatic Environment* (pp. 93-139). Pensacola, Florida: Society of Environmental Toxicology and Chemistry (SETAC) and CRC Press.
- Strickland, J. D. H., & Parsons, T. R. (1972). *A Practical Handbook of Seawater Analysis* (2nd ed.). Ottawa: Fisheries Research Board of Canada.
- Struger, J., Thompson, D., Staznik, B., Martin, P., McDaniel, T., & Marvin, C. (2008). Occurrence of Glyphosate in Surface Waters of Southern Ontario. *Bulletin of Environmental Contamination and Toxicology*, 80(4), 378-384. doi: <https://doi.org/10.1007/s00128-008-9373-1>
- Thiers, R. E., & Vallee, B. L. (1957). Distribution of metals in subcellular fractions of rat liver. *J. biol. Chem.*, 226, 911-920
- Tillitt, D. E., Papoulias, D. M., Whyte, J. J., & Richter, C. A. (2010). Atrazine reduces reproduction in fathead minnow (*Pimephales promelas*). *Aquatic Toxicology*, 99(2), 149-159. doi: <https://doi.org/10.1016/j.aquatox.2010.04.011>
- Tlili, A., Berard, A., Roulier, J. L., Volat, B., & Montuelle, B. (2010). PO43- dependence of the tolerance of autotrophic and heterotrophic biofilm communities to copper and diuron. *Aquatic Toxicology*, 98(2), 165-177. doi: <https://doi.org/10.1016/j.aquatox.2010.02.008>
- Tlili, A., Corcoll, N., Bonet, B., Morin, S., Montuelle, B., Berard, A., & Guasch, H. (2011). In situ spatio-temporal changes in pollution-induced community tolerance to zinc in autotrophic and heterotrophic biofilm communities. *Ecotoxicology*, 20(8), 1823-1839. doi: <https://doi.org/10.1007/s10646-011-0721-2>
- Tlili, A., Dorigo, U., Montuelle, B., Margoum, C., Carluer, N., Gouy, V., Bouchez, A., & Berard, A. (2008). Responses of chronically contaminated biofilms to short pulses of diuron. An experimental study simulating flooding events in a small river. *Aquatic Toxicology*, 87(4), 252-263. doi: <https://doi.org/10.1016/j.aquatox.2008.02.004>

- Tollefson, L., & Cordle, F. (1986). Methylmercury in fish: a review of residue levels, fish consumption and regulatory action in the United States. *Environmental Health Perspectives*, 68, 203-208. doi: <https://doi.org/10.1289/ehp.8668203>
- UE. (2014). Foamstream: un herbicide efficace, sans agent chimique. Bruxelles: Commission Européenne.
- Ungerer, J. R., & Thomas, P. (1996). Role of very low density lipoproteins in the accumulation of o,p'-DDT in fish ovaries during gonadal recrudescence. *Aquatic Toxicology*, 35(3-4), 183-195. doi: [https://doi.org/10.1016/0166-445X\(96\)00011-2](https://doi.org/10.1016/0166-445X(96)00011-2)
- Urho, L. (1996). Habitat shifts of perch larvae as survival strategy. *Annales Zoologici Fennici*, 33(3-4), 329-340
- Urien, N., Cooper, S., Caron, A., Sonnenberg, H., Rozon-Ramilo, L., Campbell, P. G. C., & Couture, P. (2018). Subcellular partitioning of metals and metalloids (As, Cd, Cu, Se and Zn) in liver and gonads of wild white suckers (*Catostomus commersonii*) collected downstream from a mining operation. *Aquatic Toxicology*, 202, 105-116. doi: <https://doi.org/10.1016/j.aquatox.2018.07.001>
- Vadeboncoeur, Y., & Steinman, A. D. (2002). Periphyton function in lake ecosystems. *ScientificWorldJournal*, 2, 1449-1468. doi: <https://doi.org/10.1100/tsw.2002.294>
- van de Merwe, J. P., Chan, A. K., Lei, E. N., Yau, M. S., Lam, M. H., & Wu, R. S. (2011). Bioaccumulation and maternal transfer of PBDE 47 in the marine medaka (*Oryzias melastigma*) following dietary exposure. *Aquatic Toxicology*, 103(3-4), 199-204. doi: <https://doi.org/10.1016/j.aquatox.2011.02.021>
- Van den Brink, P. J., Crum, S. J., Gylstra, R., Bransen, F., Cuppen, J. G., & Brock, T. C. (2009). Effects of a herbicide-insecticide mixture in freshwater microcosms: Risk assessment and ecological effect chain. *Environmental Pollution*, 157(1), 237-249. doi: <https://doi.org/10.1016/j.envpol.2008.07.012>
- Van Eerd, L. L., Hoagland, R. E., Zablotowicz, R. M., & Hall, J. C. (2003). Pesticide metabolism in plants and microorganisms. *Weed Science*, 51(4), 472-495. doi: [https://doi.org/10.1614/0043-1745\(2003\)051\[0472:PMIPAM\]2.0.CO;2](https://doi.org/10.1614/0043-1745(2003)051[0472:PMIPAM]2.0.CO;2)
- Vera, M. S., Juarez, A., & Pizarro, H. N. (2014). Comparative effects of technical-grade and a commercial formulation of glyphosate on the pigment content of periphytic algae.

Bulletin of Environmental Contamination and Toxicology, 93(4), 399-404. doi:

<https://doi.org/10.1007/s00128-014-1355-x>

Vera, M. S., Lagomarsino, L., Sylvester, M., Perez, G. L., Rodriguez, P., Mugni, H., Sinistro, R., Ferraro, M., Bonetto, C., Zagarese, H., & Pizarro, H. (2010). New evidences of Roundup (glyphosate formulation) impact on the periphyton community and the water quality of freshwater ecosystems. *Ecotoxicology*, 19(4), 710-721. doi:
<https://doi.org/10.1007/s10646-009-0446-7>

Wallace, W. G., Lee, B.-G., & Luoma, S. N. (2003). Subcellular compartmentalization of Cd and Zn in two bivalves. I. Significance of metal-sensitive fractions (MSF) and biologically detoxified metal (BDM). *Marine Ecology Progress Series*, 249, 183-197. doi: <https://doi.org/10.3354/meps249183>

Wallace, W. G., & Luoma, S. N. (2003). Subcellular compartmentalization of Cd and Zn in two bivalves. II. Significance of trophically available metal (TAM). *Marine Ecology Progress Series*, 257, 125-137. doi:
<https://doi.org/doi:https://doi.org/10.3354/meps257125>

Wang, F., Lemes, M., & Khan, M. A. K. (2012). Metallomics of Mercury: Role of Thiol- and Selenol-Containing Biomolecules. In G. Liu, Y. Cai & O'Driscoll (Eds.), *Environmental Chemistry and Toxicology of Mercury* (pp. 517-544). Hoboken, New Jersey: John Wiley & Sons, Inc.

Wang, K. Y., Peng, C. Z., Huang, J. L., Huang, Y. D., Jin, M. C., & Geng, Y. (2013). The pathology of selenium deficiency in *Cyprinus carpio* L. *Journal of Fish Diseases*, 36(7), 609-615. doi: <https://doi.org/10.1111/jfd.12030>

Watanabe, C., Yoshida, K., Kasanuma, Y., Kun, Y., & Satoh, H. (1999). In Utero Methylmercury Exposure Differentially Affects the Activities of Selenoenzymes in the Fetal Mouse Brain. *Environmental Research*, 80(3), 208-214. doi:
<https://doi.org/10.1006/enrs.1998.3889>

Weber, D. N. (2006). Dose-dependent effects of developmental mercury exposure on C-start escape responses of larval zebrafish *Danio rerio*. *Journal of Fish Biology*, 69(1), 75-94. doi: <https://doi.org/10.1111/j.1095-8649.2006.01068.x>

Wetzel, R. G. (1983). *Periphyton of freshwater ecosystems*. The Hague: Dr. W. Junk Publishers.

- Wetzel, R. G. (1993). Microcommunities and microgradients: Linking nutrient regeneration, microbial mutualism and high sustained aquatic primary production. *Netherlands Journal of Aquatic Ecology*, 27(1), 3-9. doi: <https://doi.org/10.1007/bf02336924>
- Whiteside, M. C., Swindoll, C. M., & Doolittle, W. L. (1985). Factors affecting the early life history of yellow perch, *Perca flavescens*. *Environmental Biology of Fishes*, 12(1), 47-56. doi: <https://doi.org/10.1007/BF00007709>
- Wickham, H. (2009). *Ggplot2: Elegant Graphics for Data Analysis*: Springer-Verlag New York.
- Wiener, J. G., Sandheinrich, M. B., Bhavsar, S. P., Bohr, J. R., Evers, D. C., Monson, B. A., & Schrank, C. S. (2012). Toxicological significance of mercury in yellow perch in the Laurentian Great Lakes region. *Environmental Pollution*, 161, 350-357. doi: <https://doi.org/10.1016/j.envpol.2011.09.025>
- Xie, R., Seip, H. M., Wibetoe, G., Nori, S., & McLeod, C. W. (2006). Heavy coal combustion as the dominant source of particulate pollution in Taiyuan, China, corroborated by high concentrations of arsenic and selenium in PM10. *Science of The Total Environment*, 370(2-3), 409-415. doi: <https://doi.org/10.1016/j.scitotenv.2006.07.004>
- Yoshida, M., Yoshida, T., Kashima, A., Takashima, Y., Hosoda, N., Nagasaki, K., & Hiroishi, S. (2008). Ecological dynamics of the toxic bloom-forming cyanobacterium *Microcystis aeruginosa* and its cyanophages in freshwater. *Applied Environmental Microbiology*, 74(10), 3269-3273. doi: <https://doi.org/10.1128/AEM.02240-07>

ANNEXE I.

Bande dessinée « La forteresse gluante »



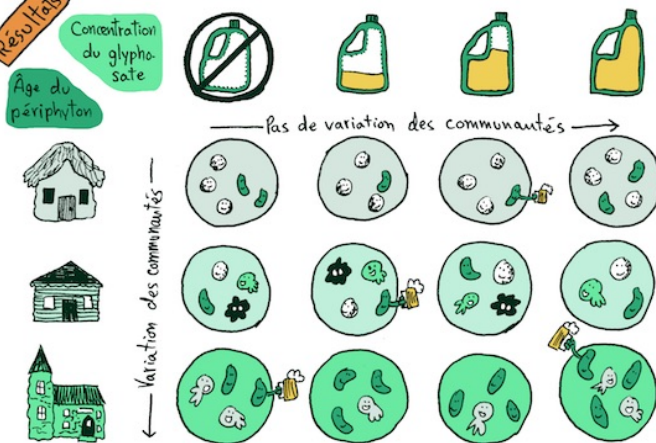
Grâce à son équipe,
elle a pu compter
sur des échantillons
de périphyton âgés
de deux mois,
un an et ...

20 ans!

La matrice (la «glue») du périphyton s'épaissit avec le temps et peut jouer un rôle de bouclier, d'où l'intérêt d'avoir des échantillons de différents âges.



Mélissa a ensuite exposé ces échantillons au glyphosate pendant une semaine.



À la vue de ces résultats, le glyphosate a peu d'effet sur la composition des communautés de périphyton.

Peu importe l'âge du périphyton, sa matrice gelatineuse agit comme une barrière contre le glyphosate.



Cette muraille permet donc aux communautés d'évoluer à travers le temps.



Bref, le glyphosate n'est pas sans danger. Mais nos écosystèmes sont complexes et résilients. Le périphyton en est un bel exemple!



ANNEXE II.

Analyses préliminaires liées à l'aperçu de la contamination en retardateurs de flamme dans les tissus de perchaude au LSP

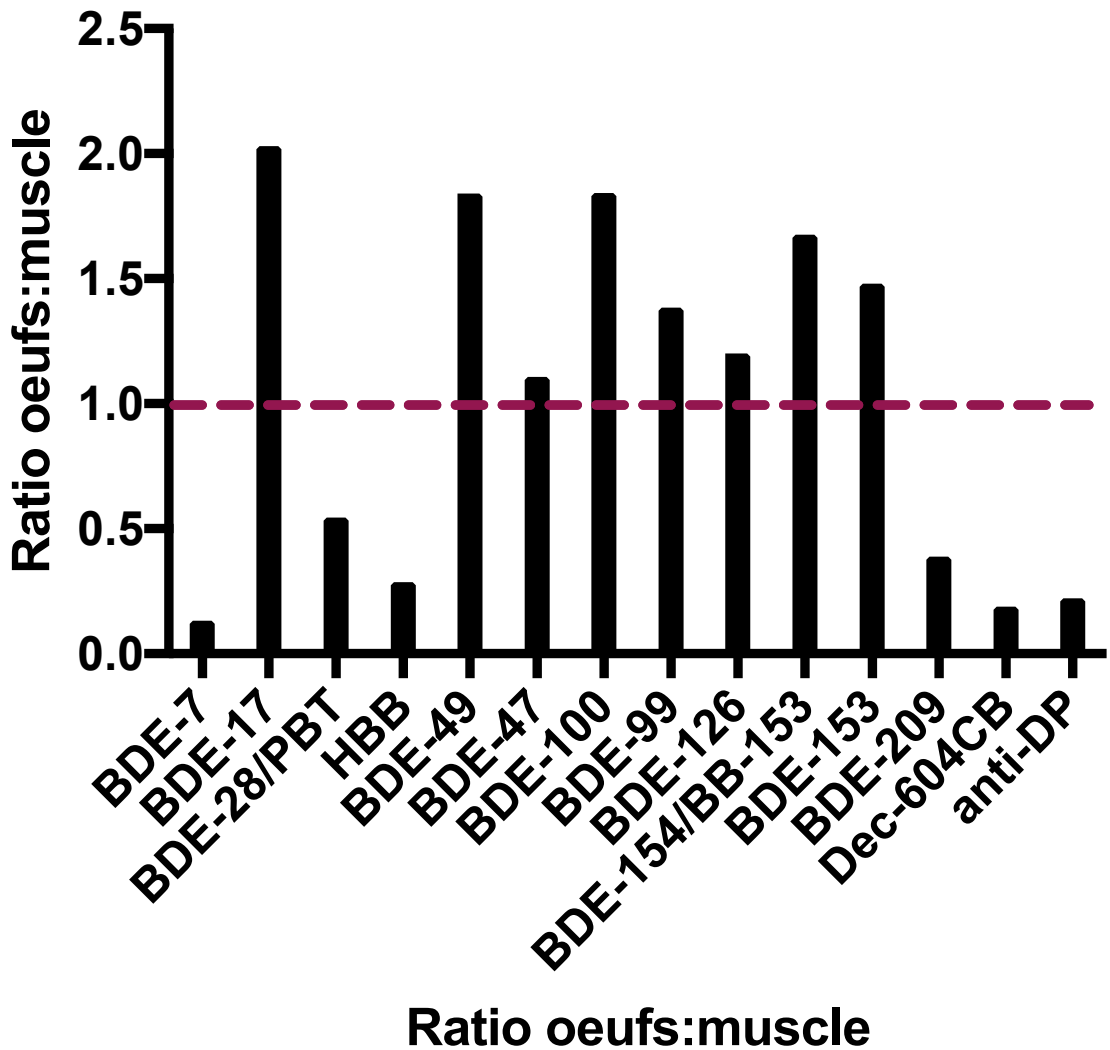


Figure 1. Ratio entre les concentrations mesurées dans les œufs et celles mesurées dans le muscle des perchaudes femelles ovigères ($n=5$) pour plusieurs retardateurs de flamme halogénés.

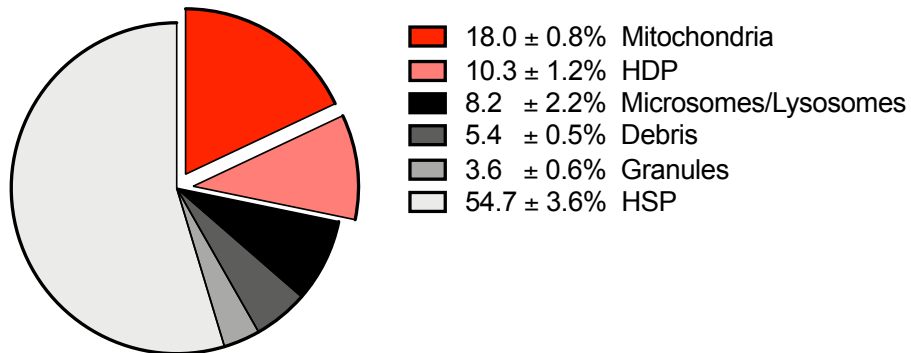
Tableau 1. Concentrations de 5 congénères de PBDE (ng/g de masse humide) dans le foie (n=2) et les gonades (n=5) de perchaudes échantillonnées au LSP et comparaison avec les RQFE. Les concentrations en rose indiquent un dépassement des RQFE.

Congénère	Concentration dans le foie	Concentration dans les gonades	RQFE
<i>BDE28-PBT</i>	0.19	0.15	120
<i>BDE-47</i>	8.57	8.26	88
<i>BDE-153</i>	0.35	0.27	420
<i>BDE-100</i>	2.29	3.47	1
<i>BDE-99</i>	2.09	1.93	1

ANNEXE III.

Fractionnement subcellulaire du cuivre, du cadmium, du manganèse et du fer dans les foies de perchaudes au LSP

a.



b.

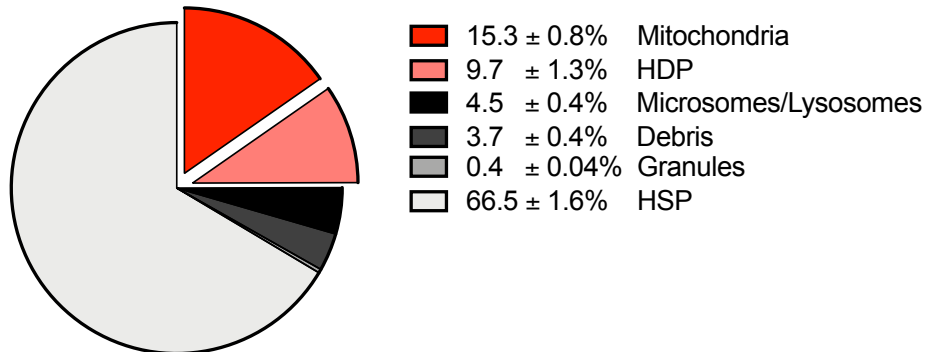
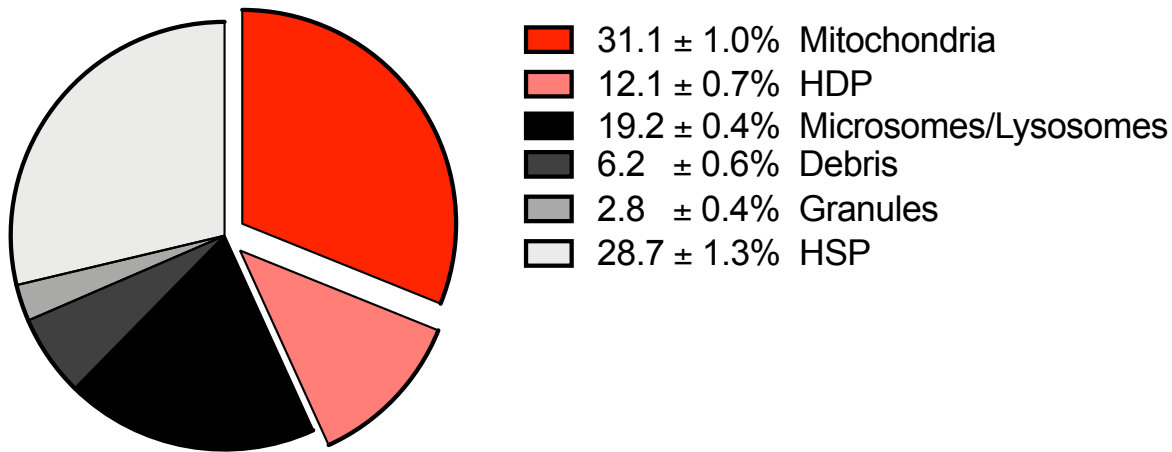


Figure 1. (a) Copper and (b) Cadmium burden distribution (% ± SEM) in subcellular fractions of liver (n=21) cells. Red and pink exploded parts represent sensitive fractions.

a.



b.

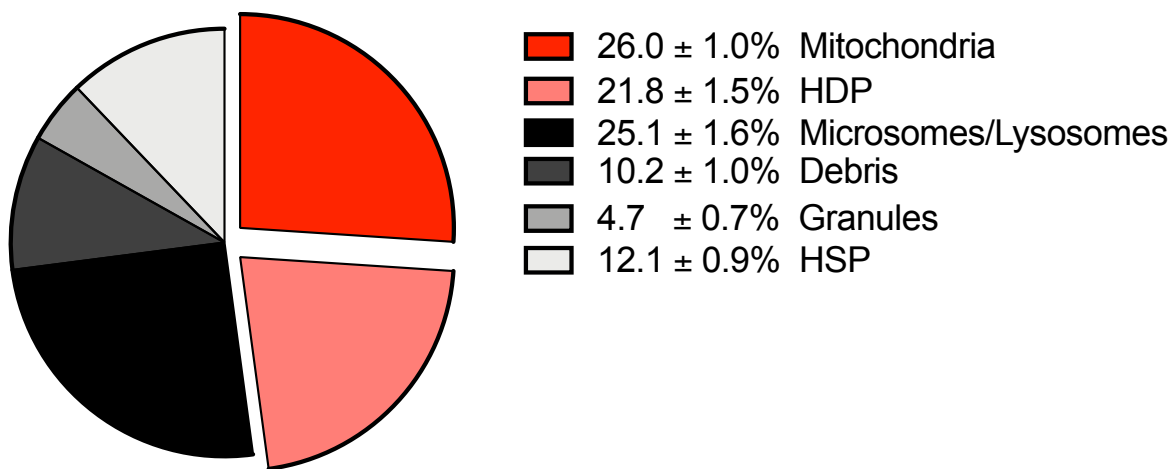


Figure 2. (a) Manganese and (b) Iron burden distribution (% ± SEM) in subcellular fractions of liver (n=21) cells. Red and pink exploded parts represent sensitive fractions.

ANNEXE IV.

Bioaccumulation du manganèse, du fer, du cuivre, de l'arsenic et du cadmium dans les tissus et les stades de vie précoce de la perchaude au LSP

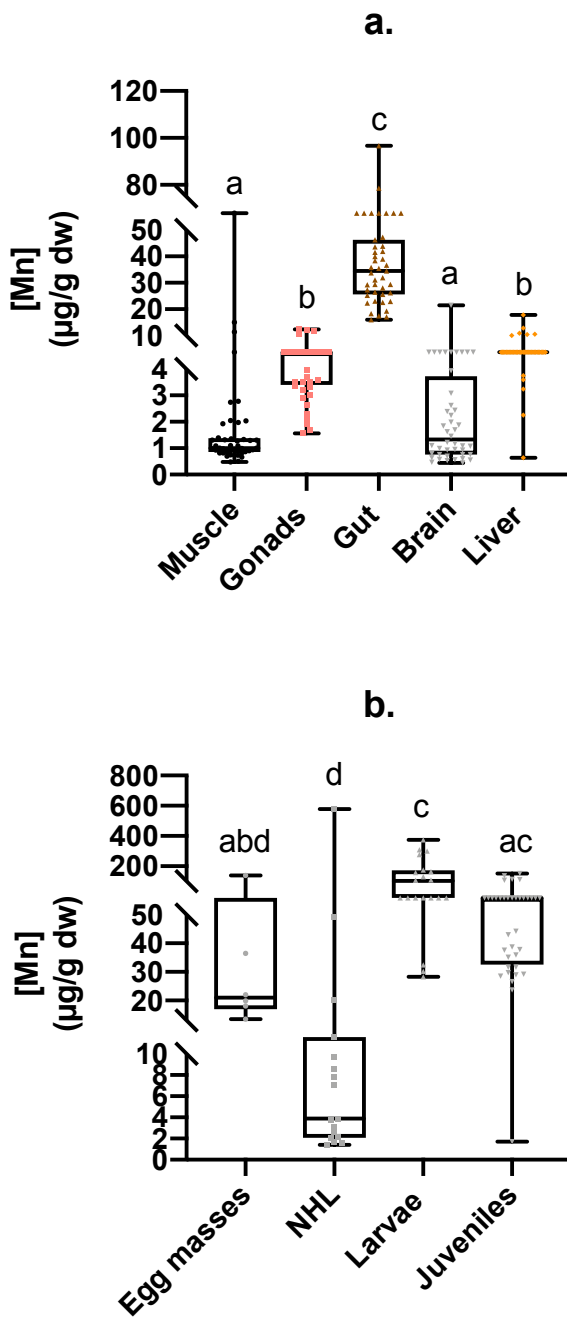


Figure 1. Manganese concentrations ($\mu\text{g/g dw}$) in (a) tissues ($n=44$) and (b) different parts of the life-cycle of Yellow Perch (egg masses ($n=6$), newly-hatched larvae (NHL) ($n=17$), larvae ($n=20$) and juvenile ($n=36$)). Letters indicate significant differences (Dunnett's T3 multiple comparisons test on log-transformed data following Brown-Forsythe and Welch ANOVA tests, $p < 0.05$ for (a) and Dunn's multiple comparisons test following a Kruskal-Wallis test, $p < 0.05$ for (b)).

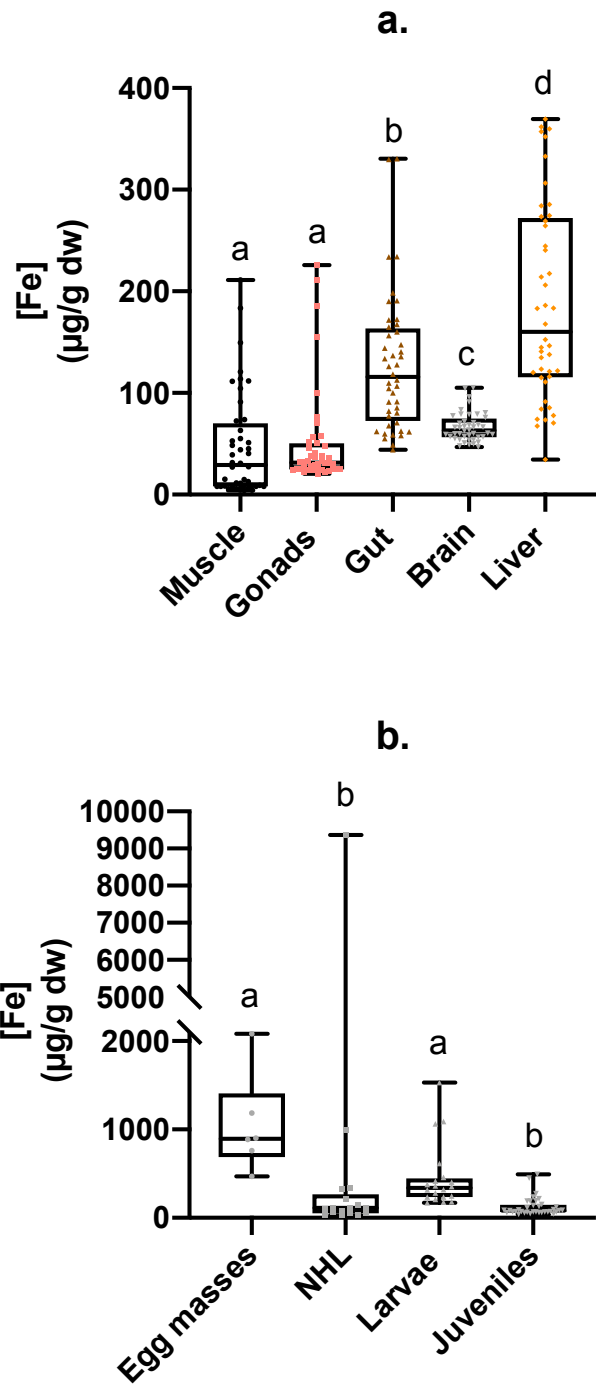


Figure 2. Iron concentrations ($\mu\text{g/g dw}$) in (a) tissues ($n=44$) and (b) different parts of the life-cycle of Yellow Perch (egg masses ($n=6$), newly-hatched larvae (NHL) ($n=17$), larvae ($n=20$) and juvenile ($n=36$)). Letters indicate significant differences (Dunnett's T3 multiple comparisons test on log-transformed data following Brown-Forsythe and Welch ANOVA tests, $p < 0.05$ for (a) and Dunn's multiple comparisons test following a Kruskal-Wallis test, $p < 0.05$ for (b)).

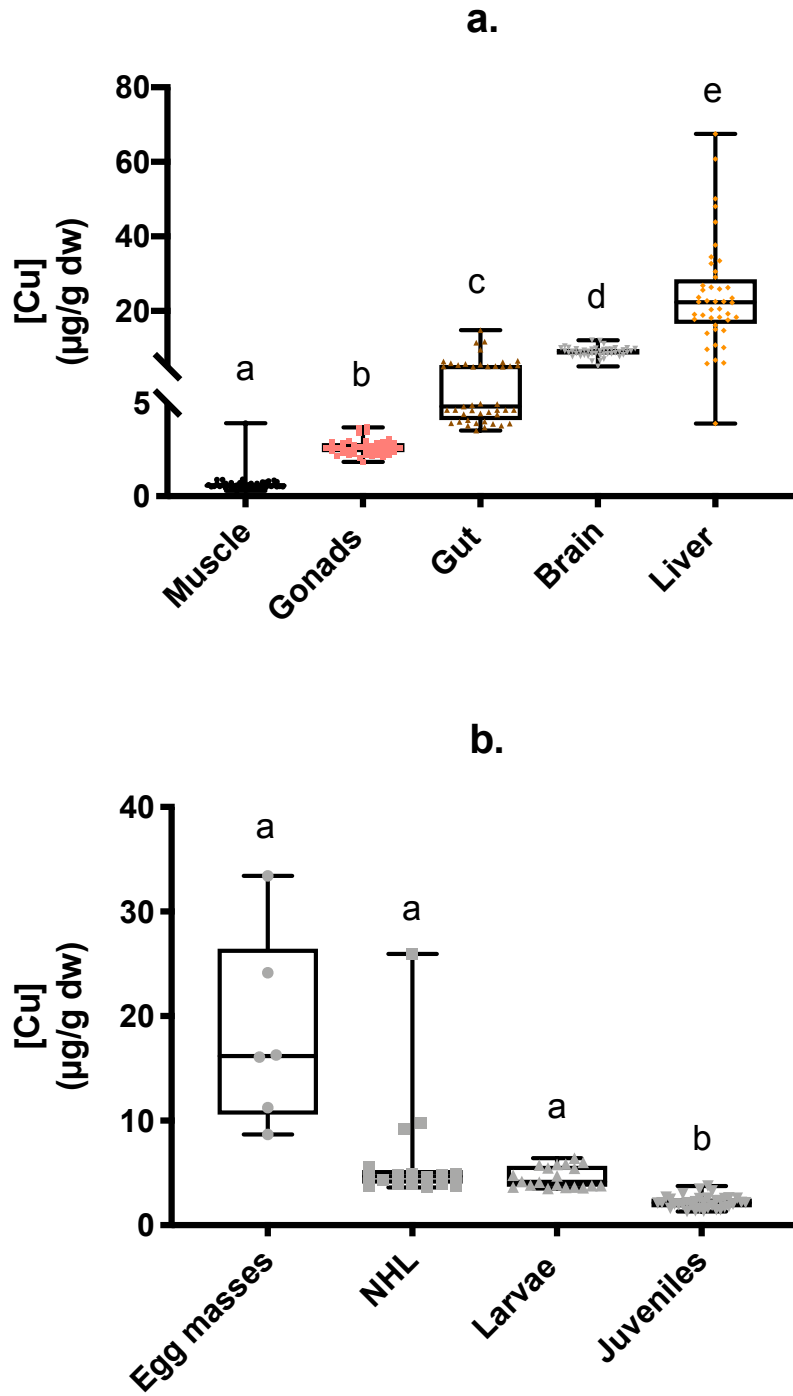


Figure 3. Copper concentrations ($\mu\text{g/g dw}$) in (a) tissues ($n=44$) and (b) different parts of the life-cycle of Yellow Perch (egg masses ($n=6$), newly-hatched larvae (NHL) ($n=17$), larvae ($n=20$) and juvenile ($n=36$)). Letters indicate significant differences (Dunnett's T3 multiple comparisons test on log-transformed data following Brown-Forsythe and Welch ANOVA tests, $p < 0.05$ for (a) and Dunn's multiple comparisons test following a Kruskal-Wallis test, $p < 0.05$ for (b)).

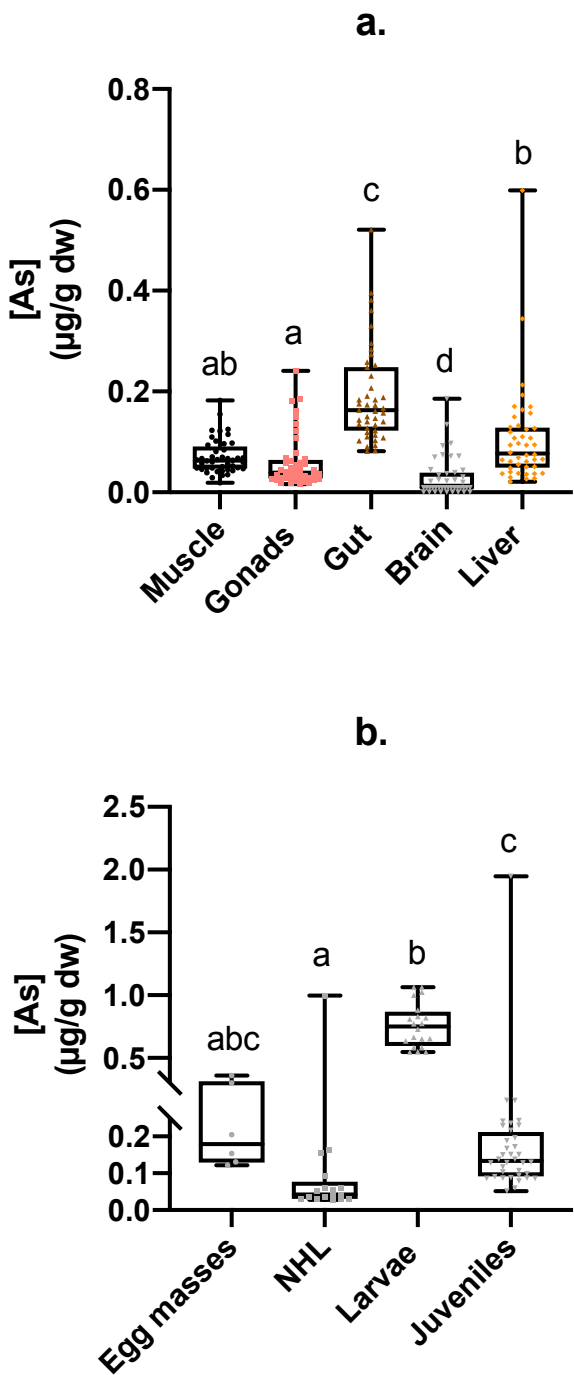


Figure 4. Arsenic concentrations ($\mu\text{g/g dw}$) in (a) tissues ($n=44$) and (b) different parts of the life-cycle of Yellow Perch (egg masses ($n=6$), newly-hatched larvae (NHL) ($n=17$), larvae ($n=20$) and juvenile ($n=36$)). Letters indicate significant differences (Dunnett's T3 multiple comparisons test on log-transformed data following Brown-Forsythe and Welch ANOVA tests, $p < 0.05$ for (a) and Dunn's multiple comparisons test following a Kruskal-Wallis test, $p < 0.05$ for (b)).

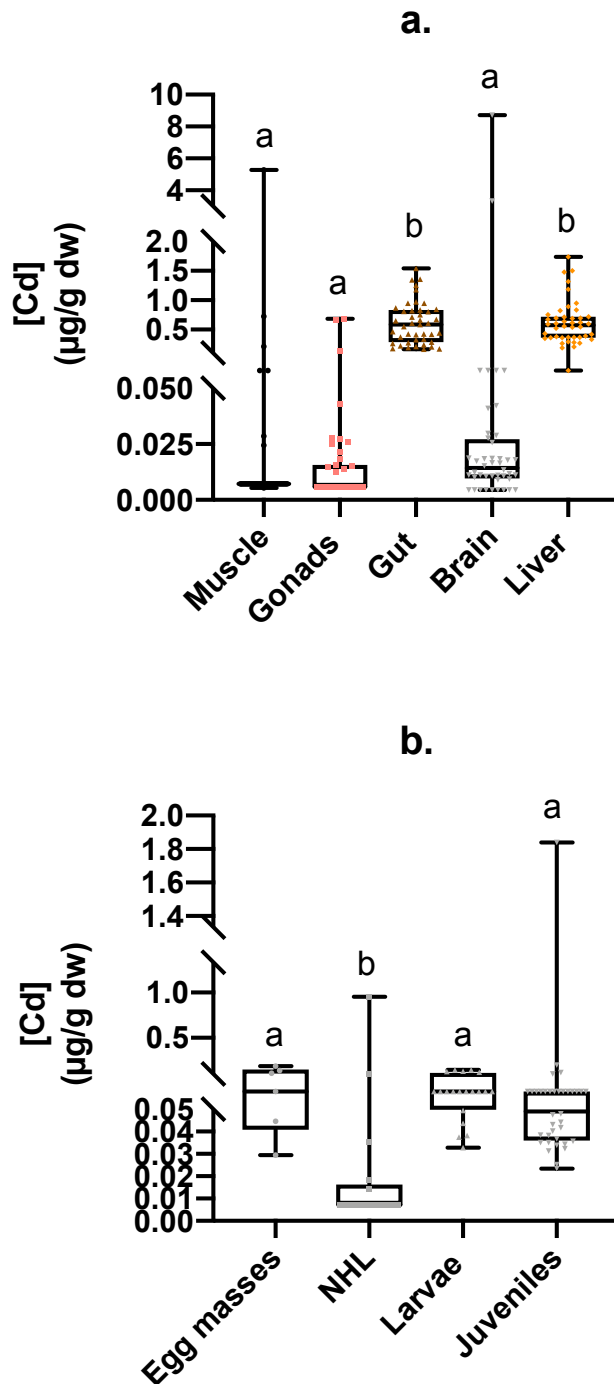


Figure 5. Cadmium concentrations ($\mu\text{g/g dw}$) in (a) tissues ($n=44$) and (b) different parts of the life-cycle of Yellow Perch (egg masses ($n=6$), newly-hatched larvae (NHL) ($n=17$), larvae ($n=20$) and juvenile ($n=36$)). Letters indicate significant differences (Dunnett's T3 multiple comparisons test on log-transformed data following Brown-Forsythe and Welch ANOVA tests, $p < 0.05$ for (a) and Dunn's multiple comparisons test following a Kruskal-Wallis test, $p < 0.05$ for (b)).